ISSN Print 1994-3237
ISSN Online 2305-6959

Abstract Volume

29th Himalaya-Karakoram-Tibet Workshop

Lucca, Italy

September 2-4, 2014

Abstract Volume 29th Himalaya-Karakoram-Tibet Workshop, Lucca, Italy, September 2-4, 2014

Journal of
Himalayan Earth Sciences

Edited By
C. Montomoli, S. Iaccarino
C. Groppo, P. Mosca
F. Rolfo, R. Carosi

Journal of Himalayan Earth Sciences

Editorial Board

Publisher

National Centre of Excellence in Geology
University of Peshawar
Peshawar 25120
Phone: +92-91-9216427, +92-91-9216767
Fax: +92-91-9218183
Email: jhes@upesh.edu.pk
Web: http://nceg.upesh.edu.pk/

29th Himalaya-Karakoram-Tibet Workshop
Lucca, Italy

2-4 September, 2014

Organizing committee

Rodolfo Carosi
Università di Torino, Torino, Italy
rodolfo.carosi@unito.it

Chiara Montomoli
Università di Pisa, Pisa, Itlay
chiara.montomoli@unipi.it

Salvatore Iaccarino
Università di Pisa, Pisa, Italy
iaccarinosalvatore@gmail.com

Scientific committee 29th Himalaya-Karakoram-Tibet Workshop

Prof. Rodolfo Carosi, *Universita` di Torino, Italy*

Dott. Isabelle Coutand, *Dalhousie University, Canada*

Prof. Eduardo Garzanti, *Univerita` di Milano Bicocca, Italy*

Prof. Laurent Godin, *Queen's University, Canada*

Prof. Arvind Kumar Jain, *CSIR-Central Building Research Institute, Roorkee, India*

Prof. Asif Khan, *Karakoram International University, Pakistan*

Prof. Rick Law, *Virginia Tech University, USA*

Dott. Chiara Montomoli, *Universita` di Pisa, Italy*

Dott. Yani Najman, *Lancaster University, UK*

Prof. Santa Man Rai, *Tribhuvan University, Kathmandu, Nepal*

Dott. Delores Robinson, *University of Alabama, USA*

Prof. Mike Searle, *University of Oxford, Great Britain*

Prof. Albrecht Steck, *University of Lausanne, Switzerland*

Prof. Igor Villa, *Universita` di Milano Bicocca, Italy and University of Bern, Switzerland*

Prof. Dario Visona`, *Universita` di Padova, Italy*

Contents

Sikkim Earthquake 2011: Bangladesh Experience

A. K. M. Khorshed Alam[1]

[1]Earthquake Research Cell, Geological Survey of Bangladesh, Dhaka 1000, Bangladesh, akmkhorshed@gmail.com

Bangladesh is mostly floored with Holocene alluvial and deltaic unconsolidated sediments and minor Tertiary folded sedimentary rocks, and located close to the one of the active tectonic regions of the world. Whole of Bangladesh was shaken due to Sikkim earthquake of 18 September 2011, although there was no serious damage. Because the country experienced the highest shaking during last 60 years so the necessity for an assessment on the impact of this earthquake was felt. As the epicenter of the earthquake of 6.9 magnitude was near the Indian-Eurasian plate boundary and 495 km away from Dhaka, the capital city, the assessment was made mostly on the basis of the reports published in the newspapers, information collected from different parts of the country and interviews of local people.

Based on these information an intensity map of the earthquake was prepared showing how the shaking affected the people, natural bodies and artificial structures. The intensity map clearly showed that response to earthquake shaking was not only related to the distance from the epicenter and magnitude but also more related to the earth material i.e. local soil condition.

The maximum intensity was estimated to be IV-V which was found in areas close to the epicentral region, and in areas of clay-rich deposits and in the Old Ganges delta. Result of the study gives a clear relationship between the earthquake shaking and response of unconsolidated sediments.

Cite as: Alam Khorshed, A.K.M., 2014, Sikkim Earthquake 2011: Bangladesh Experience, in Montomoli C., et al., eds., proceedings for the 29th Himalaya-Karakoram-Tibet Workshop, Lucca, Italy.

Characterizing the sub-surface geometry of the Main Frontal Thrust in the Dhalkebar area of central Nepal

Rafael Almeida[1], Judith Hubbard[1], Peter Polivka[1], Dana Peterson[1], Soma Nath Sapkota[2], Agathe Schmid[1], Paul Tapponnier[1], Chintan Timsina[2]

[1] Earth Observatory of Singapore, Nanyang Technological University, 50 Nanyang Avenue, Block N2-01a-15, Singapore, 639798, ralmeida@ntu.edu.sg
[2] National Seismological Centre, Department of Mines and Geology, Lainchaur, Kathmandu, Nepal

The Main Frontal Thrust (MFT) represents the most frontal surface expression of the Himalayan fold and thrust belt. It is contained within the foreland deposits of this orogenic belt, the Siwalik Group. In Nepal this structure is thought to accommodate a large majority of the convergence between India and southern Tibet (~20 mm/yr; Lave and Avouac, 2000). This conclusion was based on uplift rates of river terraces in the Siwaliks. Flights os river terraces such as these are abundant in the hanging wall of the MFT, and can be dated to determine uplift rates. However, converting these uplift rates into slip rates requires knowledge about the geometry of the MFT at depth. To better constrain this geometry as well as the slip history of the MFT, we conducted seismic reflection surveys in Central Nepal around the town of Bardibas. Previous surveys in the research area have used surface data and shallow trenches to identify the surface rupture of the great 1934 earthquake (Sapkota et al., 2013). The seismic surveys are intended to (1) confirm that the rupture identified at the surface is a large through-going feature at depth; (2) image the geometry and kinematics of the fault, in order to assess both the slip in the 1934 rupture, based on surface measurements, and the behavior of the fault at longer timescales, and (3) assess how the many fault strands visible at the surface interact at depth. Ultimately, we hope to improve the assessment of seismic hazard along this fault zone, which forms one of the largest natural hazards in Nepal.

The surveys were conducted during a nine-week period from January through March, 2014. Using a 6300 kg vibroseis Minibuggy, we acquired ~34 km of data in three long transects cutting across the Main Frontal Thrust, with two additional shorter transects and a small hammer survey (red lines in Figure 1). The vibroseis data were acquired with a split-spread configuration, using 264 channels with 5 m spacing. The source consisted of an 8 sec sweep, which changed linearly from 10 Hz to 120 Hz. The record lengths are 6 sec. Six to twelve sweeps, depending on ambient noise, were done at each source location to improve the signal to noise ratio of the data. The seismic lines follow several of the dry river-beds in the area and generally are orthogonal to the range front. The hammer survey was done at the northern end of the vibroseis line acquired in Sir Khola using a 7 kg sledgehammer. The line had a length of 200 m and 96 channels were used with a spacing of 2 m. We used 10 hammer swings at each source location. The hammer survey was acquired to constrain the shallow (down to ~20 m depth) location of a thrust fault in the river bed of Sir Khola (Figure 1). Preliminary processing of this data suggests that the fault is readily observable in the shallow subsurface.

The Siwalik Group is strongly folded in this region. Measurements of bedding attitudes were done throughout the area to complement the seismic data (Figure 1). The bedding planes are consistently tilted with a NW-SE strike. The faults at the surface are mostly E-W. This discrepancy suggests the possibility of an oblique ramp in the thrust fault. The folding near the outcropping faults is asymmetric, typically with narrow steep fore-limbs and wide shallow back-limbs. The river terraces, however, are sub-horizontal and uplifted over large areas. This difference suggests a transition from fault-propagation folding to translation along the fault sometime before the formation of the terraces, although in a few locations the terraces are also gently folded. We expect to use the serial cross-sections obtained from the seismic data to generate a pseudo-3D view of the fault system in the area to help constrain this transition as well as any complexities in the fault-ramp structure. We plan to acquire additional seismic reflection data along other portions of the MFT in the winter of 2014-2015 to gain a better understanding of how the geometry and behavior of the fault changes along strike.

Cite as: Almeida R., et al., 2014, Characterizing the sub-surface geometry of the Main Frontal Thrust in the Dhalkebar area of central Nepal, in Montomoli C., et al., eds., proceedings for the 29th Himalaya-Karakoram-Tibet Workshop, Lucca, Italy.

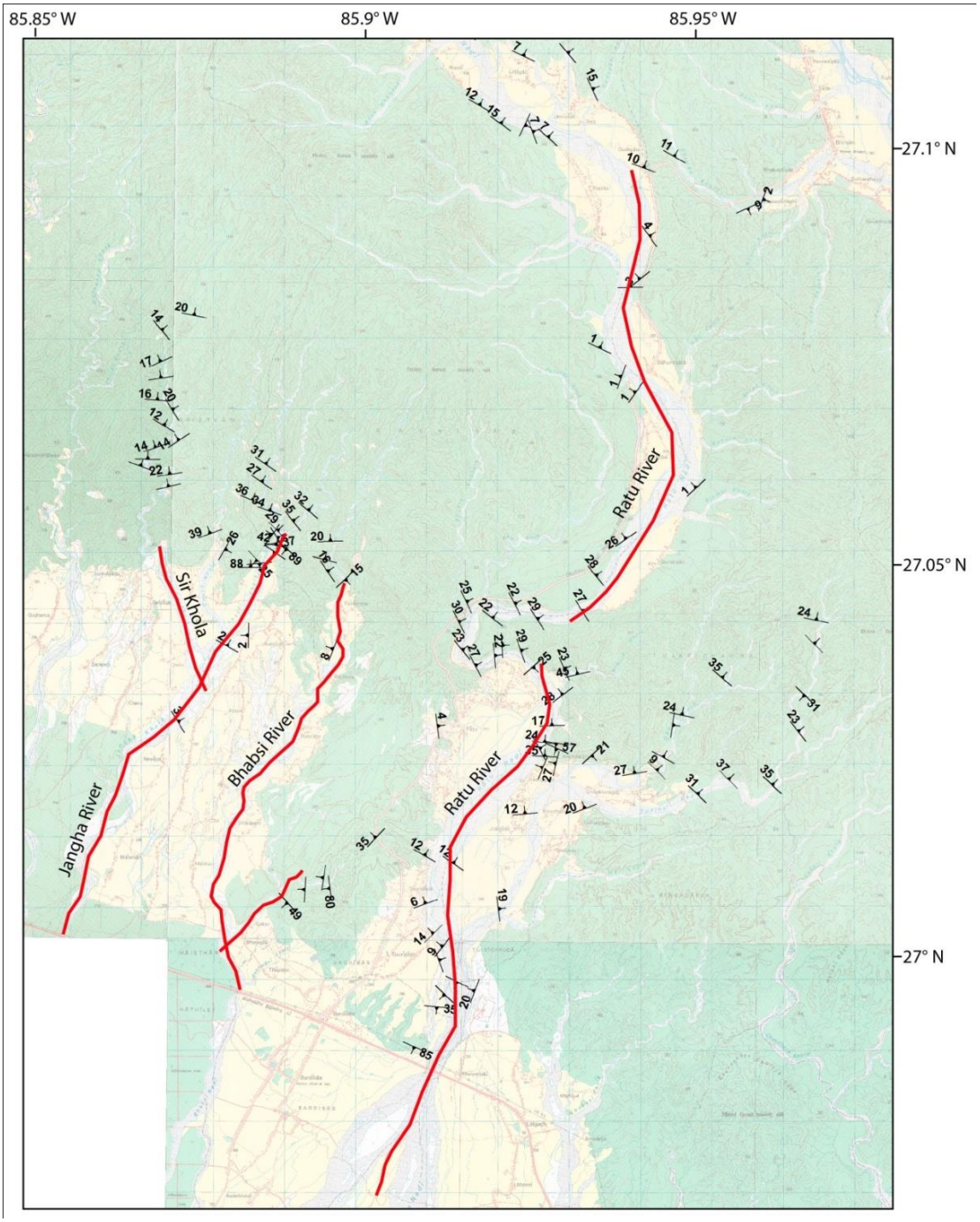

Figure 1. Topographic map of the study area showing location of acquired seismic lines (red lines) and measured bedding attitudes.

References

Lavé J. and Avouac, J.P., 2000, Active folding of fluvial terraces across the Siwalik Hills (Himalaya of central Nepal), Journal of Geophysical Research, 105, 5735-5770.

Sapkota, S.N., Bollinger, L., Klinger, Y., Tapponnier, P., Gaudemer, Y. and Tiwari, D., 2013, Primary surface ruptures of the great Himalayan earthquakes in 1934 and 1255, Nature Geoscience, 6, 71-76.

Hydrology, hillslope processes and suspended sediment transport in the central Himalayas of Nepal

Christoff Andermann[1], Martin Struck[2], Niels Hovius[1], Jens Turowski[1], Oliver Korup[3], Raj Bista[4]

[1] German Research Centre for Geosciences GFZ, Helmholtz Centre Potsdam, Germany, christoff.andermann@gfz-potsdam.de
[2] School of Earth and Environmental Sciences, University of Wollongong, Australia
[3] Institute of Earth- and Environmental Sciences, University of Potsdam, Germany
[4] Nepal Electricity Authority, Kathmandu, Nepal.

Suspended sediment load in rivers is a primary proxy for present-day mean catchment denudation rates (Dadson et al., 2003). In active mountain belts denudation is generally thought to be dominated by hillslope mass wasting. In the Himalayas, strong relief and intense monsoonal rainfall provide favourable conditions for mass wasting (Korup and Weidinger, 2011). On the other hand the suspended sediment fluxes in rivers, draining such large orogens, are mainly controlled by the transport capacity of these rivers and by the contribution of material from the adjacent hillslopes, for example by landsliding. In the Himalayas the spatio-temporal distribution of precipitation has numerous consequences for surface processes, water availability and transport capacities of the rivers. The very clear seasonality - monsoon and non-monsoon - exerts a very distinct annual cyclicity bounding surface processes almost exclusively to the monsoon season, when high rainfall feeds pore water pressures in steep hillslopes that are already prone for failure. In particular, the occurrence of mass wasting and associated highly concentrated suspended sediment fluxes in rivers are closely tied to monsoon season (Andermann et al., 2012a). However, the transfer of precipitation into rivers involves temporary water storage in reservoirs such as soils, groundwater, snow and glaciers, where different transfer times influence the hydrological cycle (Andermann et al., 2012b).

In this contribution we discuss first the interlinkage between suspended sediment concentration, river hydrology and precipitation, on the example of the three major drainage basins (Karnali, Narayani and Koshi) of the Nepal Himalayas. And secondly, we present a new unpublished and highly resolved dataset from the Kali Gandaki River where we infer hillsope processes from the grain-size distribution of the suspended load, supported by satellite imagery based landslide mapping.

For the three major drainage basins the dataset consist of daily suspended sediment and river discharge measurements from 12 hydrological stations across the Nepal Himalayas. All records are daily measurements, spanning several years (i.e. 4–6 yr) between 1973 and 2006, but are not always complete. Precipitation information is derived from the APHRODITE (Asian Precipitation- Highly-Resolved Observational Data Integration Towards Evaluation of Water Resources) precipitation dataset, the best available spatial data for this region (Andermann et al., 2011). The suspended sediment records vs. river discharge plots display seasonal clockwise hysteresis loops. By separating the discharge hydrograph into its different discharge components and only plotting direct runoff (short response time) against suspended sediments the hysteresis collapses to a linear relationship. This demonstrates that the fast flowing discharge component, caused by intense rainfall provides material from the hillslopes to the river. From the clear relationship between direct discharge and sediment fluxes we propose a new sediment transport rating model, allowing us to deduce basin wide denudation rates from the river discharge record, ranking from 0.1 to 5.9 mm/yr. Last we discuss these denudation rates in the context of basin characteristics and we propose a new conceptual model of mobilization and transportation of material within the monsoonal discharge cycle.

The second, more highly resolved dataset incorporates equally suspended sediment and river discharge measurements from two gauging sites along the Kali Gandaki River, one of Nepal's major trans-Himalayan rivers. These two strategically located gauging stations provide the opportunity of tracing at-a-station variations in discharge, sediment fluxes and potential delivery processes on either side of the

Cite as: Andermann et al., 2014, Hydrology, hillslope processes and suspended sediment transport in the central Himalayas of Nepal, in Montomoli C., et al., eds., proceedings for the 29th Himalaya-Karakoram-Tibet Workshop, Lucca, Italy.

Himalayan orographic divide. The upstream station at Lete village (2500 m asl) has an upstream area of 3450 km^2 and is located at the transition between the arid Southern Tibetan Plateau Margin in the north and the monsoon-influenced southern Himalayan front. At Lete suspended sediments have been measured twice daily (morning and evening) over two years (2011-2012). The downstream station is situated at the water intake of a run-of-the-river hydropower facility at Mirmi (520 m asl) with an upstream area of 7580 km^2. At Mirmi the data is available for seven consecutive years (2006-2012). For the first time, for both stations grain size distribution information is available in addition to the bulk suspended load. In order to examine broad scale patterns we compare the sand-to-mud ratio between the upstream and downstream station. The sand fraction clearly shows a stronger sensitivity to external forcing. We observe a distinct coarsening of the sediment flux during monsoon at the downstream station while the sediment ratio at the upstream station remains all year around constant. We attribute this coarsening to precipitation driven mass wasting during monsoon that is contributing coarse sediments to the rivers. This interpretation is confirmed by landslide mapping from Landsat Satellite image time series, indicating that landslides occur exclusively during monsoon and more than ten times more frequent in the south facing monsoon influenced part of the catchment.

Our results demonstrate that the transport of sediments in the Himalayas depends to first order on the contribution of sediments supply from the hillslope and the availability of water, rather than from in channel sediment storage. We show that erosion in the Himalayas is strongly coupled with the magnitude–frequency distribution of precipitation expressed in the fast river discharge fraction. Furthermore, the downstream coarsening of suspended load along the Kali Gandaki River is likely to be linked to sediment input by hillslope mass wasting processes preferentially occurring at the southern front of the Himalayas. Since our denudation rates are derived from a dataset of continuous contemporary sediment flux, they provide a field-based benchmark for denudation studies across multiple timescales.

References

Andermann, C., Bonnet, S. and Gloaguen, R., 2011, Evaluation of precipitation data sets along the Himalayan front, Geochemistry, Geophysics, Geosystems, 12(7), doi:10.1029/2011GC003513.

Andermann, C., Crave, A., Gloaguen, R., Davy, P. and Bonnet, S., 2012a, Connecting source and transport: Suspended sediments in the Nepal Himalayas, Earth Planetary Science Letters, 351-352(0), 158-170.

Andermann, C., Longuevergne, L., Bonnet, S., Crave, A., Davy, P. and Gloaguen R., 2012b, Impact of transient groundwater storage on the discharge of Himalayan rivers, Nature Geoscience, 5(2), 127-132, doi:10.1038/ngeo1356.

Dadson, S.J. et al., 2003, Links between erosion, runoff variability and seismicity in the Taiwan orogen, Nature, 426(6967), 648-51, doi:10.1038/nature02150.

Korup, O. and Weidinger, J.T. 2011, Rock type, precipitation, and the steepness of Himalayan threshold hillslopes, Geol. Soc. London, Spec. Publ., 353(1), 235-249, doi:10.1144/SP353.12.

Seismically reactivated Panjgran mass movement in the Northeast Himalayas of Pakistan

Muhammad Basharat[1], Joachim Rohn[2]

[1] Institute of Geology, University of Azad Jammu and Kashmir, Muzaffarabad, Pakistan, basharatgeo@yahoo.com
[2] GeoZentrum Nordbayern, Friedrich-Alexander-University Erlangen-Nuremberg, Germany

The 2005 Kashmir earthquake induced large number of mass movements throughout the affected area, in the northeast Himalayas of Pakistan. The Panjgran mass movement in the Neelum Valley area, close to the epicenter, is one that blocked the Neelum Valley road many days after the earthquake.

SPOT images and ground investigation were used to analyse the characteristics of seismically reactivated Panjgran mass movement. The mass movement travelled 650 m in the direction of north towards Neelum river and caused severe damage of Neelum road. Initial slope movement involved the slumping in weathered, jointed shale and sandstone of Miocene Murree Formation at the foot of the mass movement. While on the detachment zone the rock fall material detached from the bed rock, moved down slope and accumulated at the base of the ridge. Total volume of Panjgran mass movement was estimated about 6.75 million cubic meters.

The study shows that the mass movement is the result of pre-existing slump on over steepened slope undercut by the Neelum river and ground shaking by the 2005 Kashmir earthquake.

Cite as: Basharat, M. and Rohn, J., 2014, Seismically reactivated Panjgran mass movement in the Northeast Himalayas of Pakistan, in Montomoli C., et al., eds., proceedings for the 29th Himalaya-Karakoram-Tibet Workshop, Lucca, Italy.

Tectonic Evolution of the North-western Tibetan margin and the Pamirs as determined from the sedimentary record of Aertashi, Western Tarim Basin, China

Tamsin Blayney[1], Yani Najman[1], Guillaume Dupont-Nivet[2], Eduardo Garzanti[3], Andrew Carter[4], Ian Millar[5], Martin Rittner[4]

[1] Lancaster Environment Centre, Lancaster University, Bailrigg, Lancaster, LA1 4YW, UK, t.blayney1@lancs.ac.uk
[2] Geosciences Rennes 1, Campus de Beaulieu 35042, Rennes, France
[3] Department of Earth and Environmental Sciences, Universita degli studi di Milano-Bicocca, Italy
[4] Department of Earth Sciences, University College London, Kathleen Lonsdale Building, UK
[5] NIGL, British Geological Survey, Keyworth, UK

The India-Asia collision is the archetypal example of continent-continent collision, however little is known of how deformation has propagated internally through the northern margin of Tibet and the Pamirs. This project focuses on an area of the western Tarim basin (Aertashi (Fig 1)) where a Cenozoic sedimentary record of erosion from the northern Tibetan margin / Pamir salient can be obtained (Fig 2), providing new evidence to explore the impacts of India-Asia collision on the Asian interior, in particular the timing and evolution of the Pamir Salient and Western Kunlun mountain range.

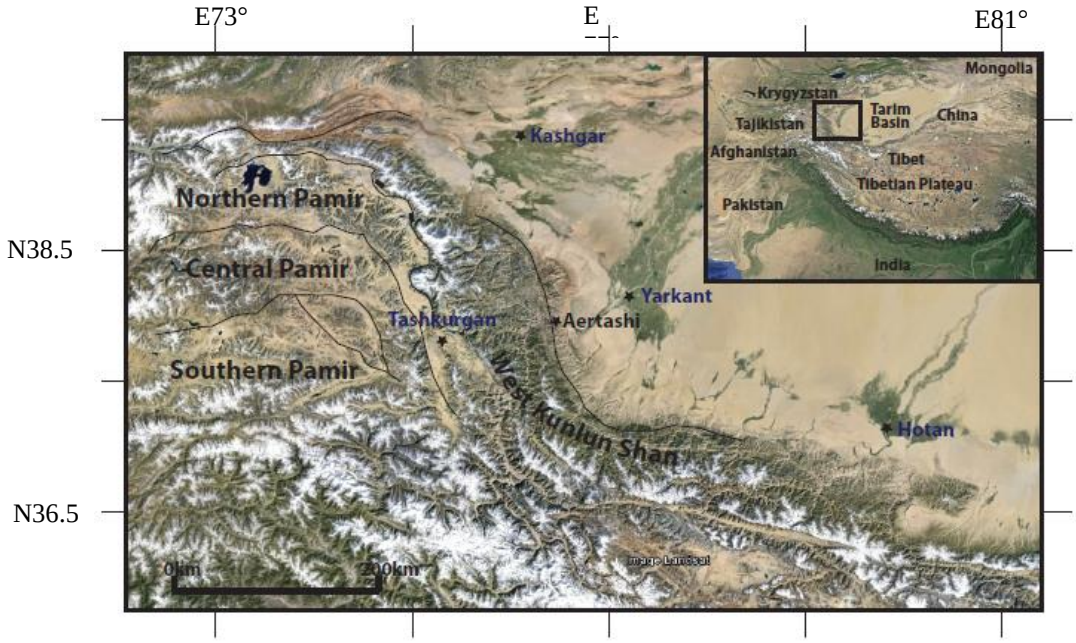

Figure 1. Location map for Aertashi, Western China.

The project has 3 key elements:

1. Characterisation of modern rivers draining the North, Central and South Pamirs and West Kunlun using U/Pb-fission track double dating on detrital zircons, Sr-Nd on muds, and petrography and heavy minerals on sands, in order to a) elucidate the regions' geological history and b) be able to identify detritus from these potential sources in the Aertashi section.
2. Use the same techniques as described above, to examine sediments throughout the Aertashi section, western Tarim basin, focussing on the Eocene – Pleistocene section in order to identify Pamir / Western Kunlun sources in the section .
3. Carry out a magnetostratigraphic study of the Aertashi section in order to a) place provenance changes identified in a temporal time frame and b) document the palaeo-rotations of the section and the subsidence history of the basin, to be interpreted in the context of adjacent hinterland tectonics. This work is a continuation of previous work conducted by Bosboom et al (2014).

Cite as: Blayney, T. et al, 2014, Tectonic Evolution of the North Tibetan margin and the Pamirs as determined from the sedimentary record of Aertashi, Western Tarim Basin, China, in Montomoli C., et al., eds., proceedings for the 29th Himalaya-Karakoram-Tibet Workshop, Lucca, Italy.

Preliminary results will be presented.

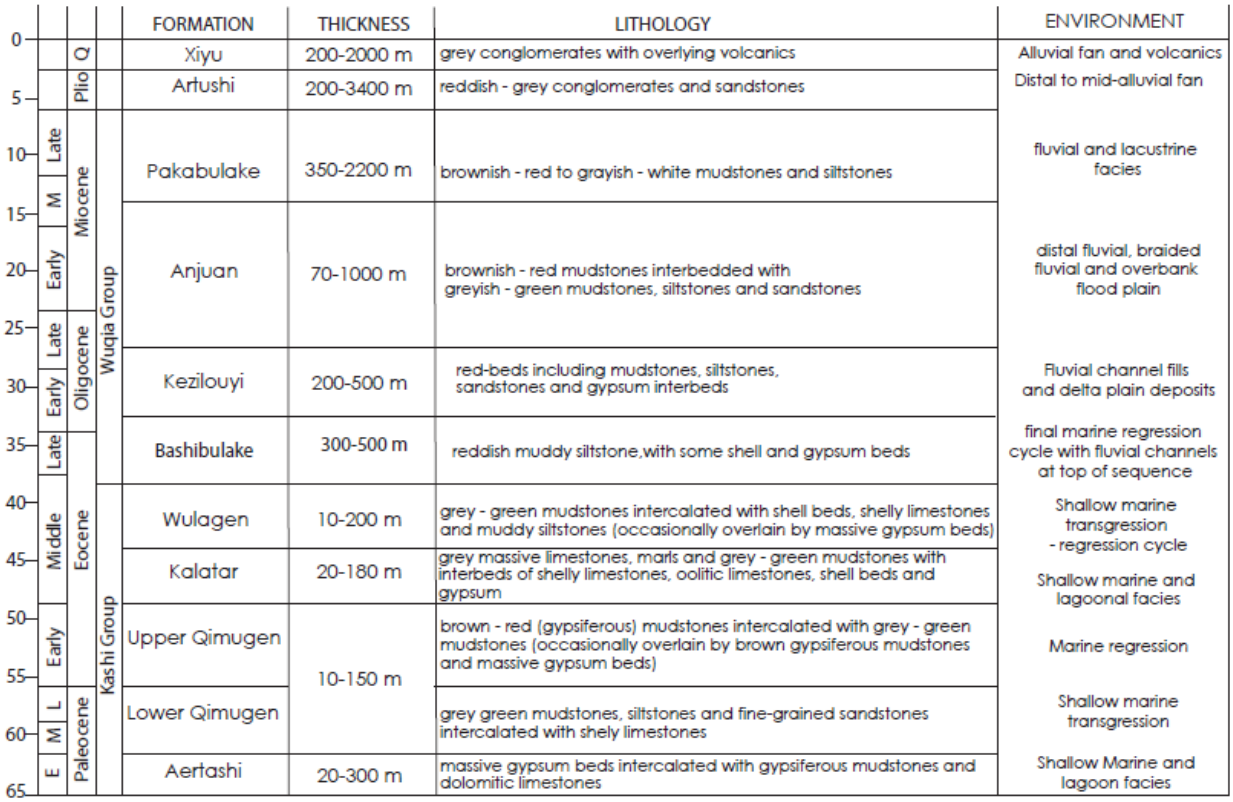

Figure 2. Lithostratigraphy of sediments in the Western Tarim Basin modified from Bosboom et al (2013), Wei et al (2013) and Zheng et al (2010)

References

Bosboom R., Dupont-Nivet, G., Grothe, A., Brinkhuis, H., Villa, G. et al., 2014, Linking Tarim Basin sea retreat west China and Asian aridification in the late Eocene, Accepted Article.

Wei, H.-H., Meng, Q.-R., Ding, L. and Li, Z.-Y., 2013, Tertiary evolution of the western Tarim basin, northwest China: a tectono-sedimentary response to northward indentation of the Pamir salient, Tectonics, 32, 3, 558–575.

Zheng, H., Tada, R., Jia, J., Lawrence, C., and Wang, K., 2010, Cenozoic sediments in the southern Tarim Basin: implications for the uplift of northern Tibet and evolution of the Taklimakan Desert, GSL Special Pub., 342, 67-78.

Controls on weathering kinetics and the δ7Li of Himalayan rivers

Madeleine Bohlin[1], Mike Bickle[1], Sambuddha Misra[1]

[1] Department of Earth Sciences, University of Cambridge, Downing Street, Cambridge, CB2 3EQ, United Kingdom, msb56@cam.ac.uk

Chemical weathering of the crust plays an important part in geochemical cycling by redistributing elements between Earth's surface reservoirs. On a geological time scale chemical weathering buffers Earth's climate as atmospheric CO_2 is consumed during the breakdown of silicate minerals and eventually stored as carbonates in the ocean. However there are many problems involved in quantifying the chemical fluxes associated with silicate weathering and their climatic impact. The key problems involve distinguishing between silicate and carbonate sources of riverine dissolved loads and understanding the nature of the cycling of solutes along groundwater and river flow paths.

An emerging field in studying chemical weathering is the use of light stable isotopes which readily fractionate during weathering reactions. They are probably the most sensitive proxies for continental weathering and have the potential of fingerprinting specific weathering processes. A recently constructed palaeo-record of the δ^7Li of seawater show a 9‰ net increase over the last 60 Ma coinciding with the uplift of the Himalayas (Misra and Froelich, 2012). As opposed to the traditionally used $^{87}Sr/^{86}Sr$ ratio which in addition to silicate weathering also reflects that of carbonates, lithium isotopes are almost exclusively associated with silicate weathering. Although records of ocean composition, where it is forced by riverine dissolved loads may reflect changes in the weathering regime on the continents it is important to understand the processes responsible for these changes. By studying the isotopic composition of dissolved and sediment loads of rivers and their tributaries it is possible to better constrain these controls. High erosion rates associated with high topographic relief give rise to incongruent weathering reactions. The rate of chemical weathering in these areas is limited by the kinetics of the chemical reactions, as opposed to areas with low erosion rates where weathering is transport-limited and congruent. The formation of secondary clays during incongruent weathering heavily fractionates Li isotopes, as the light isotope (^{6}Li) is partitioned into the forming clays. The heavy Li isotope (^{7}Li) is left in the dissolved phase which gets increasingly heavier as more clays form, i.e. the more incongruent the weathering is. This is the case for modern Himalayan rivers which have dissolved loads several per mille higher than drained source rocks. With increasing weathering intensity the difference in δ^7Li between source rocks and riverine dissolved loads decrease. Several studies have highlighted this link between δ^7Li and weathering intensity (e.g. Kisakurek et al., 2005).

In order to understand the relation between weathering intensity and stable isotopic fractionation it is important to constrain both the mineralogical reactions and the ground water flow paths. Weathering reactions likely take place continuously within catchments with water flowing through a range of shallow to deep paths as rock is progressively weathered during exhumation. To model this it is necessary to consider how kinetically-limited fluid-mineral reactions will evolve along individual water flow paths and to understand the range of inputs to river systems. We show how such modelling yields the minimum amount of controlling parameters and can offer insight to the isotopic evolution along the water flow path.

A new method of isotopic analysis is currently under development, allowing simultaneous separation of several stable isotopes in one column passing. Results from MC-ICP-MS analysis of Alaknanda river waters will be presented with the preliminary results from modelling of the isotopic evolution along the river flow path.

References

Kisakurek, B., James, R.H., and Harris, N.B.W., 2005, Li and δ7Li in Himalayan rivers: Proxies for silicate weathering? Earth and Planetary Science Letters, 237, 387-401.

Misra, S., and Froelich, P.N., 2012, Lithium isotope history of the Cenozoic seawater: changes in silicate weathering and reverse weathering, Science, 335 (6070), 818-23.

Cite as: Bohlin et al., 2014, Controls on weathering kinetics and the δ7Li of Himalayan rivers, in Montomoli C., et al., eds., proceedings for the 29th Himalaya-Karakoram-Tibet Workshop, Lucca, Italy.

Petrology and U-Pb SHRIMP zircon chronology of migmatite from Tangtse Shear Zone, eastern Ladakh Himalaya, India: Evidences of melting of granitoid protoliths and formation of leucogranite-granulite

Sita Bora[1], Santosh Kumar[1], Umesh K. Sharma[2], Keewook Yi[3], Namhoon Kim[3]

[1] Department of Geology, Centre of Advanced Study, Kumaun University, Nainital 263 002, India, skyadavan@yahoo.com
[2] Department of Science and Technology, Technology Bhavan, New Delhi 110016, India
[3] SHRIMP Centre, Korea Basic Science Institute, Ochang Campus, Korea, Chungbuk, 363-383, Korea

Tangtse Shear Zone (TSZ) separates the Pengong Metamorphic Complex (PMC) to the northeast from the Ladakh batholith to the southwest (Reichardt et al. 2010 and references therein). The TSZ is an integral part of Karakoram Shear Zone that lies in the central part of Karakoram fault of trans-tensional nature having dextral strike slip (N55°W). This is marked by the presence of slickenside showing dextral strike slip movement of mylonitized calc-alkaline granite gneiss ubiquitous near Tangtse village. Farther away from this, a mylonitic zone grades into intense network of leucogranite to pegmatitic granites hosting mesocratic to melanocratic amphibolite and granulite lithotypes together referred herewith as Tangtse Migmatite Complex (TMC).

Detailed field association, petrographic features and U-Pb SHRIMP zircon chronology of some representative lithounits constituting the TMC have been investigated in order to infer the nature of protolith, residue and timing of leucogranite melt generation. To achieve the objectives we have chosen carefully an outcrop for detailed investigation which has variegated colour indices representing almost all major components of migmatite complex. Leucogranite veins, sometimes becoming pegmatite in nature, provide concordant to discordant relationships with mesocratic to melanocratic, foliated to stromatic metamorphosed host rocks. Insitu syn-deformational melting signature producing melt stream parallel to the foliation plane are also preserved. We report herewith melanosome granulite from Tangtse region consisting of cpx-scapolite-pl±qtz±ep±ttn assemblage typically representing granulose texture. Anhedral plagioclase is included in clinopyroxene whereas quartz inclusion is found inside the epidote. Mesosome, corresponding to amphibolite facies, bears hbl (±cpx)-bt-pl-qtz assemblage with predominating hornblende. Hornblende is rimmed by chlorite and in the core of amphibole and biotite lie pyroxene, Leucosome, representing typical leucogranite melt, exhibits hypidiomorphic texture having bt-Kf-qtz assemblage and occasional plagioclase residue with inclusions of quartz blebs as partial melts. Close to the studied outcrop calc-alkaline porphyritic granodiorite of Ladakh range is exposed, which most likely served as fertile crust for partial melting at deeper and shallow levels for the TMC. Experimental studies have indicated that melting of metabasic and intermediate rocks will form 15 to 50 vol% melt at $T \leq$ 900°C, and production of such large quantity of melt will cause buffering of metamorphic temperature, which means metamorphic temperature will rarely exceed 850-900°C. Such a thermal event will generate S- and I-type granitoid liquids leaving behind granulitic residue composed of mineral assemblages depending on the composition of the involved protolith (Vielzeuf et al. 1990). Brown (2010) suggested that increase of melt volume increases the melt connectivity and generates dynamic rheological environment, and melt may escape from the source in batches during several melt-loss events. These mechanisms evidently support the occurrences of melt dykes forming cross-cutting network ubiquitous in Tangtse region overall forming the TMC.

Zircons were separated from discordant leucogranite vein, and were subjected to U-Pb SHRIMP analysis. Back Scattered Electron (BSE) and Cathodo-luminescence (CL) images suggest euhedral and zoned nature of zircons, which frequently have anhedral, rounded but zoned inherited cores derived from igneous source regions. Oscillatory zones can also be recognized, which are sometimes truncated by new growth zones. Such morphological features and observed Th/U ratios indicate magmatic origin of zircons. Most of the zircons have yielded concordant to nearly-concordant U-Pb isotopic ages. Out of twenty

Cite as: Bora, S., et al., 2014, Petrology and U-Pb SHRIMP zircon chronology of migmatite from Tangtse Shear Zone, eastern Ladakh Himalaya, India: Evidences of melting of granitoid protoliths and formation of leucogranite-granulite, in Montomoli C., et al., eds., proceedings for the 29th Himalaya-Karakoram-Tibet Workshop, Lucca, Italy.

seven analyzed spots of zircons, inherited cores (N=15) have yielded older weighted mean $^{206}Pb/^{238}U$ age of 72.1±1.9 Ma (MSWD=2.0) which corresponds to the age of granitoid protolith of Ladakh range. On the other hand, rims (N=06) of the zircons have provided younger weighted mean $^{206}Pb/^{238}U$ age of 18.24±0.29 Ma (MSWD=3.0), which suggest the primary crystallization age of zircons in leucogranite melt. Old zircons inherited from heterogeneous granodiorite-diorite protoliths, ranging in $^{206}Pb/^{238}U$ ages between 58.3 and 73.6 Ma, commonly have higher content of U (555-5076 ppm) and Th (269-3419 ppm) than the younger rims of zircons (U=592-2340 ppm, Th=79-574 ppm) crystallized in leucogranite magma. The obtained age of 18.24±0.29 Ma for leucogranite vein is consistent with the earlier suggested age of 18.0±0.4 Ma from leucogranite of Tangtse pluton (Reichardt et al. 2010). Based on available field, petrographic and chronological evidences it is suggested that Ladakh granitoid protoliths have undergone partial melting event at shallow to deeper levels during collisional events producing vast amount of leucogranite melt leaving behind granulite residue.

References

Brown, M., 2010, Melting of the continental crust during orogenesis: the thermal, rheological, and compositional consequences of melt transport from lower to upper continental crust, Canadian Journal of Earth Science, 47, 655-694.

Reichardt, H., Weinberg, R.F., Andersson, U.B. and Fanning, C.M., 2010, Hybridization of granitic magmas in the source: The origin of the Karakoram batholiths, Ladakh, NW India, Lithos, 116, 249-272.

Vielzeuf, D., Clemens, J.D., Pin, C. and Moinet, E., 1990, Granites, granulites and crustal differentiation, In: Vielzeuf, D. and Vidal, Ph. (eds.) Granulites and crustal evolution. NATO ASI Series, 311, 59-85.

Petrographic study of the andalusite-bearing graphitic schists from the Northern Karakoram (Sarpo Laggo, K2 and Gasherbrum Glaciers moreins, Xinjiang, China)

Alessia Borghini[1], Chiara Groppo[1], Franco Rolfo[1,2]

[1] Department of Earth Sciences, University of Torino, Torino, I-10125, Italy, chiara.groppo@unito.it
[2] IGG – CNR, Torino, I-10125, Italy

The Karakoram terrane comprises the southern part of the Asian side of the India-Asia collision zone and is the geological equivalent of the Central Tibet Qiangtang terrane. The geology of the Karakoram terrane can be divided into: (a) a northern dominantly sedimentary terrain intruded by diorite-granodiorite intrusions (e.g. Broad Peak diorites) with uplifted lower crustal metamorphic core complexes (e.g. K2 gneiss), (b) the Karakoram batholith, a ~700 km long granite batholith, and (c) the Southern Karakoram metamorphic complex composed of regional Barrovian facies kyanite- and sillimanite- grade gneisses. Opposite to the Southern Karakoram metamorphic complex, which has been widely studied (e.g. Desio and Zanettin, 1970; Searle et al., 1989; Searle and Tirrul, 1991; Allen and Chamberlain, 1991; Fraser et al., 2001; Rolland et al., 2001; Rolland and Pêcher, 2001; Gaetani et al., 1990b), the metamorphic terranes of the Northern Karakoram are still largely unknown and most of the geological maps of the area are highly incomplete (e.g. Searle, 2011). Most of the data actually available on the metamorphites of the Northern Karakorum terrane derive from two Italian expeditions (1988 and 2006; EV-K2-CNR) in the Shaksgam Valley, north of K2 and Gasherbrum (Desio et al., 1991; Gaetani et al., 1990a; Groppo and Rolfo, 2008). Due to the difficult accessibility of the area, most of the metamorphic rocks have been collected from the Sarpo Laggo, K2 and Gasherbrum Glaciers morains.

We present the results of a preliminary petrographic study on andalusite-bearing, two micas graphitic schists (± garnet, ± cordierite, ± staurolite): this study has allowed to define the main mineral assemblages and microstructures and to make some hypothesis on the nature of the protolith and on the P-T conditions experienced during metamorphism.

The locally well preserved clastic structure and the observed mineral assemblages suggest that the protolith of these phylladic micaschists was a sedimentary rock characterized by arenaceous levels alternating to pelitic levels. The former arenaceous levels are now dominated by quartz, with minor biotite and white mica, whereas the former pelitic levels mainly consist of fine-grained biotite and white mica, abundant graphite and Al-rich minerals (andalusite ± garnet ± staurolite).

All the studied samples show the evidence of two deformation events: the first event (D_1) was responsible for the development of a pervasive foliation (S_1), which is often crenulated by the following deformation event (D_2). The crenulation associated to the D_2 event is locally so pervasive that a new foliation S_2 develops. Both S_1 and S_2 are defined by the iso-orientation of white mica and biotite; chlorite is locally present in S_2.

The studied samples are characterized by abundant andalusite porphyroblasts that are mainly concentrated in the pelitic levels. Andalusite is generally well preserved and locally shows a chiastolitic structure; it is locally partially or completely replaced by a fine-grained aggregate of white mica ± chlorite. Andalusite growth is syn- to post-S_1. Garnet and staurolite are more rare and their growth is post-S_1.

The most complete mineral assemblage, useful to constrain peak metamorphic conditions, is syn- to post-D_1 and consists of biotite + white mica + andalusite + quartz ± garnet ± staurolite ± cordierite. This assemblage constrains peak metamorphic conditions of about 500-600°C, 1.5-2.5 kbar, i.e. low pressure amphibolite facies conditions. Late white mica and chlorite flakes statically overgrowing the S_2 suggest a retrograde evolution under greenschist facies conditions.

Cite as: Borghini, A., Groppo, C. and Rolfo, F., 2014, Petrographic study of the andalusite-bearing graphitic schists from the Northern Karakoram (Sarpo Laggo, K2 and Gasherbrum Glaciers moreins, Xinjiang, China), in Montomoli C., et al., eds., proceedings for the 29th Himalaya-Karakoram-Tibet Workshop, Lucca, Italy.

Although not collected in place, these samples thus provide important information on the nature of the metamorphic rocks outcropping at the head of Sarpo Laggo, K2 and Gasherbrum valleys.

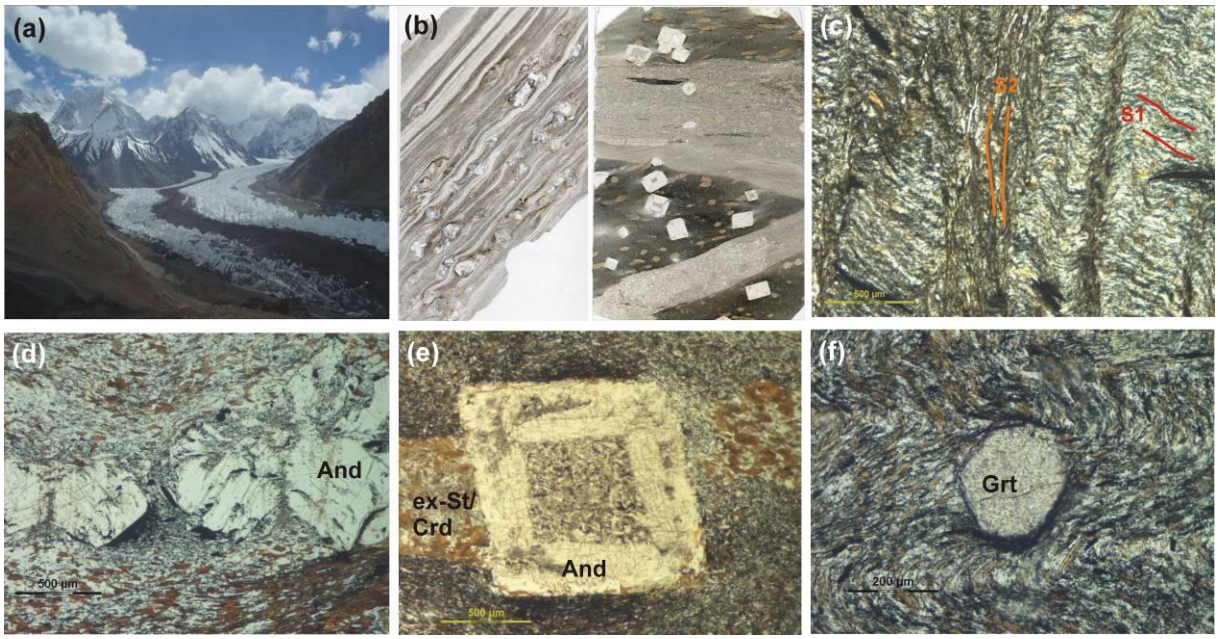

Figure 1. (a) Gasherbrum Glacier with its lateral and central morains. (b) The studied andalusite-bearing graphitic schists consists of former arenaceous levels (lighter in colour) alternating with former pelitic levels (darker). Andalusite porphyroblast mainly grew in the former pelitic layers. (c) Detail of the foliation S_1 crenulated by the deformative event D_2. A new foliation S_2 locally develops. (d,e) Details of andalusite porphyroblasts, locally with a chiastolite structure. (f) Garnet porphyroblast post-S_1.

References

Allen, T. and Chamberlain, C.P., 1991, Metamorphic evidence for an inverted crustal section with constraints on the Main Karakoram thrust, Baltistan, northern Pakistan. J. Metam. Geol., 9, 403-418.

Desio, A. and Zanettin, B., 1970, Geology of the Baltoro Basin. Scientific Report of the Italian Geological Expedition in Karakorum- Hindu Kush III/2. Brill, Leiden, 308 pp.

Desio, A., Caporali, A., Gosso, G., Pognante, U., Gaetani, M., Palmieri, F. and Rampini, L., 1991, Geodesy, geophysics and geology of the upper Shaksgam valley (Northen-east Karakorum) and south Sinkiang. Italian expedition to the Karakorum 1998. Scientific Reports, Ev-K2-CNR, Milano, 202 pp.

Fraser, J.E., Searle, M.P., Parrish, R.R. and Noble, S.R., 2001, Chronology of deformation, metamorphism, and magmatism in the southern Karakoram Mountains. Geol. Soc. Am. Bull., 113, 1443-1455.

Gaetani, M., Garzanti, E., Jadul, F., Nicora, A., Tintori, A., Pasini, M. and Kanwar, S.A.K., 1990b, The North Karakorum side of the Central Asia geopuzzle. Geol. Soc. Am. Bull., 102, 54-62.

Gaetani, M., Gosso, G. and Pognante, U., 1990a, A geological transect from Kun Lun to Karakorum (Sinkiang, China): the western termination of the Tibetan plateau. Preliminary note. Terra Nova, 2/1, 23-30.

Groppo, C. and Rolfo, F., 2008, Counterclockwise P–T evolution of the Aghil Range: Metamorphic record of an accretionary melange between Kunlun and Karakorum (SW Sinkiang, China). Lithos, 105, 365-378.

Rolland, Y. and Pêcher, A., 2001, The Pangong granulites of the Karakoram Fault (Western Tibet): vertical extrusion within a lithospheric scale fault? Compt. Rend. Acad. Sci., Paris, 332, 363-370

Rolland, Y., Maheo, G., Guillot, S. and Pêcher, A., 2001, Tectonometamorphic evolution of the Karakoram Metamorphic Complex (Dassu-Askole area, NE Pakistan): exhumation of mid-crustal HT-MP gneisses in a convergent context. J. Metam. Geol., 19, 717-737.

Searle, M.P., 2011, Geological evolution of the Karakoram Ranges. Boll. Soc. Geol. It., 130, 147-159.

Searle, M.P. and Tirrul, R., 1991, Structural and thermal evolution of the Karakoram crust. J. Geol. Soc. London, 148, 65-82.

Searle, M.P., Rex, A.J., Tirrul, R., Rex, D.C., Barnicoat, A. and Windley, B.F., 1989, Metamorphic, magmatic and tectonic evolution of the central Karakorum in the Biafo-Baltoro-Hushe regions of northern Pakistan. Geol. Soc. Am. Special Papers, 232, 47-73.

Petrographic study of the xenoliths hosted within lamprophyric dykes from the Shaksgam Valley (Xinjiang, China)

Serena Botta[1], Chiara Groppo[1], Franco Rolfo[1,2], Simona Ferrando[1]

[1] Department of Earth Sciences, University of Torino, Torino, I-10125, Italy, chiara.groppo@unito.it
[2] IGG – CNR, Torino, I-10125, Italy

The Tibetan Plateau, consisting of several terranes progressively accreted onto the stable North Asian Siberian–Mongolian craton since the Early Mesozoic, is the highest and largest topographic feature on Earth, and represents the archetypal product of continent-continent collision. Although many hypotheses have been advanced to explain the development of such high-elevation plateaus in collisional belts, the processes that formed the Tibetan Plateau remain almost unclear (e.g. Searle et al., 2011). The limited occurrence of exhumed deep crustal rocks in most of the Tibetan Plateau hampers the direct observation of the deeper crust and upper mantle beneath the orogen, whose structure is mainly interpreted basing on the results of deep crustal seismic experiments (e.g. Zhao et al. 1993; Nelson et al. 1996; Hetényi et al. 2007; Nábelek et al. 2009).

Direct information on the structure and composition of the lower crust and upper mantle can be inferred from xenoliths entrained in ultrapotassic volcanic rocks that have sampled the lower crust on their way up to the surface. Post-collisional volcanic rocks are widespread in the whole Tibetan Plateau (e.g. Chung et al., 1998, 2003, 2005; Miller, 1999; Wang et al., 2010); ultrapotassic dykes hosting lower crustal xenoliths have been reported from the Qiangtang terrane of central Tibet (Hacker et al. 2000, Jolivet et al., 2003; Ding et al., 2007), the Lhasa terrane of southern Tibet (Chan et al., 2009) and the Pamirs (Ducea et al. 2003; Hacker et al., 2005). Post-collisional potassic and ultrapotassic dykes have been also reported from the Karakoram terrane, which represents the western equivalent of the Qiangtang terrane (Pognante, 1990; Searle et al., 2010); however, so far, no crustal xenoliths have been reported from the northern Karakoram terrane.

The hereby presented preliminary petrographic data on crustal xenoliths hosted by lamprophyric dykes (Fig. 1a) from the Shaksgam valley, northern Karakoram terrane (Xinjiang, China), provide new important information on the composition of the deep, intermediate and upper crust beneath the western segment of the Himalayan-Tibetan collisional belt.

The lamprophyric dykes are mostly porphyritic minettes, consisting of abundant phlogopite fenocrysts set in a fine-grained groundmass consisting of K-feldspar ± phlogopite ± augitic clinopyroxene ± amphibole ± aegirinic clinopyroxene ± plagioclase (Fig. 1b,c). The lamprophyric dykes host various types of xenoliths sourced at different depths, from the deep to the intermediate and lower crustal levels, and variably affected by the thermo-metamorphic effects induced by the dyke intrusion.

Most of the analysed xenoliths are of deep crustal origin and include:

(i) apatite-bearing clinopyroxenite: this xenolith is mostly composed of clinopyroxene (> 90 vol%), apatite and minor phlogopite (Fig. 1d); its genesis remains uncertain, although the abundant occurrence of coarse-grained apatite suggests a deep crustal rather than a mantle source;
(ii) basic granulite: this xenoliths consists of clinopyroxene, garnet, plagioclase and magnetite (Fig. 1e) and reflects thermobaric conditions typical of the deep crust;
(iii) acid granulites (Qtz + Kfs + Grt + Pl): these xenoliths are characterized by the presence of abundant K-feldspar (up to 40 vol%) and garnet (up to 30 vol%) (Fig. 1f), the almost complete lack of hydrous minerals (biotite < 2 vol%) and by the local occurrence of relict kyanite. Rutile and graphite are common accessory minerals. Microstructures and mineral assemblages suggest that these acid granulites may represent the restitic product of a former pelitic protolith that experienced high pressure dehydration melting.

Cite as: Botta, S., Groppo, C., Rolfo, F. and Ferrando, S., 2014, Petrographic study of the xenoliths hosted within lamprophyric dykes from the Shaksgam Valley (Xinjiang, China), in Montomoli C., et al., eds., proceedings for the 29th Himalaya-Karakoram-Tibet Workshop, Lucca, Italy.

Xenoliths from intermediate to upper crustal levels include:

(i) biotite ± garnet gneiss: microstructures and mineral assemblages suggest that these xenoliths derive from a igneous protolith (e.g. granodiorite) re-equilibrated under high-temperature amphibolite-facies P-T conditions.

(ii) thermo-metamorphosed quartzitic-sandstone: this is a sedimentary rock with a well-preserved clastic structure, showing pervasive effects of the thermo-metamorphism induced by the dyke.

Overall, the analysed xenoliths allow to reconstruct a quite complete crustal section from the deeper to the upper structural levels; microstructures and mineral assemblages suggest derivation of the xenoliths from subducted ultrafemic, basic, granodioritic and pelitic crust that experienced variable degree of high pressure dehydration melting and metamorphic re-equilibration at different depths and at different P-T conditions.

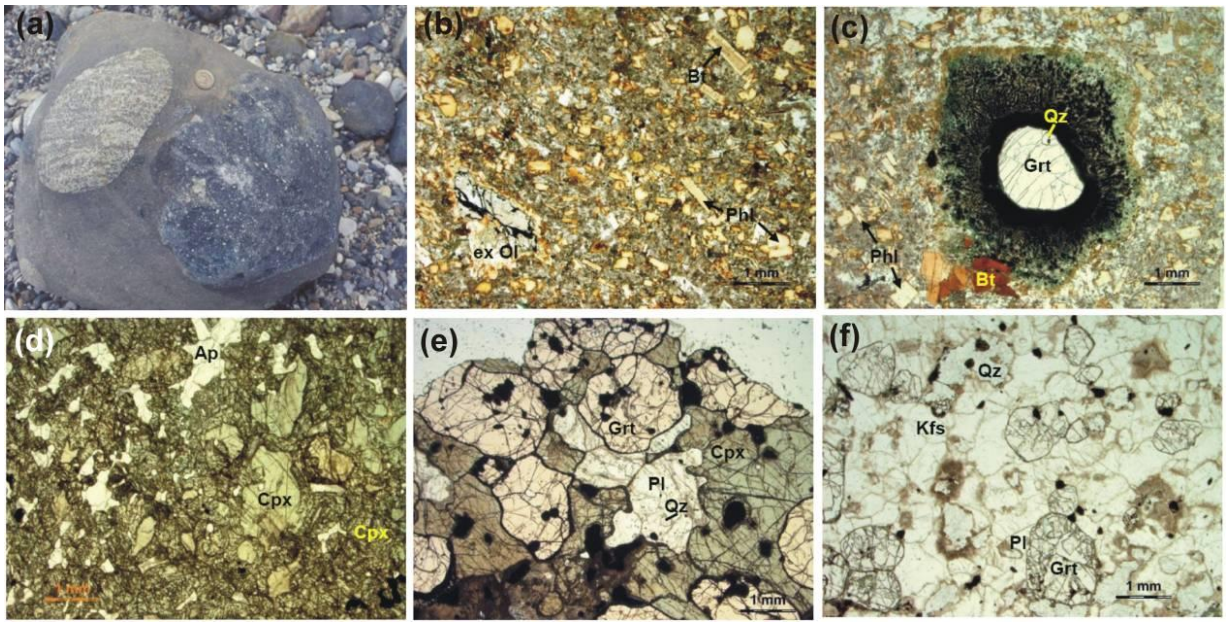

Figure 1. (a) Crustal xenoliths hosted by a lamprophyric dyke. (b-f) Representative microstructures (optical microscope, Plane Polarized Light) of the lamprophyric dykes (b,c) and of the xenoliths (d: Ap-clinopyroxenite; e: basic granulite; f: acid granulite).

References

Chan, G.H.-N., Waters, D.J. et al., 2009, Probing the basement of southern Tibet: evidence from crustal xenoliths entrained in a Miocene ultrapotassic dyke. J. Geol. Soc. London, 166, 45-52.

Chung, S.L., Chu, M.F. et al., 2009, The nature and timing of crustal thickening in Southern Tibet: Geochemical and zircon Hf isotopic constraints from postcollisional adakites, Tectonophysics, 477, 36-48.

Chung, S.-L., Liu, D.-Y., Ji, J.-Q., Chu, M.-F., Lee, H.-Y. et al., 2003, Adakites from continental collision zones: melting of thickened lower crust beneath southern Tibet, Geology, 31, 1021-1024.

Chung, S.-L., Lo, C.-H., Lee, T.-Y., Zhang, Y.-Q., Xie, Y.-W. et al., 1998, Diachronous uplift of the Tibetan plateau starting 40 Myr ago, Nature, 394, 769-773.

Ding, L., Kapp, P., Yue, Y. and Lai, Q., 2007, Postcollisional calc-alkaline lavas and xenoliths from the southern Qiangtang terrane, central Tibet. Earth Planet. Sci. Lett., 254, 28-38.

Ducea, M.N., Lutkov, V. et al., 2003, Building the Pamirs: the view from the underside, Geology, 31, 849-852.

Hacker, B., Gnos, E. et al., 2000, Hot and dry deep crustal xenoliths from Tibet, Science, 287, 2463-2466.

Hacker, B., Luffi, R., et al. 2005. Near ultrahigh pressure processing of continental crust: Miocene crustal xenoliths from the Pamir, J. Petrol., 46, 1661-1687.

Hetényi, G., Cattin, R., Brunet, F., Bollinger, L., Vergne, J. et al., 2007, Density distribution of the India plate beneath the Tibetan Plateau: Geophysical and petrological constraints on the kinetics of lower crustal eclogitization, Earth Planet. Sci. Lett., 264, 226-244.

Jolivet, M., Brunel, M. et al., 2003, Neogene extension and volcanism in the Kunlun Fault zone, northern Tibet: New constraints on the age of the Kunlun Fault, Tectonics, 22, TC1052.

Miller, C., Schuster, R., Klötzli, U., Mair, V. et al., 1999, Post-collisional potassic and ultrapotassic magmatism in SW Tibet: geochemical and Sr–Nd–Pb–O isotopic constraints for mantle source characteristics and petrogenesis. J. Petrol., 40, 1399-1424.

Nábelek, J., Hetényi, G. et al. 2009. Underplating in the Himalaya–Tibet collision zone revealed by the Hi-CLIMB experiment. Science, 325, 1371–1374.

Nelson, K.D., Zhao, W. et al. 1996, Partially molten middle crust beneath Southern Tibet: Synthesis of Project INDEPTH results, Sciences, 274, 1684-1688.

Pognante U., 1990, Shoshonitic and ultra-potassic post-collisional dykes from northern Karakoram (Sinkiang, China), Lithos, 26, 305-316.

Searle, M.P., Elliott, J.R., Phillips, R.J. and Chung, S.L., 2011, Crustal-lithospheric structure, geological evolution and continental extrusion of Tibet. J. Geol. Soc. London, 168, 633-672.

Searle, M.P., Parrish, R.R., Thow, A.V., Noble, S.R. et al., 2010, Anatomy, age and evolution of a collisional mountain belt: the Baltoro granite batholith and Karakoram Metamorphic complex, Pakistani Karakoram. J. Geol. Soc. London, 167, 183-202.

Wang, Q., Wyman, D.A. et al., 2010, Eocene north–south trending dikes in central Tibet: New constraints on the timing of east–west extension with implication for early plateau uplift. Earth Planet. Sci. Lett., 298, 205-216.

Zhao, W., Nelson, W.D. et al., 1993, Deep seismic reflection evidence for continental underthrusting beneath Tibet, Nature, 366, 557-559.

Dynamic implications of temporal gravity changes over Himalaya-Tibet

Carla Braitenberg[1]

[1] Department of Mathematics and Geosciences, University of Trieste, berg@units.it

The time variations of gravity observed with satellite GRACE or with terrestrial measurements are due to the combination of ice-volume changes and hydrologic mass changes, that add to the effects of vertical crustal movements and tectonic mass changes. The vertical crustal movement is expected to generate a long-term effect, the hydrologic and ice-mass changes being both seasonal and long-term. The superficial mass variations generate a load variation which induces vertical isostatic crustal accommodation. Apart from the glacial isostatic response, vertical movements can be generated also by tectonic effects: exhumation typically in areas of plate convergence, and subsidence due to sediment compaction, post-seismic movements or subduction. At the Himalayan orogen the ongoing uplift has been measured by GPS, and rates of a few mm/yr are typical. The horizontal convergence rates are much greater, in the order of several cm/yr. As crustal material is not destroyed, it implies that the crustal material contributes to crustal thickening, which according to the isostatic degree of compensation is divided into topographic uplift and crustal root thickening.

These different mechanisms of mass transfer generate a change in the gravity field combined to different extents of changes in the topography. The observation of this mass transfer would give a useful constraint on understanding the mountain building process. In this study first a review of the observed gravity variations and geometry variations is given, based on published results. It is found that depending on the authors, contrasting conclusions are found regarding the interpretation. The gravity changes have been determined using satellite GRACE as well as through absolute gravity observations. These two data sets differ substantially, as the first gives a spatially averaged result with wavelengths typical of the spatial resolution of the GRACE satellite, whereas the repeated absolute measurements are point-like observations.

For the Tibetan plateau GPS observations give evidence that horizontal convergence is 3-4 times the uplift rate. The absolute gravity rate at Lhasa set at the South-Eastern border of the plateau is -1.97 ± 0.66 microGal/yr, and when corrected for the observed uplift and assumed erosional denudation remains negative at a rate of -1.56 ± 0.67 microGal/yr (Sun et al., 2011). The residual negative gravity rate has been interpreted as the observation of crustal thickening, in terms of Moho deepening, at a rate of 2.3 ± 1.33 cm/yr (Sun et al., 2009). Alternatively, Matsuo and Heki (2010), determine the gravity change from GRACE observations for 2003-2009 and attribute the yearly and long term gravity change to hydrologic effects which are concentrated at the outer border of the Tibet plateau, estimated to 47 ± 12 Gigaton/yr ice-loss. These authors mention the uncertainty in the contribution of isostatic or tectonic uplift, but think the hydrologic effect to be preponderant in their observations. The GRACE observations were filtered with a Gaussian filter of radius 400km to reduce short wavelength noise. Yi and Sun (2014) extend the analysis of the GRACE satellite observations to 10 years.

Uplift may have the cause of a glacial isostatic movement, of crustal thickening, or a combination of both effects. The difference resides in the mass variations at Moho level: for crustal thickening the Moho is deepened, producing a negative gravity effect; in case of glacial isostatic accommodation the Moho is uplifting, and it produces a positive gravity effect. This signal adds to the positive gravity effect of the uplift, which increases the superficial mass. We here calculate simulations for the Tibet plateau, assuming different geometries and rates for crustal thickening and uplift rates and compare them with the published gravity changes. The simulations quantify the wavelengths and change rates of the expected gravity signal. Another product of the simulations is the so called "viscous ratio", which is defined as the ratio between terrestrial gravity change rate from absolute gravity observations and the observed uplift, which

Cite as: Braitenberg, C., 2014, Dynamic implications of temporal gravity changes over Himalaya-Tibet, in Montomoli C., et al., eds., proceedings for the 29th Himalaya-Karakoram-Tibet Workshop, Lucca, Italy.

in southern Alaska is between -0.1 to -0.2 microGal/mm (Sato et al., 2012), whereas in Tibet at the Lhasa station is much lower, -2.5 microGal/mm (Sun et al., 2009; 2011). This difference could be an indicator of the different mechanisms which are affecting the crust-mantle contact. The simulations contribute to define the requirements to future gravity missions apt to contribute to a better understanding of the genesis of the Tibet plateau.

References

Matsuo, K. and Heki, K., 2010, Time-variable ice loss in Asian high mountains from satellite gravimetry, Earth and Planetary Science Letters, 290, 30-36, doi:10.1016/j.epsl.2009.11.053.

Sato, T., Miura, S., Sun, W., Sugano, T, Freymueller, J. T., Larsen, C. F., Ohta, Y., Fujimoto, H., Inazu, D. and Motyka, R. J., 2012, Gravity and uplift rates observed in southeast Alaska and their comparison with GIA model predictions, Journal of Geophysical Research, 117, B01401, doi:10.1029/2011JB008485.

Sun, W., Wang, Q., Li, H., Wang, Y., Okubo, S., Shao, D., Liu, D. and Fu, G., 2009, Gravity and GPS measurements reveal mass loss beneath the Tibetan Plateau: Geodetic evidence of increasing crustal thickness, Geophysical Research Letters, 36, L02303, doi:10.1029/2008GL036512

Sun, W., Wang, Q., Li, H., Wang, Y. and Okubo, S., 2011, A Reinvestigation of Crustal Thickness in the Tibetan Plateau Using Absolute Gravity, GPS and GRACE Data, Terrestrial, Atmospheric and Oceanic Sciences, 22, 109-119, doi: 10.3319/TAO.2010.06.07.01(TibXS).

Yi, S., and Sun, W., 2014, Evaluation of glacier changes in high-mountain Asia based on 10 year GRACE RL05 models, Journal of Geophysical Research: Solid Earth, 119, 2504-2517, doi:10.1002/2013JB010860.

The subduction of continental lithosphere: insights from multiscale geophysical modelling of the Periadriatic region

Enrico Brandmayr[1], Fabio Romanelli[1,2], Giuliano F. Panza[1,2,3,4]

[1] Department of Mathematics and Geosciences, University of Trieste, Via Weiss 4, 34127, Trieste, Italy, enrico.brandmayr@gmail.com
[2] The Abdus Salam International Centre for Theoretical Physics, Strada Costiera 11, 34014 Trieste, Italy
[3] Institute of Geophysics, China Earthquake Administration, Minzudaxuenanlu 5, Haidian District, 100081 Beijing, China
[4] International Seismic Safety Organization (ISSO) - www.issoquake.org

The subduction of continental lithosphere has been demonstrated in the Alps (Panza and Müller, 1979) and since this pioneering paper it has been recognized in several other collisional belts such as the Apennines (Panza et al., 2007), the Himalaya (Zhang et al., 2014) and Zagros chain (Motaghi et al., 2014) by means of seismological and geophysical investigations. We present a multiscale 3D model of the crust and upper mantle of the Periadriatic region showing that the Adriatic plate, the Northern indent of the African promontory, is involved in the Apennines, Alpine, and Dinarides subduction, respectively surrounding its western, northern, and eastern margins.

The superposition of different geodynamic mechanisms in the same area is coherent with the global asymmetry of plate tectonics (Doglioni et al., 2007; Panza et al., 2010) and supports a passive origin of plate boundaries, contrary to what is usually assumed.

Data and method

The 3D model is obtained through the ensemble of cellular models expressed in terms of shear waves velocity (V_S), thickness and density of the layers, to a depth of 350 km. These physical properties are obtained by means of advanced non-linear inversion techniques, such as the "hedgehog" inversion of group and phase velocity dispersion curves for the determination of V_S (Panza et al., 2007 and references therein) and the non-linear inversion of gravity data by means of the method GRAV3D (Li and Oldenburg, 1998).

The "hedgehog" method allows for the definition of a set of structural models without resorting to any a priori model, considering the V_S and the thickness of the layers as independent variables. Given the well-known non-uniqueness of the inverse problem, the representative solution of each cell is determined through the application of optimization algorithms (Boyadzhiev et al., 2008) and is also validated with the use of independent geological, geophysical and petrological data, e.g. the distribution of seismicity with depth.

The gravimetric inversion has been constrained to the geometry of the layers defined by the V_S absolute tomography model (Foulger et al., 2013) obtained from the inversion of surface wave dispersion data. To the gravimetric data input a Gaussian noise with an amplitude of 1.5 mGal has been applied and the density anomalies obtained by the inversion process are transformed into absolute values relative to a reference model consistent with the Nafe-Drake relation.

A temperature model of the mantle is finally obtained by means of an advanced conversion technique of V_S to temperature that takes in account variable chemical composition and bulk water content (Tumanian et al., 2012 and references therein).

Results

The 3D model thus obtained at the scale of 1°x1°, analysed along selected sections perpendicular to the orogenic complexes of the study area (Apennines, Alps, Dinarides) confirms the existence of deep structural asymmetries between E- and W-directed subduction zones. The asymmetry found between the almost vertical Apenninic subduction and the Alpine-Dinaric subduction, which is characterized by a low

Cite as: Brandmayr, E. et al., 2014, The subduction of continental lithosphere: insights from multiscale geophysical modelling of the Periadriatic region, in Montomoli C., et al., eds., proceedings for the 29th Himalaya-Karakoram-Tibet Workshop, Lucca, Italy.

dip angle, can be ascribed to an eastward mantle flow taking place in the low velocity zone (LVZ) that characterizes the top of the very shallow asthenosphere beneath the Tyrrhenian basin.

The refined model obtained for the Alpine region at a scale of 0.5°x0.5°, enlightening the extreme variability of the crustal thickness as well the small scale heterogeneities in the upper mantle beneath the study area (fig. 1), shows the extreme importance of the best possible definition of the most superficial layers, which are fixed in the inversion, by means of reliable independent information.

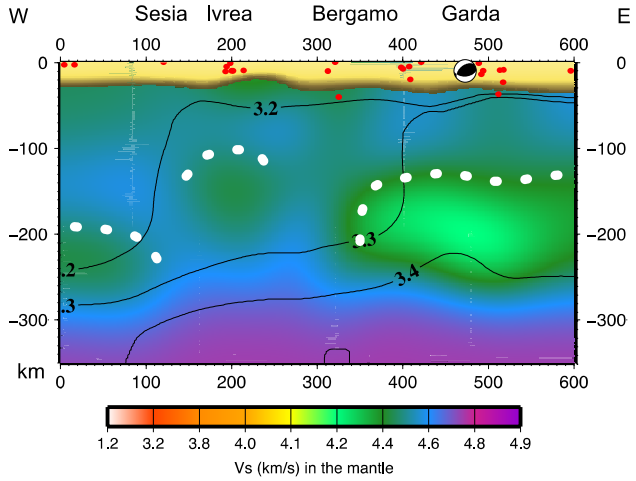

Figure 1. V_S and density (contour lines, g/cm^3) model along a W-E profile along latitude 45.75°N. Seismicity (red dots) and focal mechanisms of major events are shown as well. Dotted white lines delineate the lid-LVZ margin.

The density model clearly shows that the subducting lithosphere is less dense than the surrounding mantle (Brandmayr et al., 2011). This result opens the way to new interpretations in subduction dynamics, which in its common description relies on the "slab pull" phenomenon as a first order acting force. In the upper mantle of the whole study area temperatures are strongly variable and can reach 1500-1600°C at the top of the asthenosphere. This finding corroborates the condition of non adiabaticity of the mantle, i.e. a super adiabatic regime in the upper 200 km which would inhibit large scale upper mantle convention.

Acknowledgments

We thanks all co-authors (see references) for their contribution and we acknowledge partial financial support from PRIN 2011- 2010PMKZX7 (MIUR) and from SHARM project (FSE - Regione FVG).

References

Boyadzhiev, G., Brandmayr, E., Pinat, T. and Panza, G.F., 2008, Optimization for non linear inverse problem, Rendiconti Lincei: Sci. Fis. e Nat., 19, 17-43.

Brandmayr, E., Marson, I., Romanelli, F. and Panza, G.F., 2011, Lithosphere density model in Italy: no hint for slab pull, Terra Nova, 23, 292-299.

Doglioni, C., Carminati, E., Cuffaro, M. and Scrocca, D., 2007, Subduction kinematics and dynamic constraints, Earth Science Reviews, 83, 125-175.

Foulger, G.R., Panza, G.F., Artemieva, I.M., Bastow, I.D., Cammarano, F. et al., 2013, Caveats on tomographic images, Terra Nova, 25, 259-281.

Li, Y. and Oldenburg, D.W., 1998, 3D inversion of gravity data, Geophysics, 63/1, 109-119.

Motaghi, K., Tatar, M., Priestley, K., Romanelli, F., Doglioni, C. et al., 2014, The deep structure of the Iranian Plateau, Gondwana Research, http://dx.doi.org/10.1016/j.gr.2014.04.009.

Panza, G.F. and Mueller, S., 1979, The plate boundary between Eurasia and Africa in the Alpine area, Memorie di Scienze Geologiche, Università di Padova, 33, 43-50.

Panza, G.F., Doglioni, C. and Levshin, A., 2010, Asymmetric ocean basins, Geology, 38, 59-62.

Panza, G.F., Peccerillo, A., Aoudia, A. and Farina, B.M, 2007, Geophysical and petrological modelling of the structure and composition of the crust and upper mantle in complex geodynamic settings: The Tyrrhenian Sea and surroundings, Earth-Science Reviews, 80, 1–46.

Tumanian, M., Frezzotti, M.L., Peccerillo, A., Brandmayr, E. and Panza, G.F., 2012, Thermal structure of the shallow upper mantle beneath Italy and neighbouring areas: correlation with magmatic activity and geodynamic significance, Earth-Science Reviews, 114 , 369-385.

Zhang, Z., Teng, J., Romanelli, F., Braitenberg, C., Ding, Z. et al., 2014, Geophysical constraints on the link between cratonization and orogeny: Evidence from the Tibetan Plateau and the North China Craton, Earth-Science Reviews, 130, 1-48.

The Geodynamics of Asian continental tectonics: insights from numerical modeling

Fabio A. Capitanio[1], Anne Replumaz[2], Nicolas Riel[1]

[1] School of Geosciences, Monash University, Clayton, VIC 3800, Australia, fabio.capitanio@monash.edu
[2] Institute des Sciences de la Terre, Université de Grenoble 1, CNRS, Grenoble, France

The evolution of continental tectonics must ultimately relate to the fundamental processes of the dynamic Earth. Here, we propose that the enigmatic Asian tectonics is best seen in the broad context of the continent interactions with the Tethys plate subduction. Using three-dimensional numerical models, we show how continent entrainment, slab breakoff and forced convergence during oceanic subduction result in coupled convergent margin-upper plate interiors deformations. Continent subduction destabilizes the convergent margin, forcing neighboring oceanic trench migrations and extension in the upper plate. As slab breakoff ceases subduction along the continental margin, convergence is here accommodated by indentation and extrusion, and faulting and large-scale rotations towards the retreating trench ensue. When modeled far-field force raises above the margin's subduction forces, the whole subduction zone advances, driving indenter migrations and resisting oceanic trench retreat. The varying balance between margin and far-field forces causes upper plate-scale rotations, while thickening and compression migrate within the plate interiors. The models yield large-scale deformation and motion patterns remarkably similar to the Cenozoic Asian tectonics phases. The comparisons with observables allow inferences on the driving mechanisms of Southeast Asian margin migration and Sundaland extension, extrusion tectonics and Tibet thickening, and widespread tectonics migrations far in Asian plate, providing relevant insights in the dynamics of continent interiors.

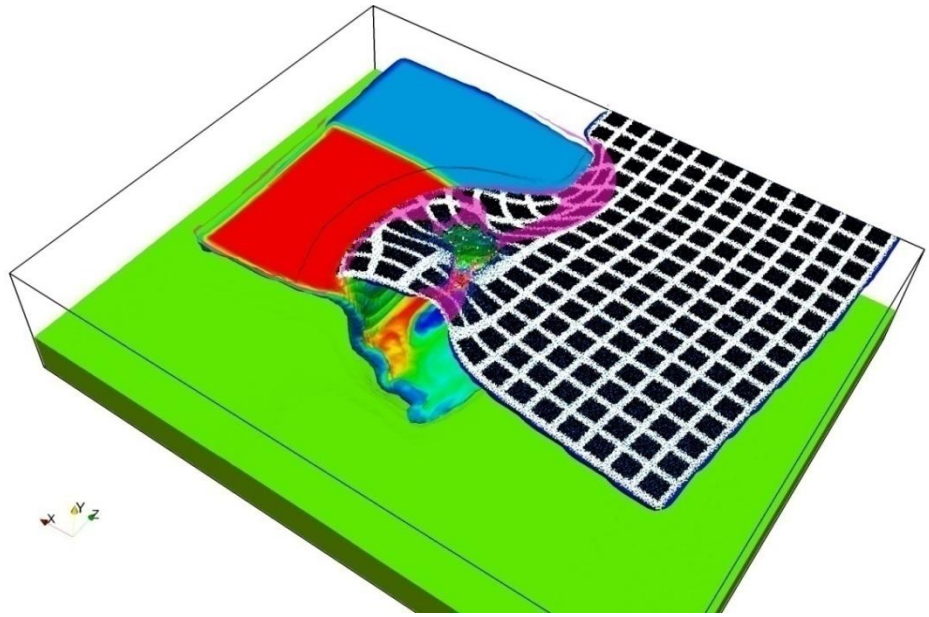

Figure 1. Top view of the numerical model of subduction of heterogeneous lithosphere and forced convergence, and coupled upper plate deformation. In this model the subducting plate hosts oceanic and continental lithospheres (red and blue, respectively, colorscale for density contrast with the mantle). Black and white dots are the Lagrangian particles in the upper plate model, gridded for reference. In purple shading the areas of largest strain rate on the upper plate. Extreme thinning is indicated by sparse particle distribution, and indicates oceanisation. In green the surface of the lower mantle. Upon continent subduction the oceanic trench has migrated driving back-arc stretching, eventually leading to spreading. Breakoff along the subducting continent margin and far-field forces drive large migration of the plate and indentation of the upper plate. The margin motions result in upper plate thickening and thinning along the advancing and retreating margin, respectively. Because margin migrations are combined, upper plate deformation is partially accommodated by large-scale extrusion and faulting.

Cite as: Capitanio, F.A. et al., 2014, The Geodynamics of Asian continental tectonics: insights from numerical modeling, in Montomoli C., et al., eds., proceedings for the 29th Himalaya-Karakoram-Tibet Workshop, Lucca, Italy.

In-sequence shearing within the Greater Himalayan Sequence in Central Himalaya: deformation and metamorphism by crustal accretion from the Indian plate

Rodolfo Carosi[1] Chiara Montomoli[2], Salvatore Iaccarino[2], Dario Visonà[3]

[1] Dipartimento di Scienze della Terra, v. Valperga Caluso, 35 10125 Torino, Italy, rodolfo.carosi@unito.it
[2] Dipartimento di Scienze della Terra, v. S. Maria, 53 56126 Pisa, Italy
[3] Dipartimento di Geoscienze, Via Gradenigo, 6 35131, Padova, Italy

The Greater Himalayan Sequence (GHS) is the main metamorphic unit of the Himalayas, running for over 2400 km, bounded to the South by the Main Central Thrust (MCT) and to the North by the South Tibetan Detachment (STD) whose contemporanous activity is considered to have guided the exhumation of the GHS between 23 and 17 Ma (Godin et al., 2006).

Several shear zones and/or faults have been recognized within the GHS, usually regarded as out of sequence thrusts (Mukherjee et al., 2012). Recent investigations in the GHS in Central Himalaya allowed the Authors to identify a tectonic and metamorphic discontinuity, localized in the middle-lower part of the GHS well-above the MCT, with a top-to-the SW contractional sense of shear (Higher Himalayan Discontinuity: HHD: Montomoli et al., 2013; in press).

U-(Th)-Pb *in situ* monazite ages provide temporal constraint of initiation of the HHD at 28-26 Ma (Carosi et al., 2010; Larson et al., 2013; Montomoli et al., 2013), older than the Main Central Thrust, and continuing up to 17 Ma. Data on the P and T evolution testify that these shear zones affected the tectono-metamorphic evolution of the belt and different P and T conditions have been often recorded in the hanging-wall and footwall of the HHD. Moreover the activity of the HHD resulted in different timing of the peak metamorphic conditions in its hanging wall and footwall rocks (Montomoli et al., in press). The correlation of the HHD with several other discontinuities recognized in the GHS led to propose that it is a regional-scale tectonic feature running for several hundreds kilometers dividing the GHS in two different portions and affecting its metamoprhic evolution and exhumation.

In Western and Central Nepal the occurrence of even more structurally higher contractional shear zone, with a top-to-the SW sense of shear, in the GHS (above the HHD): the Tyar shear zone in the Mugu – Karnali valley and the Kalopani shear zone in the Kali Gandaki valley, points out to an even more complex deformation pattern within the metamorphic core.

These recent findings suggest that GHS is build up by the progressive accretion of Indian crustal slices since the Eocene-Oligocene. The GHS is made up by several crustal slices showing younging deformation and metamorphism from the upper one to the lower one (Fig. 1). The youngest activity of the STDS in Western Nepal is constrained by the timing of intrusion of a large undeformed and cross-cutting leucogranite body at 23-24 Ma (Carosi et al., 2013). Considering that in the same area the MCT was active after ~ 18 Ma (Montomoli et al., 2013) there is no evidence of contemporaneous activity of the STD and MCT

The actual proposed models of exhumation of the GHS, based mainly on the MCT and STD simultaneous activities, are not able to explain the occurrence of the HHD and other in-sequence shear zones. Every model of the tectonic and metamorphic evolution of the Himalaya should account for the occurrence of the regional tectonic and metamorphic discontinuities within the GHS (HHD) and its consequences on the metamorphic paths and on the assembly of Himalayan belt.

Cite as: Carosi et al., 2014, In-sequence shearing within the Greater Himalayan Sequence in Central Himalaya: deformation and metamorphism by crustal accretion from the Indian plate., in Montomoli C., et al., eds., proceedings for the 29th Himalaya-Karakoram-Tibet Workshop, Lucca, Italy.

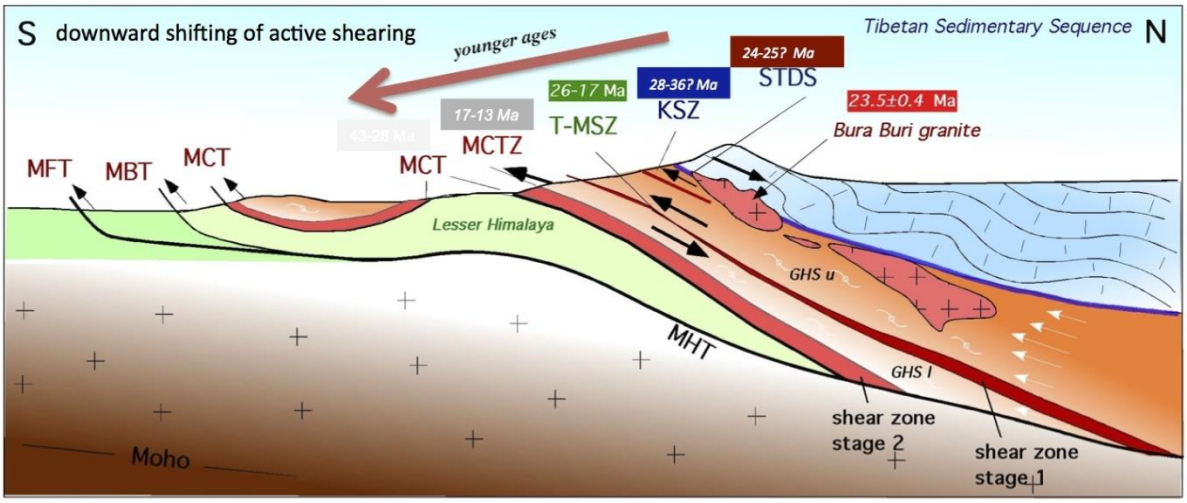

Figure 1. Schematic cross section through the Himalayas showing the localization of shear zones in the GHS (GHS u = upper, GHS l = lower) and their ages (modified after Carosi et al., 2010; 2013; in press and Montomoli et al., 2013). Ages of ductile shear zones such as Kalopani shear zone: KSZ, Tojem-Mangri Shear Zone (= Higher Himalayan Discontinuity): T-MSZ and MCT Zone and subsequent brittle faults in western Nepal indicate a deformation propagating to the foreland. Ages of STDS and MCT in central-western Nepal were taken from Godin et al. (2006) and Montomoli et al. (2013). Crosses with red background indicate Higher Himalayan granites emplaced in the hanging-wall of the HHD and cross-cutting the STDS (ages from Carosi et al., 2013).

References

Godin, L., Grujic, D., Law, R.D. and Searle, M.P., 2006, Channel flow, ductile extrusion and exhumation in continental collision zones: an introduction, Geological Society of London Special Publication, 268, 1-23.

Carosi, R., Montomoli, C., Rubatto, D. and Visonà, D., 2010, Late Oligocene high-temperature shear zones in the core of the Higher Himalayan Crystallines (Lower Dolpo,Western Nepal), Tectonics, 29, TC4029, http://dx.doi.org/10.1029/2008TC002400.

Carosi, R., Montomoli, C., Langone, A., Turina, A., Cesare, B., Iaccarino, S., Fascioli, L., Visonà, D., Ronchi, A. and Rai, S.M., Eocene partial melting recorded in peritectic garnets from kyanite-gneiss, Greater Himalayan Sequence, central Nepal. In: "Tectonics of Himalayas" (Editors: S. Mukherjie, R. Carosi, B. Mukherjie, D. Robinson, van Der Beck), Geol. Soc. London Special Publication, in press.

Carosi, R., Montomoli, C., Rubatto, D. and Visonà, D., 2013, Leucogranite intruding the South Tibetan Detachment in western Nepal: implications for exhumation models in the Himalayas, Terra Nova, 25 (6), 478–489, doi: 10.1111/ter.12062.

Larson, K.P., Gervais, F. and Kellett, D.A., 2013, A P–T–t–D discontinuity in east-central Nepal: Implications for the evolution of the Himalayan mid-crust, Lithos, 179, 275-292.

Montomoli, C., Iaccarino, S., Carosi, R., Langone, A. and Visonà, D., 2013, Tectonometamorphic discontinuities within the Greater Himalayan Sequence in Western Nepal (Central Himalaya): Insights on the exhumation of crystalline rocks, Tectonophysics, 608, 1349-1370, doi:10.1016/j.tecto.2013.06.006.

Montomoli, C., Carosi, R., and Iaccarino, S., 2013, Tectono-metamorphic discontinuities in the Greater Himalayan Sequence and their role in the exhumation of crystalline units. In: "Tectonics of Himalayas" (Editors: S. Mukherjie, R. Carosi, B. Mukherjie, D. Robinson, P. van Der Beck), Geol. Soc. London Special Publication, in press.

Mukherjee, S., Koyi, H.A. and Talbot, C., 2012, Implications of channel flow analogue models for extrusion of the Higher Himalayan Shea Zone with special reference to the out-of-sequence thrusting, International Journal of Earth Sciences (Geol. Rundsch.), 101, 253-272.

Eocene partial melting recorded in peritectic garnets from kyanite-gneiss, Greater Himalayan Sequence, central Nepal

Rodolfo Carosi[1], Chiara Montomoli[2, 7], Antonio Langone[3], Alice Turina[4], Cesare Bernardo[4], Salvatore Iaccarino[2], Luca Fascioli[4], Dario Visonà[5], Ausonio Ronchi [4], Santa Man Rai[6]

[1] Dipartimento di Scienze della Terra, v. Valperga Caluso, 35 10125 Torino, Italy, rodolfo.carosi@unito.it
[2] Dipartimento di Scienze della Terra, v. S. Maria, 53 56126 Pisa, Italy
[3] C.N.R.-Istituto di Geoscienze e Georisorse, UOS Pavia, via Ferrata 1 27100 Pavia, Italy
[4] Dipartimento di Scienze della Terra, Via Ferrata, 1 27100, Pavia, Italy
[5] Dipartimento di Geoscienze, Via Gradenigo, 6 35131, Padova, Italy
[6] Department of Geology, Tribuhuvan University, Ghantaghar, Kathmandu, Nepal
[7] C.N.R.-Dipartimento di Geoscienze e Georisorse, v. Moruzzi, 1 56124 Pisa, 56100 Pisa, Italy

The Himalayan mountain belt is characterized by the impressive continuity over 2500 km of tectonic units, thrusts and normal faults, as well as large volumes of high-grade - metamorphic rocks and granite exposed at the surface (Visonà et al., 2012).

Although there are many studies on metamorphism, melt generation and deformation concentrated in the same time span as activity on the MCT and STD (~ 23 - 17 Ma; Godin et al. 2006), much fewer data on deformation, metamorphism, melt generation and geochronology in the Greater Himalayan Sequence (GHS) is available for the large time span (~ 30 M.y.) between collision at ~ 55 Ma and MCT-STD activities (Carosi et al., 2010; 2013; Montomoli et al., 2013).

Melt generation and granite emplacement have been mainly related to the exhumation stage of the GHS during Early Miocene (Harris and Massey, 1994). Very few evidences of partial melting during prograde metamorphism have been reported until now in the southern part of the belt (Godin et al. 2001; Imayama et al. 2012). The GHS of eastern Nepal and Sikkim (India) shows the occurrence of melting at the bottom of the GHS (Barun gneiss) at nearly 33-27 Ma (Imayama et al., 2012; Ferrero et al., 2012; Rubatto et al., 2012).

Anatectic melt inclusions (nanogranites and nanotonalites) have been found in garnet of kyanite-gneiss at the bottom of the Greater Himalayan Sequence (Fig. 1) along Kali Gandaki valley, Central Nepal, nearly ~ 1 km structurally above the Main Central Thrust. In situ U-Th-Pb dating of monazite included in garnets, in the same structural positions as melt inclusions, allowed to constrain partial melting starting at ~36-41 Ma (Carosi et al., in press).

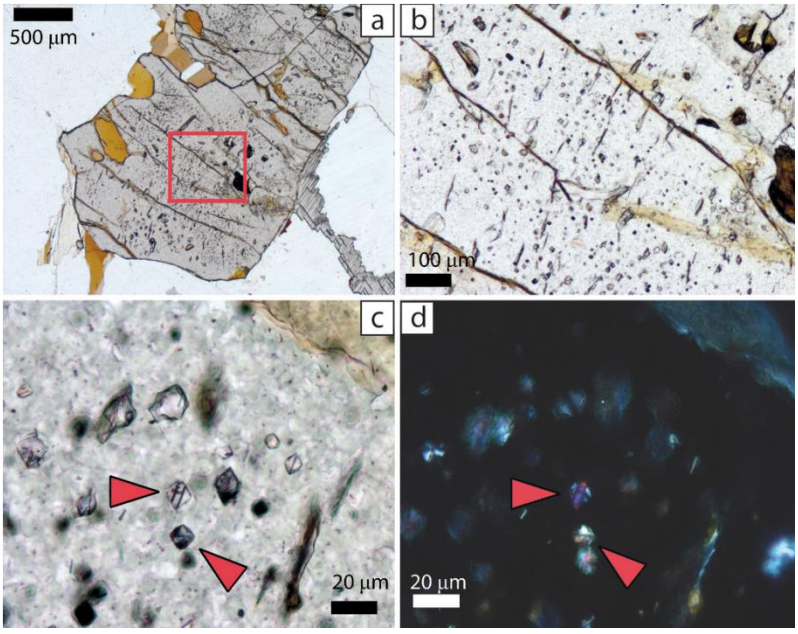

Figure 1. a) A porphyroblast of garnet in contact with kyanite, showing abundant inclusions and a set of subparallel, spaced fractures. Red box: area enlarged in (b). b) aninclusion-rich area of the garnet. A second set of small fractures, oriented subvertically, can be observed. c) and d) Close up (plane-polarized light and crossed polars, respectively) of crystallized melt inclusions from the area in (b). Inclusions (red arrows) show negative crystal shape and consist of polycrystalline aggregates.

Cite as: Carosi et al., 2014, Eocene partial melting recorded in peritectic garnets from kyanite-gneiss, Greater Himalayan Sequence, central Nepal, in Montomoli C., et al., eds., proceedings for the 29th Himalaya-Karakoram-Tibet Workshop, Lucca, Italy.

Compositional X-ray maps of garnets allow to better constrain monazite ages and melting within the prograde/retrograde path of the rocks.

Eocene partial melting occurred during prograde metamorphism in the kyanite stability field (Eo-himalayan event). Sillimanite-bearing mylonitic foliation wraps around garnets showing a top-to-the SW sense of shear linked to the Main Central Thrust Zone ductile activity and to the exhumation of the GHS. These findings highlight the occurrence of an older melting event in the GHS during prograde metamorphism in the kyanite stability field before the more diffuse Miocene melting event (King et al., 2011).

The growth of prograde garnet and kyanite at 36-41 Ma in the MCT zone, affecting the bottom of the GHS, suggests that inverted metamorphism in the MCT zone and folded isograds in the GHS should be carefully proved with the aid of geochronology, because not all Barrovian minerals grew during the same time span and they grew in different tectonic settings.

References

Carosi, R., Montomoli, C., Rubatto, D. and Visonà, D., 2010, Late Oligocene high-temperature shear zones in the core of the Higher Himalayan Crystalline (Lower Dolpo, Western Nepal), Tectonics, 29, TC4029, doi:10.1029/2008TC002400.

Carosi, R., Montomoli, C., Rubatto, D., and Visonà, D., 2013, Leucogranite intruding the South Tibetan Detachment in western Nepal: implications for exhumation models in the Himalayas, Terra Nova, 25, 478-489, doi: 10.1111/ter.12062.

Carosi, R., Montomoli, C., Langone, A., Turina, A., Cesare, B., Iaccarino, S., Fascioli, L., Visonà, D., Ronchi A. and Rai S.M., Eocene partial melting recorded in peritectic garnets from kyanite-gneiss, Greater Himalayan Sequence, central Nepal. In: "Tectonics of Himalayas" (Editors: S. Mukherjie, R. Carosi, B. Mukherjie, D. Robinson, P. van Der Beck), Geol. Soc. London Special Publication, in press.

Ferrero, S., Bartoli, O., Cesare, B., Salvioli-Mariani, E., Acosta-Vigil, A., Cavallo, A., Groppo, C. and Battiston, S., 2012, Microstructures of melt inclusions in anatectic metasedimentary rocks, Journal of Metamorphic Geology, 30, 303-322.

Godin, L., Parrish, R.R., Brown, R.L. and Hodges, K.V., 2001, Crustal thickening leading to exhumation of the Himalayan metamorphic core of central Nepal: Insight from U-Pb geochronology and 40Ar/39Ar thermochronology, Tectonics, 20 (5), 729-747.

Godin, L., Grujic, D., Law, R.D. and Searle, M.P., 2006, Channel flow, ductile extrusion and exhumation in continental collision zones: an introduction, Geological Society of London Special Publication, 268, 1-23.

Harris, N, and Massey J., 1994, Decompression and anatexis of Himalayan metapelites, Tectonics, 13, 1537-1546.

Imayama, T., Takeshite, T., Yi, K., Cho, D. -Y., Kitajima, K., Tsutsumi, Y., Kayama, M., Nishido, H., Okumura, T., Yagi, K., Itaya, T. and Sano, Y., 2012, Two-stage partial melting and contrasting cooling history within the Higher Himalayan Crystalline Sequence in the far-eastern Nepal Himalaya, Lithos, 134-135, 1-22.

King, J., Harris, N., Argles, T., Parrish, R., and Zhang, H., 2011, Contribution of crustal anatexis to the tectonic evolution of Indian crust beneath southern Tibet, Geological Society of America Bulletin, 123, 218-239.

Montomoli, C., Iaccarino, S., Carosi, R., Langone, A. and Visonà, D., 2013, Tectonometamorphic discontinuities within the Greater Himalayan Sequence in Western Nepal (Central Himalaya): Insights on the exhumation of crystalline rocks, Tectonophysics, 608, 1349-1370.

Rubatto, D., Chakraborty, S. and Dasgupta, S., 2012, Timescale of crustal melting in the Higher Himalayan Crystallines (Sikkim, Eastern Himalaya) inferred from trace element-constrained monazite and zircon chronology, Contributions to Mineralogy and Petrology, 165, 349-372.

Visonà, D., Carosi, R., Montomoli, C., Peruzzo, L. and Tiepolo, M., 2012, Miocene andalusite leucogranite in central-east Himalaya (Everest–Masang Kang area): low-pressure melting during heating, Lithos, 144, 194-208.

Origin of Late Cretaceous-Paleocene granites from Tengchong terrene, Western Yunnan: implications for continental arc evolution and lithosphere subduction

Xijie Chen[1], Zhiqin Xu[1], Zhihui Cai[1], Huaqi Li[1]

[1]State Key Laboratory of Continental Tectonics and Dynamics, Institute of Geology, Chinese Academy of Geological Sciences, Beijing, China, xijiechen2008@gmail.com

The Cenozoic geology of West Yunnan is characterized by widespread Jurassic to Cretaceous igneous rocks consisting predominantly of granites and rhyolites and subordinate mafic lithologies. However, the tectonic regime responsible for the inland Eocene granites remains controversial. We report here U–Pb zircon ages, geochemical and Sr–Nd–Hf isotopic data for Tengliang granitoid belt (Guyong Pluton, Lushui pluton, Mangdan Pluton) and West Yingjiang complex Batholith in West Yunnan. Mineralogical and geochemical features suggest that the West Yinjiang and Tengliang granitoid rocks are I- and aluminous S-type granites, respectively. LA-ICPMS U–Pb zircon analyses yield consistent ages ranging from 50.4 Ma to 60.8 Ma for three samples from the Yinjiang Batholith, and three ages of 68 Ma, 68 Ma and 66 Ma from Guyong pluton, Lushui pluton and Mangdan pluton.

The rocks from West Yingjiang are characterized by metaluminous and weakly peraluminous hornblende-bearing gneissic granites with A/CNK = 1.01-1.11, $K_2O > Na_2O$, coupled with low initial Sr isotopic values of 0.7076–0.7106 and high εNd(t) values from -4.6 to -11.9. The metamorphosed granitoids crystallized during the early Eocene (~60–50 Ma) with zircons showing εHf(t) values from +10.88 to −2.75 and crustal model ages of 1.30 to 0.59 Ga, comparable to those of coeval I-type granitoids from the Gangdese batholith, southern Lhasa. Meanwhile, the granite of 60-50 Ma which mostly distributed in the western Yingjiang area could be the direct products of Neo-Tethys northern subduction. The Tengliang granites situated west of the Gaoligong belt, were emplaced in late Cretaceous (66-68 Ma) and displayed a strong peraluminous affinity and negative εHf(t) (-24~-4) and crustal model ages of 1.41 to 2.66 Ga, indicating a provenance from a Proterozoic sedimentary source with little mantle contribution. While the magmatic arc was related to eastward subduction of the Neo-Tethys beneath the Asian continent, the S-type granites represented the melting products of thickened crust in the hinterland. Initial $^{87}Sr/^{86}Sr$ ratios are 0.7101-0.7139 and εNd(t) values from -8.91 to -13.8, considerably lower than High Himalayan leucogranites (0.74-0.79), and are indicative of a lower continental crust source. The Mesozoic granitoids of this area may have been generated mainly by reworking of deeply-buried Neoproterozoic biotite-rich pelitic materials due to thermal perturbations triggered by the subduction of Neo-Tethys in Mesozoic time. Intrusion of mantle melts provided heat to promote crustal melting and may have selectively contaminated the granite magma.

On the basis of geological, geochemical data of Late Cretaceous - Cenozoic igneous rocks in West Yunnan, we suggest that during the period from 80 to 40 Ma, the slab dip angle of Neo-Tethys plate subduction underneath Tengchong terrane increased from a very low angle to a median angle. Consequently, magmatic activity of the West Yunnan continental margin migrated oceanward to the west.

During subduction process, various degrees of mantle wedge melting and basaltic underplating provided the necessary heat to cause partial melting of lower- and middle- crust, and generation of voluminous felsic magmas. A combination of these processes is responsible for the formation of the famous Cenozoic granitoids, volcanic rocks and related ore deposits in West Yunnan.

Cite as: Chen, X.J. et al., 2014, Origin of Late Cretaceous-Paleocene granites from Tengchong terrene, Western Yunnan: implications for continental arc evolution and lithosphere subduction, in Montomoli C., et al., eds., proceedings for the 29th Himalaya-Karakoram-Tibet Workshop, Lucca, Italy.

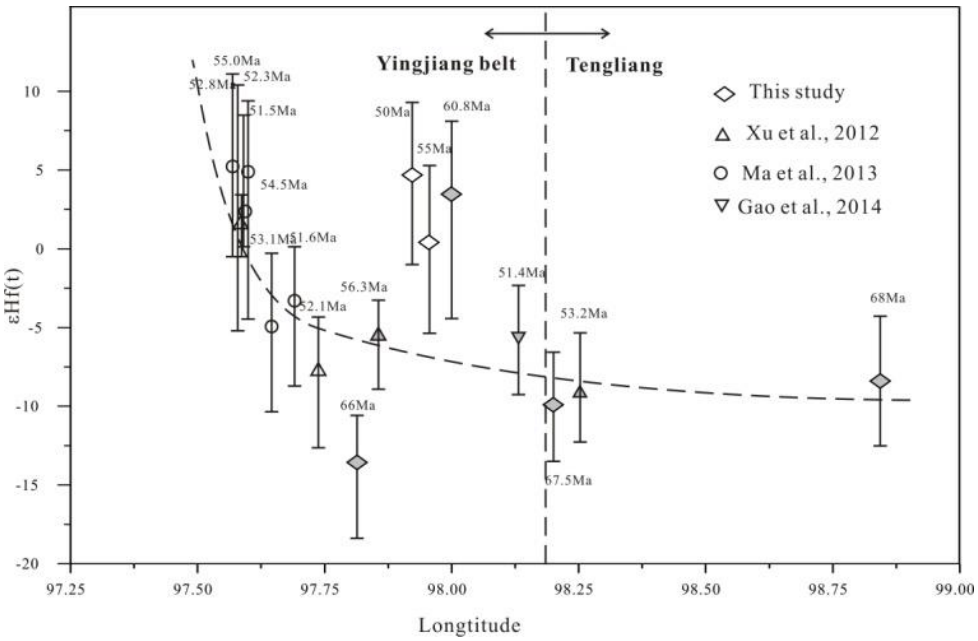

Figure 1. The spatial variation of average εHf(t) for zircons from the early Eocene granitic samples from west Yingjiang across Tengliang area. The gray color denotes the S-type granite; the white color denotes the I-type granite.

References

Ma, L., Wang, Y., Fan, W., Geng, H., Cai, Y., et al., 2014, Petrogenesis of the early Eocene I-type granites in west Yingjiang (SW Yunnan) and its implication for the eastern extension of the Gangdese batholiths, Gondwana Research, 25(1), 401-419.

Xu, Y.G., Yang, Q.J., Lan, J.B., Luo, Z.Y., Huang, X.L., et al., 2012, Temporal–spatial distribution and tectonic implications of the batholiths in the Gaoligong–Tengliang–Yingjiang area, western Yunnan: Constraints from zircon U–Pb ages and Hf isotopes, Journal of Asian Earth Sciences, 53, 151-175.

Gao, Y.J., Lin, S.L., Cong, F., Zou, G.F., Xie, T., et al., 2014, Zircon U-Pb Geochronology, Zircons Hf isotope and bulk Geochemistry of paleogene granite in the Tengchong-Lianghe Area, West Yunnan, Acta Geologica Sinica, 88(1), 63-71.

From Continental Collision to the Earth's Deep Water Cycle

Wang-Ping Chen[1,2], Tai-Lin Tseng[3], Shu-Huei Hung[3], Chi-Yuen Wang[4]

[1] Ocean College, Zhejiang University, Hangzhou, 310058, China, wpchen@uiuc.edu
[2] Formerly Dept. of Geology, University of Illinois, Urbana-Champaign, Urbana, IL 61801, USA
[3] Dept. of Geosciences, National Taiwan University, Taipei, Taiwan 10617, R.O.C.
[4] Dept. of Earth & Planetary Science, University of California, Berkeley, CA 94720, USA

While there is a general consensus that the Himalayan-Tibetan orogen is a consequence of collision between the Asian continent and the Indian shield, a broad array of different tectonic models have been proposed. Mantle dynamics is important in all these models, but processes in the mantle are not explicitly addressed in most cases. Here we address this important issue emphasizing new methodology and high-resolution, broadband seismic array data that are readily available in the public domain. The latter aspect is critical in that our results are independently verifiable – a basic tenet of any scientific endeavor.

Combining results from a variety of seismic methods and additional constraints from plate motions, mineral physics, geodesy, and petrology, the current configuration of overlapping lithospheres is constrained down to depths above the lower mantle (Fig. 1). We then reconstruct position of the Indian lithospheric mantle relative to Asia back to 15 Ma ago or the onset of the latest magmatic activity in Tibet. By then the leading (northern) edge of the Indian lithospheric mantle (Indian mantle front, IMF) has advanced sub-horizontally past the entire Lhasa terrane (now southern Tibet), and thickened the lithospheric mantle of the Qiangtang terrane (now central Tibet). Rayleigh-Taylor instability ensued, causing widespread but small volume of magmatic activity in northern Tibet (Fig. 1). Meanwhile, detached lithospheric mantle foundered quickly through the upper mantle and now rests at the bottom of the mantle transition zone (MTZ) just above the lower mantle. The remnant of detached lithospheric mantle of the Qiangtang terrane manifests itself as a large-scale seismic anomaly of high compressional wave speed (V_P) but curiously is undetectable through shear-waves.

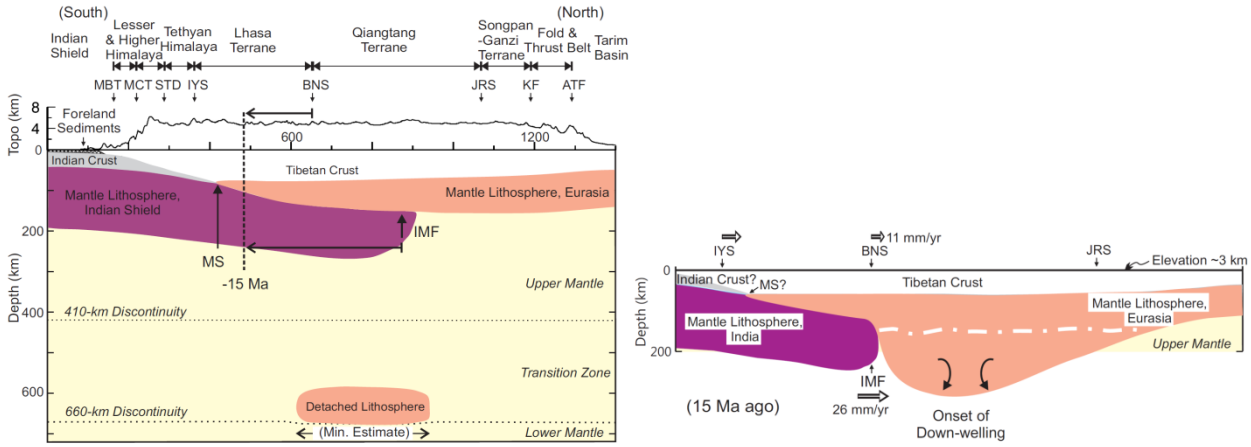

Figure 1. (Left panel) A north-south trending cross section showing our interpretation of the current configuration of lithospheres. The detached lithosphere in the MTZ is inferred from the minimum lateral extent of seismic anomaly of high V_P. The dashed vertical line marks the reconstructed position of the IMF and the BNS at 15 Ma ago. (Right panel) A schematic cross section showing reconstructed positions of the IMF and the BNS at 15 Ma ago when the IMF is near the southern edge of thickened Qiangtang terrane. (Chen and Tseng, 2007; Tseng and Chen, 2008; Chen et al., 2013).

The discordant results between *P*- and *S*-waves indicate that the foundered lithospheric mantle is rich in hydroxyls, a conclusion supported by other evidence including hydrous minerals in recent volcanic rocks found in northern Tibet. Since olivine and its high-pressure polymorphs, all nominally anhydrous

Cite as: Chen W.P. et al., 2014, From Continental Collision to the Earth's Deep Water Cycle, in Montomoli C., et al., eds., proceedings for the 29th Himalaya-Karakoram-Tibet Workshop, Lucca, Italy.

minerals, can hold ~1 wt% of water throughout the upper mantle and the MTZ, foundering of thickened lithospheric mantle caused by continental collision is an unappreciated but effective pathway for water to enter the deep mantle. In fact, the global distribution of deep earthquake foci is inconsistent with the traditional notion that subduction of oceanic lithosphere is the major pathway for recycling water into the Earth's deep interior (Green et al., 2010).

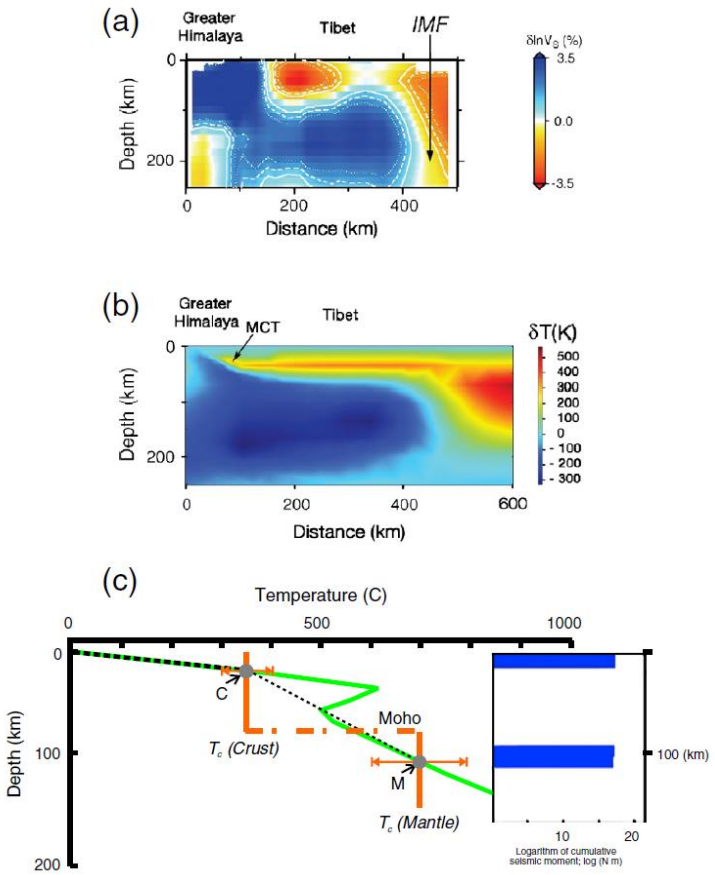

Figure 2. (a) North–south trending, vertical cross-section of V_S anomalies (Hung et al., 2011). (b) Simulated temperature anomalies (relative to an average continental geotherm) beneath Tibet along the same cross-section as in (a) (Wang et al., 2013). (c) Temperature as a function of depth beneath southern Tibet where the distribution of focal depths is bimodal (inset). The step-function (in orange) shows limiting temperatures for seismicity in crustal and mantle materials, giving two constraints in temperature from focal depths (near points "C" and "M"): Shallow crustal earthquakes indicate a high geotherm in the upper crust, while mantle events specify a low temperature of only about 700°C at a depth of approximately 100 km (dashed lines). The green curve is predicted temperature from numerical simulations by Wang et al. (2013); where the combined effect of cooling by underthrust Indian plate and viscose shear heating along the top of the Indian plate results in a temperature inversion in the now thickened lower crust of southern Tibet.

Currently, a clear, subhorizontal seismic anomaly of high V_P and V_S (but low V_P/V_S) in the upper mantle can be traced from under northern India all the way to beneath part of the Qiangtang terrane (Figs. 1 & 2a). This configuration of the "Greater India" (GI), or the submerged, northern portion of the Indian shield, is a vast heat sink that readily explains why the upper mantle is cold under southern Tibet, including the occurrence of large, sub-crustal earthquakes (down to depths about 100 km) where the temperature is below about 700 ± 100°C (Fig. 2b). Yet the upper crust of Tibet is hot, including crustal earthquakes that are no deeper than about 15 km where the temperature is above ~350 ± 100°C. Based on results of numerical simulations, we attribute the high temperature there to the self-limiting, localized nature of shear heating along the top of GI (Fig. 2c).

References

Chen, W.P. and Tseng, T.L., 2007, Small 660-km seismic discontinuity beneath Tibet implies resting ground for detached lithosphere, Journal of Geophysical Research, 112, B05309.

Chen, W.P., Tseng, T.L., Yang, Z., Wang, C.Y., Yu, C.-Q. et al., 2013, Moho, seismogenesis, and rheology of the lithosphere, Tectonophysics, 609, 491-503.

Green, H.W., Chen W.P. and Brudzinski, M., 2010, Seismic evidence of negligible water carried below 400 km depth in subducting lithosphere, Nature, 467, 828-831.

Hung, S.H., Chen, W.P. and Chiao, L.Y., 2011, A data-adaptive, multi-scale approach of finite-frequency, travel-time tomography with special reference to P- and S-Wave data from central Tibet, Journal of Geophysical Research, 116, B06307.

Tseng, T.L. and Chen, W.P., 2008, Discordant contrasts of P- and S-wave speeds across the 660-km discontinuity beneath Tibet: A case for hydrous remnant of sub-continental lithosphere, Earth and Planetary Science Letters, 268, 450-462.

Wang, C.Y., Chen, W.P. and Wang, L.P., 2013, Temperature beneath Tibet, Earth and Planetary Science Letters, 375, 326-337.

First tectonic-geomorphology study along the Longmu – Gozha Co fault system, Western Tibet: Insights on the youngest segment of the Altyn Tagh fault

Marie-Luce Chevalier[1], Jiawei Pan[1], Haibing Li[1], Zhiming Sun[2], Dongliang Liu[1], Junling Pei[2], Wei Xu[3], Chan Wu[1]

[1] State Key Laboratory of Continental Tectonics and Dynamics, Institute of Geology, Chinese Academy of Geological Sciences, Beijing 100037, China, mlchevalier@hotmail.com

[2] Key Laboratory of Paleomagnetism, Institute of Geomechanics, Chinese Academy of Geological Sciences, Beijing 100081, China

The Longmu – Gozha Co left-lateral strike-slip fault system (LGCF) is located in remote western Tibet, intersecting both the Altyn Tagh fault (ATF) and the Karakorum fault (KF), the two major strike-slip faults in the region. The Ashikule, the Gozha Co and the Longmu Co faults are clear and distinct left-stepping en-echelon faults, together forming the LGCF system. Although poorly documented, quantifying its activity remains a key problem to understand the kinematics and the tectonics history of the westernmost Tibetan Plateau. Indeed, the Karakax fault (westernmost segment of the ATF), LGCF and KF together control the tectonics of western Tibet which itself controls the extrusion of Tibet towards the east. The LGCF system shows clear and impressive morphological indications of left-lateral active shear, that we here attempt to quantify using field measurements (terrestrial LIDAR) along with ^{10}Be surface-exposure dating. Our preliminary data suggest a slip-rate <3 mm/yr, consistent with geodetic and block model studies. While it is on the order of the Karakax fault slip-rate (~2 mm/yr), it is smaller than those along the ATF and KF (>9 and >8 mm/yr, respectively), yielding a possible ~4 mm/yr slip accommodated most likely in the Ashikule graben located between the ATF and Karakax faults, as well as along the thrusts in the south Tarim basin. In addition to evidence of recent tectonic-related events in the vicinity, such as the 1951 volcanic eruption, the 2008 and 2014 Mw7.3 Yutian earthquakes, the LGCF's en-echelon geometry, as well as relatively low slip-rate compared to those of the surrounding faults, suggests that this segment of the ATF may be the most recent, > 9-21 Ma.

Cite as: Chevalier, M-L.,et al., 2014, First tectonic-geomorphology study along the Longmu – Gozha Co fault system, Western Tibet: Insights on the youngest segment of the Altyn Tagh fault, in Montomoli C., et al., eds., proceedings for the 29th Himalaya-Karakoram-Tibet Workshop, Lucca, Italy.

Oligocene activity on the eastern margin of the Tibetan Plateau

Kristen L. Cook[1], Yuan-Hsi Lee[2], Xibin Tan[3]

[1] German Research Center for Geosciences GFZ, Potsdam, 14473, Germany, klcook@gfz-potsdam.de
[2] Department of Earth and Environmental Sciences, National Chung-Cheng University, Taiwan, R.O.C.
[3] Institute of Geology, China Earthquake Administration, Beijing 100029, China

Differing proposed mechanisms of plateau formation and growth have different implications for the propagation of the Tibetan Plateau towards its current margins, and therefore for the timing of onset of uplift and deformation on the margins. On the eastern plateau margin, the Cenozoic uplift and deformation history has been extensively studied in recent years, but questions still remain. Numerous thermochronology studies have been conducted in the area, but the interpretations vary depending on the thermochronometers used and the sample distribution – particularly on whether the study is regional or is focused on specific structures. Many studies identify uplift at 10-12 Ma in the Longmenshan, and initiation of river incision within the plateau at the same time (Clark et al., 2005; Godard et al., 2009; Wilson and Fowler, 2011). However, there is increasing evidence of earlier uplift and deformation in the region. Wang et al. (2012) recognize a phase of rapid uplift at ~30 Ma in the central Longmenshan. We find activity at this time throughout the eastern margin region. In the southwestern Longmenshan, apatite and zircon fission track thermochronology shows a two-phase uplift history with rapid exhumation at ~30 Ma and at 3-5 Ma, roughly similar to the exhumation history of the central Longmenshan. To the west, in the Danba region, fission track and Ar/Ar thermochronology show that a portion of the folding and exhumation of the Danba region took place in the Cenozoic, starting at ~30 Ma and accelerating at ~10 Ma. Both apatite and zircon fission track ages are youngest in the core of the Danba antiform and increase steadily toward the antiform margins. Biotite and muscovite Ar/Ar ages from the region are highly variable, with Oligocene ages within shear zones and 50-90 Ma ages elsewhere throughout the region. These data allow us to constrain the magnitude, distribution, and timing of Cenozoic exhumation in the region. To the southwest of the Danba antiform, migmatite on the eastern boundary of the Gongga granite contains zircons with U-Pb ages of ~30-35 Ma. These ages have been attributed to high temperature metamorphism and crustal melting by Li et al., (2013), but the driver of this melting remains unclear. Elsewhere on the eastern margin, there is evidence of Oligocene hydrothermal and magmatic activity with gold deposits, a large REE complex, and high potassium intrusive rocks, all dated to ~25-35 Ma (Hou and Cook, 2009). The contemporaneous uplift and deformation in the Longmenshan and Danba regions and emplacement of ore deposits and magmatic rocks throughout the eastern margin suggests a regional response to plateau propagation on the eastern margin by the Oligocene.

References

Clark, M.K., House, M.A., Royden, L.H., Burchfi el, B.C., Whipple, K.X., Zhang, X., and Tang, W., 2005, Late Cenozoic uplift of southeastern Tibet, Geology, 33, 525-528, doi:10.1130/G21265.1.

Godard, V., Pik R., Lavé J., Cattin R., Tibari B., de Sigoyer J., Pubellier M., and Zhu J., 2009, Late Cenozoic evolution of the central Longmen Shan, eastern Tibet: Insight from (U-Th)/He thermochronometry, Tectonics 28, doi 10.1029/2008TC002407.

Hou, Z., and Cook, N. J., 2009, Metallogenesis of the Tibetan collisional orogen: A review and introduction to the special issue, Ore Geology Reviews, 36, 2-24.

Li, H. and Zhang, Y., 2013, Zircon U-Pb geochronology of the Konggar granitoid and migmatite: constraints on the Oligo Miocene tectono-thermal evolution of the Xianshuihe fault zone, East Tibet, Tectonophysics, 606, 127-139.

Wang, E., E. Kirby, K. P. Furlong, M. van Soest, G. Xu, X. Shi, P. J. J. Kamp, and K. V. Hodges (2012), Two-phase growth of high topography in eastern Tibet during the Cenozoic, Nature Geoscience, 5, 640-645, doi:10.1038/ngeo1538.

Wilson, C.J.L., and Fowler, A.P., 2011, Denudational response to surface uplift in east Tibet: Evidence from apatite fission track thermochronology: Geological Society of America Bulletin, 123, 1966-1987, doi:10.1130/B30331.1.

Cite as: Cook, K.L., Lee, Y.-H., and Tan, X., 2014, Oligocene activity on the eastern margin of the Tibetan Plateau, in Montomoli C., et al., eds., proceedings for the 29th Himalaya-Karakoram-Tibet Workshop, Lucca, Italy.

Active tectonic uplift in the eastern Himalayan Syntaxis: geomorphic traces of the 1950 Assam earthquake rupture

Aurélie Coudurier-Curveur[1], Elise Kali[2], Paul Tapponnier[1], Jérôme van Der Woerd[2], Saurabh Baruah[3], Swapnamita Choudhury[4], Paramesh Banerjee[1], Sorvigenaleon Ildefonso[1], Çağıl Karakaş[1]

[1] Earth Observatory of Singapore, Nanyang Technological University, Singapore 639798, acoudurierc@ntu.edu.sg
[2] Institut de Physique du Globe de Strasbourg, CNRS, UDS, Strasbourg , France
[3] North-East Institute of Science and Technology, Jorhat, India
[4] Wadia Institute of Himalayan geology, Dehradun, India

On August 15, 1950, the M ≈ 8.7 Assam earthquake devastated the Abor and the Mishmi foothills, in Arunachal Pradesh, triggering large landslides and debris flows all around the eastern Himalayan Syntaxis and eastern Assam plain (Poddar, 1950; Tandon, 1950; Tillotson, 1951; Kingdon-Ward, 1953). No surface rupture, however, was ever documented, whether at the time of the event, or in the 6 decades since.

We present here the first evidence for a primary rupture of that event, along both the Main Himalayan Frontal Thrust (MFT) and the Mishmi Thrust. Geomorphic features indicative of tectonic surface uplift and recent active faulting were first identified in field reconnaissance surveys guided by satellite image interpretation. Topographic profiles across fault scarps crossing at high angle fluvial terrace risers were then leveled with a Total Station, to quantify the vertical offsets of uplifted, perched Quaternary alluvial terraces. Such offsets range from ≈ 2.6 to ≈ 29 m. At a few sites, the analysis of the profile shapes and slopes enables a preliminary assessment of the co-seismic throws of the 1950 earthquake and its predecessors. At Pasighat and Wakro, for instance, the minimum heights of the steepest scarps along the MFT and Mishmi Thrust are 2.6 ± 0.1 and 7.3 ± 0.1 m, respectively. We interpret them to represent the vertical co-seismic offsets of the 1950 earthquake. On the Mishmi Thrust near Wakro, our topographic profiles also show evidence for about 14 m of cumulative vertical offset - the sum of two identical 7 m throw amounts - suggestive of locally characteristic slip in the 1950 and penultimate earthquake. The differences in co-seismic throw on the MFT and Mishmi Thrust may result from large changes in dip around the eastern Syntaxis, which would be consistent with large-scale changes in the topography of the corresponding mountain ranges.

References

Poddar, M.C., 1950, The Assam earthquake of 15th August, 1950, Indian Minerals, 4/4, 167-176.
Tandon, A.N., 1950, The very great earthquake of August 15, 1950, Science and Culture, 16/4, 147-155.
Tillotson, E., 1951, The Great Assam earthquake of August 15, 1950, Nature, 167, 128-130.
Kingdon-Ward, F., 1953, The Assam earthquake of 1950, The Geographical Journal, 119/2, 169-182.

Cite as: Coudurier-Curveur, A. et al., 2014, Active tectonic uplift in the eastern Himalayan Syntaxis: geomorphic traces of the 1950 Assam earthquake rupture, in Montomoli C., et al., eds., proceedings for the 29th Himalaya-Karakoram-Tibet Workshop, Lucca, Italy.

Geometry and kinematics of the Main Himalayan Thrust and Neogene crustal exhumation in the Bhutanese Himalaya derived from inversion of multi-thermochronologic data

Isabelle Coutand[1], David M. Whipp Jr.[2], Djordje Grujic[1], Matthias Bernet[3], Maria Giuditta Fellin[4], Bodo Bookhagen[5], Kyle R. Landry[1], S. K. Ghalley[6], Chris Duncan[7]

[1] Department of Earth Sciences, Dalhousie University, PO BOX 15000, Halifax, NS, B3H 4R2, Canada, icoutand@dal.ca
[2] Institute of Seismology, Department of Geosciences and Geography, P.O. Box 68, FI-00014 University of Helsinki, Finland
[3] ISTerre, Université Joseph Fourier, 1381 Rue de la piscine, BP 53, 38041 Grenoble Cedex, France
[4] Institute for Geochemistry and Petrology, Sonneggstrasse 5 8092, ETH-Zürich, Zürich, Switzerland
[5] Department of Geography, 1832 Ellison Hall, UC Santa Barbara, Santa Barbara, CA 93106-4060, USA
[6] Department of Geology and Mines, Ministry of Economic Affairs, P.O. Box 173, Thimphu, Bhutan
[7] Department of Geosciences, University of Massachusetts, Amherst, MA 01003, USA

Both climatic and tectonic processes affect bedrock erosion and exhumation in convergent orogens, but determining their respective influence is difficult. A requisite first step is to quantify long-term (~10^6 yr) erosion rates within an orogen. In the Himalaya, past studies suggest long-term erosion rates varied in space and time along the range front, resulting in numerous tectonic models to explain the observed erosion rate distribution. Here, we invert a large dataset of new and existing thermochronological ages to determine both long-term exhumation rates and the kinematics of Neogene tectonic activity in the eastern Himalaya in Bhutan (Coutand et al., 2014). New data include 31 apatite and 5 zircon (U-Th)/He ages, and 49 apatite and 16 zircon fission-track ages along two North-South oriented transects across the orogen in western and eastern Bhutan. Data inversion was performed using a modified version of the 3-D thermo-kinematic model PECUBE, with parameter ranges defined by available geochronologic, metamorphic, structural and geophysical data. Among several important observations, our three main conclusions are: (1) Thermochronologic ages do not spatially correlate with surface traces of major fault zones, but appear to reflect the geometry of the underlying Main Himalayan Thrust; (2) our data are compatible with a strong tectonic influence, involving a variably dipping Main Himalayan Thrust geometry and steady-state topography; and (3) erosion rates have remained constant in western Bhutan over the last ~10 Ma, while a significant decrease occurred at ~6 Ma in eastern Bhutan, which we partially attribute to convergence partitioning into uplift of the Shillong plateau.

References

Coutand, I. et al., 2014, Geometry and kinematics of the Main Himalayan Thrust and Neogene crustal exhumation in the Bhutanese Himalaya derived from inversion of multithermochronologic data, Journal of Geophysical Research: Solid Earth, 119, doi:10.1002/2013JB010891.

Cite as: Coutand et al., 2014, Geometry and kinematics of the Main Himalayan Thrust and Neogene crustal exhumation in the Bhutanese Himalaya derived from inversion of multi-thermochronologic data, in Montomoli C., et al., eds., proceedings for the 29th Himalayan-Karakorum-Tibet Workshop.

Neogene exhumation history of the Bhutan Himalaya quantified using multiple detrital proxies

Isabelle Coutand[1], David M. Whipp Jr.[2], Bodo Bookhagen[3], Matthias Bernet[4], Eduardo Garzanti[5], Djordje Grujic[1]

[1] Department of Earth Sciences, Dalhousie University, PO BOX 15000, Halifax, NS, B3H 4R2, Canada, icoutand@dal.ca
[2] Institute of Seismology, Department of Geosciences and Geography, P.O. Box 68, FI-00014 University of Helsinki, Finland
[3] Department of Geography, 1832 Ellison Hall, UC Santa Barbara, Santa Barbara, CA 93106-4060, USA
[4] ISTerre, Université Joseph Fourier, 1381 Rue de la piscine, BP 53, 38041 Grenoble Cedex, France
[5] Department of Earth and Environmental Sciences, Università di Milano-Bicocca, Milano, Italy

Proper sampling to constrain the evolution of fault geometries and kinematics, and quantify erosion rates in active orogens using *in situ* bedrock thermochronological data is often difficult, due to logistical and infrastructural challenges in high-elevation areas. Detrital thermochronology of modern river sands is an appealing alternative that has been used successfully in many instances, but typical assumptions that underlie the interpretation of detrital data, such as uniform catchment-wide erosion rates, can introduce bias in detrital data interpretation. Numerical tools able to predict detrital cooling ages subject to differential exhumation rates across individual catchments are now available (e.g. Whipp et al., 2009; Braun et al., 2011) to overcome some of these limitations. The aim of this paper is to quantitatively test whether the detrital thermochronometer record from modern river sands supports the tectonomorphic scenario extracted from *in situ* thermochronometer data along the Bhutanese range front (Coutand et al., 2014). In a second step, we use various topographic indices (e.g., channel steepness, relief, specific stream power) to test how topographic expression correlates with predicted exhumation patterns.

Our study focuses on the Bhutanese Himalaya, where the spatial and temporal evolution of Neogene exhumation was recently constrained by inverting a large dataset of strategically located *in situ* multi-thermochronological ages using a modified version of the 3-D thermokinematic model Pecube (Coutand et al., 2014). We have collected 18 sand samples from the modern channels of the main rivers draining the Bhutan Himalaya and processed them for apatite and zircon fission-track thermochronology (AFT and ZFT, respectively), cosmogenic radionuclide dating (CRN) and sandstone petrography. Measured thermochronometer age distributions are first compared to predicted age distributions generated using the preferred fault kinematics and thermal parameters from Coutand et al. (2014) using the approach of Whipp et al. (2009). Preliminary results suggest the measured age distributions are statistically equal to ≥99% predicted age distributions from Monte Carlo sampling of predicted basin ages for 12 of 14 basins dated thus far. Predicted age distributions from the other 2 basins show a poor fit to the measured ages; <2% of the predicted age distributions are statistically equal to the measured ages.

It is important to note that our predicted detrital ages are from a thermokinematic model that is not coupled to a surface process or landscape-evolution model; as a consequence, the model topography does not evolve through time and exhumation is exclusively controlled by a combination of modern steady-state topography and the underlying fault kinematics/geometry (i.e., tectonic processes, Coutand et al., 2014). To identify and quantify the contribution of surface processes to exhumation in each catchment, we compare the measured detrital thermochronologic ages and CRN records to a number of geomorphic indices including channel steepness, relief, and specific stream power (Bookhagen and Strecker, 2012). Ultimately, this research will help to understand how transient landscape evolution in active orogens affects erosion rates measured at different temporal and spatial scales.

References

Whipp, D.M., Ehlers, T.A., Braun, J. and Spath, C. D., 2009, Effects of exhumation kinematics and topographic evolution on detrital thermochronometer data, Journal of Geophysical Research, F04021, doi:10.1029/2008JF001195.

Braun, J. et al., 2011, Quantifying rates of landscape evolution and tectonic processes by thermochronology and numerical modeling of crustal heat transport using PECUBE, Tectonophysics 524-525, 1-28.

Coutand, I. et al., 2014, Geometry and kinematics of the Main Himalayan Thrust and Neogene crustal exhumation in the Bhutanese Himalaya derived from the inversion of multithermochronologic data. Journal of Geophysical Research - Solid Earth, doi:10.1002/2013JB010891.

Bookhagen, B. and Strecker, M.R., 2012, Spatiotemporal trends in erosion rates across a pronounced rainfall gradient; examples from the southern Central Andes, Earth and Planetary Science Letters 327-328, 97-110, doi:10.1016/j.epsl.2012.02.005.

Cite as: Coutand, I., et al., 2014, Neogene exhumation history of the Bhutan Himalaya quantified using multiple detrital proxies, in Montomoli C., et al., eds., proceedings for the 29th Himalaya-Karakoram-Tibet Workshop, Lucca, Italy.

Precipitation stochasticity and its effects on discharge and erosion in the Himalaya

Eric Deal, Jean Braun[1]

[1]ISTerre, University Grenoble Alpes, Grenoble, France, eric.deal@ujf-grenoble.fr

Despite the modern availability of high quality datasets for climate, topography, and erosion rates in the Himalaya, it remains challenging to untangle the importance of climate on observed landforms and erosion rates. Due to the importance of water for erosional processes, it is often expected that precipitation rates and erosion rates will correlate positively. However this is not always the case, as shown for example by the Pliocene uplift of the Shillong plateau in northeast India that has created a strong east-west gradient in rainfall downwind on the southeastern front of the Himalaya not matched by a measurable gradient in exhumation rate (Adlakha et al, 2012). Modelling studies have shown that such discrepancies between rainfall and erosion can be well explained by an erosion threshold, a water runoff rate below which no erosion occurs (Snyder et al, 2003). This discharge threshold leads to a complex relationship between precipitation, river discharge and erosion rates, obfuscating the effect of rainfall on erosion. Additionally, it implies that the characterization of precipitation and discharge must take into account not just magnitude but also stochasticity because the relative ratio of discharge events below the threshold to discharge events above the threshold is important.

Therefore, to better elucidate the effect of rainfall patterns in the Himalaya on erosion rates we have described precipitation for the region by measuring magnitude and stochasticity with the TRMM satellite dataset. Using this more complete characterization of precipitation over the Himalaya, we work to establish a statistical relationship between the stochasticity of precipitation and that of river discharge. The development of this important link between climate patterns and discharge patterns will allow for the upscaling of climate data for use in landscape evolution models (LEMs). This opens up several interesting possibilities for future work with LEMs such as using modern climate data and erosion rates to constrain certain parameters such as the erosion discharge threshold or using climate data from paleo-GCMs in conjunction with erosion rates derived from the sedimentary record to test past climate scenarios for the region.

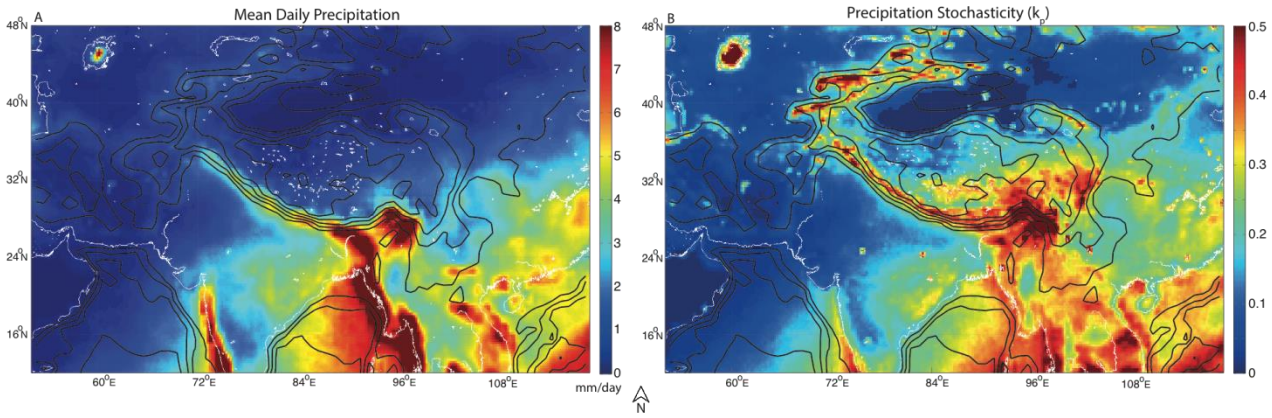

Figure 1. On the left a map of mean daily precipitation over the Tibetan plateau as measured by the TRMM dataset from 1998 until 2013. On the right a map of stochasticity for the same region. The black lines are 1000m contours and the white lines delineate coastlines and lakes.

References

Adlakha, V., Lang, K.A., Patel, R.C., Lal, N. and Huntington, K.W., 2012, Rapid long-term erosion in the rain shadow of the Shillong Plateau, Eastern Himalaya, Tectonophysics, 582, 76-83.

Snyder, N.P., Whipple, K., Tucker, G.E. and Merritts, D.J., 2003, Importance of a stochastic distribution of floods and erosion thresholds in the bedrock river incision problem. Journal of Geophysical Research: Earth Surface, 108(B2). doi:10.1029/2001JB001655.

Cite as: Deal, E. and Braun, J., 2014, Precipitation stochasticity and its effects on discharge and erosion in the Himalaya, in Montomoli C., et al., eds., proceedings for the 29th Himalaya-Karakoram-Tibet Workshop, Lucca, Italy.

Orographic and Tectono - Geomorphic controls of recent disasters in Himalaya: An appraisal from East to West Himalaya

Chandra S. Dubey[1], Nitu Singh[1], Dericks P. Shukla[1], Ravindra P. Singh[1]

[1] Department of Geology, Centre for Advanced Studies, University of Delhi, Delhi, 110007, India, csdubey@gmail.com, dericks.82@gmail.com

The massive change in the climatic conditions have increased the frequency of extreme events and have played a significant role in enhancing the tectonics of the Himalaya. High precipitation along the Himalaya has played a significant role in evolution of its landscapes enhancing hill slopes and fluvial erosion processes leading to huge amount of mass removal. Most of the landslides of the world occur in South Asia out of which, Himalayas are the most plausible, due to their topography and extreme precipitation conditions. High precipitation often leads to flooding, cloud burst, landslides, bank erosion etc. In this work, TRMM (Tropical Rainfall Measuring Mission) data for 16 years (1998-2013) was utilized to visualize the present variation of precipitation pattern along whole Himalaya. Not just precipitation but extreme events such as cloud burst, flash floods, landslides collected from various sources such as research papers, articles, and news reports were plotted for whole of Himalaya. It is observed (Figure 1) that the extreme events in Himalayas are mainly restricted to the south of the Higher Himalayas or near the foothills of the Siwaliks where coincidently high precipitation is also detected. Since, both the Higher Himalayas and Siwaliks are bound by MCT and MBT in north and south respectively, it could be envisaged that these thrusts have been acting as orographic barriers because most of the extreme events and the high precipitation is confined in these thrust areas. These orographic barrier in Himalayas play a significant role in controlling the expectancy and extant of rainfall. It is seen that in the south of hanging wall of MCT, the precipitation is high as compared to its foot wall in the north. Since the presence of high mountains does not allow the monsoon winds of Indian Summer Monsoon (ISM) to cross over and it generates large amplitude stationary waves which are responsible for the dry climate in Tibetan areas. While the winter monsoon (Northwest disturbance) causes high precipitation (mostly snowfall) on the vicinity of Higher Himalaya. Most of the precipitation during Monsoon occur below the MCT while during Post Monsoon precipitation is seen on either side of the MCT. These thrusts mainly MCT, MBT present whole along the Himalayas have a huge impact on the precipitation pattern along them.

Cite as: Dubey, et al., 2014, Orographic and Tectono - Geomorphic controls of recent disasters in Himalaya: An appraisal from East to West Himalaya., in Montomoli C., et al., eds., proceedings for the 29th Himalaya-Karakoram-Tibet Workshop, Lucca, Italy.

Pluton crystallization and petrogenesis in the Eastern Hindu Kush, NW Pakistan

Shah Faisal[1,2], Kyle P. Larson[2]

[1] Earth and Environmental Sciences, IKBAS, University of British Columbia, Okanagan, 3333 University Way, Kelowan, BC V1V 1V7, Canada, shahfaisal@upesh.edu.pk
[2] National Centre of Excellence in Geology, University of Peshawar, Peshawar-25120, KPK, Pakistan

New in situ U-(Th)/Pb zircon and monazite geochronology and geochemical analyses from plutonic bodies in the Hindu Kush range, NW Pakistan, provide insight on the crustal growth and tectonic evolution of the southern Eurasian margin. These new data outline a protracted magmatic history that spans the Cambrian to the Neogene (~538 to 23 Ma) and record a variety of petrogenetic associations variably influenced by within plate, volcanic arc, and collision tectonic environments.

Major and trace elements of the Kafiristan pluton reflect two different phases, both of which indicate a source derived from partially melted lower crust consistent with an anorogenic tectonic environment. Zircon geochronological data from both phases overlap between 538 and 487 Ma. We interpret that this protracted magmatic event is related to extensional plutonism during rifting and detachment of Cimmerian blocks from Gondwana.

The geochemical signatures of Tirich Mir pluton may be attributed to partial melting of lower crust/mantle wedge material. There is significant heterogeneity in the geochemistry, which may reflect upper crustal contamination during magma ascent. Zircon from the Tirich Mir pluton yield an age of 126 ± 1 Ma contemporaneous with northward subduction of the Paleotethys along the southern margin of Eurasia following the accretion of the Hindu Kush-Karakoram blocks in the Mesozoic.

Petrography and and mineral assemblages outline distinct felsic and intermediate phases within the Buni-Zom pluton; however, geochemical signatures indicate a similar deep crust-mantle wedge source for both. Specimens from the two phases yield indistinguishable U-Pb zircon ages that indicate the Buni-Zom body was emplaced during Early Cretaceous at ca. 107 Ma. Combined with the data from the Tirich Mir body, the Buni-Zom pluton helps outline a semi-continuous subduction environment along the southern margin of Eurasia throughout the Early Cretaceous.

The Garam Chasma pluton is the youngest plutonic body in the study area. It yields an Early Miocene crystallization age (23.5 ± 0.1 Ma; Th-Pb on monazite) and a geochemical signature consistent with derivation from a sedimentary source. The age of the Garam Chasma pluton coincides with widespread melting generated during crustal thickening and anatexis across the Himalayan arc.

These new geochemical data and geochronologic constraints from the Hindu Kush not only provide crucial constraints on the melt production in the region prior to the Cenozoic India-Eurasia collision but also help provide insight into the pre-Himalayan tectonomagmatic evolution of the southern margin of Eurasia.

Cite as: Faisal, S. and Larson, K.P., 2014. Pluton crystallization and petrogenesis in the Eastern Hindu Kush, NW Pakistan, in Montomoli C., et al., eds., proceedings for the 29th Himalaya-Karakoram-Tibet Workshop, Lucca, Italy.

The pulsing glaciers of Vanj Valley (Pamir)

Abdulkhak R. Faiziev[1], Firuz A. Malakhov[2], Nosir S.Safaraliev[2]

[1] Institute of geology, earthquake engineering and seismology of the Academy of sciences of the Republic of Tajikistan, 263 Ayni street, Dushanbe, 734063, Tajikistan, faiziev38@mail.ru
[2] Tajik National University, 17 Rudaki av., Dushanbe,734025, Tajikistan

Tajikistan is a mountainous country; 93 % of its territory is occupied by mountain ranges of the Tien Shan and Pamir. The absolute height of the earth's surface ranges from 300 to 7995 m above sea level, with nearly half of its territory located at an altitude of over 3000 m. About 6 % of Tajikistan's territory is covered by glaciers. There are more than 9139 glaciers with a total area equal to 9000 square km. Among them, glacier Fedchenko is the biggest not only in Tajikistan, but in the mid-latitudes of the Earth. It extends to a distance of 70 km. Around 60 of the total number of glaciers are able to pulsate, i.e. can make many kilometre-size "throws" with devastating consequences. The largest number are in the Gorno-Badakhshan (Kohistani Badakhshan) Autonomous Region. The most famous of them are Khirs (Bear), Byrs, Fortambek, Muzgazi etc. Frequency shifts surging glaciers varied and ranges from 5-6 to 10-12 years or more. Often these glaciers damming (blocking) mountain rivers. Thus formed are unstable dam and at any moment can happen catastrophic release of water from these lakes with all the attendant adverse effects. Among river valleys of Badakhshan the r.Vanj Valley with a population of over 30,000 people is considered the most vulnerable, where houses 33 village and hundreds of hectares of arable land. At the source of the river, one of the major rivers of the Pamirs, among numerous glaciers are several major surging glaciers (Khirs, Abdukagor, Dastirost) that threaten the inhabitants of the valley for many years, with catastrophic consequences. For example, in 1963, 1973 and 1989 the glacier Khirs kept in suspense all the inhabitants of the river valley of Vanj when the glacier blocked the riverbed. As a result, the lake was formed, which could be realized in the form of powerful mudflow, causing enormous economic damage and numerous casualties. In fact, the river broke through its ice dam, destroyed and demolished bridges, embankments, some buildings and acreage of crops in the territory of the former Soviet Union and Afghanistan. There were slight casualties. However, given the global warming must be prepared for greater disaster. In Soviet times, in the seventies of the last century to solve this problem was drafted bypass tunnel for safe landslide in case of a disaster, which has not been realized. Meanwhile, it was found that the glacier Khirs, for the periods between the pulsations in the centre accumulated an average of 270 million tons of ice. Such a mass and can serves as a "signal" of a possible beginning of the next progress. The problem is so great that a solution is possible only on the national and international levels. Currently, the Tajik government alone cannot solve this problem. Natural disasters do not recognize political boundaries and only by joint efforts, using the knowledge and experience of neighbours, other residents of mountainous areas of the world, you can reduce the damage from exposure to these dangerous natural phenomena. Thus, the inhabitants of the river valley Vanj and adjacent areas River Valley Panj as a sword of Damocles hanging dangerous threat of catastrophic natural phenomena.

Cite as: Faiziev, A.R. and Malakhov, F.A., 2014, The pulsing glaciers of Vanj Valley (Pamir), in Montomoli C., et al., eds., proceedings for the 29th Himalaya-Karakoram-Tibet Workshop, Lucca, Italy.

NAO effect on winter precipitation in the Hindu-Kush Karakoram and its secular variations

Luca Filippi[1,2], Elisa Palazzi[1], Jost von Hardenberg[1], Antonello Provenzale[1]

[1] Institute of Atmospheric Sciences and Climate of the National Research Council (ISAC-CNR), Torino, Italy, l.filippi@isac.cnr.it
[2] Dipartimento di Ingegneria Meccanica e Aerospaziale, Politecnico di Torino, Torino, Italy

The Hindu-Kush Karakoram (HKK), encompassing parts of Afghanistan, Pakistan, India and China, constitutes the westernmost part of the Himalayan range. During the winter season, from December to March, it is strongly impacted by westerly perturbations (Western Weather Patterns, WWPs) originating from the Mediterranean and Atlantic regions. The dynamics of WWPs is affected by the North Atlantic Oscillation (NAO), which is the dominant pattern of atmospheric variability in the North Atlantic sector (Hurrell et al. 2003). As a consequence, above (below) than normal precipitation amounts are typically recorded in the HKK during the positive (negative) NAO phase (Archer and Fowler 2004; Syed et al. 2006). However, this relationship underwent secular variations during the 20th Century, showing an alternation of periods of strong and weaker influence of the NAO on precipitation in the HKK (Yadav et al. 2009).

In the present study, we further investigate the relationship between the NAO and precipitation in the HKK, and the mechanisms responsible for this link. We also address the secular variations that occurred in the NAO-precipitation signal and we show that these multi-decadal changes are associated with spatial shifts in the position of the NAO centers of action (COAs). To this end, we consider an ensemble of precipitation datasets, including three rain-gauge-based archives - the Asian Precipitation Highly-Resolved Observational Data Integration Towards Evaluation of Water Resources (APHRODITE), the Global Precipitation Climatology Centre (GPCC) and the Climate Research Unit (CRU) data - and the ERA40 reanalysis. We also use another reanalysis product - the Twentieth Century Reanalysis (20CR) - extending further back in time, in order to study multi-decadal variations occurring in the NAO-precipitation relationship and to reconstruct the atmospheric variability from 1871 to the present.

All the considered datasets coherently exhibit enhanced precipitation over the HKK during the positive NAO phase. Some differences arise in the spatial distribution, intensity and significance of the NAO-associated precipitation anomalies, reflecting the difficulty of having reliable precipitation estimates over this region due to the complex orography, problems in detecting snowfall and the sparse coverage of stations (Palazzi et al., 2013).

The NAO exerts its control on precipitation in the HKK by regulating the intensity of westerly winds in the region of the Middle East jet stream, from North Africa to southeastern Asia. During the positive NAO phase, westerlies over this area are intensified from the upper-tropospheric jet to the lower levels. The strengthening of the jet intensifies the WWPs, while the anomaly in the middle-lower troposphere produces a faster transport of humidity towards the HKK. Our results indicate that evaporation from the Persian Gulf, the northern Arabian Sea and the Red Sea plays an important role. These basins, which constitute the main moisture sources for precipitation in the HKK, show enhanced evaporation during the positive NAO phase, mainly because of higher surface wind speed. The combination of enhanced humidity coming from evaporation and faster westerly winds results into an increased moisture transport towards the HKK. Wetter than normal conditions are experienced over northern Pakistan and northern India, and larger precipitation amounts occur as the WWPs reach this region.

The study of correlations between the NAO and precipitation in the HKK shows the multi-decadal variations that occurred in the NAO-precipitation relationship during the past century. The alternation of periods of strong and weaker control by the NAO is coherently reproduced by all the datasets. To investigate if these variations are associated with changes in the spatial structure of the NAO in the North

Cite as: Filippi, L., et al., 2014, NAO effect on winter precipitation in the Hindu-Kush Karakoram and its secular variations, in Montomoli C., et al., eds., proceedings for the 29th Himalaya-Karakoram-Tibet Workshop, Lucca, Italy.

Atlantic, we adopt the Angle Index metric introduced by Wang et al. (2012), a measure of the spatial displacements of the NAO COAs on decadal timescales. It is found that significant correlations between the NAO and precipitation mostly occur when the Angle Index is negative, that is, when the northern node of the NAO is shifted to the west and/or the southern node is shifted to the east. In the opposite configuration, the Angle Index is positive and the NAO-precipitation correlation is weaker. Shifts of the NAO COAs have significant implications for the circulation response to the NAO phase. Our analysis shows that, when the Angle Index is negative, the NAO has a strong control on the Middle East jet stream, and the mechanism of regulation of the HKK precipitation by the NAO is activated. Viceversa, when the Angle Index is positive, the NAO does not project – or projects weakly – onto the Middle East jet stream and the relationship between the NAO and winter precipitation in the HKK weakens.

References

Archer, D. R. and Fowler, H. J., 2004, Spatial and temporal variations in precipitation in the Upper Indus Basin, global teleconnections and hydrological implications, Hydrol. Earth. Syst. Sc., 8 (1), 47–61.

Hurrell, J. W., Kushnir, Y., Ottersen, G. and Visbeck, M., 2003: An Overview of the North Atlantic Oscillation, Geoph. Monog. Series, 134, 1–35.

Palazzi, E., von Hardenberg, J. and Provenzale, A., 2013, Precipitation in the Hindu-Kush Karakoram Himalaya: Observations and future scenarios, J. Geophys. Res., 118 (1), 85–100.

Syed, F. S., Giorgi, F., Pal, J. S. and King, M. P., 2006, Effect of remote forcings on the winter precipitation of central southwest Asia part 1: observations, Theor. Appl. Climatol., 86 (1-4), 147–160.

Yadav, R. K., Kumar, K. R. and Rajeevan, M., 2009, Increasing influence of ENSO and decreasing influence of AO/NAO in the recent decades over northwest India winter precipitation, J. Geophys. Res., 114 (D12), 112.

Wang, Y.-H., Magnusdottir, G., Stern, H., Tian, X. and Yu, Y., 2012, Decadal variability of the NAO: Introducing an augmented NAO index, Geophys. Res. Lett., 39 (21), L21 702.

The Tethys Himalaya in the Cretaceous/Paleocene: anorogenic evolution driven by Deccan-related uplift

Eduardo Garzanti[1], Xiumian Hu[2]

[1] Laboratory for Provenance Studies, Department of Earth and Environmental Sciences, Università di Milano-Bicocca, 20126 Milano, Italy, eduardo.garzanti@unimib.it
[2] State Key Laboratory of Mineral Deposits Research, School of Earth Sciences and Engineering, Nanjing University, Nanjing, China

The Cretaceous to Lower Paleocene succession of the Tethys Himalaya records an entirely anorogenic evolution that both began and ended with flood-basaltic eruptions. Uplift associated with emplacement of the Rajmahal Traps was followed by thermal subsidence and quasi-synchronous shelf drowning at the end of the Early Cretaceous (Garzanti, 1993; Hu et al., 2010). Widespread deposition of upper-bathyal foraminiferal oozes ensued. A similar cycle was repeated at the end of the Late Cretaceous. The widespread Campanian hiatus associated with re-suspension and faunal reworking was followed by a major pulse of terrigenous supply and drastic increase in accumulation rates. This major erosional event recorded across the Indian subcontinent is ascribed to magmatic upwelling at the base of the Indian lithosphere, begun around 80-75 Ma or even some Ma earlier. The shallowing-upward Maastrichtian succession of the Tethys Himalaya is capped by Lower Paleocene coastal quartzarenites testifying to rejuvenation of the Indian subcontinent in the south. Volcanic rock fragments and Cr-spinels virtually identical geochemically to Deccan spinels resisted the coupled effect of strong weathering at subequatorial latitudes and subsequent diagenetic dissolution, and are preserved throughout the Maastrichtian to Danian succession (Garzanti and Hu, 2014). This is "smoking-gun" evidence that detritus from Deccan lavas reached the passive margin of northern India. At the close of the Danian (~62 Ma), transgression of marine carbonates documents a synchronous drowning event all along the Tethys Himalaya. Thermal subsidence took place at the same time as India moved away from the magma source and Deccan volcanism eventually ceased. The sedimentary record of the northern Indian margin excludes any postulated orogenic event associated with ophiolite obduction, arc-continent or continent-continent collision in the Late Cretaceous, and indicates that Neotethys remained open until the Late Paleocene (Fig. 1).

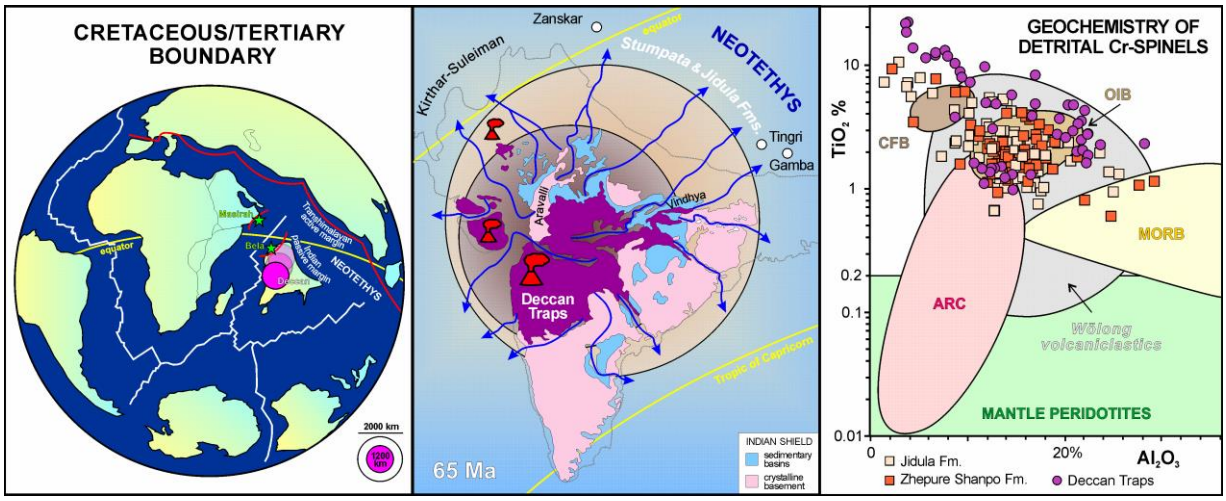

Figure 1. The simple anorogenic scenario for the Tethys Himalaya in the latest Cretaceous/earliest Paleocene (Cande and Stegman, 2011). Passive-margin evolution of northern India is indicated by stratigraphic and mineralogical data, while ophiolite obduction was taking place along the western transpressive boundary of the Indian plate (Gnos et al., 1997). Detrital Cr-spinels in Maastrichtian to Danian sandstones of the Tethys Himalaya are both derived first-cycle from Deccan basalts and recycled from Lower Cretaceous lavas and volcaniclastics (data for comparison from Kamenetsky et al., 2001, Melluso et al., 2010, and Hu et al., 2014).

Cite as: Garzanti, E. and Hu, X., 2014, The Tethys Himalaya in the Cretaceous/Paleocene: anorogenic evolution driven by Deccan-related uplift, in Montomoli C., et al., eds., proceedings for the 29th Himalaya-Karakoram-Tibet Workshop, Lucca, Italy.

References

Cande, S.C. and Stegman, D.R., 2011, Indian and African plate motions driven by the push force of the Reunion plume head, Nature, 475, 47-52.

Garzanti, E., 1993, Sedimentary evolution and drowning of a passive margin shelf (Giumal Group; Zanskar Tethys Himalaya, India): palaeoenvironmental changes during final break-up of Gondwanaland, in: Treloar P.J. and Searle M.P. (eds.), Himalayan tectonics, Geological Society London, Special Publications, 74, 277-298.

Garzanti, E. and Hu, X., 2014, Latest Cretaceous Himalayan tectonics: Obduction, collison or Deccan-related uplift? Gondwana Research, http://dx.doi.org/10.1016/j.gr.2014.03.010.

Gnos, E., Immenhauser, A. and Peters, T., 1997, Late Cretaceous/early Tertiary convergence between the Indian and Arabian plates recorded in ophiolites and related sediments, Tectonophysics, 271, 1-19.

Hu, X., Jansa, L., Chen, L., Griffin, W.L., O'Reilly, S.Y. et al., 2010, Provenance of Lower Cretaceous Wölong Volcaniclastics in the Tibetan Tethyan Himalaya: Implications for the final breakup of Eastern Gondwana, Sediment. Geol., 223, 193-205.

Hu, X., An, W., Wang, J., Garzanti, E. and Guo, R., 2014, Himalayan detrital chromian spinels and timing of Indus-Yarlung ophiolite erosion, Tectonophysics, 621, 60-68.

Kamenetsky, V.S., Crawford, A.J. and Meffre, S., 2001, Factors controlling chemistry of magmatic spinel: an empirical study of associated olivine, Cr-spinel and melt inclusions from primitive rocks, Journal of Petrology, 42, 655-671.

Melluso, L., de'Gennaro, R. and Rocco, I., 2010, Compositional variations of chromiferous spinel in Mg-rich rocks of the Deccan Traps, India, Journal of Earth System Science, 119, 343-363.

Isotope provenance of Eastern Himalayan rivers draining to the south into India, Nepal and Bhutan

L. Gemignani[1], J.R. Wijbrans[1], Y. Najman[2], P. van der Beek[3], G. Govin[2]

[1] Department of Earth Sciences, Faculty of Earth and Life Sciences VU University, Amsterdam, The Netherlands, l.gemignani@vu.nl
[2] University of Lancaster, Lancaster Environmental Centre, Lancaster, LA1 4YQ, UK
[3] ISTerre, University Joseph Fourier, Grenoble, France

The Himalayas represent a unique natural laboratory where the interactions between tectonics, erosion, climate and drainage evolution can be investigated. The purpose of this work is to understand, in collaboration with other PhD students and researchers collaborating in the iTECC Marie Curie Initial Training Network, the importance of processes involving the complex links and feedbacks between climate, tectonics and erosion.

The two syntaxes of the Himalaya (eastern and western) show anomalously fast recent exhumation compared to the rest of the Himalaya, as typified by mineral ages <10 Ma (Zeitler et al., in press). Various hypotheses and models have been proposed to explain this anomaly, for example those include coupling between tectonics and erosion, such as the Tectonic Aneurism model (Zeitler et al., 2001; Zeitler et al., in press), which calls on ductile upwelling of weak lower crust (Beaumont et al., 2001).

Understanding the timing of onset of this rapid exhumation is critical to informing these models. Bedrock studies suggest rapid exhumation since 4 Ma (Seward and Burg, 2008) or maybe 10 Ma. However, detrital studies (Ar-Ar micas, ZFT), using the record of material eroded from the syntaxis and preserved in the foreland basin, show no evidence of anomalously young grains and thus rapid exhumation throughout the duration of the sedimentary succession studied (Bracciali et al., 2012; Chirouze et al., 2013). However, both these detrital studies were conducted in regions distal to the syntaxes, and it is possible that downstream dilution may have affected the signal.

The purpose of this research is to investigate the potential effect of dilution on the detrital signal by 1) looking at how the detrital signal evolves downstream i.e. the degree to which the "young" grain signal is diluted at increasing distance from the source and 2) a comparison of ZFT and Ar-Ar mica ages from the same samples, to investigate whether there is any distinction in the dilution effect depending on mineral type.

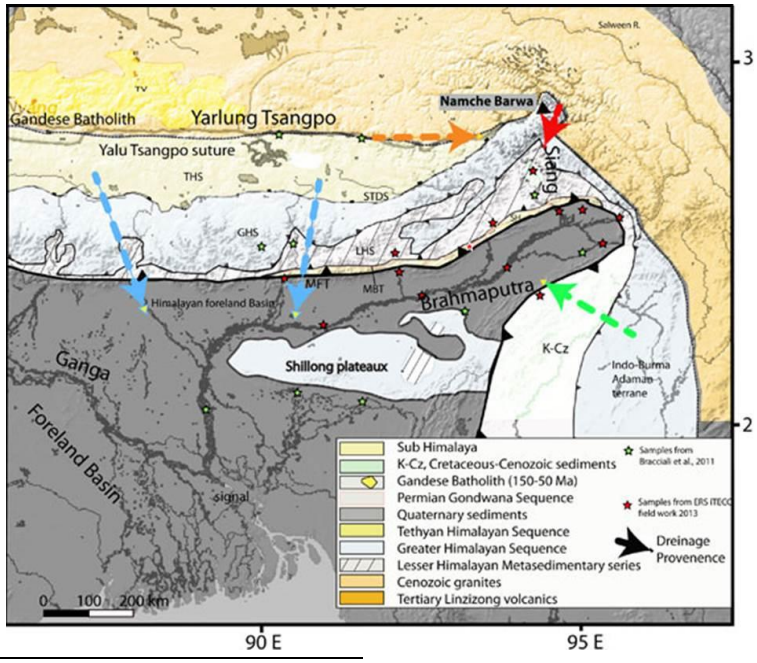

Figure 1. Regional tectonic map showing sampled geology and location of major rivers. The red stars indicates the location of the samples collected during the fieldwork. The arrows indicates the main provenance sediments into the Yarlung Tsangpo-Bramaputra River system. (modified after Chirouze et al., 2012).

Cite as: Gemignani, L. et al., 2014, Isotope provenance of Eastern Himalayan rivers draining to the south into India, Nepal and Bhutan, in Montomoli C., et al., eds., proceedings for the 29th Himalaya-Karakoram-Tibet Workshop, Lucca, Italy.

Building on the existing database, eleven samples from the Yarlung-Brahmaputra River system and from tributaries draining the Himalaya, the Arakan belt and the Shillong plateau have been collected in the Arunachal Pradesh and Assam regions of the North-east India (Fig. 1). We will analyse this potentially important aspect in detail, using high-resolution dating of micas of different grain sizes. To analyse smaller and younger grains, newly developed high-sensitivity multi-collection noble-gas mass spectrometry will be used. In this way, we will determine the extent to which dilution should be taken in to account when interpreting detrital signals, and also contribute further to our knowledge of exhumation ages in the source regions.

References

Beaumont, C. et al., 2001, Himalayan tectonics explained by extrusion of a low-viscosity crustal channel coupled to focused surface denudation, Nature, 414, 738-742.

Bracciali et al., 2012, Using Detrital Zircon, Rutile and White Mica Chronometry to Constrain Exhumation and Provenance of the Brahmaputra River in the Eastern Himalaya, Abstract T33C-2671 AGU fall meeting.

Chirouze, F. et al., 2013, Magnetostratigraphy of the Neogene Siwalik Group in the far eastern Himalaya: Kameng section, Arunachal Pradesh, India, Journal of Asian Earth Sciences, 44, 117-135.

Seward, D. and Burg, J.-P, 2008, Growth of the Namche Barwa Syntaxis and associated evolution of the Tsangpo Gorge: Constraints from structural and thermochronological data, Tectonophysics, 451, 282-289.

Zeitler, P.K. et al., 2001, Erosion, Himalayan geodynamics, and the geology of metamorphism, GSA Today, 11, 4-8.

Zeitler, P.K. et al., in press, Tectonics and topographic evolution of Namche Barwa and the easternmost Lhasa Block. Towards and improved understanding of uplift mechanisms and elevation history of the Tibetan Plateau, GSA Special Paper.

Along-strike strain variation and timing of deformation in the lower Himalayan metamorphic core, west-central Nepal

Rohanna Gibson[1], Laurent Godin[1], John M. Cottle[2], Dawn A. Kellett[3]

[1] Department of Geological Sciences and Geological Engineering, Queen's University, Kingston, ON K7L 3N6, Canada, rohanna.gibson@queensu.ca
[2] Department of Earth Science, University of California, Santa Barbara, CA 93106, USA
[3] Geological Survey of Canada, 601 Booth Street, Ottawa, ON K1A 0E8, Canada

Orogens are typically simplified as two-dimensional systems, downplaying potentially significant along-strike strain variation. In the Himalaya, along-strike variations in seismicity (Arora et al., 2012), topographic profile (Duncan et al., 2003), precipitation (Bookhagen and Burbank, 2006), collision rates (Larson et al., 1999), and crustal architecture (Goscombe et al., 2006; Yin, 2006) have been documented. Along-strike comparisons of the deformation history of the metamorphic core are lacking, despite the extensive debate surrounding the mechanism of its emplacement (Beaumont et al., 2001; Bollinger et al., 2006; Beaumont and Jamieson, 2010; Larson et al., 2010). Contrasting tectonic interpretations may reflect locally or regionally distinct pressure-temperature-time-deformation paths due to along-strike strain variation in the metamorphic core.

Our study examines how strain and the timing of deformation vary along-strike in the lower metamorphic core in west-central Nepal. The study area was selected due to documented along-strike variation in the thickness and regional strike of the metamorphic core, a wealth of existing structural and metamorphic data available for comparison along strike (Larson et al., 2010; Vannay and Hodges, 1996; Catlos et al., 2001; Martin et al., 2005; Carosi et al., 2007; Larson and Godin, 2009; Corrie and Kohn, 2011), and the possible presence of cross-strike basement structures (Godin and Harris, 2014) that could influence strain partitioning (Fig. 1). The lower metamorphic core is defined here as the 'Lower Greater Himalayan sequence', which includes lithotectonic units previously referred to as upper 'Lesser Himalaya' (Martin et al., 2005; Carosi et al., 2007), the base of which is the top-to-the-south reverse-sense Main Central thrust (MCT) (Sarle et al., 2008). This study investigates how the style and age of deformation vary along-strike of the lower metamorphic core, and attempts to reconcile disparate tectonic models and place constraints on three-dimensional orogenic models.

Along-strike analysis of the lower metamorphic core is based on fieldwork in the lower Dolpo and Annapurna foothills, west-central Nepal (Fig. 1). The base of the metamorphic core is a ~1-5 km thick top-to-the-south reverse-sense high strain zone; the lower boundary is mapped as the MCT. The immediate footwall rocks of the MCT are characterized by multiple cleavages, relic detrital grains, and an absence of shear-sense indicators. Hanging-wall rocks contain dynamically recrystallized minerals and predominantly top-to-the-south shear-sense indicators. Lower metamorphic core rocks typically exhibit a penetrative schistosity and down-dip mineral elongation lineation. From northwest to southeast in lower Dolpo, the schistosity shifts from moderately E-dipping to steeply NE-dipping; this shift corresponds to a more westerly-strike. In the Annapurna foothills, the schistosity gradually shifts from gently NNE-dipping in the west to moderately NE-dipping in the east with a WNW to NW strike. A slight increase in metamorphic grade and mylonitization in the MCT hanging-wall rocks corresponds with a decrease in the structural thickness of the high strain zone.

Quartz-rich tectonites from near the base of the lower metamorphic core are characterized by well-developed plane strain top-to-the-south quartz crystallographic preferred orientation fabrics, consistent with deformation temperatures of ~400-450ºC. The quartz petrofabrics are similar along strike, though samples from the central Annapurna foothills yield slightly more constrictional strain and higher apparent deformation temperatures. The minimum age of these quartz petrofabrics, as constrained by muscovite $^{40}Ar/^{39}Ar$ ages, ranges in the Annapurna foothills from ~6.8 in the west to ~4.1 Ma in the east. At a higher

Cite as: Gibson, R., et al., 2014, Along-strike strain variation and timing of deformation in the lower Himalayan metamorphic core, west-central Nepal, in Montomoli C., et al., eds., proceedings for the 29th Himalaya-Karakoram-Tibet Workshop, Lucca, Italy.

structural level, near the kyanite isograd, the muscovite $^{40}Ar/^{39}Ar$ age in the central Annapurna foothills is ~19.4 Ma, which decreases to the west (~13.0 Ma) and east (~5.3 Ma). The $^{232}Th/^{238}Pb$ ages and corresponding yttrium zonation of *in situ* monazite from samples along the kyanite isograd illustrate protracted prograde metamorphism in the Eocene-Oligocene followed by a Miocene retrograde metamorphic phase, with ages of each phase varying along-strike. The age of early prograde metamorphism is constrained with Th/Pb age peaks from zones of pre-garnet monazite crystallization; these ages range from ~39 Ma in lower Dolpo to ~31 and ~27 Ma in the western and eastern Annapurna foothills, respectively. The minimum age of peak metamorphism ranges, from western lower Dolpo to the eastern Annapurna foothills, from ~25 Ma to ~18 Ma. Retrograde metamorphic Th/Pb age peaks from post-garnet monazite zones yield ~19 to ~23 Ma from west to east in lower Dolpo, and ~21 to ~16 Ma from west to east in the Annapurna foothills.

Results indicate there is along-strike variability in the deformation and metamorphic history of the lower Himalayan metamorphic core. Variations in the style and timing of strain, thickness of the high strain zone, and timing of metamorphism have occurred. A thicker high strain zone correlates to more distributed strain, and relatively old monazite Th/Pb and muscovite $^{40}Ar/^{39}Ar$ ages. Variation in the metamorphic core proximal to the across-strike basement structure[17] include structural thinning, a shift in the regional strike, and a decrease in muscovite $^{40}Ar/^{39}Ar$ and monazite Th/Pb ages. These results illustrate the importance of incorporating along-strike variation into the interpretation of the Himalayan orogen and the potential influence of across-strike basement structures on strain partitioning.

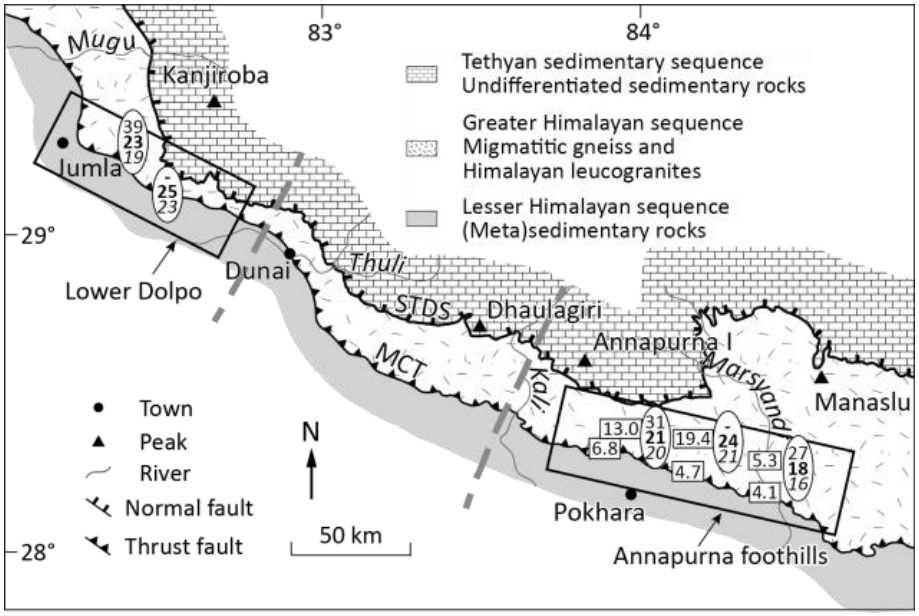

Figure 1. Simplified geologic map of west-central Nepal with field areas highlighted by black rectangles. STDS=South Tibetan Detachment System. Approximate muscovite $^{40}Ar/^{39}Ar$ (rectangle) and monazite $^{232}Th/^{238}Pb$ (ellipse) ages are listed at approximate sample location.

References

Arora, B.R., Gahalaut, V.K. and Kumar, N., 2012, Structural control on along-strike variation in the seismicity of the northwest Himalaya, J. Asian Earth Sci., 57, 15–24.

Beaumont, C. and Jamieson, R., 2010, Himalayan-Tibetan Orogeny: Channel Flow versus (Critical) Wedge Models, a False Dichotomy? U.S.G.S. Open-File Report 2010-1099.

Beaumont, C., Jamieson, R.A., Nguyen, M.H. and Lee, B., 2001, Himalayan tectonics explained by extrusion of a low-viscosity crustal channel coupled to focused surface denudation, Nature, 414, 738–742.

Bollinger, L., Henry, P. and Avouac, J., 2006, Mountain building in the Nepal Himalaya: Thermal and kinematic model, Earth Planet. Sci. Lett., 244, 58–71.

Bookhagen, B. and Burbank, D.W., 2006, Topography, relief, and TRMM-derived rainfall variations along the Himalaya, Geophys. Res. Lett., 33, L08405.

Carosi, R., Montomoli, C. and Visonà, D., 2007, A structural transect in the Lower Dolpo: Insights on the tectonic evolution of Western Nepal, J. Asian Earth Sci., 29, 407–423.

Catlos, E.J. et al., 2001, Geochronologic and thermobarometric constraints on the evolution of the Main Central Thrust, central Nepal Himalaya, J. Geophys. Res., 106, 16–177–16–204.

Corrie, S.L. and Kohn, M.J., 2011, Metamorphic history of the central Himalaya, Annapurna region, Nepal, and implications for tectonic models, Geol. Soc. Am. Bull., 123, 1863–1879.

Duncan, C., Masek, J. and Fielding, E., 2003, How steep are the Himalaya? Characteristics and implications of along-strike topographic variations, Geology, 31, 75–78.

Godin, L. and Harris, L.B., 2014, Tracking basement cross-strike discontinuities in the Indian crust beneath the Himalayan orogen using gravity data - relationship to upper crustal faults, Geophys. J. Int.

Goscombe, B.D., Gray, D.R. and Hand, M., 2006, Crustal architecture of the Himalayan metamorphic front in eastern Nepal, Gondwana Res., 10, 232–255.

Larson, K.M., Bürgmann, R., Bilham, R. and Freymueller, J.T., 1999, Kinematics of the India-Eurasia collision zone from GPS measurements, J. Geophys. Res., 104, 1077–1093.

Larson, K.P. and Godin, L., 2009, Kinematics of the Greater Himalayan sequence, Dhaulagiri Himal: implications for the structural framework of central Nepal, J. Geol. Soc., 166, 25–43.

Larson, K.P., Godin, L. and Price, R.A., 2010, Relationships between displacement and distortion in orogens: Linking the Himalayan foreland and hinterland in central Nepal, Geol. Soc. Am. Bull., 122, 1116–1134.

Martin, A.J., DeCelles, P.G., Gehrels, G.E., Patchett, P.J. and Isachsen, C., 2005, Isotopic and structural constraints on the location of the Main Central thrust in the Annapurna Range, central Nepal Himalaya, Geol. Soc. Am. Bull., 117, 926.

Searle, M.P. et al., 2008, Defining the Himalayan main central thrust in Nepal, J. Geol. Soc., 165, 523–534.

Vannay, J.-C. and Hodges, K.V., 1996, Tectonometamorphic evolution of the Himalayan metamorphic core between the Annapurna and Dhaulagiri, central Nepal, J. Metamorph. Geol., 14, 635–656.

Yin, A., 2006, Cenozoic tectonic evolution of the Himalayan orogen as constrained by along-strike variation of structural geometry, exhumation history, and foreland sedimentation, Earth-Sci. Rev., 76, 1–131.

Large-scale organization of carbon dioxide discharge in the Nepal Himalayas: Evidence of a 110-km-long facilitated pathway for metamorphic CO_2 release

Frédéric Girault[1,2], Frédéric Perrier[1], Mukunda Bhattarai[3], Bharat Prasad Koirala[3], Christian France-Lanord[4], Laurent Bollinger[5], Sudhir Rajaure[3], Jérôme Gaillardet[1], Monique Fort[6], Soma Nath Sapkota[3]

[1] Institut de Physique du Globe de Paris, Sorbonne Paris Cité, Univ. Paris Diderot, UMR 7154 CNRS, F-75005 Paris, France
[2] Currently at: Laboratoire de Géologie, École Normale Supérieure, UMR 8538 CNRS, F-75005 Paris, France (girault@biotite.ens.fr)
[3] National Seismological Centre, Department of Mines and Geology, Kathmandu, Nepal
[4] Centre de Recherches Pétrographiques et Géochimiques, CNRS-Univ. de Nancy, BP20 F-54501, France
[5] CEA, DAM, DIF, F-91297 Arpajon, France
[6] Département de Géographie, Sorbonne Paris Cité, Univ. Paris Diderot, UMR Prodig 8586 CNRS, F-75013, Paris, France

Convergent zones play an essential role in the global carbon dioxide (CO_2) balance of the Earth (Kerrick and Caldeira, 1998). In addition to their role of atmospheric CO_2 sink through weathering (Gaillardet et al., 1999), large orogens are also the location of the production and release of CO_2-rich fluids (Irwin and Barnes, 1980). Major active fault zones appear therefore as a dynamically complex system where fluid circulation, crustal permeability and possibly earthquake occurrence might be interrelated (Ingebritsen and Manning, 2010; Manga et al., 2012). The Himalayas offers a privileged natural laboratory where this essential dynamical coupling can be studied. High seismic activity is concentrated on a mid-crustal ramp located in the Main Central Thrust (MCT) zone on the Main Himalayan Thrust accommodating the 2 cm year^{-1} convergence (Ader et al., 2012), where fluid occurrence might explain the high electrical conductivity observed by magneto-telluric sounding (Lemonnier et al., 1999). Seasonal variations of seismicity (Bollinger et al., 2007) and deformation (Chanard et al., 2014) can be accommodated by surface hydrological forcing, possibly leading to fluid overpressures at depth. Direct evidence of the fluid release in the MCT zone has been given recently. First, the high alkalinity of hot springs was observed to contribute to tremendous CO_2 fluxes in the main rivers (Evans et al., 2004). The high carbon isotopic ratios of the hot springs suggested the presence of a metamorphic decarbonation source at depth and of massive CO_2 degassing (Becker et al., 2008; Evans et al., 2008). Second, direct evidence of CO_2 emission from the ground was discovered in the Syabru-Bensi hydrothermal system (SBHS), central Nepal (Perrier et al., 2009), where it was found to be associated with a radon-222 signature, a valuable asset for long-term monitoring (Girault et al., 2009), and was subsequently mapped in detail (Girault et al., 2014),. In this study, we present the results of systematic search and measurement of CO_2 release from the ground in the vicinity of other significant hot springs from western to eastern Nepal (Figure 1).

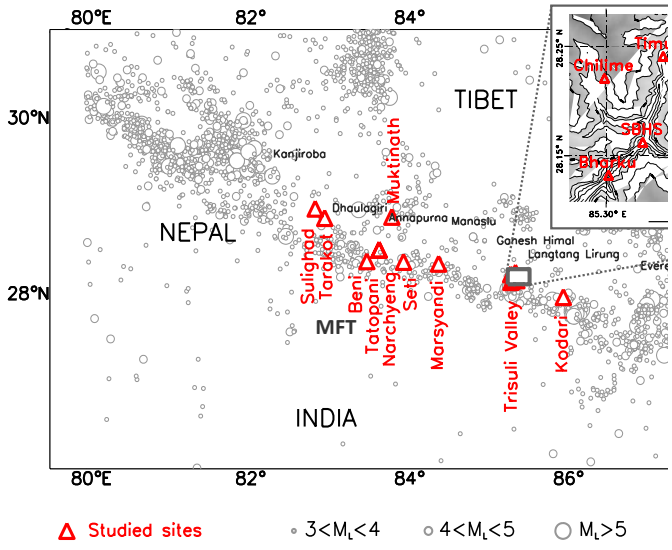

Figure 1. Overview of sites in the Nepal Himalayas. Main Central Thrust (MCT), Main Frontal Thrust (MFT) and highest summits (closed triangles) are shown. Earthquakes epicenters are taken from the 1995-2005 catalogue (Nepal National Seismological Centre). The inset shows location of sites in the upper Trisuli Valley. SBHS corresponds to the Syabru-Bensi hydrothermal system in central Nepal.

Cite as: Girault, F. et al., , 2014, Large-scale organization of carbon dioxide discharge in the Nepal Himalayas: Evidence of a 110-km-long facilitated pathway for metamorphic CO_2 release, in Montomoli C., et al., eds., proceedings for the 29th Himalaya-Karakoram-Tibet Workshop, Lucca, Italy.

Gaseous CO_2 and radon-222 (radioactive gas with half life of 3.8 d) release from the ground was investigated along the MCT zone in the Nepal Himalayas and quantified using the accumulation chamber technique. From >2200 CO_2 and >900 radon-222 flux measurements in the vicinity of 13 hot springs from western to central Nepal, we obtained total CO_2 and radon discharges varying from 10^{-3} to 1.6 mol s^{-1}, and from 20 to 1600 Bq s^{-1}, respectively. We observed a coherent organization at spatial scales of ≈10 km in a given region (Figure 2) (Girault et al., submitted): low CO_2 and radon discharges (Group III) around Pokhara (midwestern Nepal) and in the Bhote Kosi Valley (east Nepal); low CO_2 but large radon discharges (Group II) in Lower Dolpo (west Nepal); large CO_2 and radon discharges (Group I) in the upper Trisuli Valley (central Nepal).

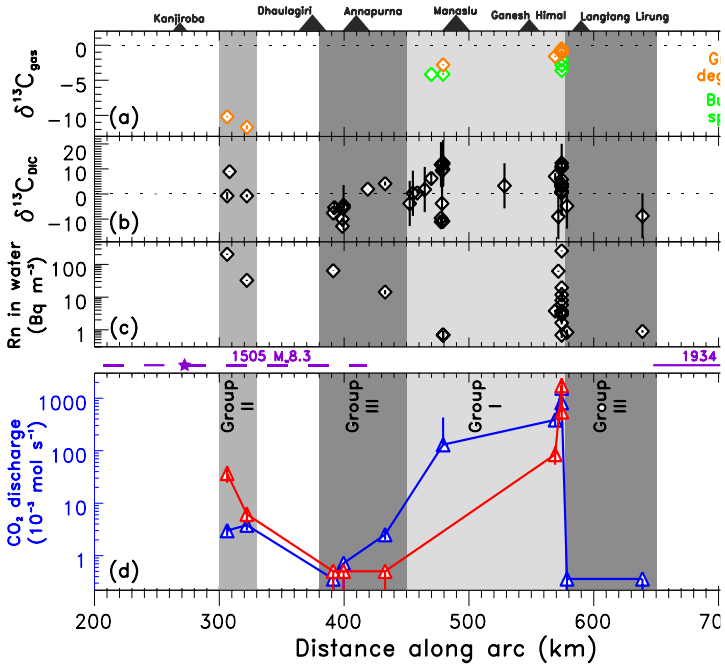

Figure 2. Characteristics of CO_2 degassing from the ground and from water along the Nepal Himalayan arc: (a) carbon isotope ratios of the gaseous CO_2 from the ground and from bubbles in springs, (b) carbon isotope ratios of water (dissolved inorganic carbon), (c) radon concentration in spring waters, and (d) CO_2 and radon discharges from the ground. Data include original and published works. Epicenter and rupture length of the two last megaquakes (1505 and 1934) are displayed.

This large-scale organization suggests different gas transport mechanisms. While the simultaneous degassing of dissolved CO_2 and radon from hot spring waters can be considered in Lower Dolpo, in the upper Trisuli Valley, by contrast, the CO_2 and radon discharge can likely be the evidence at the surface of a gaseous-dominated transport through a large-scale fault network (Girault and Perrier, 2014). A 110-km-long CO_2-producing segment, with high carbon isotopic ratios indicating most likely metamorphic decarbonation, is thus evidenced from 84.5°E to 85.5°E, which suggests interactions between geological conditions, crustal permeability, and, possibly, large Himalayan earthquakes. This hypothesis needs to be tested in detail. First, we need a better understanding of the mechanisms producing metamorphic CO_2 in the Himalayas (Groppo et al., 2013). Then, we need a more comprehensive mapping of CO_2 emission in the Himalayas.

References

Ader, T. et al., 2012, Convergence rate across the Nepal Himalaya and interseismic coupling on the Main Himalayan Thrust: Implications for seismic hazard, J. Geophys. Res., 117, B04403.

Becker, J.A., Bickle, M.J., Galy, A. and Holland, T.J.B., 2008, Himalayan metamorphic CO_2 fluxes: Quantitative constraints from hydrothermal springs, Earth Planet. Sci. Lett., 265, 616-629.

Bollinger, L. et al., 2007, Seasonal modulation of seismicity in the Himalaya of Nepal, Geophys. Res. Lett., 34, L08304.

Chanard, K., Avouac, J.-P., Ramilien, G. and Genrich, J., 2014, Modeling deformation induced by seasonal variations of continental water in the Himalaya region: Sensitivity to Earth elastic structure, J. Geophys. Res., 119, DOI: 10.1002/2013JB010451.

Evans, M.J., Derry, L.A. and France-Lanord, C., 2004, Geothermal fluxes of alkalinity in the Narayani river system of central Nepal, Geochem. Geophys. Geosyst., 5(8), Q08011.

Evans, M.J., Derry, L.A. and France-Lanord, C., 2008, Degassing of metamorphic carbon dioxide from the Nepal Himalaya, Geochem. Geophys. Geosyst., 9, Q04021.

Gaillardet, J., Dupré, B., Louvat, P. and Allègre, C.J., 1999, Global silicate weathering and CO_2 consumption rates deduced from the chemistry of large rivers, Chem. Geol., 159, 3-30.

Girault, F. and Perrier, F., 2014, The Syabru-Bensi hydrothermal system in central Nepal: 2. Modeling and significance of the radon signature, J. Geophys. Res. Solid Earth, 119, doi:10.1002/2013JB010302.

Girault, F., Koirala, B.P., Perrier, F., Richon, P. and Rajaure, S., 2009, Persistence of radon-222 flux during monsoon at a geothermal zone in Nepal, J. Environ. Radioact., 100, 955-964.

Girault, F. et al., 2014, The Syabru-Bensi hydrothermal system in central Nepal: 1. Characterization of carbon dioxide and radon fluxes, J. Geophys. Res. Solid Earth, 119, doi:10.1002/2013JB010301.

Girault, F. et al., submitted, Large scale organization of CO_2 discharge in the Nepal Himalayas, Geophys. Res. Lett.

Groppo, C., Rolfo, F., Castelli, D. and Connolly, J.A.D., 2013, Metamorphic CO_2 production from calc-silicate rocks via garnet-forming reactions in the CFAS–H2O–CO2 system, Contrib. Mineral. Petrol., 166, 1655-1675.

Ingebritsen, S.E. and Manning, C.E., 2010, Permeability of the continental crust: dynamic variations inferred from seismicity and metamorphism, Geofluids, 10, 193-205.

Irwin, W.P. and Barnes, I., 1980, Tectonic relations of CO_2 discharges and earthquakes, J. Geophys. Res., 85, 3115-3121.

Kerrick, D.M. and Caldeira, K., 1998, Metamorphic CO_2 degassing from orogenic belts, Chem. Geol., 145, 213-232.

Lemonnier, C. et al., 1999, Electrical structure of the Himalaya of Central Nepal: high conductivity around the mid-crustal ramp along the MHT, Geophys. Res. Lett., 26(21), 3261-3264.

Manga, M. et al., 2012, Changes in permeability caused by transient stresses: Field observations, experiments, and mechanisms, Rev. Geophys., 50, RG2004.

Perrier, F. et al., 2009, A direct evidence for high carbon dioxide and radon-222 discharge in Central Nepal, Earth Planet. Sci. Lett., 278, 198-207.

Tracking basement cross-strike discontinuities in the Indian crust beneath the Himalayan orogen using gravity data – relationship to upper crustal faults

Laurent Godin[1], Lyal B. Harris[2]

[1] Department of Geological Sciences & Geological Engineering, Queen's University, Kingston, ON K7L 3N6, Canada, godinl@queensu.ca
[2] Institut national de la recherche scientifique, Centre – Eau Terre Environnement, 490 de la Couronne, Quebec City, QC G1K 9A9, Canada

The Himalaya is the result of the on-going convergence and collision of India and Asia, two plates with complex and protracted geological evolutions. The internal configuration and processes that govern the rise of the Himalaya and Tibetan Plateau are crucial to understand continental collision zones. However, knowledge of the prior configuration of the colliding plates is equally important, since inherited (pre-orogenic/basement) structures can undeniably influence the development of the orogenic architecture throughout the orogen's cycle of collision and eventual collapse. Three northeast-trending palaeotopographic ridges of faulted Precambrian Indian basement underlie the Ganga Basin south of the Himalaya (Oil and Natural Gas Commission 1968; Valdiya 1976; Gahalaut & Kundu, 2012). Our study (Godin & Harris, 2014) illustrates a crustal-scale fault origin for these ridges and succeeds in determining how far north beneath the Himalayan system they extend and how they ultimately govern the location of upper crustal faults in southern Tibet.

Spectrally filtered EGM2008 Bouguer gravity data and edges in its horizontal gradient at different source depths ('gravity worms') over northern Peninsular India, the Himalaya, and southern Tibet reveal several continuous Himalayan cross-strike discontinuities interpreted to represent crustal faults (Fig. 1). Gravity lineaments in Peninsular India coincide with edges of the Precambrian basement ridges and megakinks up to 100 km wide develop in foreland cover sequences between the interpreted basement faults. The interpreted basement faults project northward beneath the Himalayan system and southern Tibet. Our results suggest that several active Himalayan cross-strike faults, such as the ones related to many graben in southern Tibet, are rooted in the underplated Indian lower crust or step *en échelon* along interpreted basement faults. Our interpretation thus suggests that south Tibet graben are spatially related to deep-seated crustal-scale faults rooted in the underplated Indian crust. These major discontinuities partition the Himalayan range into distinct zones, and could ultimately contribute to lateral variability in tectonic evolution along the orogen's strike.

References

Godin, L. and Harris, L.B., 2014, Tracking basement cross-strike discontinuities in the Indian crust beneath the Himalayan orogen using gravity data – relationship to upper crustal faults, *Geophys. J. Int*., **197** doi:10.1093/gji/ggu131.

Gregory, L.C., Meert, J.G., Pradhan, V., Pandit, M.K., Tamrat, E. et al., 2006, A paleomagnetic and geochronologic study of the Majhgawan kimberlite, India: Implications for the age of the Upper Vindhyan Supergroup, *Precam. Res*., **149**, 65-75.

Gahalaut, V.K. and Kundu, B., 2012, Possible influence of subducting ridges on the Himalayan arc and on the ruptures of great and major Himalayan earthquakes, *Gondwana Res*., **21**, 1080–1088.

Masun, K, Sthapak, A.V., Singh, A., Vaidya, A. and Krishna C., 2009, Exploration history and geology of the diamondiferous ultramafic Saptarshi intrusions, Madhya Pradesh, India, *Lithos*, **112S**, 142–154.

Oil and Natural Gas Commission, India, 1968, Tectonic Map of India, eds Negi, B.S. & Eremenko, N.A., Dehra Dun, India.

Rao, N.C., 2006, Mesoproterozoic diamondiferous ultramafic pipes at Majhgawan and Hinota, Panna area, central India: Key to the nature of sub-continental lithospheric mantle beneath the Vindhyan basin, *J. Earth Syst. Sci*., **115**, 161-183.

Valdiya, K.S., 1976, Himalayan transverse faults and folds and their parallelism with subsurface structures of north Indian planes, *Tectonophysics*, **32**, 353–386.

Cite as: Godin, L. and Harris, L.B., 2014, Tracking basement cross-strike discontinuities in the Indian crust beneath the Himalayan orogen using gravity data – relationship to upper crustal faults, in Montomoli C., et al., eds., proceedings for the 29th Himalaya-Karakoram-Tibet Workshop, Lucca, Italy.

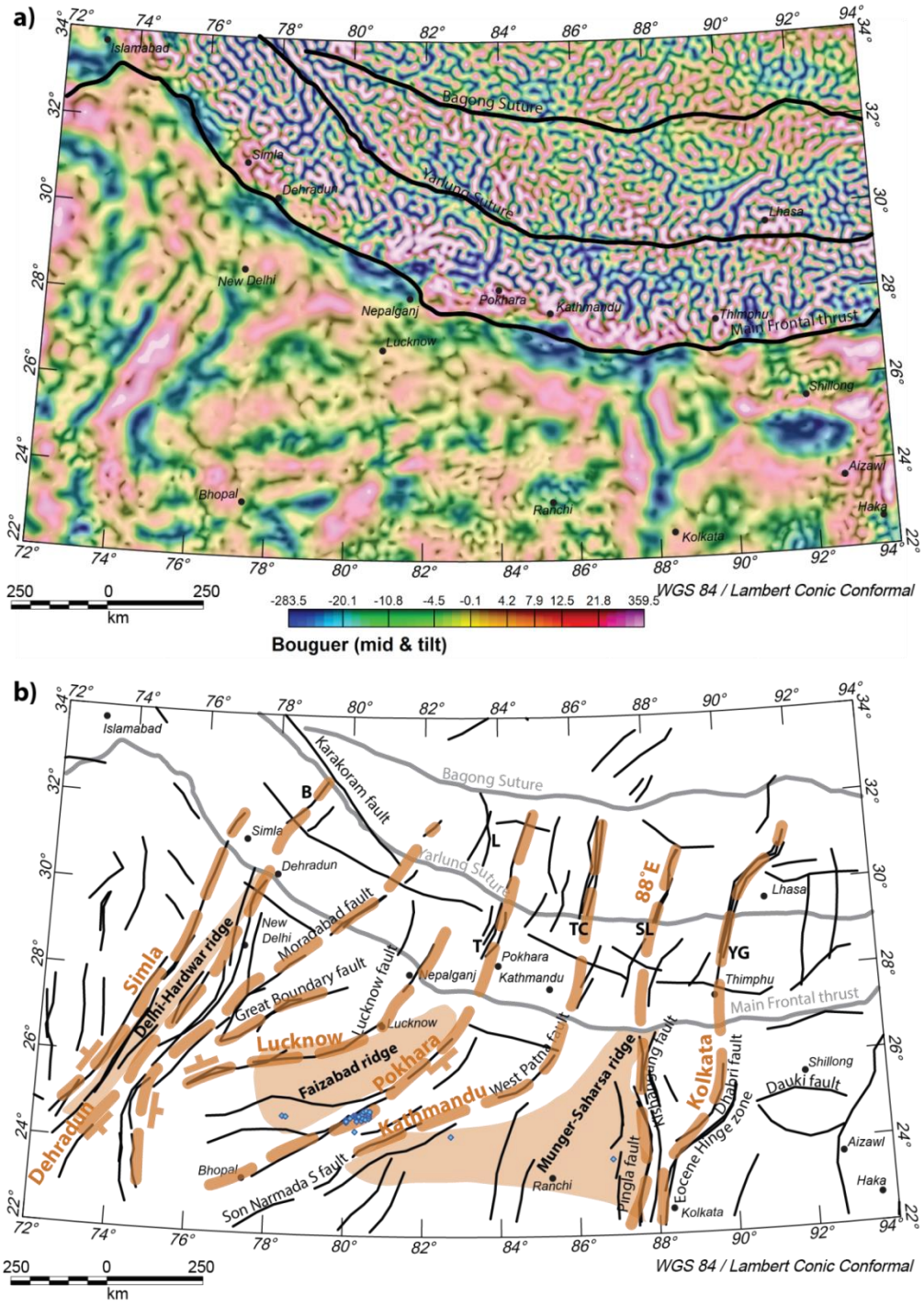

Figure 1. (**a)** Bouguer gravity map with high-frequency noise removed and data isolated to show the 'mid-' wavelength component only, on which a tilt angle enhancement was overlain. **(b)** Map showing location of the three Indian basement ridges, major graben systems developed in southern Tibet (B, Burang; L: Lunggar; TC: Tangra Yum Co; T, Thakkhola; SL, Senza-Laze; YG, Yadong-Gulu), and traces of the most important lineaments interpreted from the 'mid-' and 'long-' wavelength components of the Bouguer gravity data (black lines). The dashed light brown lines are interpreted as major cross-strike Indian basement lineaments connecting underplated Indian faults with upper crustal graben faults developed on the overlying crust north of Main Frontal thrust. Dip directions are indicated based on worm data; lineaments without one are interpreted to represent near vertical discontinuities. Blue diamonds locate known late Mesoproterozoic kimberlites and lamproites (Gregory et al. 2006; Rao 2006; Masun et al. 2009).

Farwestern Tibet: evolution of the relief since Oligo-Miocene times, from sedimentology and low-temperature thermochronometry

Loraine Gourbet [1], Gweltaz Mahéo [1], Philippe Hervé Leloup [1], Philippe Sorrel [1], David L. Shuster [2], Jean-Louis Paquette [3], Frédéric Quillévéré [1]

[1] Laboratoire de géologie de Lyon, UMR 5276, UCB Lyon 1 – ENS Lyon, Villeurbanne, France, loraine.gourbet@ens-lyon.fr
[2] Department of Earth and Planetary Science, UC Berkeley -and- Berkeley Geochronology Center, CA, USA
[3] Laboratoire Magmas et Volcans, UMR6524, Clermont-Ferrand, France

Western Tibet, between the Karakorum fault and the Gozha-Longmu Co fault system, is internally drained and has a 2-km-amplitude relief with km-large valleys and several peaks higher than 6000 m, as shown on Figure 1. These features differ from central Tibet, which has lower relief and mean elevation, and from southeastern Tibet, where the strong relief is due to river incision. Western Tibet relief is not systematically associated with active faults. This raises the question of the origin of a strong relief zone with no connection with major rivers, within the Tibetan plateau.

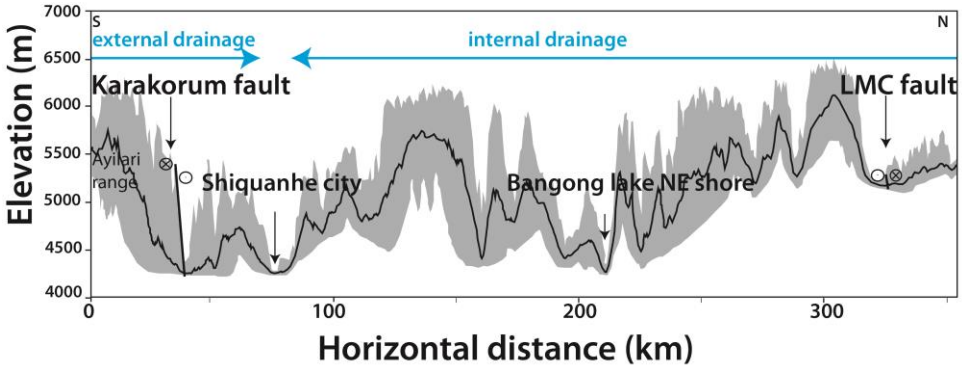

Figure 1. S-N topographic profile across Western Tibet. Grey envelope shows minimum and maximum elevations; mean elevation is shown by the black line. LMC : Lungmu Co strike-slip fault system. The external drainage area is connected to the Indus river.

We investigate the Oligocene-Miocene morphology evolution in the Lungmu Co - Rutog - Shiquanhe area by constraining the erosion history: its spatial distribution, timing, and rates. To do so, we combined mapping tertiary detrital sediments using field data and satellite imaging, and a sedimentology and geochronology analysis. Erosion rates are also investigated through exhumation reconstructions based on low-temperature thermochronometry. We performe a (U-Th-Sm)/He and $^{4}He/^{3}He$ study on apatites from a vertical profile in a granodiorite pluton south of the Bangong lake.

Tertiary continental strata (or red beds) lithology indicates a proximal, detrital fan depositional environment. U-Pb dating was performed *in situ* by LA-ICPMS on zircons from trachytic flows interbedded within the red beds, and indicates a deposition age range between 24.3 +/- 1.1 and 22.6 +/- 1.4 Ma. These results are similar to a previous $^{39}Ar/^{40}Ar$ dating by Kapp et al., 2003, and show that a detrital sedimentation coming from a local relief occurred at that time. Continental deposits are mostly distributed on flanks of km-large, 1000m deep valleys and seem to fill a palaeorelief formed by Cretaceous-Permian sediments. This suggests that the main valleys were already formed by the Oligocene.

Apatites cooling age range from 13 to 22 Ma, as shown on Figure 2. Age-elevation relationship indicate an apparent exhumation rate of 70 m/Ma, and modelled thermal histories based on AHe ages and $^{4}He/^{3}He$ data suggest that erosion rates were already low during the early Miocene.

Cite as: Gourbet, L., Mahéo, G., Leloup, P.H., Sorrel, P., Shuster, D.L., Paquette, J.-L., and Quillévéré F., 2014, Farwestern Tibet: evolution of the relief since Oligo-Miocene times, from sedimentology and low-temperature thermochronometry, in Montomoli C., et al., eds., proceedings for the 29th Himalaya-Karakoram-Tibet Workshop, Lucca, Italy.

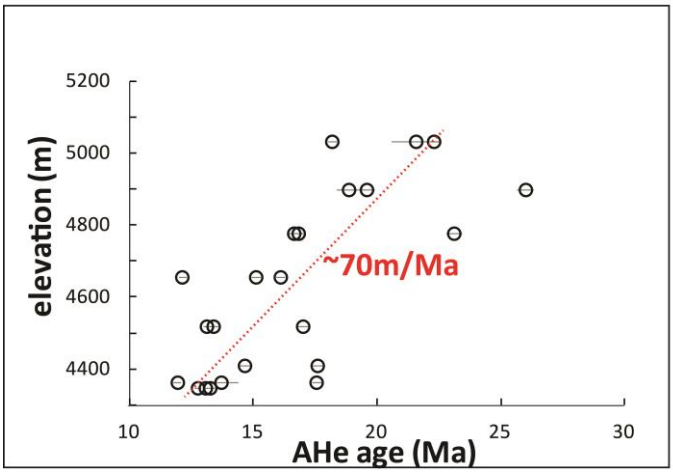

Figure 2. Apatites (U-Th-Sm)/He cooling ages from 8 granodiorite samples from an elevation profile south from the Bangong lake. Each open circle corresponds to a single apatite grain; grains at the same elevation come from the same sample. Ages at 23 and 26 Ma likely reflect U-rich inclusions inside the crystals. Grey horizontal lines are analytical errors. Linear regression through the median ages is shown by the red dotted line.

The modern 2-km amplitude relief appears to be incompatible with present day arid climate and very low erosion conditions. Therefore, we suggest that today's internally drained farwestern Tibet was externally drained until late Oligocene, and experienced significant fluvial incision. The relief carved by the incision was then preserved, presumably because the offset of the Karakorum fault partly blocked the palaeo-Indus drainage system.

References

Kapp P., Murphy M.A.,Yin A., and Harrison T.M., 2003, Mesozoic and Cenozoic tectonic evolution of the Shiquanhe area of western Tibet, Tectonics, 22, doi:10.1029/2001TC001332.

Constraining the timing of exhumation of the Eastern Himalayan syntaxis, from a study of the palaeo-Brahmaputra deposits, Siwalik Group, Arunachal Pradesh, India

Gwladys Govin[1], Yani Najman[1], Peter van der Beek[2], Ian Millar[3], Matthias Bernet[2], Guillaume Dupont-Nivet[4], Jan Wijbrans[5], Lorenzo Gemignani[5], Natalie Vögeli[2], Pascale Huyghe[2]

[1] Lancaster Environment Centre, Lancaster University, UK, g.govin1@lancaster.ac.uk
[2] Institut des Sciences de la Terre, Université Joseph Fourier, Grenoble, France
[3] NERC Isotope Geosciences Laboratory, Keyworth, UK
[4] Géosciences Rennes UMR-CNRS, France
[5] VU University Amsterdam, Faculty of Earth and Life Sciences, Netherlands

The evolution of Himalayan syntaxes is debated: they have been subjected to anomalously young (<10 Ma) high grade metamorphism, melting and unusually high rates of exhumation (~10mm/yr), compared to the main arc of the range where peak metamorphism / melting occurred in the Early Miocene and exhumation rates of ca 2mm/yr are more common (Rasmus et al., 2004). The history of the young metamorphism and rapid exhumation of the eastern syntaxis is debated. Bedrock studies have been interpreted to imply rapid exhumation since either 3-4 Ma (Seward and Burg, 2008) or 8-10 Ma (Zeitler et al., in press). However, the earlier history of the sampled region is removed by erosion and should be preserved in the sedimentary record. Bracciali et al. (2012) focused on distal detrital deposits and suggested a much more recent onset, during the Quaternary.

A number of models have been proposed to explain the syntaxial evolution, supporting different controlling influences, from lithospheric channel flow, to tectonic-surface process interactions.

Ductile extrusion of weak lower crust from beneath Tibet by "channel flow" (Beaumont et al., 2001) is a process that has been proposed to account for the outward growth of the plateau to the east (Clark and Royden, 2000), exhumation of the Higher Himalaya in the Miocene when coupled with high erosion rates, and could be responsible for rapid exhumation of the syntaxis (Booth et al., 2009). Ehlers and Bendick (2013) propose that initiation of rapid and localised exhumation at subduction arc terminations may result from the 3D geometry imposed by subducting curved shells at such locations. Clark and Bilham (2008) evoke a change in regional stress along the India-Asia-Burma plate boundary, perhaps due to the introduction of denser (oceanic and transitional crust) material into the eastern part of the boundary late in the orogen's history. Zeitler et al. (2001) consider that exhumation of the syntaxis is driven by surface processes.

In order to understand how and why the syntaxis formed, this project aims to better constrain the onset of exhumation of the Namche Barwa using the proximal detrital record of material eroded from the syntaxis by the paleo-Brahmaputra. We analyse the sedimentary record to have access to earlier erosion products than preserved in the bedrock itself, in a proximal location. The Remi River section, in the Siwalik Group, is located directly downstream of the syntaxis and therefore is the most likely location to contain these sediments. Sediment provenance is characterized by U-Pb dating on detrital zircons, which allows specifically documenting an Indus-Yarlung suture-zone (and therefore paleo-Brahmaputra) provenance.

Detrital U-Pb rutile, zircon fission track and Ar/Ar mica dating is used to document rapid exhumation. When ages of the youngest population for all analysis types are essentially the same (stacked thermochronological ages), a period of very rapid exhumation at this time is indicated.

Depositional ages are determined through magnetostratigaphic dating of the Upper and Middle Siwaliks in the Remi section. Comparison of the detrital mineral cooling ages with their host sediment depositional age will allow us to determine the lag time and then exhumation rates.

Preliminary results will be discussed; they better constrain the period of rapid exhumation history of the syntaxis and will better inform the crustal deformation models presented above.

Cite as: Govin, G. et al., 2014, Constraining the timing of exhumation of the Eastern Himalayan syntaxis, from a study of the palaeo-Brahmaputra deposits, Siwalik Group, Arunachal Pradesh, India, in Montomoli C., et al., eds., proceedings for the 29th Himalaya-Karakoram-Tibet Workshop, Lucca, Italy.

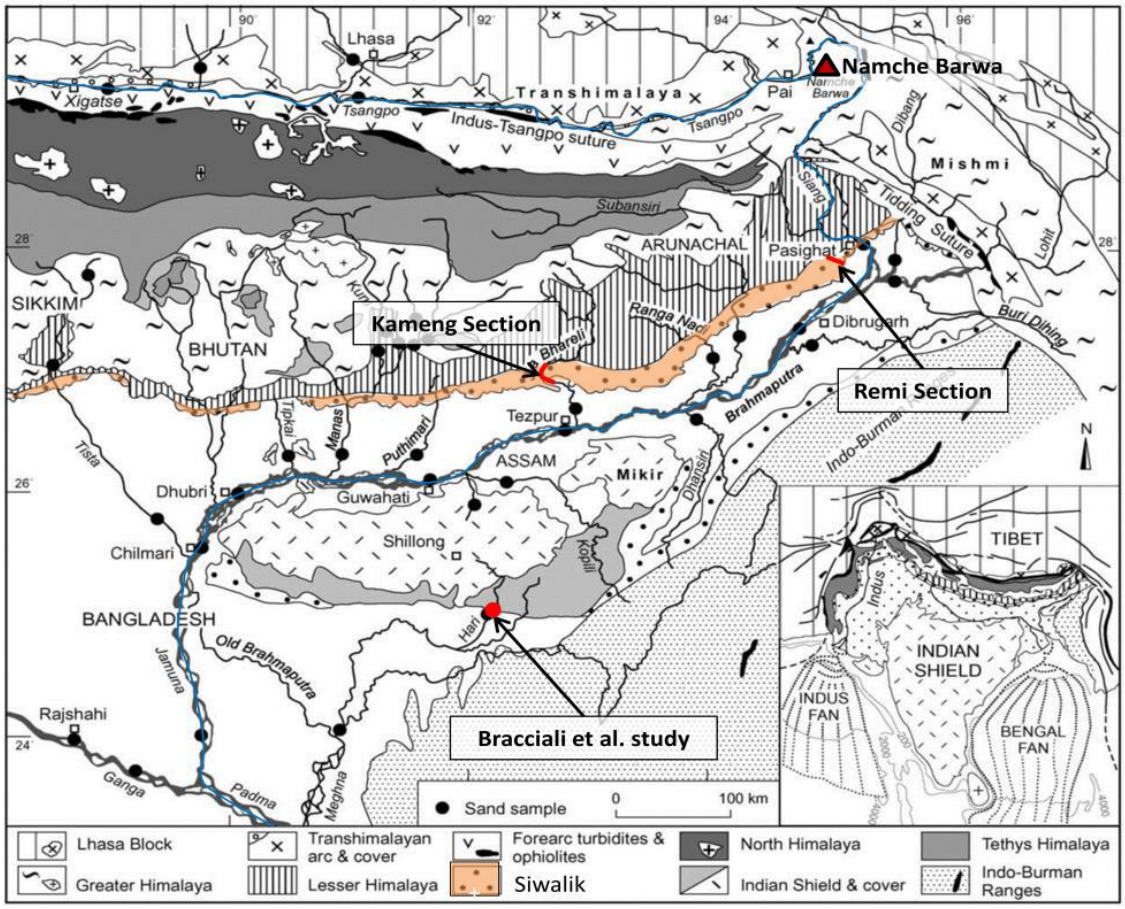

Figure 1. Geological map of the eastern syntaxis, Chirouze et al. (2012) and Bracciali et al. (2012) study locations, after Garzanti et al. (2004).

References

Rasmus, C., Thiede, R.C., Bookhagen, B., et al., 2004, Climatic control on rapid exhumation along the Southern Himalayan Front, Earth and Planetary Science Letters, 222, 791-806.

Seward, D. and Burg, J.-P., 2008, Growth of the Namche Barwa Syntaxis and associated evolution of the Tsangpo Gorge: Constraints from structural and thermochronological data, Tectonophysics, 451(1-4), 282-289.

Zeitler, P.K., Meltzer, A.S. and Brown, L., in press, Tectonics and topographic evolution of Namche Barwa and the easternmost Lhasa Block. Towards and improved understanding of uplift mechanisms and elevation history of the Tibetan Plateau, GSA Special Paper.

Bracciali, L., Parrish, R., Najman, Y. et al., 2012, Using Detrital Zircon, Rutile and White Mica Chronometry to Constrain Exhumation and Provenance of the Brahmaputra River in the Eastern Himalaya, Abstract T33C-2671 AGU Fall Meeting.

Beaumont, C., Jamieson, R.A., Nguyen, M.H., et al., 2001, Himalayan tectonics explained by extrusion of a low-viscosity crustal channel coupled to focused surface denudation, Nature, 414(6865), 738-742.

Clark, M.K. and Royden, L.H., 2000, Topographic ooze: Building the eastern margin of Tibet by lower crustal flow, Geology, 28(8), 703-706.

Booth, A.L., Chamberlain C.P., et al., 2009, Constraints on the metamorphic evolution of the eastern Himalayan syntaxis from geochronologic and petrologic studies of Namche Barwa, Geological Society of America Bulletin, 121(3-4), 385-407.

Ehlers, T.A. and Bendick R., 2013, "Bottom up" subduction geometry initiation of extreme localised exhumation at orogeny snytaxes, GSA Abstracts with Programs, 45(7), 222.

Clark, M.K. and Bilham, R., 2008, Miocene rise of the Shillong Plateau and the beginning of the end for the Eastern Himalaya, Earth and Planetary Science Letters, 269(3-4), 336-350.

Zeitler, P.K., Meltzer, A.S., Koons, et al., 2001, Erosion, Himalayan Geodynamics and the geomorphology of metamorphism, GSA Today, January 4-9.

Chirouze, F., Dupont-Nivet, G., Huyghe, P., et al., 2012, Magnetostratigraphy of the Neogene Siwalik Group in the far eastern Himalaya: Kameng section, Arunachal Pradesh, India, Journal of Asian Earth Sciences, 44, 117-135.

Garzanti, E., Vezzoli, G., Andó, S., et al., 2004, Sediment composition and focused erosion in collision orogens: the Brahmaputra case, Earth Planet. Sci. Lett., 220, 157-174.

Metamorphic CO_2 production in scapolite-bearing calc-silicate rocks from the upper Greater Himalayan Sequence (eastern Nepal Himalaya)

Chiara Groppo[1], Franco Rolfo[1,2], Pietro Mosca[1], Daniele Castelli[1]

[1] Department of Earth Sciences, University of Torino, Torino, I-10125, Italy, chiara.groppo@unito.it
[2] IGG – CNR, Torino, I-10125, Italy

The "long-term carbon cycle" operates over millions of years and involves the slow exchange of carbon between rocks and the surficial system; the volume of CO_2 involved in these processes is still far from being constrained. So far, the degassing flux was mainly estimated based on the flux emitted by volcanoes in different geodynamic contexts, and additionally include carbon from the mantle and carbon degassed from subduction zones. This estimated flux does not take into account CO_2 derived from orogenic zones, where organic rich sediments and limestone may be buried at depths at which CO_2 is formed by metamorphic reactions. However, recent studies suggest that metamorphic degassing from active collisional orogens supplies a significant fraction of the global solid-Earth derived CO_2 to the atmosphere, thus playing a fundamental role, even in today's Earth's carbon cycle (Gaillardet and Galy, 2008; Evans, 2011; Skelton, 2011).

In order to test if calc-silicate rocks may act as metamorphic CO_2-source rocks, a petrologic study of K-feldspar + scapolite -bearing calc-silicate rocks from eastern Nepal Himalaya has been performed. These rocks are hosted in anatectic kyanite-sillimanite- bearing gneisses (i.e. Barun Gneiss, see Groppo et al., 2012) and often occur as tens to hundreds of meter thick, folded or boudinated, levels occasionally associated to layers of impure marbles. The transition between the hosting paragneiss and the calc-silicate granofels is generally gradual and is characterized by the progressive disappearance of biotite, the appearance of clinopyroxene and the modal increase of plagioclase. This suggest that calc-silicate rocks derive from former marly intercalations within a thick sedimentary sequence.

Mineral assemblage consists of K-feldspar + clinopyroxene + scapolite + calcite + plagioclase + quartz ± zoisite (Fig. 1a, b), and later epidote and green amphibole. Clinopyroxene often shows oriented inclusions of phlogopite + scapolite + calcite ± muscovite ± quartz (Fig. 1e), whereas zoisite includes scapolite + quartz + calcite + Na-rich plagioclase (Fig. 1c, d) and is intergrown with K-feldspar and Ca-rich plagioclase. Clinopyroxene is often partially replaced by later green Ca-amphibole ± epidote, whereas scapolite is locally partially replaced by symplectitic aggregates of plagioclase + calcite (Fig. 1f). In addition to the ubiquitous titanite, a strongly pleochroic allanite and a bluish to colourless tourmaline (Fig. 1a) locally occur, whereas graphite is always absent.

The K-feldspar + scapolite -bearing calc-silicate rocks can be modelled in the NKCMAS-CO_2-H_2O system, including plagioclase and scapolite solid solutions, in addition to the fluid of variable composition. The results of petrologic modelling suggest that most of the key-microstructures in the studied rocks correspond to invariant assemblages in the classical T-XCO_2 grids. In such a complex system, the use of mixed-volatile phase diagram projections (in which the volatile composition of the system is projected onto the P–T coordinate frame: Connolly and Trommsdorff, 1991; Castelli et al., 2007; Groppo et al., 2013), is the best approach for simultaneously considering the effects of the three variables P, T and X_{fluid} on phase relations; fluid-present univariant curves in a mixed-volatile P–T projection correspond to invariant points in the correspondent isobaric T–XCO_2 sections.

Preliminary petrologic data demonstrates that K-feldspar + scapolite -bearing calc-silicate rocks may act as CO_2-source during prograde heating, releasing internal-derived CO_2-rich fluids (XCO_2=0.5-0.6) through clinopyroxene, K-feldspar and zoisite -forming, and scapolite -consuming, reactions such as:
Qtz + Cal + Mu + Scp = Zo + Pl + Kfs + F
Qtz + Phl + Scp + Zo + Cal = Cpx + Kfs + Pl + F
Mu + Scp + Phl + Qtz + Zo = Cpx + Kfs + Pl + F

Cite as: Groppo, C., Rolfo, F., Mosca, P. and Castelli, D., 2014, Metamorphic CO_2 production in scapolite-bearing calc-silicate rocks from the upper Greater Himalayan Sequence (eastern Nepal Himalaya), in Montomoli C., et al., eds., proceedings for the 29th Himalaya-Karakoram-Tibet Workshop, Lucca, Italy.

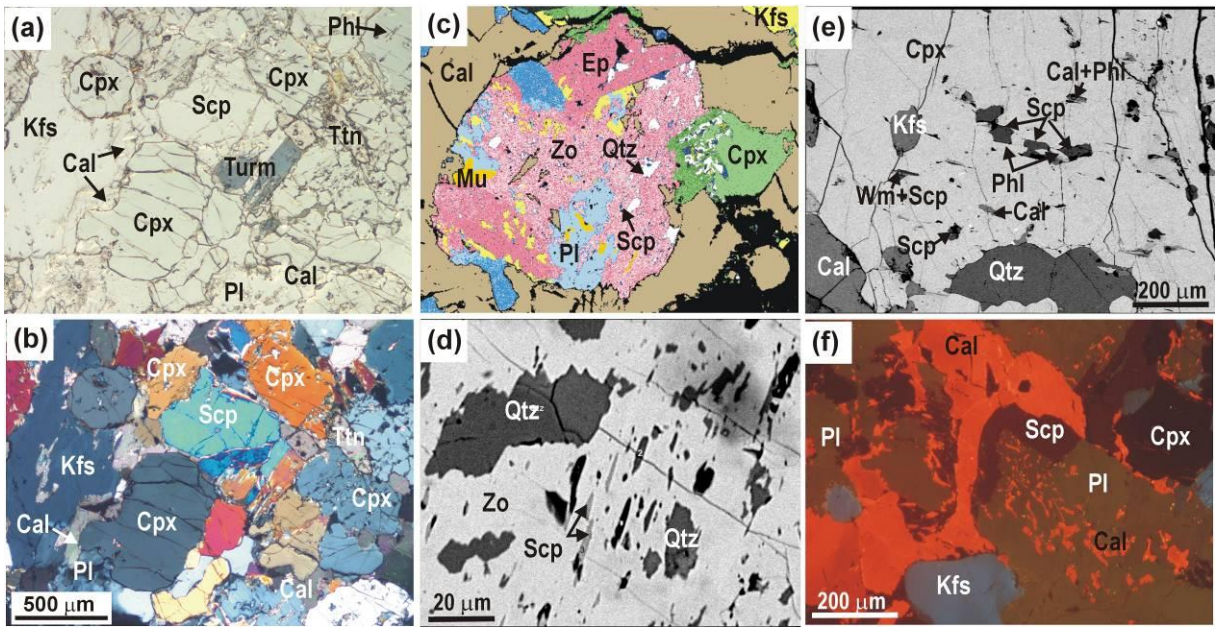

Figure 1. (a,b) Representative microstructure (a: Plane Polarized Light; b: Cross Polarized Light) of the K-feldspar + scapolite -bearing calc-silicate rocks. Note the oriented phlogopite inclusions in the up-right clinopyroxene. (c) Compositioal map of a zoisite crystal including quartz, scapolite muscovite and Na-rich plagioclase and intergrown with K-feldspar. (d) Detail of oriented scapolite and quartz inclusions within zoisite (BSE image). (e) Detail of oriented scapolite + phlogopite + calcite + muscovite inclusions within clinopyroxene (BSE image). (f) Detail of a plagioclase + calcite symplectitic aggregate partially replacing scapolite in the rock matrix (CL image).

References

Castelli, D., Rolfo, F., Groppo, C., Compagnoni, R., 2007, Impure marbles from the UHP Brossasco-Isasca Unit (Dora-Maira Massif, western Alps): evidence for Alpine equilibration in the diamond stability field and evaluation of the X(CO2) fluid evolution. J. Metam. Geol., 25, 587-603.

Connolly, J.A.D. and Trommsdorff, V., 1991, Petrogenetic grids for metacarbonate rocks: pressure–temperature phase-diagrams for mixed-volatile systems. Contrib. Mineral. Petrol., 108, 93-105.

Evans, K.A., 2011, Metamorphic carbon fluxes: how much and how fast? Geology, 39,95-96.

Gaillardet, J. and Galy, A., 2008, Himalaya-carbon sink or source? Science, 320, 1727-1728.

Groppo, C., Rolfo, F. and Indares, A., 2012, Partial melting in the Higher Himalayan Crystallines of Eastern Nepal: the effect of decompression and implications for the "channel flow" model. J. Petrol., 53, 1057-1088.

Groppo, C., Rolfo, F., Castelli, D., Connolly, J.A.D., 2013. Metamorphic CO_2 production from calc-silicate rocks via garnet-forming reactions in the CFAS-H_2O-CO_2 system. Contrib. Mineral. Petrol., 166, 1655-1675.

Skelton, A., 2011, Flux rates for water and carbon during greenschist facies metamorphism. Geology, 39, 43-46.

What controls the growth and shape of the Himalayan foreland fold-and-thrust belt?

Djordje Grujic[1], John Hirschmiller[1], Deirdre Mallyon[1]

[1] Dalhousie University, Department of Earth Sciences, Halifax, Canada, dgrujic@dal.ca

We provide empirical evidence for the impact of surface processes on the structure and geometry of the present-day foreland fold-and-thrust belt (FTB) of the Himalaya. We have reconstructed and analysed ten balanced cross sections distributed along the entire length of the Himalayan arc (Hirschmiller et al., 2014). Although published opinions vary, we contend that the active Himalayan FTB is delineated by the Main Frontal thrust (frontal thrust) and Main Boundary thrust (backstop), with foreland sediments deformed in the style of fold-and-thrust belts lying between the two. Here, we focus on the Siwalik Group, which represents the deformed part of the foreland basin and consists of synorogenic middle Miocene to Pleistocene sediments that form the youngest and frontal part of the Himalayan orogen.

Within the active foreland fold-and-thrust belt of the Himalaya, extension, strain rate, and belt morphology vary systematically from west to east. Strain rates correlate well with west to east increases in convergence rates according to both long-term plate velocity data and GPS data, suggesting that Pliocene to Holocene shortening is externally imposed and related to plate convergence rates. Conversely, the eastward decrease in belt width corresponds to an eastward increase in rainfall rates and specific stream power. Although mass accretion rates have not been well constrained, we argue that they remain relatively constant along the FTB. We suggest that the morphology of the Himalayan FTB is controlled primarily by erosion, in accordance with the critical taper model. Surface material removal is mainly controlled through rainfall and runoff and can be expressed as specific stream power. Thus, we propose that climatically induced erosion is the principal control on Himalayan foreland fold-and-thrust belt morphology.

We test this hypothesis through a series of 1D numerical models. Among the parameters controlling the form of a wedge, lithology, erodibility, and rock mechanical properties are relatively homogeneous throughout the belt. Hence, within the range of observed values in the Himalaya, we investigate the sensitivity of the shape of the Himalayan fold-and-thrust belt to the sole-out depth of the basal décollement, flux of tectonically added material, and the erosional constant.

For parameter values within the range of those observed in nature, the models successfully reproduce the observed variations in width of the Himalayan fold-and-thrust belt. The experimental results suggest:

- The value of the rock erodibility constant (K) varies over one order of magnitude or less along-strike of the Himalaya.
- Orogen-parallel variations in erosion rate can dominate over variations in accretion flux in controlling critical Coulomb wedge width.

Cite as: Grujic, D., et al.,, 2014, What controls the growth and shape of the Himalayan foreland fold-and-thrust belt?, in Montomoli C., et al., eds., proceedings for the 29th Himalaya-Karakoram-Tibet Workshop, Lucca, Italy.

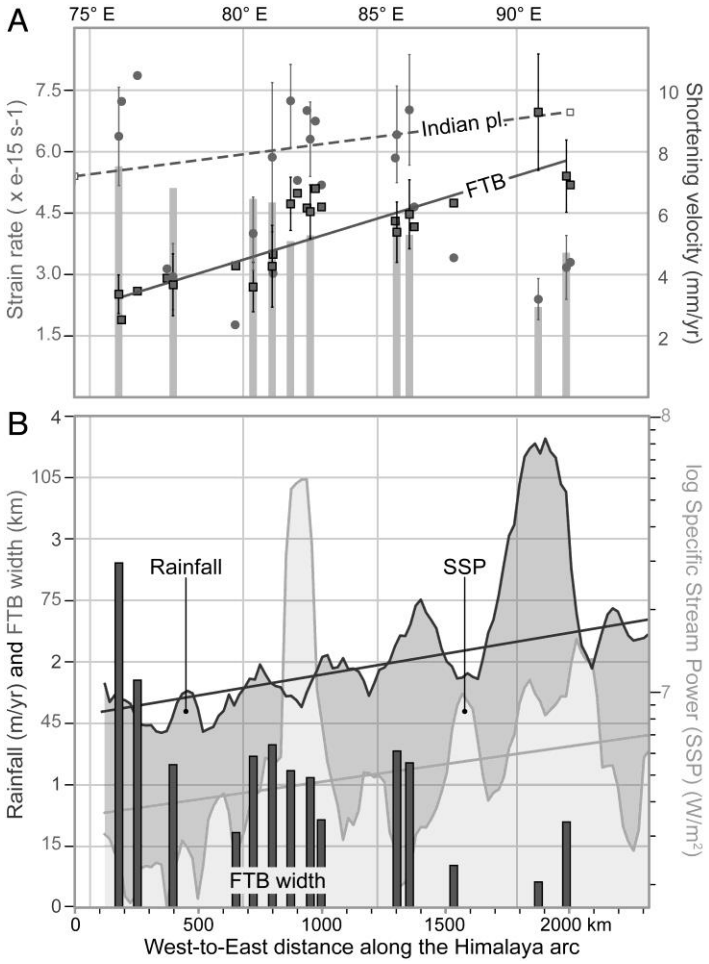

Figure 1. A) Graph of shortening velocity, strain rate, and sediment thickness of the Siwalik Group plotted against distance along the Himalayan arc. Dark and pale colours represent data from this study and published sections, respectively. Red line is the best fit of strain rate in the Himalayan FTB. The plate strain rate was calculated from the plate convergence rate of Molnar and Stock (2009), assuming the Indian plate motion is distributed over a lithosphere with a thickness of 200 km. Grey circle is the average shortening velocity and the grey line is the shortening velocity scaled to vary at the same rate as the plate convergence velocity. B) Graph plotting the width of the Himalayan fold-and thrust belt with distance along the Himalayan arc against total annual rainfall and specific steam power. From Hirschmiller et al. (2014).

References

Hirschmiller, J., Grujic, D., Bookhagen, B., Coutand, I., Huyghe, P., Mugnier, J.-L. and Ojha, T., 2014, What controls the growth of the Himalayan wedge? Pliocene to recent shortening of the Siwalik group in the Himalayan foreland belt, Geology, 42, 247–250, doi:10.1130/G35057.1.

Molnar, P., and Stock, J.M., 2009, Slowing of India's convergence with Eurasia since 20 Ma and its implications for Tibetan mantle dynamics, Tectonics, 28, TC3001, doi:10.1029/2008TC002271.

Siginficance of HP to UHP metamophism along Himalaya - What we learn from the Bohemian massif

Stéphane Guillot[1], Karel Schulmann[2,3], Kéiko Hattori[4], Ondrej Lexa[2], Vojtech Janoušek[2,5], Petra Maierová[2], Anne Replumaz[1], Pavla Stipska [2,3]

[1] ISTerre, Université Grenoble I, CNRS, 1381 rue de la Piscine, 38400 Grenoble Cedex 09, France, stephane.guillot@ujf-grenoble.fr
[2] Czech Geological Survey, Centre for Lithospheric Research, Klárov 3, 118 21 Prague 1, Czech Republic
[3] EOST, IPG, UMR 7516, Université de Strasbourg, 1 Rue Blessig, 67084 Strasbourg, France
[4] Department of Earth Science, University of Ottawa, Ottawa, Ontario K1N 6N5, Canada
[5] Institute of Petrology and Structural Geology, Charles University, Albertov 6, 128 43 Prague 2, Czech Republic

It is well recognized that the Eocene ultra-high pressure (UHP) metamorphism recorded in the Kaghan and Tso Morari Massifs in NW Himalaya is the direct result of the subduction of the Indian continent beneath the south Indian margin (Guillot et al., 2008). In contrast, the origin of the Oligocene high-pressure (HP) granulites in domal/antiformal structures along the Higher Himalayan Crystalline belt is highly debated. Do these rocks record the thickened crust in Oligocene time or relamination of deeply subducted continental material to the base of the South Tibetan block (Hacker et al., 2011).

The Variscan Bohemian massif in Czech Republic provides an insight of the origin of these Himalayan granulites. In the Bohemian massif, the root of the orogenic belt is well exposed.

Recent studies show that the Carboniferous HP granulites retain vertical mylonitic fabrics, suggesting that large-scale overturn produced crustal-scale dome-like structures. Numerical modelling by Maierova et al. (2014) for the Variscan evolution of Bohemian Massif demonstrates that the vertical exchange of the felsic lower crust with overlying dense material, which is followed by the development of a major decoupling zone separating the superstructure from the deep orogenic infrastructure. This decoupling zone, called here the infrastructure– superstructure transition zone, is responsible for the transfer of material and heat resulting in channel flows. Thermal structure of this zone suggests that mid-crustal rocks produce partial melting and a thick layer of migmatite as observed in the Higher Himalayan Crystallines.

It is proposed that the Carboniferous evolution of the Bohemian Massif may be analogous to Tertiary crustal dynamics of the Higher Himalayan system. Based on the model we thus predict a multistage evolution of large hot orogens including massive vertical movement of material and heat transfers.

Cite as: Guillot, S. et al., 2014, Siginficance of HP to UHP metamophism along Himalaya - What we learn from the Bohemian massif, in Montomoli C., et al., eds., proceedings for the 29th Himalaya-Karakoram-Tibet Workshop, Lucca, Italy.

The intense weathering condition in the Middle Miocene period supplied from the fluvial sediments in central Japan

Nozomi Hatano[1], Kohki Yoshida[2], Saori Mori[2], Shiori Irie[3]

[1] Division of Science and Technology, Graduate School of Shinshu University, Japan, 13sm407f@shinshu-u.ac.jp
[2] Department of Geology, Faculty of Science, Shinshu University
[3] Inpex Cooperation

Introduction

In the middle Miocene - early Pliocene period, the climate condition in the Japanese Islands was subtropical on the basis of the distribution of fossil mollusc assemblage (Ozawa et al., 1995). Especially, in the middle Miocene period, the Eastern Asian Monsoon was enhanced (Quade et al., 1989). In this study, the middle Miocene Tokiguchi Porcelain Clay Formation (9 - 11Ma; Yoshida et al., 1997) and the lower Pliocene the Kobiwako Group (3 - 6 Ma; Yokoyama and Takemura, 1983) in central Japan, they are thought to be the fluvial sediments, were examined for the paleopedology, mineralogy and geochemistry in order to reveal the paleoweathering condition in the Eastern Asian region in the middle Miocene - early Pliocene period. As a result, it is revealed that the middle Miocene period (9 - 11Ma) had been under intense weathering condition dominated by wet - warm climate.

Geological background - paleopedology and sedimentary environment

The middle Miocene Tokiguchi Porcelain Clay Formation and the early Pliocene Kobiwako Group were deposited under warm and wet climatic condition proved by the fossil plants and diatom assemblages. The middle Miocene formation is known as high quality resource of ceramics because of their clay minerals composed of kaolin. Many paleosol horizons, besides, can be recognized in the backswamp and lake deposits in the formation. These paleosol horizons with many organic materials and peat, like a histosol of the USDA soil taxonomy (Soil Survey Staff, 1998), were formed thickly and show relatively wet condition in soils. On the other hand, the early Pliocene Kobiwako Group almost has never been paleosol horizons that suggest the formation under strong weathering condition.

Paleoweathering - mineralogy and geochemistry

The chemical weathering degree was examined for the chemical index alternation (CIA; Nesbitt and Young, 1982). In the Miocene formation, the mud samples show intense weathering condition with the CIA value over 80. In the Pliocene formation, on the one hand, the mud samples show just weakly weathering with the CIA values of approximately 70 though the degree is still higher than one of the Pleistocene (Omori, 1968). The clay mineral assemblage shows the variation of the parent rocks in the middle Miocene formation. For example, the assemblage composed of almost kaolinite indicates the plutonic rocks in origin, besides the assemblage consists of common expandable clay mineral and almost kaolinite suggests the heterogeneity of parent rocks, e. g. the mixture of sedimentary and plutonic rock. In the lower Pliocene formation, then, the clay mineral assemblage composed of almost expandable clay mineral and mica mineral in spite of their plutonic nature. These results suggest that the weathering degree of the middle Miocene sediments is higher than the one of the Pliocene and Pleistocene sediments in the Japanese Islands regardless of their parent materials.

Discussion

Consequently, this result suggests the severe weathering condition in the middle Miocene (9 - 11Ma) and the relatively weak weathering condition in the lower Pliocene (3 - 6Ma) in the Japanese Islands. The middle Miocene, besides, includes paleosol horizons that supply the wet soil condition. The weathering condition in the middle Miocene time in the Japanese Islands, therefore, implies wet - warm climatic condition, like a semi tropical climate, affected by the Eastern Asian summer monsoon. It is pointed that the initiation of the Eastern Asian monsoonal climate, in the late Miocene period (Quade et al., 1989), is

Cite as: Hatano, N., Yoshida, K., Mori S. and Irie, S., 2014, The intense weathering condition in the Middle Miocene period supplied from the fluvial sediments in central Japan, in Montomoli C., et al., eds., proceedings for the 29th Himalaya-Karakoram-Tibet Workshop, Lucca, Italy.

caused by accretion of the south wind from the monsoonal depression due to heating the Tibetan Plateau and meandering the westerly wind due to wind barrier Himalayan range (Prell and Kutzback, 1992). As a trigger of the initiation of the climate, uplifting of the Himalayan range and Tibetan Plateau in the middle Miocene period (10 - 15Ma) is proposed (Royden et al., 2008). The weathering condition in the middle Miocene in the Japanese Islands, therefore, may reflect the initiation of the Eastern Asian monsoonal climate caused by uplifting of the Himalayan range and Tibetan Plateau. There, however, is possibility that the wet - warm climatic condition in the middle Miocene period reflects the increasingly of the Kuroshio currents in the middle Miocene (10.4 - 11.5Ma; Ozawa et al., 1995).

References

Nesbitt, H. W. and Young, G. M., 1982, Early Proterozoic climates and plate motions inferred from major element chemistry of lutites, Nature, 299, 715-717.

Omori, T., 1968, On the Chemical composition of bottom sediments in Lake Biwa, Central Japan, Bull. Geol. Surv. Japan, 19, 103-114.

Ozawa, T., Inoue, K., Tomida, S., Tanaka, T. and Takami, N., 1995, An outline of the Neogene warm-water molluscan faunas in Japan, Fossils, 58, 20-27.

Prell, W. L. and Kutzbach, J. E., 1992, Sensitivity of the Indian monsoon to forcing parameters and implications for its evolution, Nature, 360, 647-652.

Quade, J., Cerling, T. E. and Bowman, J. E., 1989, Development of Asian monsoon revealed by marked ecological shift in the latest Miocene of northern Pakistan, Nature, 342, 163-166.

Royden, L. H., Burchfiel, B. C. and der Hilst, R. D, 2008, The geological evolution of the Tibetan Plateau, Science, 321, 1054-1058.

Soil Survey Staff, 1998, Keys to Soil Taxonomy, 8th edition U.S. Dept. Agri. Nat. Res. Conserv. Serv. 327p.

Yokoyama, T., and Takemura, K., 1983, Geologic column obtained by the Deep Drilling from the bottom surface of Lake Biwa, Japan, IPP-CCE Newsletter, 3, 21-23.Yoshida, F., Nakayama, K. and Danhara, T., 1997, Fission-track ages of the lower part of the Seto Group, Aichi and GifuPrefectures, JPGU Meet. 1997, Abstr., 584p.

Geochemistry and geobarometry of Eocene dykes intruding the Ladakh Batholith

Alexandra R. Heri[1], Jess A. King[1], Franco Rolfo[2], Jonathan C. Aitchison[1], Justin Bahl[3], Igor M. Villa[4,5]

[1] Dept. of Earth Sciences, The University of Hong Kong, Hong Kong, China, heri.alexandra@gmail.com
[2] Dipartimento di Scienze della Terra, Università di Torino, 10125 Torino, Italy
[3] School of Public Health, The University of Texas, Houston, TX 77030, USA
[4] Dipartimento di Scienze della Terra, Università di Milano Bicocca, 20126 Milano, Italy
[5] Institut für Geologie, Universität Bern, 3012 Bern, Switzerland

We present further distinguishing characteristics among Eocene dykes found along the Southern margin of the Ladakh batholith (NW-India). Coupled evidence from field structures and Nd-Sr isotope data showed that there are two broad dyke provinces extending over 50 km: between Leh and Tunglung, an "eastern", ENE-trending family with higher crustal assimilation; between Tunglung and Hemis Shugpachan, the "western" dykes trend NNW and have higher eps(Nd). The hornblende-bearing dykes of both families revealed crystallisation ages between 50 and 54 Ma, i.e. formed in the same tectonic setting at roughly the same time. In this study we present the geochemistry of these dykes and test hypotheses of common origin (i.e. formation from same magma chamber) through a novel statistical analysis.

The dykes show a large range in differentiation from basaltic to rhyolitic, but most are of an intermediate composition. High K_2O concentrations classify them as High-K calk-alkaline or shoshonitic. All dykes exhibit LREE enrichment and HREE depletion as well as negative Tb and Nb anomalies characteristic for subduction-related intrusives and extrusives. They are chemically similar to undated dykes E of Leh described by Ahmad et al. (1998), but show higher enrichment in incompatible elements and Pb in respect to Primitive mantle.

According to preliminary petrologic data, the emplacement pressure of the dykes appears to be lower in the west than in the east. A more comprehensive and extended study of a good number of selected samples will likely provide tighter thermobarometric constraints.

Although the dykes share many characteristics, they have not formed from the same batch of magma. Their REE patterns support a clear subdivision into chemically distinct groups. To test whether these groups formed from the same magma chamber, we used hierarchical clustering and multidimensional scaling. These tools are used to assess similarity/dissimilarity amongst individuals of a group - e.g. in evolutionary biology. Even though in hierarchical clustering we assume common origins, the analysis creates a hierarchy of groups by similarity. Multi-dimensional scaling allows for the natural grouping of samples with similar characteristics, without any assumption of origin. Therefore, these two methods are complementary. The results show the dykes are cogenetic, but clearly not consanguineous, i.e. have not formed from one, progressively differentiating magma chamber but from different batches of melt.

References

Ahmad, T., Thakur, V.C., Islam, R., Khanna, P.P., Mukherjee, P.K., 1998, Geochemistry and geodynamic implications of magmatic rocks from the Trans-Himalayan arc, Geochemical Journal, 32, 383-404.

Cite as: Hery, A.R. et al., , 2014, Geochemistry and geobarometry of Eocene dykes intruding the Ladakh Batholith, in Montomoli C., et al., eds., proceedings for the 29th Himalaya-Karakoram-Tibet Workshop, Lucca, Italy.

Crustal structure, seismicity and landslide activity in Bhutan – preliminary results from a temporary seismological network

György Hetényi[1,2], Julia Singer[2], Edi Kissling[2], Tobias Diehl[1], Jamyang Chophel[3,4], Arnaud Burtin[5], Simon Löw[3], Dowchu Drukpa[4]

[1] Swiss Seismological Service, ETH Zürich, 8092 Zürich, Switzerland, gyorgy.hetenyi@sed.ethz.ch
[2] Institute of Geophysics, Department of Earth Sciences, ETH Zürich, 8092 Zürich, Switzerland
[3] Institute of Geology, Department of Earth Sciences, ETH Zürich, 8092 Zürich, Switzerland
[4] Seismology Division, Department of Geology and Mines, Thimphu, Bhutan
[5] Section 5.1 Geomorphology, GFZ German Research Centre For Geosciences, 14473 Potsdam, Germany

Project GANSSER focuses on the Geodynamics ANd Seismic Structure of the Eastern-Himalaya Region. Its main tool of observation is a temporary network of 38 broadband seismological stations (Fig. 1), which was deployed in Bhutan in January 2013 and operated until April 2014. While 13 of these stations continue to acquire data in the field, preliminary results on crustal structure, seismic activity and landslide-generated seismic noise are presented here.

The structure of the crust is targeted to deduce two types of information. First, the main interfaces at which seismic properties change in space – such as the crust-mantle boundary (Moho) and the Main Himalayan Thrust (MHT) – are investigated by converted waves (receiver functions). Second, the P- and S-wave velocity structure of the crust and the underlying mantle are the aim of various seismic imaging techniques (tomography, active source seismology principles). Details of these are presented in the companion paper by Singer et al. (this volume).

The level of seismic activity in Bhutan is of interest as the region is considered a seismic gap, i.e. a segment of the Himalayan arc where fewer earthquakes happen than elsewhere in the orogen. Also, regarding very large and destructive earthquakes (magnitude M>8), there is neither instrumental nor historical record of such events in Bhutan, but palaeoseismological results suggest two M>8 events in the past 1000 years (Berthet et al. 2014). Characterizing the level of seismicity is of importance to assess seismic hazard and to understand the seismotectonics of Bhutan. With the first 9 months of the data analyzed, our preliminary results show two clusters of seismicity in the Southwestern and in the Eastern part of the country. The two M>4 events that have been detected globally were located more accurately: one of them occurred at about 70 km depth in Northern Bhutan, the other was followed by a series of aftershocks. Several other felt events in the region that have not been located by global networks were detected by our network. The processing of the full catalogue, including the now continuing monitoring, is planned to come to more representative conclusions (i.e. based on a longer time period).

Detecting landslides from seismic noise is an emerging field of seismology. Based on a seismically well-characterized debris flow event in Nepal and the applied methods there (Burtin et al., 2009), we screened the dataset acquired in Bhutan for landslide activity during the 2013 monsoon season. Compared to our expectations to detect a large number of events in such a steep country, the number of observed landslides remained relatively low. With observations made during a field campaign, we propose the following reasons to explain this: the relatively small size of events; the relatively dry 2013 monsoon season; the dense forest coverage; the strength of the rocks of the Greater Himalayan Sequence occupying most of the region; and the relatively sparse station distribution in the centre of the country. Nevertheless, a number of events could be detected and located, and some were confirmed by Landsat composite satellite image pairs (before and after the event). Many of these landslides are in: areas of geologically weaker rocks (phyllites); in the Southern part of the country where the combination of active tectonics, rainfall and steep slopes is most favourable for landslides; or near new road constructions. The ca. one dozen events reported by the media could not be located seismically: their size was large enough to cause road blocks (and due to the elementary road network trigger media appearance) but not enough to be detected by a

Cite as: Hetényi, G., et al., 2014, Crustal structure, seismicity and landslide activity in Bhutan – preliminary results from a temporary seismological network, in Montomoli, C., et al., eds., Proceedings for the 29th Himalaya-Karakoram-Tibet Workshop, Lucca, Italy.

sufficient number of stations. From a seismological point of view: it seems most advantageous if a landslide monitoring network is designed for a specific region (including adequate station spacing), and if it undergoes a phase of calibration with ground truth from field verifications.

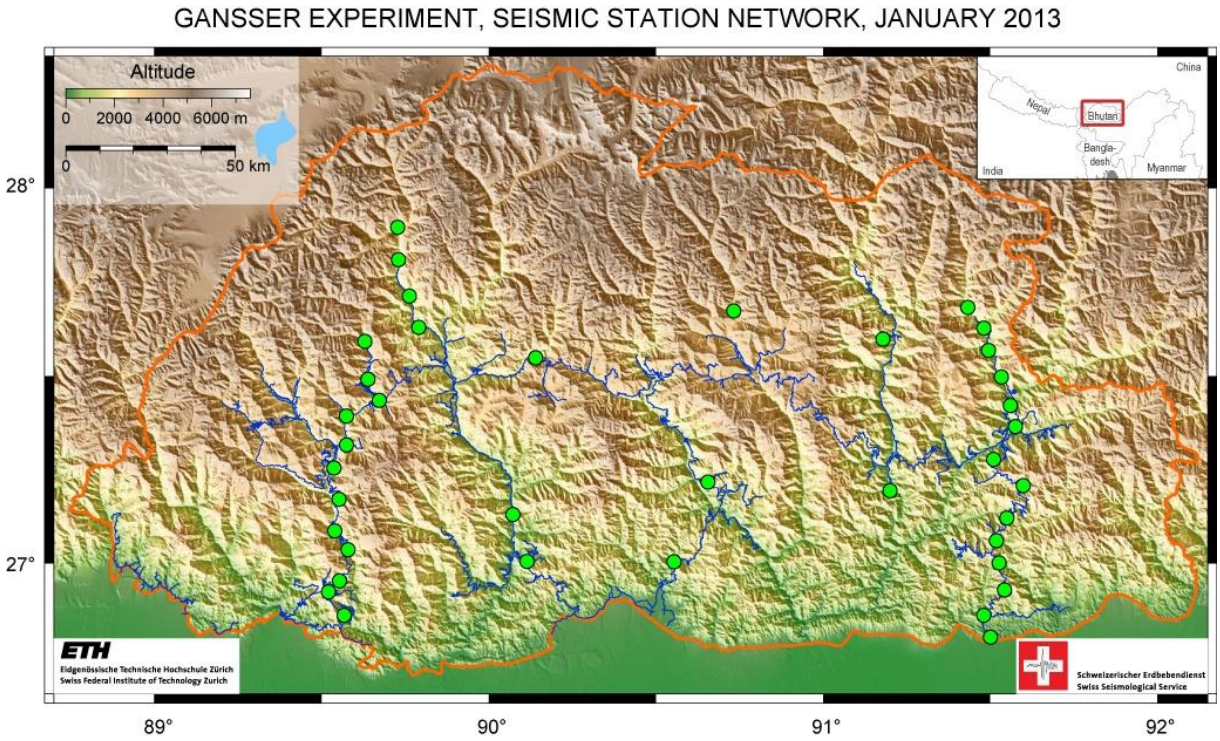

Figure 1. Station geometry of the GANSSER project's broadband seismological network in Bhutan.

References

Berthet, T. et al., 2014, Active tectonics of the eastern Himalaya: new constraints from the first tectonic geomorphology study in southern Bhutan, Geology, 42, 427-430. doi:10.1130/G35162.1

Burtin, A., Bollinger, L., Cattin, R., Vergne, J. and Nábělek, J.L., 2009, Spatiotemporal sequence of Himalayan debris flow from analysis of high-frequency seismic noise, J. Geophys. Res., 114, F04009. doi:10.1029/2008JF001198

Chemical evolution of Himalayan leucogranites based on an integrated zircon O, U-Pb, Hf study

Thomas N. Hopkinson[1], Clare J. Warren[1], Nigel B.W. Harris[1], Sam Hammond[1], Randall R. Parrish[2]

[1] Department of Environment, Earth and Ecosystems, The Open University, Milton Keynes, MK7 6AA, United Kingdom, thomas.hopkinson@open.ac.uk
[2] NERC Isotope Geoscience Laboratory, Kingsley Dunham Centre, Keyworth, Notts, NG12 5GG, United Kingdom.

Crustal melting and leucogranite intrusion are common features of most collision zones around the world. In the Himalayas, multiple Miocene leucogranite plutons and sheet complexes intrude the Greater Himalayan Series (GHS) across the orogen, in particular at upper structural levels towards the South Tibetan Detachment.

Previously-published Himalayan whole-rock data show that the leucogranites formed from a meta-sedimentary source (e.g. Deniel et al., 1987; Guillot and Le Fort, 1995). However the bulk rock approach carries inherant uncertainties. Post-crystallization processes such as fluid-rock interaction can have a large effect on whole rock chemistry and bulk analyses may mask more subtle influences from (differing) contributing sources. Zircons have been shown to retain precise information of the contributing sources of the melt from which they crystallise due to the resistant nature of the zircon structure to post-magmatic processes (Appleby et al., 2010).

This study focuses on detailed geochemical investigations of zircon to differentiate between varying geochemical processes in granite formation. O and Hf isotopes are used to detect discrete changes in source while U-Pb analyses yield the timing of zircon crystallisation. This study of Oligocene-Miocene (35-12 Ma) leucogranite zircons from the Bhutan Himalaya presents the first application of this novel technique that links Hf and O isotope data to the U-Pb age in zircons, to anatexis in the Himalayan orogeny.

The dataset shows that the majority of zircon rim analyses yield O-Hf signatures that lie within the previously-reported whole-rock GHS field, suggesting no discernable mantle source has contributed to Himalayan leucogranite formation (Fig. 1). In contrast zircon cores inherited from earlier orogenic episodes reveal a significant mantle component during Paleozoic and Precambrian events.

A change in Hf isotope composition through time during Himalayan orogenesis is documented, with a tendency for younger (17-12 Ma) leucogranites to yield significantly lower εHf values. The maximum εHf stays constant at -11 through all samples, however the minimum value drops as low as -23 in the youngest leucogranites (Fig. 2). This correlates to a change in Hf model age from 1.4 Ga to 2.4 Ga. These data suggest either a change of source within the GHS over time, or an increasing contribution from older Lesser Himalayan (LHS) material in the melt. LHS Nd model ages are significantly older than those of the GHS (2.4-2.9 Ga compared with 1.4-2.4 Ga; Ahmad et al., 2000), and even minor amounts of LHS material incorporated into a melt would significantly increase the Hf model age of the resulting leucogranite. If this inference is confirmed, it would have large implications for tectonic models of the Himalaya.

Cite as: Hopkinson, T. et al., 2014. Chemical evolution of Himalayan leucogranites based on an integrated O, U-Pb, Hf study of zircons, in Montomoli C., et al., eds., proceedings for the 29th Himalaya-Karakoram-Tibet Workshop, Lucca, Italy.

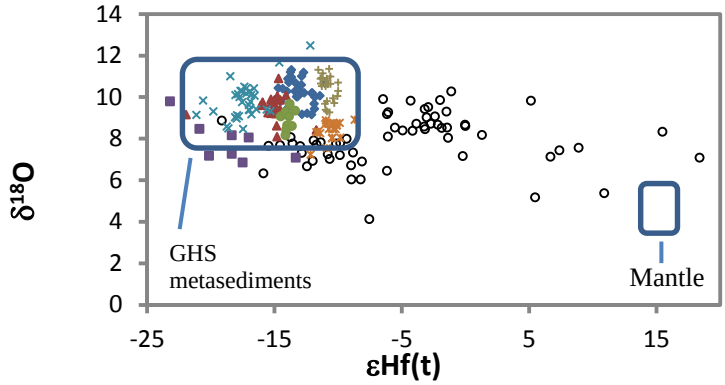

Figure 1. Graph of oxygen and hafnium isotope data for leucogranite zircon rims. Each colour/shape represents one sample. The vast majority of samples lie within the GHS (whole-rock) metasediment field, suggesting there is no mantle interaction with Himalayan melts. Open circles represent zircon core values. Data for GHS field from Harris and Massey (1994) and Massey et al. (1995). Mantle values from Vervoort and Blichert-Toft (1999) and Valley et al. (2005).

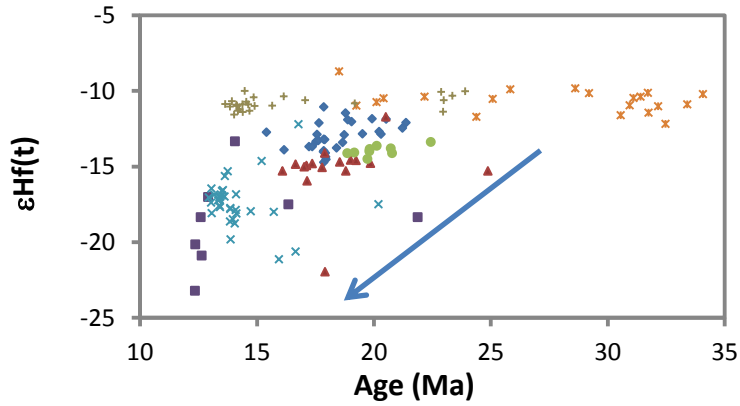

Figure 2. Plot of Hf isotope composition against age for leucogranite zircon rims. Each colour/shape represents one sample.

References

Ahmad, T., et al., 2000, Isotopic constraints on the structural relationships between the Lesser Himalayan Series and the High Himalayan Crystalline Series, Garhwal Himalaya, Bulletin of the Geological Society of America, 112, 467-477.

Appleby, S.K. et al., 2010, Do S-type granites commonly sample infracrustal sources? New results from an integrated O, U-Pb and Hf study of zircon, Contrib. Mineral. Petrol., 160, 115-132.

Deniel, C. et al., 1987, Isotopic study of the Manaslu granite (Himalaya, Nepal): inferences on the age and source of Himalayan leucogranites, Contrib. Mineral. Petrol., 96, 78-92.

Harris, N.B.W. and Massey, J., 1994, Decompression and anatexis of Himalayan metapelites, Tectonics, 13, 1537-1546.

Guillot, S. and Le Fort, P., 1995, Geochemical constraints on the bimodal origin of High Himalayan leucogranites, Lithos, 35, 221-334.

Massey, J. et al., 1994, Contrasting retrograde oxygen isotope exchange behaviour and implications: examples from the Langtang Valley, Nepal, Journal of Metamorphic Geology, 12, 261-272.

Valley, J.W. et al., 2005, 4.4 billion years of crustal maturation: oxygen isotope ratios of magmatic zircon, Contrib. Mineral. Petrol., 150, 561-580.

Vervoort, J.D. and Blichert-Toft, J., 1999, Evolution of the depleted mantle: Hf isotope evidence from juvenile rocks through time, Geochim. Cosmochim. Acta, 63, 533-556.

The early Cretaceous Xigaze ophiolites formed in the Lhasa forearc: evidence from paleomagnetism, sedimentary provenance, and stratigraphy*

Wentao Huang[1,2], Douwe J.J. van Hinsbergen[2], Marco Maffione[2],Devon A. Orme[3], Guillaume Dupont-Nivet[1,2,4,5], Peter C. Lippert[3],Carl Guilmette[6], Nathaniel Borneman[7], Kip Hodges[7], Lin Ding[8]; Zhaojie Guo[1]; Paul Kapp[3]

[1] Key Laboratory of Orogenic Belts and Crustal Evolution, Ministry of Education, School of Earth and Space Sciences, Peking University, Beijing 100871, China, W.Huang@uu.nl
[2] Department of Earth Sciences, Utrecht University, Budapestlaan 17, 3584 CD, Utrecht, The Netherlands
[3] Department of Geosciences, University of Arizona, Tucson, Arizona 85721, USA
[4] Géosciences Rennes, UMR 6118, Université de Rennes 1, Campus de Beaulieu, 35042 Rennes Cedex, France
[5] Institute of Earth and Environmental Science, University of Potsdam, Karl-Liebknecht-Str. 24-25, 14476 Potsdam-Golm, Germany
[6] Département de Géologie et de Génie Géologique, Université Laval, Québec, Qc., Canada G1K 7P4
[7] School of Earth and Space Exploration, Arizona State University, Tempe, Arizona, USA
[8] Key Laboratory of Continental Collision and Plateau Uplift, Institute of Tibetan Plateau Research, Chinese Academy of Sciences, Beijing, China

The Xigaze ophiolite belt, exposed in the Yarlu-Tsangpo suture zone, contains thinned remnants of an oceanic lithosphere formed during the closing of the Tethys Ocean in early Cretaceous. At this time, its latitudinal position between the converging Indian and Asian continents has direct implications on understanding the timing and processes of the subsequent continental collision. Here we report paleomagnetic investigations on the Lower Cretaceous sedimentary rocks unconformably covering mantle lithosphere of the Xigaze ophiolites in Sangsang, and interfingering with radiolarian sequences in Qunrang (Southern Tibet). Detrital zircon U–Pb ages of the Sangsang sedimentary rocks indicate a clear Gondwanan suggestive of a Lhasa terrane provenance. The youngest peak of the age spectrum constrains the deposition age to be ~120 Ma, which is further tested through calcareous nannofossil biostratigraphy of this section. A positive fold test of the isolated characteristic remanent magnetization (ChRM) shows that these sediments from Sangsang likely carry a primary magnetization. At face value, the paleomagnetic results from the Sangsang sedimentary rocks suggest the deposition at rather low latitude, of ~8°N, consistent with previous findings. However, rock magnetic tests and ChRM direction analyses show us that it is very likely that these Sangsang sedimentary rocks were affected by compaction/compression-induced inclination shallowing. We apply two different correction methods to estimate the magnitude of inclination shallowing. Using the elongation/inclination (E/I) correction method, the mean inclination is corrected from 16.9° to 30.2° within 95% confidence limits between 24.8° and 37.3°; Using an anisotropy-based inclination correction method steepens the mean inclination to 31.1 ± 9.6° after a curve fitting-determined particle anisotropy of 1.40 is applied. These corrected inclinations are statistically indistinguishable from each other and yield an estimated paleolatitude of ~17°N. We also investigated the Qunrang sediments deposited ca. 116 Ma as indicated by the zircon U–Pb dating of the interbedded tuff. Isolated ChRM directions from the Qunrang sediments correspond to a paleolatitude of ~12°N. Although we cannot correct the potential inclination shallowing in these sediments due to limited dataset of the ChRM directions and unavailability of anisotropy data, the distribution of the ChRM directions strongly suggest that these were also affected by inclination shallowing. Our new findings imply that spreading and extensional dismemberment of the Xigaze ophiolites occurred around ~17°N, immediately adjacent to the southern margin of the Lhasa terrane from which a contemporaneous ~16°N paleolatitude estimate was published. The Xigaze forearc sediments are Lhasa-derived and unconformably cover the Xigaze ophiolites ocean floor. Previously published interpretations of an equatorial formation latitude, and the existence of a major subduction thrust between the Xigaze ophiolites and the Xigaze forearc sediments are inconsistent with our observations of their contact, our paleomagnetic measurement, and our sediment provenance results.

Cite as: Huang, et a., 2014, The early Cretaceous Xigaze ophiolites formed in the Lhasa forearc: evidence from paleomagnetism, sedimentary provenance, and stratigraphy in Montomoli C., et al., eds., proceedings for the 29th Himalaya-Karakoram-Tibet Workshop, Lucca, Italy.

Geological and tectono-metamorphic characterization of the Himalayan metamorphic core (HMC) in the Mugu Karnali valley (Western Nepal, Central Himalaya)

Salvatore Iaccarino[1], Chiara Montomoli[1], Rodolfo Carosi[2], Hans-Joachim Massonne[3], Antonio Langone[4], Dario Visonà[5]

[1] Dipartimento di Scienze della Terra, Univ. of Pisa, Italy, iaccarino@dst.unipi.it
[2] Dipartimento di Scienze della Terra, Univ. of Torino, Italy
[3] Institut für Mineralogie und Kristallchemie, Univ. of Stuttgart, Germany
[4] C.N.R. Istituto di Geoscienze e Georisorse, U.O.S. Pavia, Italy
[5] Dipartimento di Geoscienze, Univ. of Padova, Italy

The Himalayan range, extending over 2500 km, has played a central role in shaping our understanding of the orogenesis by colliding continental plates (*e.g.* Kohn, 2014). Several first order geodynamic processes, currently among the major topics of geosciences, like syn-compressional extension, feedback relations between climate and tectonics, rheological implications and exhumation consequences in response to crustal melting, have been developed starting from studies of the Himalayas (*e.g.* Jamieson and Beaumont, 2013).

In this contribution we present the structural and tectono-metamorphic evolution of the Himalayan metamorphic core (HMC) in the Mugu Karnali valley, in Western Nepal, where very few geological data are currently available in the literature (see Montomoli et al., 2013 and references therein). Along this transect a complete and quite well-exposed cross section of the belt, starting from the Lesser Himalayan Sequence (LHS) up to the Tethyan Sedimentary Sequence (TSS), is present. The LHS is characterized by poorly deformed very low-grade metamorphic quartzites, graphitic schists, chlorite-bearing phyllites, and dolomitic marbles. Meso- and microscopic investigations reveal that the main foliation, S2, is a crenulation cleavage since an older foliation is recognized within the microlithons and within intertectonic porhyroblasts. Approaching the tectonic contact of LHS and Greater Himalayan Sequence (GHS), the Main Central Thrust (MCT), we observe an increase of deformation, with developing S-C-C' fabrics in the chlorite-bearing phyllites and L, L>S tectonites in the quartzite layers, as well as, an increase of metamorphic grade with a sporadic appearance of garnet in the pelitic layers just before the MCT. The MCT in this transect, is neither a sharp fault nor a protolith boundary, but a large (kilometre thick) ductile shear zone affecting both quartzites and phyllites of the LHS and high-grade metamorphic rocks (up to the kyanite zone) of the GHS (Carosi et al., 2007).

According to Larson and Godin (2009) the GHS has been subdivided into two portions, the lower GHS (GHS_L), composed of locally anatectic metapelites (garnet zone up to sillimanite zone), orthogneisses, and minor garnet-bearing calcsilicates and amphibolites, and an upper portion (GHS_U) with migmatized para- and orthogneisses and high grade calcsilicates with olivine. The main foliation in the GHS is S2 with an older foliation observable within the microlithons and only sporadically preserved within the porphyroblasts in the highest grade samples. Both GHS and LHS main foliations are folded by late kink-like folds with subvertical axial planes, without developing a clear axial plane foliation and mineral re-crystallization/re-orientation. Moreover, a several km-sized leucogranitic body, the Mugu granite, intruded the migmatitic portion of the GHS_U and likely the base of the TSS. Several magmatic "*textures*" have been observed in the field ranging from equigranular to porphyric.

At the base of the TSS we observed boudinage on orthogonal outcrop surfaces, suggesting a strain pattern typical of field I of Ramsay and Huber (1983). Moreover, the presence of monoclinic structures like flanking folds and asymmetric boudins, coexisting with orthorhombic structures like symmetric boudins, suggest a general flow deformation regime. Near the base of the TSS a very high temperature gradient is suggested by the rapid passage from calcsilicate occasionally with some wollastonite to low grade fossiliferous meta-limestone.

Cite as: Iaccarino, S. et al., 2014, Geological and tectono-metamorphic characterization of the Himalayan metamorphic core (HMC) in the Mugu Karnali valley (Western Nepal, Central Himalaya), in Montomoli C., et al., eds., proceedings for the 29th Himalaya-Karakoram-Tibet Workshop, Lucca, Italy.

More than two hundred samples were collected for optical and microstructural studies. Representative samples along the whole section were selected, ranging from garnet-chlorite-bearing rocks (>500°C, 0.8 GPa) up to kyanite/sillimanite-bearing migmatites (*c.* 750°C, 1.1-0.7 GPa) for a detailed petrological characterization, combining pseudosection modeling, trace element thermometry (*e.g.* Zr-in-rutile thermometry, Tomkins et al., 2007), as well as multi-equilibrium thermobarometry (MET) approach. Monazite geochronology is in progress, in order to obtain time constraints for the evolution of these rocks. Preliminary data for samples from different structural position (*i.e.* GHS_L vs GHS_U) reveal a diachronic mineral equilibration within the GHS and support the occurrence of a tectonic and metamorphic discontinuity.

References

Carosi, R., Montomoli, C. and Visonà, D., 2007, A structural transect in the Lower Dolpo: Insights on the tectonic evolution of Western Nepal, Journal of Asian Earth Sciences, 29, 407-423.

Jamieson, R.A. and Beaumont, C., 2013, On the origin of orogens, Geological Society of America Bulletin, 125, 1671-1702.

Kohn, M.J., 2014, Himalayan Metamorphism and Its tectonic Implications, Annual Review of Earth and Planetary Sciences, 42, 381-419.

Larson, K.P. and Godin, L., 2009, Kinematics of the Greater Himalayan sequence, Dhaulagiri Himal: implications for the structural framework of central Nepal, Journal of the Geological Society, London, 166, 25-43.

Montomoli, C., Iaccarino, S., Carosi, R., Langone, A. and Visonà, D, 2013, Tectonometamorphic discontinuities within the Greater Himalayan Sequence in Western Nepal (Central Himalaya): Insights on the exhumation of crystalline rocks, Tectonophysics, 608, 1349-1370.

Ramsay, J.G. and Huber, M.I., 1983, The Techniques of Modern Structural Geology. Vol I: Strain Analysis. London: Academic Press.

Tomkins, H.S., Powell, R. and Ellis, D.J., 2007, The pressure dependence of the zirconium-in-rutile thermometer, Journal of Metamorphic Geology, 25, 703-713.

Higher Himalayan Crystalline (HHC) Belt: its shear sense indicators and their implications on its tectonic evolution

Arvind K. Jain[1], Mrinal Shreshtha[2], Puneet Seth[2], Lawrence Kanyal[2], Sandeep Singh[2], Rodolfo Carosi[3], Chiara Montomoli[4], Salvatore Iaccarino [4]

[1] CSIR-Central Building Research Institute, Roorkee-247667 India, himalfes@gmail.com
[2] Department of Earth Sciences, Indian Institute of Technology, Roorkee-247667
[3] Università degli Studi di Torino, Dipartimento di Scienze della Terra via Valperga Caluso, 35, 10125 Torino, Italy
[4] Dipartimento di Scienze della Terra, University of Pisa, Via S. Maria 53, 56126 Pisa, Italy

As a consequence of the Cenozoic India–Himalayan convergence, the Himalaya exhibits some of the most spectacular features like ductile, inverted metamorphism and generation of migmatite/leucogranite within the Higher Himalayan Crystalline (HHC) Belt, and its subsequent thrusting along the Main Central Thrust (MCT) over the Lesser Himalayan Sedimentary Belt (LHSB). In central parts of Uttarakhand, more than 20 km thick and homoclinal NE-dipping HHC is almost continuously exposed between Helang and Malari along the Dhauli Ganga Valley. This road dip-section traverse provides an excellent opportunity to investigate the (i) ambiguity regarding the position of the MCT in terms of the Munsiari Thrust (the MCT–I), and the Vaikrita Thrust (the MCT–II), and the South Tibetan Detachment System (STDS), (ii) intense ductile shearing of the HHC, having top-to-the-southwest and top-to-the-northeast shear indicators, (iii) structural control on melt accumulation of the Himalayan migmatites, (iv) Himalayan inverted metamorphism, and (vi) assessment of channel flow or other models.

Based on lithologies and grade of metamorphism from the lower to higher structural levels northwards, the HHC is divisible into two main groups above the Munsiari Thrust. In the lower parts, the Munsiari Group of low to medium grade contains garnet mica schist/gneiss, quartzite, amphibolite and biotite-rich phyllonite, mylonitic gneiss and augen gneiss. Overlying the Vaikrita Thrust, the Vaikrita Group is comprised of the Joshimath Formation (garnet-biotite-muscovite schist/psammitic gneiss), the Suraithota Formation (kyanite-garnet-biotite schist/psammitic gneiss and amphibolite), and the Bhapkund Formation (sillimanite/fibrolite- kyanite-garnet-biotite psammitic gneiss/schist with pervasive migmatite, concordant to discordant pegmatite veins, and small tourmaline-rich leucogranite lenses/dykes and the Malari leucogranite). The Vaikrita Group is typically characterized by inverted metamorphism, where sillimanite–K-feldspar gneiss and migmatite in the uppermost parts of the Bhapkund Formation was metamorphosed under upper amphibolite facies at about >800 °C (Spencer et al., 2012). The Bhapkund Formation constitutes the footwall of the STDS, which separates it from the very low biotite-grade to unmetamorphosed quartzite and slates/phyllite of the Martoli Formation of the basal Tethyan Sedimentary zone under peak metamorphic conditions of 450±50 °C.

Various shear sense indicators proliferate the HHC between Helang and Malari. From the asymmetry of structures like S-C and S-C' fabric, boudins, mantled porphyroclasts, folds etc., sense of ductile to brittle-ductile shearing reveals two phases of ductile shear deformation: (a) an older top-to-the-SW upwards phase throughout the HHC having an overall thrust geometry, and (b) a younger superposed top-to-the-NE downwards phase with normal fault sense from the middle to upper parts (Shreshtha et al. communicated).

In the upper parts of the HHC migmatite is ubiquitously distributed up to Malari in the upper parts of the Bhapkund Formation, having five different phases of melt accumulation (Jain et al. 2013). The oldest migmatite phase (Me1) parallels the main foliation S_m as the stromatite layers and concordant leucogranite bands. Younger melt phases Me2, Me3 and Me5 are recorded along small-scale ductile thrusts, extensional fabric and structureless patches, respectively. It is only the Me4 melting phase that is evidenced by large-scale melt migration along cross-cutting irregular veins. These were possible conduits for migration and accumulation of melt into larger leucogranite bodies like the Malari granite (19.0±0.5 Ma).

Cite as: Jain, A.K. et al., 2014, Higher Himalayan Crystalline (HHC) Belt: its shear sense indicators and their implications on its tectonic evolution, in Montomoli C., et al., eds., Proceedings for the 29th Himalayan-Karakoram-Tibet Workshop, Lucca, Italy.

Various tectonic models for the evolution of the Himalayan metamorphic belt can be critically assessed in this section, as these shear indicators provide invaluable constraints on various tectonic models currently in use for the evolution of the Himalayan metamorphics.

References

Jain, A.K., Seth, Puneet, Shreshtha, Mrinal, Mukherjee, P.K. and Singh, Keser, 2013, Structurally-controlled Melt Accumulation: Himalayan Migmatites and Related Deformation – Dhauli Ganga Valley, Garhwal Himalaya, Journ. Struct. Geol., 82, 313-318.

Shreshtha, M., Jan, A.K. and Singh Sandeep, Shear sense analysis of the Higher Himalayan Crystalline (HHC) belt, and tectonics of the South Tibetan Detachment System (STDS), Alaknanda – Dhauli Ganga Valley, Uttarakhand Himalaya, Communicated.

Spencer, C.J., Harris, R.A. and Dorais, M.J., 2012, The metamorphism and exhumation of the Himalayan metamorphic core, eastern Garhwal region, India, Tectonics, 31, TC1007, doi:10.1029/2010TC002853.

Continental subduction vs. collision: What shaped the Himalaya?

Arvind K. Jain[1]

[1] INSA Senior Scientist, CSSI-Central Building Research Institute Roorkee-247667, India, himalfes@gmail.com

Two major processes appear to have shaped the youngest mountain belts on the Earth– the Himalaya and the Trans-Himalaya mountains: subduction of (i) the Tethyan oceanic lithosphere and (ii) the Indian continental lithosphere. Against the common concepts that the Himalaya originated due to continent-to-continent collision of the India-Asian Plates, recent geological, geophysical and geochronological data from the northern parts of the Himalaya and Trans-Himalayan mountains have been critically evaluated to highlight evolution of these mountains through time.

As the vast Neo-Tethyan Ocean separated the continents of the Indian and Asian Plates, these continents would not have collided initially to start with. It became therefore evident that leading Tethyan oceanic lithosphere in front of the Indian continent initially subducted and melted to produce the calc-alkaline magmatic Shyok-Dras Volcanic Arc, which was subsequently intruded by the Ladakh Batholith. Hence, these mountains did not initially evolve by the collision of continents of the Indian and Asian Plates.

Timing of the first impingement of the Indian and Asia Plates has been better constrained at around 58 Ma by comparing the (i) bulk ages from the Ladakh Batholith (product of partial melting of the Tethyan oceanic lithosphere) with the (ii) subducted continental lithospheric and UHP metamorphosed Indian crust in the Tso Morari, and (iii) biostratigraphy of the youngest marine sedimentation in Zanskar. Thus, the Himalaya first rose and emerged from the deeply exhumed terrain in the Tso Morari only between 53 and 50 Ma. It was followed by sequential imbrication of the Indian continental lithosphere, its subduction at ~45-35 Ma and ~25-15Ma to produce the Eo- and Neo-Himalayan metamorphism and associated exhumation episodes during rise of the Himalayan Mountains from north to the south since 45 Ma.

Current sub-horizontal geometry of the Indian Plate, deciphered by seismic tomography, focal plane mechanism of recent earthquakes, gravity, and magnetotelluric methods, bespeaks continental lithosphere subduction in the Himalaya; this geometry can only be achieved by episodic sub-horizontal push of the Indian Plate towards north.

Cite as: Jain, A.K., 2014, Continental subduction vs. collision: What shaped the Himalaya?, in Montomoli C., et al., eds., proceedings for the 29th Himalaya-Karakoram-Tibet Workshop, Lucca, Italy.

Topographic evolution and climate aridification during continental collision: insights from numerical modeling

Ivone Jiménez-Munt[1], Daniel Garcia-Castellanos[1]

[1] Institute of Earth Sciences Jaume Almera, ICTJA-CSIC, Barcelona, Spain, ivone@ictja.csic.es

What is the relative importance of tectonics, sediment transport and climate in shaping the topographic evolution of the Earth? And how much does the erosion and sedimentation at the crust's surface influence the distribution of tectonic deformation? During the last three decades, these questions have been often addressed via numerical models constrained with thermochronological and geomorphological data at scales ranging from local to orogenic.

Here we present a new numerical model that aims at reproducing these phenomena at the continental scale (Fig. 1). For this purpose, we couple in a single computer model: 1) a thin-sheet viscous model of continental deformation; 2) a stream-power surface transport approach; 3) flexural isostasy allowing for the formation of large sedimentary foreland basins; and 4) a orographic precipitation model that reproduces basic climatic effects such as continentality and rain shadow.

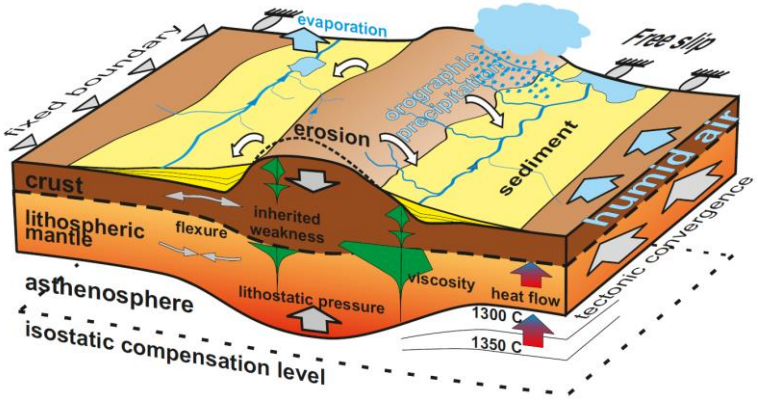

Figure 1. Conceptual cartoon with the processes integrated in the model. River erosion and sediment transport is calculated using a stream power approach and allowing the water follow the maximum slope. Evaporation is explicitly accounted for in lakes. The horizontal tectonic velocity is predefined at the boundaries. The viscosity of the lithospheric layer is dependent on the thermal regime and lithological parameters. The thickness of crustal and mantle varies according to the accommodation of the boundary velocities, depending on the viscosity distribution.

We quantify the feedbacks between these 4 processes in a synthetic scenario inspired by the India-Asia collision. The model reproduces first-order characteristics of the growth of the Tibetan Plateau as a result of the Indian indentation. A large endorheic, intramountain basin representing the Tarim Basin develops when predefining a hard inherited area in the undeformed foreland (Asia). The amount of sediment trapped in this basin is very sensitive to climatic parameters, particularly to evaporation, because it crucially determines its endorheic/exorheic drainage. We identify some degree of feedback between the deep and the surface processes, leading locally to a <50% increase in deformation rates in places where orographic precipitation is concentrated. This climatically-enhanced thickening of the crust takes place in areas of concentrated precipitation and steep slope as at the upwind flank of the growing plateau and the corners of the indenter (syntaxes). We hypothesize that this may provide clues for better understanding the mechanisms underlying the intriguing tectonic aneurisms documented in the Himalayas. In the continental scale, however, the overall distribution of topographic ranges and basins seems insensitive to climatic factors, despite these do have important, sometimes counterintuitive effects on the amount of sediments trapped within the continent. The dry climatic conditions that naturally develop in the interior of the continent, for example, are key in triggering large intra-continental basins and sediment trapping. Finally, the complex surface-tectonic interactions identified make the development of steady-state topography at the continental scale unlikely.

Cite as: Jiménez-Munt, I. and Garcia-Castellanos, D., 2014, A numerical model of continental-scale topographic evolution integrating thin sheet tectonics, river transport, and orographic precipitation, in Montomoli C., et al., eds., proceedings for the 29th Himalaya-Karakoram-Tibet Workshop, Lucca, Italy.

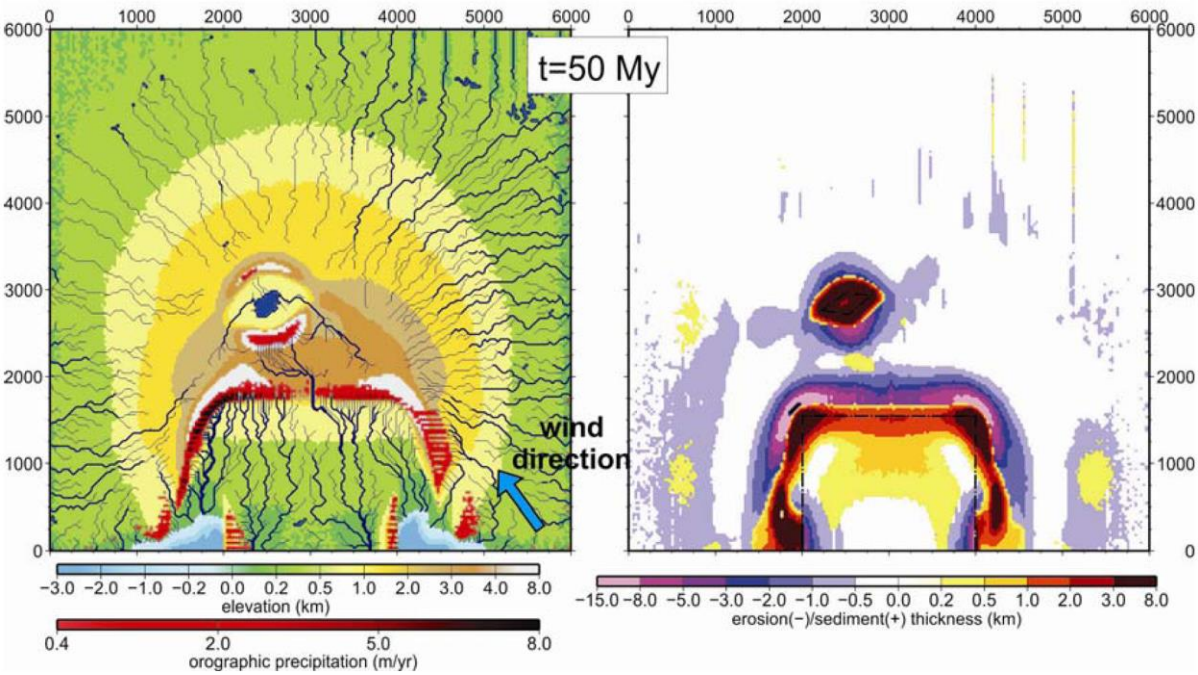

Figure 2. Final topography, precipitation, drainage (left panel), and erosion and sediment distribution (right panel) resulting from orographic precipitation and NW wind direction.

Prospects of Precious and Semiprecious stones in Nepal Himalaya and their Mining Opportunities

Krishna P. Kaphle[1], Hans C. Einfalt[2]

[1] Central Department of Geology, Tribhuvan University, Kirtipur, Kathmandu, Nepal,kpkaphle@gmail.com
[2] Bretten, Federal Republic of Germany, hcv.einfalt@t-online.de

Prospects of precious and semiprecious stone from different parts of the Higher Himalayas and Crystalline Klippe/ Nappe in the Lesser Himalayas in Nepal are known since more than six decade. Few, very small scale quarries are also in operation since that time. Almost all of them are mined applying crude methods without any technical knowhow. As a result more than 75% of the valuable resources are destroyed and wasted during blasting for mining and applying crude mining methods to separate them from the host rocks.

This paper epitomizes these prospects by studying existing prospects/ mines all across Nepal while referencing existing literatures, documents and findings. Among the well known precious stones from Nepal Himalaya are ruby, sapphire and topaz. Similarly among the semiprecious stones constitute various coloured tourmaline, aquamarine, amazonite, gahnite, danburite, kyanite, garnet, epidote, amethyst, citrine, smoky quartz, agate, jasper and colourless transparent rock crystals (Kaphle, 2011). Some of the mines of these stones are closed, few are operational and others are in development stage.

Among the precious stones gem quality small crystals of light red to red ruby and light to dark blue sapphire exist in Chumar and Ruyil villages in the northern remote part of Dhadhing district and in Shelghar, Songlahas, Pola and Sublay in Rasuwa district. They occur in highly tectonized intensely folded en-chelon lenses of saccharoidal dolomite within the high grade metamorphic rocks in MCT zone (Smith et. al., 1997, Basset, 1987). Some corundum, sapphire, and green and straw yellow topaz are also known from Ilam, Taplejung and Rasuwa districts respectively.

Gem quality distinctive multihued tourmaline (Elbaite) and pink, bright green, light orange sometimes with repeated colour banding olive green with amber coloured core tourmaline from Hyakule and Phakuwa are mined from the complex pegmatites in Sankhuwasabha, eastern Nepal are known since 1934 (UN/ESCAP with DMG, 1993). Pegmatites of Ikabu and Lodantar (Taplejung), few places in Panchthar, Langtang valley (Rasuwa), Naje (Manang), Garkhakot (Jajarkot) are also promising for tourmaline. Similarly aquamarine and quartz crystals from Ikabu and Lodantar and hambergite, danburite and ijolite are the important prospects in Taplejung. Aquamarine from Phakuwa (Sankhuwasabha); aquamarine and green coloured tourmaline from Naje (Manang), Lekhpatan and Tikachaur (Jajarkot); Jagat, Panchmane and Kagtigaon (Kathmandu); Baguwa, Tarkeghyang, Nibuwagaon (Sindhupalchok); Khaptad (Bajhang), and few places of Darchula and Panchthar are the other promising sites for aquamarine/ beryl.

Light green amazonite from pegmatites in Hyakule, Phakuwa, Naje and some parts of Taplejung are not minable deposits. Yellowish green to pistachio-green transparent crystals of epidote are recorded in epidote garnet schist, epidote bearing amphibolites and gneiss in Manang. However, there is no epidote mine as such. Gem quality inky blue kyanites are known from Dolakha, Sankhuwasabha, Taplejung, Rasuwa, Dhadhing, Bajhang, Jajarkot, and Achham districts. Kyanite mines are in operation in Daha and Suneri area in Jajarkot in Mid western and Barah area of Achham district in Farwestern Nepal. Garnet is another important gemstone which is widely found mainly in the Higher Himalayan region in Sankhuwasabha, Taplejung, Ilam, Dhadhing, Rasuwa, Jajarkot and few other districts. Deep red and red coloured almandine, hessonite and pyrope garnet are mined from Sankhuwasabha and Taplejung. Quartz crystals are known from pegmatite located in different parts of Taplejung, Ilam, Sankhuwasabha, Nuwakot, Dhadhing, Rashuwa, Manang, Dailekh, Jajarkot and Darchula districts. Smokey quartz crystals, amethyst, citrine, and rock crystals of gem quality are also available in different parts of Nepal. At present

Cite as: Kaphle, K.P. and Einfalt, H. C., 2014, Prospects of Precious and Semiprecious stones in Nepal Himalaya and their Mining Opportunities, in Montomoli C., et al., eds., proceedings for the 29th Himalaya-Karakoram-Tibet Workshop, Lucca, Italy.

only two small scale mines are in operation in Khejemi/ Sirku (Taplejung) and Raluka (Nuwakot). Some crypto crystalline red coloured jaspers are recorded in heavy mineral concentrate samples from major rivers but no mineable deposit is traced so far. Agate with attractive alternating layers of chalcedony and opal are present in few places in Sankhuwasabha and Taplejung districts. Most of these prospects are yet to be mined commercially because of lack of infrastructures, technical knowhow, less attractive government policy and contradiction in existing Mining Act, Local Governance Act and Forest Act. Modern faceting gems cutting and polishing machine was introduced in 1985, and a few lapidary works and gem shops were opened in Kathmandu. At present more than six such gem cutting and polishing industries are operational while a number of gem shops are running their business in various major cities. According to the record of DMG, 37 prospecting licenses and 8 mining licenses for different types of gemstones were issued in the Fiscal Year 2009/2010. Few small scale gem stone mines are in operation in Dailekh, Jajarkot, Manang, Dhadhing, Nuwakot, Sindhupalchok, Sankhuwasabha and Taplejung districts but their actual production figures are not known. More than 50% precious and semiprecious raw stones and cut and polished gemstones are imported by Nepal mainly from Burma, Thailand, Hong Kong, Indonesia, Sri-Lanka, Pakistan, India and Russia. The Himalayan gems are very famous and on demand in the international market which make the gemstone prospects very attractive.

There is high opportunity to explore and exploit these stones in Nepal and it demands detail investigations that are yet to be carried out, especially, in the Higher Himalayan region. Therefore, it is recommended to conduct detail exploration and technical evaluation of such prospects prior to mining. By introducing advance mining methods and suitable technology in conjunction with the expert's technical advice there are tremendous opportunities to exploit such deposits in the Higher Himalaya. These well crystallized, attractive fancy coloured, precious and semiprecious stones can be cut and polished as gemstones. Completion of under construction East – West Mid Highway and North – South Highways which pass through the Lesser Himalayan and Higher Himalayan mountain region will facilitate detail investigations in virgin areas and proper mining of known deposits. Mining of these natural resources will not only help to develop infrastructures in remote areas and upgrade the living standard of the local people but also contribute to Nepal's National GDP.

References

Kaphle, K.P., 2011, Himalayan Gemstones and their prospects in Nepal, Bulletin of Nepal Geological Society, 28, 43-50.

Basset, A.M., 1987, Nepal gem tourmaline, Jour. of Nepal Geol. Soc., 4, n°1 and 2, 31-41.

Smith, C.P., Gubelin, E. and Basset, A.M., 1997, Rubies and Fancy- color sapphire from Nepal. Gems and Gemology vol.XXXIII, Quaternary Jour. Of the Gemological Inst. Of America, 24-41.

UN/ESCAP with DMG, 1993, Geology and Mineral Resources of Nepal. Atlas of Mineral resources of the ESCAP region. Published by UN/ESCAP in coordination with DMG. MIC&S/ HMG Nepal, 9, 107 pp.

Paleoseismic geomorphology of the Main Frontal Thrust between 85°49' and 86°27' E

Çağıl Karakaş[1], Paul Tapponnier[1], Somanath Sapkota[2], Laurent Bollinger[3], Yann Klinger[4], Magali Rizza[5], Aurélie Coudurier Curveur[1]

[1] Earth Observatory of Singapore, Nanyang Technological University, Singapore 639798, Singapore, ckarakas@ntu.edu.sg
[2] National Seismic Center, Department of Mines and Geology, Lainchaur, Kathmandu, Nepal.
[3] Département Analyse et Surveillance Environnement, CEA, DAM, DIF, F-91297 Arpajon, France
[4] Institut de Physique du Globe de Paris, UMR 7154, 75238 Paris, France.
[5] CEREGE, Aix-Marseille Université, Marseille France

Our recent fieldwork in eastern Nepal has shown that the M ≈ 8.4, 1934 Bihar-Nepal earthquake ruptured the surface. Traces of that rupture and of more ancient ones are clear along the Main Frontal Thrust between at least 85°49' and 86°27' E. We document and quantify the amounts and ages of relative uplift - including co-seismic – on the thrust using geomorphic markers and OSL, 10Be cosmogenic and radiocarbon dating. Our systematic mapping and sampling of uplifted terrace surfaces and abandoned paleo-channels truncated by the MFT at an increasing number of localities is based on extensive field observations, with interpretation of stereoscopic air photos and high-resolution (HR) satellite images, topographic maps and newly acquired Digital Elevation Models from Total station and Terrestrial Lidar Scanner (TLS) surveys. Our long-term goal is to build a synoptic comparison, over as long a stretch of the mega-thrust as feasible, of the heights and ages of potentially coeval co-seismic and cumulative scarps. We present here a preliminary assessment of the extension of the co-seismic ruptures between the Mahara and Khutti Khola, ~ 65 km apart. We discuss the geomorphic correlation between the sites to better determine the seismic behavior of the MFT and its relationship with underlying tectonic structures. A few sets of measurements may be taken to imply characteristic increments of throw during sequences of 2 to perhaps as many as 8 earthquakes.

Cite as: Karakaş, Ç., Tapponnier, P., Sapkota, S., Bollinger, L., Klinger, Y., Rizza, M., Coudurier Curveur, A., 2014, Paleoseismic Geomorphology of the Maint Frontal Thrust between 85°49' and 86°27' E, in Montomoli C., et al., eds., proceedings for the 29th Himalayan-Karakorum-Tibet Workshop.

The potential record of far-field effects of the India-Asia collision: Barmer Basin, Rajasthan, India

Michael J. Kelly[1,4], Yani Najman[2], Premanand Mishra[1], Alex Copley[3], Stuart Clarke[4]

[1] Cairn India Limited, 3rd Floor, Vipul Plaza, Sun City, Sector 54, Gurgaon – 122 002, India, Michael.Kelly@cairnindia.com
[2] Lancaster Environment Centre, Lancaster University, Lancaster, Lamcashire, UK, LA1 4YQ
[3] Department of Earth Sciences, Bullard Laboratories, Univeristy of Cambridge, Cambridge, Cambridgeshire, UK, CB3 0EZ
[4] Basin Dynamics Research Group, Keele University, Keele, Staffordshire, UK, ST5 5BG

The timing of the collision of the Indian plate with the Asian plate to create the Himalayas is broadly dated at ca 55-50 Ma. However, the extent and duration of deformation caused by the collision remote from the Himalayan mountain belt remains poorly understood. In particular, the nature and extent of foreland uplift and the initial Himalayan fore-bulge is poorly defined (Bera and Mandal, 2013), as is the extent of Himalayan compression. The Barmer Basin, Rajasthan, situated 800 km from the Himalayan front and 400 km from the Kirthar Mountains / Central Bruhui Range of Pakistan, is one basin where it has been proposed that far-field effects of India-Asia collision are evident (Compton, 2009). It is a major oil and gas producing region, with hydrocarbon generation and migration potentially influenced by Himalayan tectonic events. Until recently, the scale, structure and geology of the Barmer Basin were poorly constrained and only since subsurface and well data became available over the last decade has an appreciation of the significance of the basin been achieved (Bladon et al., in review; Dolson et al., in review); a rift-related setting but with regional tilting and reactivation of basement structures on the Indian craton potentially due to the India-Asia collision.

The Barmer Basin is a long (200 km), narrow (<40 km) and deep (<6 km), north-northwest trending, failed continental rift covering ~6800 km^2 principally situated in Rajasthan, northwest India (Figure 1a). The basin forms the northward extension of the Kutch and Cambay basins via the Sanchor and Tharad sub-basins within the West-Indian Rift System (Bladon et al., in review).

The main phase of extension within the Barmer Basin *sensu stricto* occurred between the late Cretaceous (Maastrichtian) and mid-Eocene (Lutetian) (Bladon et al., in review). The basin fill incorporates Lower Jurassic (Lathi Fm.) and Lower Cretaceous (Ghaggar-Hakra Fm.) pre-rift continental clastic successions. Syn-rift sedimentary successions are predominantly Paleocene to Eocene in age, and indicate a relative increase in water depth, with a progression from fluvial, through lacustrine, to shallow marine deposition (Dolson et al., in review). Latest Cretaceous (Maastrichtian) to Lower Palaeocene (Selandian) fluvial sandstones and lacustrine deposits (Fatehgarh Fm.) are deposited following a ~30 Ma hiatus. The Barmer Hill Formation overlies this succession, recording a complex array of different sedimentary styles filling the basin including: gravity flow deposits, lake margin deltaic sediments, diatomites, and pelagic mudstones. Deposition of these units is followed by the predominantly claystones of the Dharvi Dungar Formation (upper Thanetian-Ypresian) and the Thumbli, Akli and Nagarka Formations (Ypresian-Lutetian). Finally Miocene to Recent sediments unconformably overlie this succession (Jagadia and Uttarlai Formations). A major unconformity separates Lutetian and Miocene sediments, the Oligo-Miocene Unconformity (Compton, 1999).

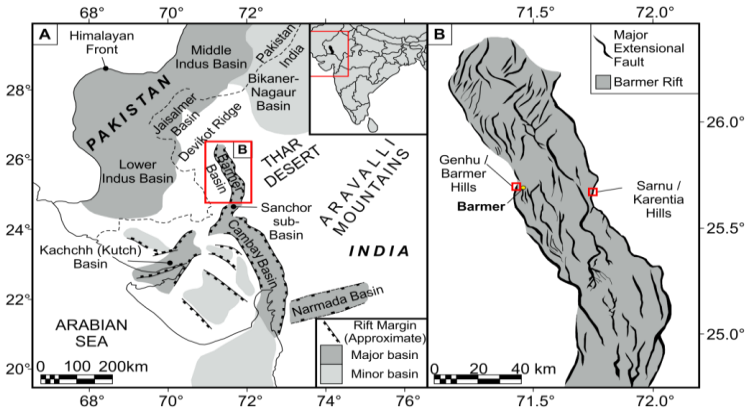

Figure 1: a) Onshore rift basins of northwest India, the West Indian Rift System (WIRS), incorporating the Kachchh (Kutch), Cambay, Barmer, and Narmada basins (location within India inset). b) Current basin-wide structural interpretation based on subsurface data alone [location highlighted in (a)] (Adapted after Bladon et al., in review)

Cite as: Kelly, M.J., Najman, Y., Mishra, P., Copley, A. and Clarke, S., 2014, The potential record of far-field effects of the India-Asia collision: Barmer Basin, Rajasthan, India, in Montomoli C., et al., eds., proceedings for the 29th Himalaya-Karakoram-Tibet Workshop, Lucca, Italy

Previous workers have proposed effects of the Himalayan Orogeny to explain a number of features present in the Barmer Basin, including the small angular unconformity at the Paleocene-Eocene transition, the influx of sediment in the Early Eocene which is ascribed to uplift of the northern margin of the basin, and the Oligo-Miocene unconformity (Compton 2009; Dolson et al., in review), evidence of N-S and NNE-SSW compressive stress directions (Compton 2009), and >1km of uplift in the north of the Basin (Dolson et al., in review). This work documents and investigates the regional compression and Oligo-Miocene uplift, and considers it in light of the possible far-field effects of the India-Asia collision. To achieve this, the work:

1. Documents and dates compressional structures providing evidence of inversion using public and company seismic data to record the amount of inversion along reactivated structures and determine which successions are affected, thus dating compressional events. Previous work has not identified any evidence of inversion or reactivation at outcrop scale within the eastern basin margin (e.g., Sarnoo (Sarnu) Hills; Figure 1b; Bladon et al., in review). However, non-coaxial extension structures have been identified leading to differential fault networks within the Barmer Basin (Bladon et al., in review). Within the western basin margin, potential small-scale reactivations of Malani basement-derived faults and steepening of pre-existing extensional faults have been suggested to indicate inversion (e.g. Barmer Hills; Figure 1b). Structural inheritance combined with potential reactivation of pre-existing non-coaxial fault networks during the India-Asia collision has major implications for basin compartmentalisation.
2. Documents, dates and considers the extent of the Base Miocene (Oligocene) Unconformity (BMU) within the Barmer Basin using public and company seismic data. Previous work has identified a major Oligocene unconformity along the entire length of the Himalayan peripheral foreland basin (e.g., Kohat Plateau; Hazara Syntaxes; Sabathu / Jammu / Kangra sub-basins e.g., DeCelles et al., 1998; Najman et al., 2004; Bera & Mandel, 2013). Development of this unconformity has previously been suggested as a result of tectonic processes associated with collision and / or a passage of a flexural forebulge (Najman et al., 2004; DeCelles et al., 1998; 2004; Irfan et al., 2005; Bhatia and Bhargava, 2006; Bera et al., 2010). This has been contradicted by Bera and Mandal (2013). A similar-aged unconformity is identified within the Barmer Basin (Compton, 1999) but is not present in all surrounding basins. Documentation of this unconformity beyond the extent of the foreland basin and Himalayan fore-bulge could require a revision of previous suggestions regarding the cause of the foreland basin unconformity and opens up the possibility of different interpretations to explain the hiatus (e.g. perturbations in the mantle such as those potentially caused by slab break off).

References

Bera, M.K. and Mandal, A., 2013. Forced regression across the marine to continental transition in Jammu sub-basin: Implication to the Oligo-Miocene unconformity in the Himalayan foreland. Journal of Asian Earth Sciences, 67-68, 37-45.

Bera, M.K., Sarkar, A., Chakrabarty, P.P., Ravikant, V. and Choudhury, A.K., 2010. Forced regressive shoreface sandstone from Himalayan foreland: implications to early Himalayan tectonic evolution. Sedimentary Geology, 229, 268–281.

Bhatia, S.B. and Bhargava, O.N., 2006. Biochronological continuity of the Paleogene sediments of the Himalayan foreland basin: Paleontological and other evidences. Journal of Asian Earth Sciences, 26, 477-487.

Bladon, A.J., Clarke, S.M., Burley, S.D. and Beaumont, H., Geology and regional significance of the Sarnoo Hills, eastern rift margin of the Barmer Basin, NW India. Basin Research. In review.

Bladon, A.J., Clarke, S.M. and Burley, S.D., Complex rift geometries resulting from inheritance of pre-existing structures: Insights from the Barmer Basin rift and their regional implications. Journal of Structural Geology Special Publication "Deformation of the Lithosphere: How Small Structures Tell a Big Story". In review.

Compton, P.M., 2009. The geology of the Barmer Basin, Rajasthan, India, and the origins of its major oil reservoir, the Fatehgarh Formation. Petroleum Geoscience, 15, 117-130.

DeCelles, P.G., Gehrels, G.E., Quade, J., Ojha, T.P., 1998. Eocene-early Miocene foreland basin development and the history of Himalayan thrusting, western and central Nepal. Tectonics, 17, 741-765.

DeCelles, P.G., Gehrels, G.E., Najman, Y., Martin, A.J. and Garzanti, E., 2004. Detrital geochronology and geochemistry of Cretaceous–Early Miocene strata of Nepal: implications for timing and diachroneity of initial Himalayan orogenesis. Earth Planetary Science Letters, 227, 313-330.

Dolson, J., Burley, S.D., Sunder, V.R., Kothari, V., Naidu, B., *et al.*, 2014. The discovery of the Barmer Basin, Rajasthan, India, and its Petroleum Geology. In review.

Irfan, M., Shadid, M., Haroon, M. and Zaidi, N.A., 2005. Sargodha High: A flexure fore-bulge of the Himalayan Foreland Basin. Geological Bulletin of the University of Peshawar, 38, 149-156.

Najman, Y., Johnson, K., White, N. and Oliver, G., 2004. Evolution of Himalayan foreland basin, NW India. Basin Research, 16, 1-24.

Assessment of land covers change due to flooding alongside Jhelum and Chenab rivers

Bushra Khalid[1,2], Hira Ishtiaq[2], Nageen Fatima[2]

[1] Department of Meteorology, COMSATS Institute of Information Technology, Islamabad, Pakistan, kh_bushra@yahoo.com
[2] Department of Environmental Sciences, International Islamic University, Islamabad, Pakistan

Pakistan is highly vulnerable to weather-related disasters. The country has increasingly been suffering from recurring cycles of intense droughts followed by enormous floods in the last few years. Massive floods of 2010 resulted into a cumulative financial loss of 10 billion US $, life loss of about 2,000 people, 17,553 villages were reportedly damaged and a total area of 160, 000 Km2 was affected. Punjab was severely damaged especially districts of Jhang, D.G. Khan, Rajanpur and Muzaffargarh. This devastating flood in 2010 was unusually intense and much bigger in scope as compared to other extreme events. Floods result in serious economic, social and environmental setback. Floods also change the land by making the farmland unworkable, affecting the vegetation cover, destructing the buildings and roads and thus changing the land use and land cover. Land cover change detection is very important to study or deduce the effects of any natural phenomenon or disaster on ecological system. Satellite Remote Sensing is an evolving technology with a potential to estimate and monitor the effects of any catastrophe. Flooding and flood induced land cover and land use change can be detected by using satellite imageries. This research focuses on the flood impact assessment of Jhang district of Punjab province using multi-temporal satellite images for year 2009 (May and August) and 2010 (July, August, September and December). The motivation of this study is the flood of 2010 in which Jhang was severely affected by flooding in River Chenab and Jhelum. Landsat ETM+ 30 meter multispectral imageries were used for flood assessment by employing maximum likelihood algorithm for supervised classification. Three instances i.e. pre-flood, during flood and post-flood were compared to estimate the change in Land use and Land Cover of district Jhang along Jhelum and Chenab Rivers. Comparison of pre and post flood images shows that there was significant decrease in built up area during flooded instances i.e. from 44% to 13%. Built up area again increased in post-flood month probably due to receding of water and rehabilitation activities. Water content was maximum in the month of August due to flooding while it slowly receded back in post flood month. Vegetation is 41% in August 2009 and 54% in August 2010 as this is a cropping season, and in this month crops like rice, maize etc. start to cultivate, so chlorophyll content is found largely in crops which was identified in NIR band while in May 2009 and December 2010, vegetation is less and bare soil has increased. Water is 2% in August 2009 due to monsoon rains. As flood struck Jhang in August 2010 so water covered about 10% of area. Water class was increased to about 5 times of the pre-flood instance. Post Flood instant clearly depicts that flooded water has almost completely receded and again the land preparation period for new cultivation has been started. The information as a result of this research can be used in further planning for natural resource management, land and water resource management. Climatic modeling and sustainability research can also be facilitated. The data of this research can be used by researchers, policy planners, and other decision makers requiring improved means of projecting land-use/ cover change.

Cite as: Khalid, B., Ishtiaq, H. and Fatima, N., 2014, Assessment of land covers change due to flooding alongside Jhelum and Chenab rivers, in Montomoli C., et al., eds., proceedings for the 29th Himalaya-Karakoram-Tibet Workshop, Lucca, Italy.

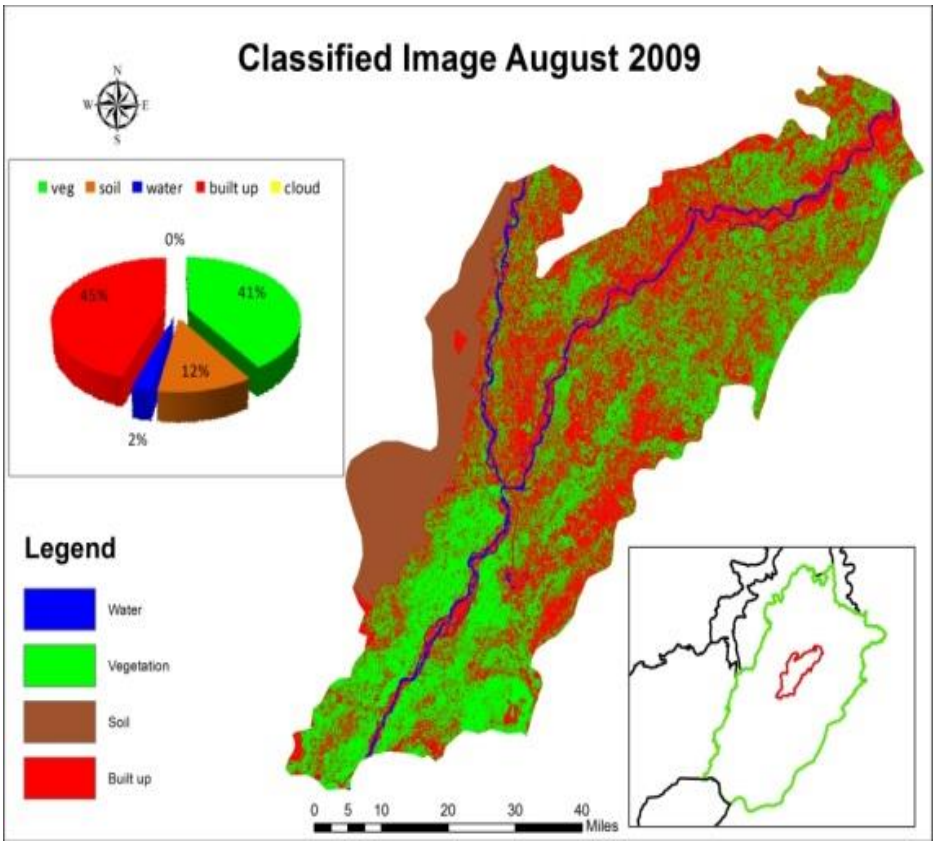

Figure 1. Classified image of August 2009. This is pre-flood classified image. Water has clearly concentrated in the river channels and only 2% area is covered with water.

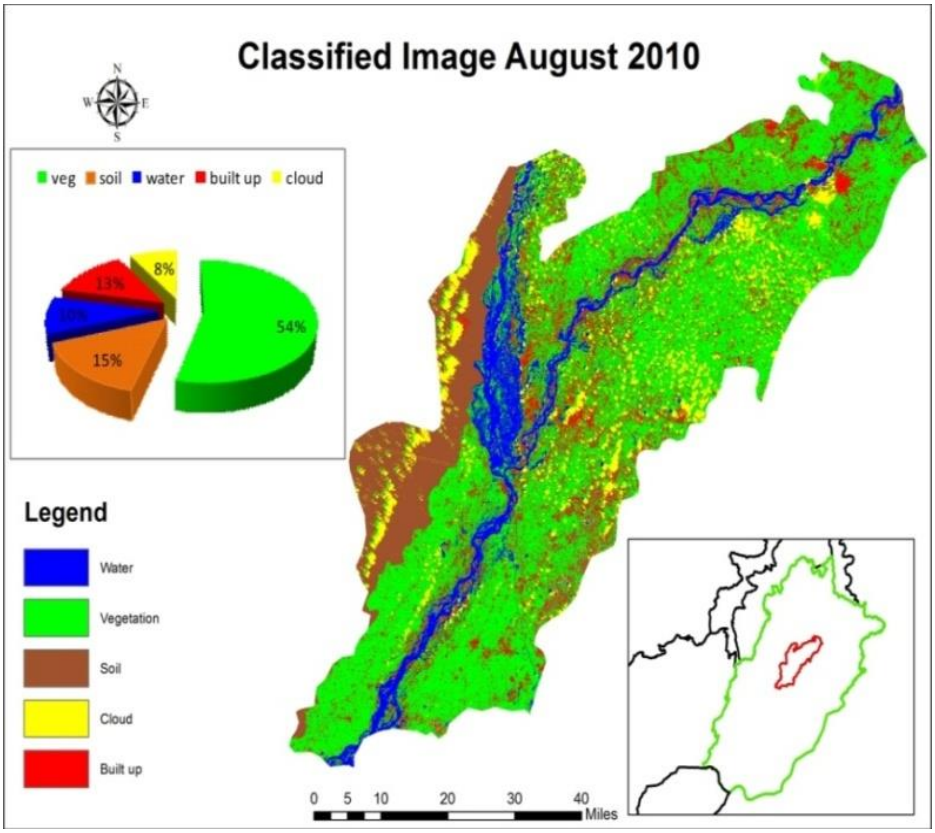

Figure 2. Classified image of August 2010. This figure shows that the area covered with water has significantly increased due to flooding.

Bearing of topography and converging plate geometry on earthquake incidences in the Central Himalaya

Prosanta K. Khan[1], Md. Afroz Ansari[1], Virendra M. Tiwari[2], S. Mohanty[3], Jayashree Banerjee[1]

[1] Department of Applied Geophysics, Indian School of Mines, Dhanbad, India, pkkhan_india@yahoo.com
[2] National Geophysical Research Institute, Hyderabad, India
[3] Department of Applied Geology, Indian School of Mines, Dhanbad, India

We critically examine the occurrences of great damaging earthquakes in the backdrop of topography, gravity and finite element modeling. We find positive correlation between blocks of concentrated seismicity and higher topography along Main Central Thrust (MCT) with the areas of northward-extended Gandak and Sarda depressions. Instead, the penetrating ridges (Monghyr-Saharsa, Faizabad, Delhi-Hardwar), around the gaps of seismicity and lower topography along MCT, might be prohibiting the occurrences of earthquakes (Khan et al., 2014). The less active seismic zone or the gaps possibly represent the areas of quiescence of recent episode of tectonic pulse. We further carry out gravity and finite element stress modeling of the strike-orthogonal converging Indian lithosphere and the overriding Asian land mass for the Nepal and Sikkim-Darjeeling sectors. We delineate the geometries of different intra-crustal layers and their interfaces through gravity modeling. The optimum model parameters along with rheological parameters of different layers are used for finite element modeling. Finite element modeling is done with boundary conditions of keeping the upper surface free, and rigidly fixing the section of the northern boundary below the Main Himalayan Thrust (MHT). We impart a force of amount 6×10^{12} N/m on its frontal section, which is equivalent to resistive force of the Himalayan-Tibet system, and analyze the maximum and minimum compressive stress fields evolved in the lithosphere. We testify our observations with earthquake database. We analyze 114 earthquake events (magnitude ≥ 4.0) occurring during the period 1902 to 2012 in these sectors of the Himalayan arcuate belt. The earthquake data were taken from the catalogues of Indian Society of Earthquake Technology, International Seismological Centre and US Geological Survey. A total of 13 focal mechanisms of earthquakes of magnitude $M_w \geq 4.7$ are also compiled from the Harvard Centroid Moment Tensor Catalogue and other different sources for better understanding the deformation processes.

We note an increasing flexing of the penetrating Indian lithosphere beyond the Main Boundary Thrust (MBT) becomes maxima between MCT and South Tibetan Detachment (STD) in both the areas; however, more steepening of the Moho boundary is identified in the Sikkim-Darjeeling Himalaya (Ansari et al., 2014). The more steepening Moho boundary in Sikkim-Darjeeling Himalaya is likely correlated with higher seismicity concentration in this region. Further, a significant distribution of seismicity in the upper-most part of the mantle clearly shows its higher degree of deformation. It is also apparent from the finite element modeling that the maximum compressive stress field is more confined right within the bending zone of the penetrating Indian lithosphere beneath the Greater Himalaya. Instead, the upper surface of different layers record extensional tectonics. Amplitude of estimated stresses in the present calculation might change due to uncertainties in the several parameters utilized to compute the stresses; however, the pattern would remain same, and the inferences drawn from the present study remain valid.

Focal mechanisms of earthquake events reveal that the sharp bending section of the lithosphere is associated with both strike-slip and thrust dominated movements, and shear planes of most of these events are more or less parallel with the interfaces of the different crustal layers of the converging Indian lithosphere. We find one event lying on the surface of Indian lower crust is dominated by normal faulting, and likely associated with operative extensional stress field. Another significant observation is the dominant right-lateral shear movements in the crustal part of the converging lithosphere, which is possibly controlled by either local or regional changes of plate obliquity, and presumably associated with the general dynamics and kinematics of the Himalaya (Ansari and Khan, 2014). We finally propose that

Cite as: Khan, P. K, Ansari, M. A., Tiwari, V. M., Mohanty, S. and Banerjee J., 2014, Bearing of topography and converging plate geometry on earthquake incidences in the Central Himalaya, in Montomoli C., et al., eds., proceedings for the 29th Himalaya-Karakoram-Tibet Workshop, Lucca, Italy.

the zone of sharp bending of the descending Indian lithosphere is the nodal area of major stress accumulation, occasionally released in form of earthquakes. Motivated thrust-dominated movements along this margin possibly support this inference. Similar type of deforming domain of higher seismic potential right within the bending portion of the converging lithosphere was also identified elsewhere (Khan and Chakraborty, 2009; Khan, 2011; Khan et al., 2012).

References

Khan, P.K. and Chakraborty, P.P., 2009, Bearing of plate geometry and rheology on shallow-focus mega thrust seismicity with special reference to 26 December 2004 Sumatra event, Journal of Asian Earth Sciences, 34, 480–491.

Khan, P.K., 2011, Role of unbalanced slab resistive force in the 2004 off Sumatra mega earthquake (Mw > 9.0) event, International Journal of Earth Sciences, 100, 1749–1758, doi:10.1007/s00531-010-0576-4.

Khan, P.K., Chakraborty, P.P., Tarafder, G. and Mohanty, S., 2012, Testing the intraplate origin of mega-earthquakes at subduction margins, Geoscience Frontiers, 3, 473-481. doi:10.1016/j.gsf.2011.11.012.

Khan, P.K., Ansari, M.A. and Mohanty, S., 2014, Earthquake source characteristics along the arcuate Himalayan belt: dynamic implications, Journal of Earth System Science (accepted).

Ansari, M.A., Khan, P.K., Tiwari, V.M. and Banerjee, J., 2014, Gravity anomaly, flexure and deformation of the converging Indian lithosphere in Nepal and Sikkim-Darjeeling Himalayas. International Journal of Earth Sciences, doi:10.1007/s00531-014-1039-0.

Ansari, M.A. and Khan, P.K., 2014, Occurrences of damaging earthquakes between the Himachal and Darjeeling Himalayas: tectonic implications, Acta Geophysica, 62, 699-73, doi:10.2478/s11600-013-0190-5.

Geochronology of the volcanic rocks from the Luobusha Conglomerates in Tibet and their implications

Ming Kong [1], Chengdong Liu [1] , Wan Jiang [2], Xiaoxiong Li [3], Yunhan Yang [1], Peisheng Ye[2]

[1] State Key Laboratory Breeding Base of Nuclear Resources and Environment, East China Institute of Technology, Nanchang, 330013, China, chdliu@ecit.cn
[2] Institute of Geomechanics, CAGS, Beijing, 100081, China.
[3] State Key Laboratory of Geological Processes and Mineral Resources, and School of Earth Science and Mineral Resources, China University of Geosciences, Beijing 100083, China.

Luobusa conglomerates crop along the east end of The Yarlung Tsangpo suture zone(nearly, Zedong County), interbedded with acidic volcanic rocks(Thickness of 15M) at the bottom of the conglomerates, and the similar stratigraphic units, Kailas Formation, Qiuwu Formation and Dazhuqu Formation crop along the whole Yarlung Tsangpo suture zone from west to east.

We reported the age of the felsic tuff interbedded with the luobusha conglomerates in the western of Zedong County for the first time. Zircon LA-ICP-MS U-Pb analysis shows that the acidic volcanic rocks was formed at 18.66±0.22Ma ago, consequently, It is inferred that the time of the initial deposition of Luobusa conglomerates was about 20Ma, combined the zircon LA-ICP-MS U-Pb age of granite underlying the Luobusa conglomerates is 29.90±0.36Ma. The existence of the volcanic rocks documents a volcanic activity developed at 18.66±0.22Ma ago, together with volcanic rocks in the Kailas Formation and Dazhuqu Formation aged ~24Ma (Decelles, P. et al., 2011) and 24.1-19Ma (Aitchison, C. J. et al., 2000) respectively, a volcanic activity developed all along Yarlung Tsangpo suture zone and moved from west to east, meaning the 're-activation' of the suture zone, which is remarkably similar to the potassic – ultrapotassic volcanism caused by the movement of deep material along Gangdese zone in time and space (MO X.X, 2010).

Making further efforts, we inferred that under the area of Zedong County, the east end of The Yarlung Tsangpo suture zone, the deep material motion and the 're-activation' of the suture zone led the deep material up to the surface, and this volcanic activity hint that the evolution of the Tibetan Plateau transformed from Plates interactions into intraplate lithosphere interactions.

References

Aitchison C. J, Jason R.A, Angel C. et al., 2000, Tectonic Implications of Felsic Tuffs Within the Lower Miocene Gangrinboche Conglomerates, Southern Tibet, Journal of Asian Earth Sciences, 34, 287-297.

Decelles, P.G, Kapp, P., Quade. J. et al., 2011,Oligocene-miocene Kailas Basin, Southwestern Tibet Record of Postcollisional Upper-plate Extension in the Indus-yarlung Suture Zone, Geological Society of America Bulletin, 123(7), 1337-1362.

MO X.X, 2010, A review and prospect of geological researches on the Qinghai-Tibet Plateau, Geology in China, 4, 841-853.

Cite as: Kong, M. et al., 2014, Geochronology of the volcanic rocks from the Luobusha Conglomerates in Tibet and their implications, in Montomoli C., et al., eds., proceedings for the 29th Himalaya-Karakoram-Tibet Workshop, Lucca, Italy.

Retrogression and recrystallization of the Stak eclogite in the northwestern Himalaya: constrains from Raman spectroscopy of residual pressures of quartz in garnet

Yui Kouketsu[1], Kéiko Hattori[2], Stéphane Guillot[3], Nicole Rayner[4]

[1] Gehchemical reserch center, Graduate School of Science, The University of Toyko, Tokyo 113-0033, Japan, kouketsu.yui@eqchem.s.u-tokyo.ac.jp
[2] Department of Earth Science, University of Ottawa, Ottawa, Ontario K1N 6N5, Canada
[3] ISTerre, Université Grenoble I, CNRS, 1381 rue de la Piscine, 38400 Grenoble Cedex 09, France
[4] Geological Survey of Canada, 601 Booth Street, Ottawa, Ontario K1A 0E8, Canada

Several eclogites have been reported along the western Himalayas. Among them, the rocks in the Stak massif in northern Pakistan were extensively retrogressed and Le Fort et al. (1997) was the first to recognize the relict evidence of eclogitic metamorphism. Recent study by Lanari et al. (2013) unravelled the condition of this eclogitic metamorphism, 750 °C and 2.5 GPa, using electron microprobe X-ray compositional mapping. These results suggest that the rocks in the Stak massif have undergone high-pressure metamorphism, ~ 2.5 GPa. We present residual pressures preserved in quartz enclosed by garnet in the Stak massif and discuss the evolution of pressure (P)–temperature (T) conditions of the unit together with new U–Pb ages of zircon grains measured in-situ using SHRIMP.

Residual pressure is commonly preserved in a mineral enclosed by a sturdy metamorphic mineral, such as garnet, and detected as a frequency shift of the Raman spectrum (e.g., Nasdala et al. 2003). Kouketsu et al. (2014) recently calculated the residual pressure of quartz inclusion in garnet and proposed a method to constrain the metamorphic P–T conditions using the residual pressure. We used this method to evaluate the P–T conditions of quartz grains in highly retrogressed Stak rocks. We measured Raman spectra of more than 100 grains of quartz from five samples. The quartz grains in garnet show residual pressures of up to 0.52 GPa, which correspond to the metamorphic conditions of 1.6 GPa at 600 °C and 1.8 GPa at 700 °C. The evidence of high pressures, ~ 2.5 GPa, calculated by Lanari et al. (2013) was not detected by the residual pressure of quartz inclusions in garnets.

Zircon grains occur both within garnets and the matrix and are all small, <50 μm, which makes the separation difficult. Therefore, U–Pb ages of zircon grains were measured in situ using a SHRIMP. The ages range from 158 to 27 Ma. Zircon grains containing low Yb and low Th/U, < 0.03, yielded the age between 36–30 Ma. The compositions suggest that they are metamorphic ages, but the values are much younger than that of the peak UHP metamorphic ages for the nearby eclogitic units: ~ 51 Ma for the Tso Morari massif (St-Onge et al. 2013) and ~ 47 Ma in the Kaghan massif (Wilke et al. 2010). Considering the proximity of these eclogitic units, it is difficult to consider ~ 36–30 Ma as the peak metamorphic age. Furthermore, the Stak massif occurs adjacent to the Nanga Parbat-Haramosh massif (NPHM) and the metamorphic ages of the granulite-migmatites of the massif vary from 25 to 30 Ma (Zeitler et al. 1989). Based on the evidence, we suggest that the rocks in the Stak massif were heated to amphibolite to granulite facies conditions with NPHM at around 36–30 Ma and are almost totally recrystallized after the peak metamorphic condition. These data imply that the Stak massif continued to underthrust beneath the Asian plate while the other HP and UHP massifs in the western Himalaya were exhumed.

References

Kouketsu, Y., Nishiyama, T., Ikeda, T. and Enami, M., 2014, Evaluation of residual pressure in an inclusion–host system using negative frequency shift of quartz Raman spectra, Amer. Mineral., 99, 433–442.

Lanari, P., Riel, N., Guillot, S. et al., 2013, Deciphering high-pressure metamorphism in collisional context using microprobe mapping methods: Application to the Stak eclogitic massif (northwest Himalaya), Geology, 41, 111–114.

Le Fort, P., Guillot, S. and Pêcher, A., 1997, HP metamorphic belt along the Indus suture zone of NW Himalaya: new discoveries and significance, Comptes Rendus de l'Académie des Sci., Ser. IIA, Earth and Planetary Sci., 325, 773–778.

Nasdala, L., Hofmeister, W., Harris, J.W. and Glinnemann, J., 2005, Growth zoning and strain patterns inside diamond crystals as revealed by Raman maps, Amer. Mineral., 90, 745–748.

St-Onge, M.R., Rayner, N., Palin, R.M. et al., 2013, Integrated pressure-temperature-time constraints for the Tso Morari dome (Northwest India): Implications for the burial and exhumation path of UHP units in the western Himalaya, J. Metamorphic Geol., 31, 469–504.

Wilke, F.D.H., O'Brien, P.J., Gerdes, A. et al., 2010, The multistage exhumation history of the Kaghan Valley UHP series, NW Himalaya, Pakistan from U-Pb and $^{40}Ar/^{39}Ar$ ages, Eur. J. Mineral., 22, 703–719.

Zeitler, P., Sutter, J., Williams, I.S. et al., 1989, Geochronology and temperature history of the Nanga Parbat–Haramosh massif, Pakistan, Geol. Soc. Am. Spec. Pap., 232, 1–22.

Cite as: Kouketsu, Y., Hattori, K., Guillot, S. and Rayner, N., 2014, Retrogression and recrystallization of the Stak eclogite in the northwestern Himalaya: constrains from Raman spectroscopy of residual pressures of quartz in garnet, in Montomoli C., et al., eds., Proceedings for the 29th Himalaya-Karakoram-Tibet Workshop, Lucca, Italy.

Palaeobiogeographical distribution of the Early Jurassic *Lithiotis*-type bivalves *versus* Lhasa Block history

Michal Krobicki[1,2], Jan Golonka[2]

[1] Polish Geological Institute – National Research Institute, Upper Silesian Branch, Krolowej Jadwigi 1, 41-200 Sosnowiec, Poland, michal.krobicki@pgi.gov.pl
[2] AGH University of Science and Technology, Mickiewicza 30, 30-059 Krakow, Poland, krobicki@geol.agh.edu.pl

The supercontinent Pangea was formed during the Carboniferous time as the result of the Hercynian orogeny. However, separation of the Cimmerian Continent [Iran (Alborz)-Qiangtang-Malaysia-Sibumasu] from the Gondwanan part of Pangea during the latest Carboniferous–earliest Permian times by rifting and drifting event originated Neothethyan Ocean (Golonka et al., 2006). Northwards migration of this continent took place during Permian-Triassic times causing wide opening of the Neotethys and closing of the Paleotethys Ocean. During the latest Permian and earliest Triassic quick rifting of this ocean and drifting of several Gondwana-derived blocks caused strong Indosinian orogeny during Late Triassic times. This orogeny was the result of collision of Indochina with both Sibumasu and South China blocks, which closed part of the Paleotethys Ocean. The time of new break-up of northernmost part of the Gondwanan Pangea is still enigmatic but most probably took place during earliest Jurassic times. An especially relationship between Qiangtang and Lhasa blocks in space and time causes a lot of controversies. By this reason palaeogeographical position of the Lhasa Block during Mesozoic times is still matter of discussion. Its Late Paleozoic (Carboniferous-Permian) and Triassic south Pangean (peri-Gondwanan) affinities on the southern margin of the Paleotethys are indicated both by paleomagnetic and facies studies. After this break-up the Lhasa Block very quickly drifted northward from Gondwana.

From the palaeobiogeographical point of view the world-wide distribution of Pliensbachian-Early Toarcian large bivalves of the so-called *Lithiotis*-facies (*sensu* Fraser et al., 2004 with literature cited therein), dominated by *Lithiotis*, *Cochlearites*, *Litioperna* genus, indicates very rapid expansion of such type of bivalves, and could be good evidence of palaeogeographical position of the Lhasa Block in this time. The huge, up to 40-50 cm long, these bivalves are most significant representatives of buildup-maker of shallow marine/lagoonal bivalve mounds (reefs) in numerous places of Tethyan-Panthalassa margins during Pliensbachian-Early Toarcian times. The distribution of *Lithiotis*-facies bivalves from Western (Spain, Italy) and Middle Europe (Slovenia, Croatia, Albania and Romania) trough north Africa (Morocco) and westernmost Asia/Arabia (eastern Turkey, Iran, Iraq, Kuwait, Oman, Arabian Emirates) up to central Asia – Timor Island, Himalaya Mts (Nepal, China) and western margin of both Americas (USA, Peru) indicates world-wide, rapid expansion of such *Lithiotis*-type bivalves (Leinfelder et al., 2002; Fraser et al., 2004; Krobicki and Golonka, 2009). Especially, the Himalayan (Nepal – Garzanti & Frette, 1991) and Tibetan (Nyalam area – Yin et al., 1998, 1999; Yin & Enay, 2004; Yin & Wan, 1998; Shi et al., 2006; see also – Jadoul et al., 1998) occurrences of *Lithiotis* and/or *Cochlearites* bivalves could help to reconstruct of Early Jurassic position of the Lhasa Block. These occurrences may suggest migration path from western Tethys trough Panthalassa Ocean up to western margin of North and South America (USA, Peru). The Early Jurassic migration routes were connected both with break-up of Pangea and oceanic circulation, which facilitated high speed of distribution of larva's of such oyster-like bivalves. Previously in Triassic time the migration of sea fauna (Late Triassic crinoids, mollusks, crustaceans and so on) was going through the vast eastern Tethys branch of the Panthalassa Ocean which is perfectly visible in the distribution of the typical Alpine fauna of the western Tethys found in the numerous terranes along the western coasts of South and North America. The fauna did not have a possibility to migrate westward, but it could use the numerous terranes within Panthalassa as s*tepping-stones* allowing relatively free migration eastward from the Alpine Tethys (Kristan-Tollmann and Tollmann, 1985). Similarly, *Lithiotis*-type bivalves during larval-stage episodes could use the numerous terranes within Panthalassa Ocean as *„stepping-stones*" allowing free migration eastward from the Alpine Tethyan Ocean to Himalayan/Tibetan one.

Cite as: Krobicki, M., and Golonka, J., 2014, Palaeobiogeographical distribution of the Early Jurassic Lithiotis-type bivalves versus Lhasa Block history, in Montomoli C., et al., eds., proceedings for the 29th Himalaya-Karakoram-Tibet Workshop, Lucca, Italy.

On the other hand, the separation of Laurusia and Gondwana, which was initiated by the Triassic break-up of Pangea, continued during Early-Middle Jurassic time. The Early Triassic continental rifting was magnified at the Triassic/Jurassic boundary and the Atlantic Ocean originated as a consequence of this break-up. In effect, the origin of the narrow sea strait, so-called *Hispanic Corridor* took place between these two continents and connection of the Panthalassa Ocean (Proto-Pacific) and western (Alpine) Tethys gradually started in Early Jurassic, most probably in Sinemurian-Pliensbachian times. Therefore the widespread distribution of numerous fossil invertebrate groups took place during these times (Hallam, 1983; Damborenea, 2000; Arias, 2006, 2007, 2008; see also Damborenea & Mancenido, 1979; Boomer & Ballent, 1996; Venturi et al., 2006; Krobicki & Golonka, 2009). It is still open question, which migration route has been used by *Lithiotis*-facies bivalves to their whole world dispersion – trough Hispanic Corridor or by Panthalassa Ocean?

Recovery of marine fauna after Triassic/Jurassic mass extinction event was mainly marked by *Lithiotis*-type bivalves buildups distribution (e.g. Leinfelder et al., 2002; Fraser et al., 2004; Krobicki & Golonka, 2009). Their world-wide distribution indicate both very rapid occupation of specific ecological niches (mainly shallow-marine/lagoon-type carbonate sedimentation) and palaeogeographic/geodynamic regimes during break-up of Pangea in Pliensbachian-Early Toarcian times (Krobicki & Golonka, 2009). The key to understand of migration pattern of these bivalves is connection with geodynamic reconstruction, mainly including Asian palaeogeography.

References

Arias, C., 2006, Northern and Southern Hemispheres ostracod palaeobiogeography during the Early Jurassic: possible migration routes, Palaeogeography, Palaeoclimatology, Palaeoecology, 233, 63-95.

Arias, C., 2007, Pliensbachian-Toarcian ostracod biogeography in NW Europe: evidence for water mass structure evolution, Palaeogeography, Palaeoclimatology, Palaeoecology, 251, 398-421.

Arias, C., 2008, Palaeoceanography and biogeography in the Early Jurassic Panthalassa and Tethys Oceans, Gondwana Research, 14, 306-315.

Boomer, I. and Ballent, S., 1996, Early-Middle Jurassic ostracod migration between the northern and southern hemispheres: further evidence for a proto Atlantic-Central Atlantic connection, Palaeogeography, Palaeoclimatology, Palaeoecology, 121, 53-64.

Damborenea, S.E., 2000, Hispanic Corridor: its evolution and the biogeography of bivalve molluscs, GeoResearch Forum, 6, 369-380.

Damborenea, S. and Mancenido, M., 1979, On the palaeogeographical distribution of the pectinid genus *Weyla* (Bivalvia, Lower Jurassic), Palaeogeography, Palaeoclimatology, Palaeoecology, 27, 85-102.

Fraser, N.M., Bottjer, D.J. and Fischer, A.G., 2004, Dissecting „*Lithiotis*" bivalves: implications for the Early Jurassic reef eclipse, Palaios, 19, 51-67.

Garzanti, E. and Pagni Frette, M., 1991, Stratigraphic succession of the Thakkhola region (Central Nepal) – comparison with the northwestern Tethys Himalaya, Rivista Italiana di Paleontologia e Stratigrafia, 97, 3-26.

Golonka, J., Krobicki, M., Pajak, J., Nguyen Van Giang and Zuchiewicz W., 2006, Global Plate Tectonics and Paleogeography of Southeast Asia. Faculty of Geology, Geophysics and Environmental Protection, AGH University of Science and Technology, Arkadia. pp. 1-128.

Hallam, A., 1983, Early and mid-Jurassic molluscan biogeography and the establishment of the central-Atlantic seaway, Palaeogeography, Palaeoclimatology, Palaeoecology, 43, 181-193.

Jadoul, F., Berra, F. and Garzanti, E., 1998, The Tethys Himalayan passive margin from Late Triassic to Early Cretaceous (South Tibet), Journal of Asian Earth Sciences, 16, 2-3, 173-194.

Kristan-Tollmann, E.K. and Tollman, A., 1985, The Tethys. In: Nakazawa, K. & Dickius, J.M. (eds), The Tethys. Tokai University Press, Tokyo, 3-22.

Krobicki, M. and Golonka, J., 2009, Palaeobiogeography of Early Jurassic *Lithiotis*-type bivalves buildups as recovery effect after Triassic/Jurassic mass extinction and their connections with Asian palaeogeography. Proceedings of the 5th International Symposium of IGCP-516; Geologial Anatomy of East and South Asia: Paleogeography and Paleoenvironment in Eastern Tethys; 22-30 September 2009, Kunming, China. *Acta Geoscientica Sinica*, 30 Supplement 1, 30-33.

Leinfelder, R.R., Schmid, D.U., Nose, M. and Werner, W., 2002, Jurassic reef patterns the expression of a changing globe. In: Kiessling W., Flgel, E. & Golonka J. (eds): Phanerozoic reef patterns. SEPM (Society for Sedimentary Geology) Special Publication, 72, 465-520.

Shi, X., Sha, J. and Deng, S., 2006, The Jurassic system of China main characteristics and recent advances in research. In: Sha, J., Wang, Y. & Turner, S. (eds.), Marine and non-marine Jurassic: boundary events and correlation, Progress in Natural Science, 16 (special issue), 90-107.

Venturi, F., Bilotta, M. and Ricci, C., 2006, Comparison between western Tethys and eastern Pacific ammonites: further evidence for a possible late Sinemurian-early Pliensbachian trens-Pangaean marine connection, Geological Magazine, 143, 699-711.

Yin, J. and Enay R., 2004, Tithonian ammonoid biostratigraphy in eastern Himalayan Tibet, Geobios, 37, 667-686.

Yin, J. & Wan, X., 1998, Discovery of Early Jurassic *Lithiotis* (Bivalvia) bioherm in Tethyan-Himalaya and its migration, Acta Palaeontologica Sinica, 37, 2, 253-256.

Yin, J., Enay, R. and Wan, X., 1999, The first report of the Late Triassic-Early Jurassic passage beds in the Eastern Tethyan Himalaya, Compte Rendu Academie des sciences, 329, 125-133.

Yin, J., Wan, X. and Pei, S., 1998, Discovery of *Lithiotis* reef in Nyalam, south Tibet, Acta Palaeontographica Sinica, 37, 253-256.

Investigation of sub-surface structure and anisotropy in the Himalaya-Karakoram-Tibet collision using Seismic tomography

Naresh Kumar[1,2], Abdelkrim Aoudia[1]

[1] The Internationa Centre for Theoretical Physics (ICTP), Strada Costiera 11, 34151 Trieste, Italy, nkumar_d@ictp.it
[2] Permanent Institute: Wadia Institute of Himalayan Geology, 33 GMS Road, Dehradun – 248001, Uttrakand, India, nkd@wihg.res.in

The 3D variation of the upper lithosphere in the form of seismic shear wave velocities is performed for the western part of the Himalaya and Tibet collision zone. The broadband seismic data of over 200 earthquakes of magnitude range 4.5 to 7.0 is utilized that is recorded at regional distances on broadband seismic stations located in the southern and northern parts of the study region. Dense ray paths between the location of seismic stations and earthquake epicentres enabled us to investigate the sub-surface structures. The data is also divided into different clusters/groups making the ray path of each cluster sampling different structural elements. The seismic wave ray paths between clusters and recording station cover different zones with different orientations respective to the strikes of major structural elements of the Himalaya and Tibet. These paths are perpendicular as well as parallel to the tectonic discontinuities and some paths also cover the western part of Indo-Gangetic plains. The ray paths sample the Himalayan region, the south Tibetan detachment zone, the Indo-Tsangpo suture zone, as well as the Karakoram fault zone and Tibetan plateau regions.

The dispersion curves of both Rayleigh and love waves are obtained from each earthquake event. For both waves, the observations are performed for periods in the range 6-80 sec, and most of the data are within the period range 10 to 50 sec. The data of dispersion curves of different paths is also utilised to obtain 2D tomographic maps, representing the lateral variations of group velocities. These maps suggest changes of shear wave velocities for the study region indicating a high variation at intermediate period ranges for different paths. This variation is for both waves although higher variation is found in case of Rayleigh waves. The average trend is also calculated for one cluster of events that is mainly traversing a single unit of structural element. Weighted averaging of computed dispersion curve for a group of events of a single cluster is obtained based on the fitting of higher order polynomial and also the standard deviation is computed. The variation of fundamental group velocity for the events of single cluster is small however a higher variation is exhibited among different paths. The paths passing through the Indo-Gangetic plains indicates very low velocities for both Rayleigh and Love waves for periods less than 15 sec. It is observed that the waves passing perpendicular to the major structural elements have high variation in velocities in the period range 10 to 30 sec and specifically due to the low velocities of Rayleigh waves. These differences are measured to assess the anisotropic behaviour of the medium for different periods.

The dispersion curves obtained at regular interval through 2D tomography is further inverted to obtain a 3D image of the S-wave velocity structure for the study area. The upper part of the crust has low group/shear velocities corresponding with the Indo-Gangetic plains as the southern part of the study region. In the central part towards south of the Karakoram fault the upper crust is coupled with a very high velocity under thrusting Indian plate. A broad low velocity mid crustal zone is observed along the Indo-Tibetan boundary and Karakoram fault region and north of the Karakoram fault the thick low velocity layer is reported reaching to depths of 45 km with a lateral extent to the north, up to the southern limit of the Tarim basin. Along a profile from NW to SE, the inverted shear wave velocity for the upper part of the lithosphere indicates variable depth of the Moho discontinuity indicating Indian plate Moho dipping towards north and the Eurasian plate dipping towards south. The variation of group velocities and inverted shear wave velocities in different depth sections are weighted to account for the effects of anisotropy, tectonics and partially fluid saturated zones. These results will shed new light on the long-lasting debates regarding processes governing continental deformation of mountain ranges and the formation of the Tibetan plateau.

Cite as: Kumar, N. and Aoudia A., 2014, Investigation of sub-surface structure and anisotropy in the Himalaya-Karakoram-Tibet collision using seismic tomography, in Montomoli C., et al., eds., proceedings for the 29th Himalaya-Karakoram-Tibet Workshop, Lucca, Italy.

Petrology and U-Pb SHRIMP zircon chronology of granitoids from Shyok Suture Zone, Ladakh Himalaya, India: Evidence of Early Cretaceous subvolcanic calc-alkaline granitoid magmatism

Santosh Kumar[1], Sita Bora[1], Umesh K. Sharma[2], Keewook Yi[3], Namhoon Kim[3]

[1] Department of Geology, Centre of Advanced Study, Kumaun University, Nainital 263 002, India, skyadavan@yahoo.com
[2] Department of Science and Technology, Technology Bhavan, New Delhi 110016, India
[3] SHRIMP Centre, Korea Basic Science Institute, Ochang Campus, Korea, Chungbuk, 363-383, Korea

Ladakh Himalaya is an integral part of Trans-Himalaya system, and the lithounits constituting this sector are exposed all along the vast zones of Indus and Shyok Sutures Zones of northwest Himalaya. Shyok Suture Zone (SSZ) separates the Dras island arc in the south from Karakoram-Tibet in the north (Gansser, 1977). The SSZ represents tectonized remainder of a marginal (back-arc) basin while experiencing crustal shortening and is mainly composed of volcano-sedimentary formations (Rai, 1982). Ladakh, Saltoro, and Karakoram blocks form a triple point at intersection of Karakoram Fault (KF) and Khalsar Thrust (KT) while moving from south to north in Nubra-Shyok confluence area (Weinberg, 2000). In this area Ladakh range is delineated by Khardung Formation in the north and Shyok Formation in the northeast, which separates Ladakh block from Saltoro block along Khalsar Thrust (KT), which is most often considered eastern continuation of the Main Karakoram Thrust.

Saltoro block of Nubra-Shyok confluence area is mainly comprised of vast amount of calc-alkaline granitoids of batholithic dimension exposed in and around Tirit region of Nubra valley referred herein Tirit granitoids, which are intimately associated with volcanics of Khardung Formation. In this region marginal parts of Ladakh granitoids have been found intruding the Shyok Formation whereas Tirit granitoids are intrusive into dacite and andesite of Khardung Formation. Field relationships particularly between Tirit granitoids and volcanics, Al-in-hornblende barometers, U-Pb SHRIMP zircon chronology have been carried out in order to understand intrusive nature, depth of emplacement and crystallization age of Tirit granitoid magma. Presence of mm to cm-sized dacitic and large-sized andesitic xenoliths ubiquitous in Tirit granitoids suggest strong assimilation, stopping and collapse of overlying volcanic materials while intrusion of Tirit granitoid melts at epizonal-subvolcanic emplacement level. Al-in-hornblende barometers (~1.08-2.1 Kbar) further corroborate emplacement and solidification of Tirit granitoid melt at subvolcanic level. The obtained pressures also indicate that the Tirit magma chamber has experienced a minimum overburden of *ca* 4 Km or to a maximum of *ca* 8 Km thick volcanic sequences (lithostatic pressure assuming $P_{TOTAL}= P_{LOAD}$) which are at places either partly preserved or completely removed at present erosional levels. On the other hand, tectonically separated marginal parts of Ladakh granitoids contain less frequent xenoliths of shale and metabasics of Shyok Formation, which suggest winty intrusive contact relation of granitoid melt with country-rocks. Both Ladakh and Tirit granitoids contain mafic to hybrid microgranular enclaves, which suggest mixing and mingling of mafic-felsic magmas in plutonic environment, a typical feature observed in calc-alkaline I-type granitoid complex.

Three representative granitoid samples, one each from assimilated and unassimilated parts of Tirit granitoid and one sample from Ladakh granitoid close to the contact with country-rocks, were chosen for U-Pb SHRIMP zircon chronology. Back scattered electron (BSE) and cathodo-luminescence (CL) images suggest euhedral and oscillatory zoned nature of zircons, which sometimes bear inherited zircon cores recycled from source regions. Total thirty four areas were analyzed from seventeen zircon crystals of unassimilated, free from any assimilative signature with volcanics, Tirit granitoid. Twelve zircon spots have yielded weighted mean $^{206}Pb/^{238}U$ age of crystallization 109.4±1.1 Ma (MSWD=3.5) corresponding to Early Cretaceous. It is interesting to observe that inherited cores of some zircons have provided three groups of older $^{206}Pb/^{238}U$ ages in the range of 278-393 Ma, 519-713 Ma and 1933 Ma, which suggest involvement of heterogeneous Carboniferous, Cambrian-Neoproterozoic and Paleoproterozoic crustal

Cite as: Kumar, S., et al., 2014, Petrology and U-Pb SHRIMP zircon chronology of granitoids from Shyok Suture Zone, Ladakh Himalaya, India: Evidence of Early Cretaceous subvolcanic calc-alkaline granitoid magmatism, in Montomoli C., et al., eds., proceedings for the 29th Himalaya-Karakoram-Tibet Workshop, Lucca, Italy.

sources in the generation of Tirit granitoid. It is likely that sediments derived from ancient continental crust were mixed with juvenile crust before the onset of subduction of oceanic crust below the Asian plate. Zircons from Tirit granitoid having strong assimilative features yield weighted mean $^{206}Pb/^{238}U$ age of crystallization 105.30±0.80 Ma (MSWD=1.4). Two inherited cores of zircons from unassimilated Tirit granitoid also yield $^{206}Pb/^{238}U$ ages of 476 Ma and 952 Ma again pointing involvement of minor amount of older continental crust in the genesis of Tirit granitoids. Although there are strong evidences of intrusion and assimilation of volcanics by Tirit granitoids, zircons derived from volcanics in Tirit granitoid are absent. The obtained two ages (*ca* 110 Ma and 105 Ma) at least suggest episodic nature of Tirit granitoid magmatism during Early Cretaceous, and the dacite and andesite as early eruptive phases of Khardung volcanism must have occurred prior to 105 Ma. Earlier suggested ages (~68-74 Ma) for calc-alkaline Tirit granitoids (Weinberg et al. 2000, Upadhyay, 2008) are much younger than the present ones, and correlate well with the ages of Ladakh granitoids. Dunlap and Wysoczanski (2002) have suggested thickness of Khardung Formation about 7 Km deposited between 60.5 Ma and 67.4 Ma, which constrain minimum age of Late Cretaceous for Shyok Formation. However, we suggest minimum age of Early Cretaceous for Khardung volcanics. Zircons from Ladakh granitoids which contain xenoliths of shales and metabasics have yielded weighted mean $^{206}Pb/^{238}U$ age of crystallization 67.32±0.66 Ma (MSWD=1.3), and it is remarkable that these zircons are completely devoid of inherited cores. Based on strong field and chronological evidences we opined that the Tirit granitoids in SSZ most likely represent early pulses of Early Cretaceous calc-alkaline magmatism formed in subduction environment, which intrude the dacite and andesite (>105 Ma) layers of Khardung volcanics at subvolcanic-epizonal levels.

References

Dunlap, W.J. and Wysoczanski, R., 2002, Thermal evidence for Early Cretaceous metamorphism in the Shyok suture zone and age of the Khardung volcanic rocks, Ladakh, India, Journal of Asian Earth Sciences, 20, 481-490.

Gansser, A., 1977, The great suture zone between Himalaya and Tibet, a preliminary account. Sci. Terre Himalaya, CNRS, 268, 181-192.

Rai, H., 1982, Geological evidences against the Shyok palaeosuture, Ladakh Himalaya. Nature, 297, 142-144.

Weinberg, R.F., Dunlap, W.J. and Whitehouse, M., 2000, New field structural and geochronological data from the Shyok and Nubra valleys, northern Ladakh: linking Kohistan to Tibet, Geol. Society. London. Spec. Publ., 170, 253-275.

Upadhyay, R., 2008, Implication of U-Pb zircon age of the Tirit granitoids on the closure of the Shyok Suture Zone, northern Ladakh, India. Current Science, 94, 1635-1640.

Tectonics of the Chamba Nappe, NW Himalaya and its regional implications

S. Lahoti[1], Yash Gupta[1], Kislay Kumud[1], Arvind Kumar Jain[2]

[1] Department of Earth Sciences, Indian Institute of Technology, Roorkee-247667 India
[2] CSIR-Central Building Research Institute, Roorkee-247667 India

Southern parts of the Himalaya in western Himachal Pradesh along the Ravi River and its tributaries are remarkable in narrowing down of the Lesser Himalayan Shali/Panjal sedimentary zone between the Main Boundary Thrust (MBT) and the Panjal Thrust (PT) due to southward propagating Chamba Nappe. This nappe is comprised of the Proterozoic-Paleo-Mesozoic Tethyan sedimentary zone with infolded Triassic-Jurassic Kalhel-Tandi carbonates having diverging vergence towards southwest and northeast, respectively.

Over the vast terrain of this succession, the low grade Chamba Group metamorphics of psammite-pelite sequence can be regionally traced into the Salkhala Group of Kashmir in the west, Chail-Jutogh metamorphics further southeast, and the Haimanta Group of Spiti-Lahaul regions. The Chamba Nappe thrusts over the Higher Himalayan Crystalline (HHC) Belt of Chenab-Miyar valleys and cuts through it in such a manner that the HHC is not exposed along the frontal parts. Intensely mylonitized 'Outer Granite Band' in the frontal parts within low grade metamorphics at the base of the Chamba Nappe probably represents the subthrust extension of Kulu-Bajura Nappe/Munsiari thrust belt.

The Chamba Nappe contains four formations: Chamba Formation (quartzite-phyllite alternations), Manjir Formation (pebbliferous slate, quartzite, diamictite), Salooni Formation (metagreywacke, siltstone, carbonaceous slate) and Kalhel Formation (fossiliferous dolomite, sandstone, shale, volcanics). These have suffered three deformation phases of which the first phase D1 appears to be the most pervasive simple shearing during southward propagating Chamba Nappe. It has produced NE-trending down-thedip plunging pebble, pyrite and mineral lineations on equally-prominent foliation, transverse to the general regional trend of the Chamba Nappe. Subsequent deformation phases D2 and D3 produced regional superposed folds and their axial planar foliations. Bedding-cleavage relationships at several localities in monotonous quartzite-phyllite sequence of the Chamba Nappe provide indisputed evidences for the presence of large D3 folds.

Cite as: Lahoti , et al., 2014, Tectonicsof the Chamba Nappe, NW Himalaya and its regional implications, in Montomoli C., et al., eds., proceedings for the 29th Himalaya-Karakoram-Tibet Workshop, Lucca, Italy.

Late Miocene-present exhumation kinematics of the Sikkim Himalaya derived from inversion of zircon (U-Th)/He and apatite fission-track ages using 3-D thermokinematic modelling

Kyle Landry[1], Isabelle Coutand[1], David M. Whipp Jr.[2], Djordje Grujic[1]

[1] Department of Earth Sciences, Dalhousie University, PO BOX 15000, Halifax, NS, B3H 4R2, Canada, kyle.landry@dal.ca
[2] Institute of Seismology, Department of Geosciences and Geography, P.O. Box 68, FI-00014 University of Helsinki, Finland

Erosion and exhumation of upper crustal material in the Himalayas results from a combination of tectonic and surface processes (Beaumont et al., 2001; Hodges et al., 2004; Grujic et al., 2006). Although recent studies have well defined the Miocene-Pliocene exhumation history and deformation kinematics along much of the Himalayan arc (Hodges et al., 2004; Wobus et al., 2005; Herman et al., 2010;) , the exhumation history of the Sikkim Himalaya is unknown despite being intriguing. The Sikkim Himalaya (Figure 1) is located in a transition zone between two regions of the Himalaya with substantial structural and geomorphological differences, the Nepal Himalaya to the west (Robert et al., 2011; Whipp et al., 2007) and the Bhutan Himalaya to the east (Grujic et al., 2006; Coutand et al., 2014). Late Miocene-present deformation of the Sikkim Himalaya is driven by slip along the Himalayan basal décollement (Main Himalayan thrust; MHT) and duplex development in the Lesser Himalaya. In addition, coupling and feedbacks between duplexing and efficient fluvial erosion have exposed meta-sedimentary rocks of the Lesser Himalayan Sequence (LHS) in a large, double tectonic window (Bhattacharyya and Mitra, 2009) from beneath the structurally overlying Greater Himalayan Sequence (GHS; Figure 1). The comparative contribution of the two processes is relatively poorly understood in particular in the study area.

This study adopts a multi-disciplinary approach coupling zircon (U-Th)/He (ZHe), and apatite fission-track (AFT) thermochronology with 3D thermokinematic modelling, to define the Neogene-present deformation and exhumation history of the Sikkim Himalaya. 44 rock samples were collected along two N-S-trending profiles across the windows (Figure 1). 15 samples were processed for ZHe and 34 for AFT dating. Published AFT data (Figure 1), collected in the footwall of the South Tibetan Detachment Zone (Kellett et al., 2013; STDZ in Figure 1), were used to augment our dataset. The ZHe cooling ages range from 11.87 ± 0.49 Ma to 1.30 ± 0.07 Ma. Approximately 20-30 km north of the Main Boundary Thrust (MBT; Figure 1), ZHe cooling ages show a marked age decrease; south of this break cooling ages range from 12 to 6 Ma, and north of the break, within the double window and beyond, ages are younger than ~4 Ma. This break corresponds roughly to the southern exposure of the LHS units within the windows. Analysis of AFT samples is ongoing.

The age dataset is inverted using the thermo-kinematic modelling software Pecube (Braun, 2003) to define the Late Miocene-present deformation and exhumation kinematics of the Sikkim Himalaya. We combine our dataset with published AFT (Kellett et al., 2013), structural (Bhattacharyya and Mitra, 2009) and geophysical data (Acton et al., 2011) to define the model input parameters and their ranges. Rock exhumation results from rock uplift determined by the underlying fault kinematics and geometry, and surface erosion, which maintains modern steady-state topography. Late Miocene-present deformation of the Sikkim Himalaya is driven by slip along the Himalayan basal décollement (Main Himalayan thrust; MHT) and duplex development in the Lesser Himalaya. Duplexing is simulated by a zone of enhanced rock uplift focussed on the northward dipping segment of the MHT located in northern Sikkim. Free parameters in the inversions include: basal temperature, radiogenic heat production, convergence rate, the ratio of under-thrusting to over-thrusting, the position of ramp and flat portions of the MHT as well as the location, timing and rate of duplex driven rock uplift. Our numerical models focus on defining the exhumation kinematics (fault geometry, slip rate) over the last 12 Ma that are most consistent with the observed age data for tectonic scenarios with and without upper-crustal duplexing.

We find that duplex-driven rock uplift in the LHS is required to produce the young ages observed in the core of the double tectonic window in the Sikkim region. The tectonic scenario involving slip only on the basal

Cite as: Landry, K., et al., 2014, Late Miocene-present exhumation kinematics of the Sikkim Himalaya derived from inversion of zircon (U-Th)/He and apatite fission-track ages using 3-D thermokinematic modelling, in Montomoli C., et al., eds., proceedings for the 29th Himalaya-Karakoram-Tibet Workshop, Lucca, Italy.

décollement and no duplexing does not provide a satisfactory fit to the age data. Specifically, modelled cooling ages from samples in and around the tectonic windows tend to be too old while the samples north of the windows (≥70 km north of the MBT) tend to be too young. Additional uplift as a result of simulated duplexing in the model provides a much better fit to the age data, with many of the predicted cooling ages within the uncertainty of the observed ages. Combined, these results suggest that duplexing is a dominant process in the tectonic evolution of Sikkim during the late-Miocene.

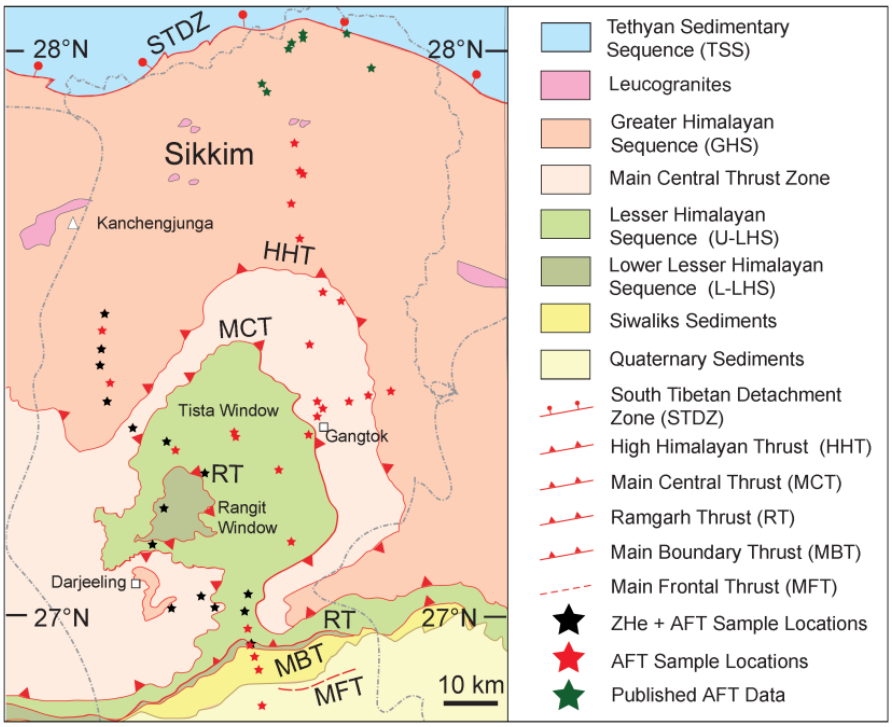

Figure 1. Geologic Map of the Sikkim Himalaya. The Tista and Rangit windows are shown in the centre of the map, bounded by the Main Central Thrust and Ramgarh Thrust respectively. Samples dated by AFT are denoted in by red stars, samples dated using both ZHe and AFT are denoted by black stars. Green stars show previously published AFT data[11]. After Kellett et al., 2013.

References

Acton, C. E., Priestley, K., Mitra, S., and Gaur, V.K., 2011, Crustal structure of the Darjeeling–Sikkim Himalaya and southern Tibet, Geophysical Journal International, 184 (2), 829-852.

Beaumont, C., Jamieson, R.A., Nguyen, M.H., and Lee, B., 2001, Himalayan tectonics explained by extrusion of a low-viscosity crustal channel coupled to focused surface denudation, Nature, 414 (6865), 738-742.

Bhattacharyya, K. and Mitra, G., 2009, A new kinematic evolutionary model for the growth of a duplex - an example from the Rangit duplex, Sikkim Himalaya, India, Gondwana Research, 16, 697-715.

Braun, J., 2003, Pecube: a new finite-element code to solve the 3D heat transport equation including the effects of a time-varying, finite amplitude surface topography, Computers & Geosciences, 29, 787-794.

Coutand, I. et al., 2014, Geometry and kinematics of the Main Himalayan Thrust and Neogene crustal exhumation in the Bhutanese Himalaya derived from inversion of multithermochronologic data, Journal of Geophysical Research: Solid Earth.

Grujic, D. et al., 2006, Climatic forcing of erosion, landscape, and tectonics in the Bhutan Himalayas, Geology, 34 (10), 801-804.

Herman, F. et al., 2010, Exhumation, crustal deformation, and thermal structure of the Nepal Himalaya derived from the inversion of thermochronological and thermobarometric data and modeling of the topography, Journal of Geophysical Research: Solid Earth, 115, (B6).

Hodges, K.V., Wobus, C., Ruhl, K., Schildgen, T., and Whipple, K., 2004, Quaternary deformation, river steepening, and heavy precipitation at the front of the Higher Himalayan ranges, Earth and Planetary Science Letters, 220 (3), 379-389.

Kellett, D.A., Grujic, D., Coutand, I., Cottle, J. and Mukul, M., 2013, The South Tibetan detachment system facilitates ultra-rapid cooling of granulite-facies rocks in Sikkim Himalaya, Tectonics, 32, 252-270

Robert, X., Van Der Beek, P., Braun, J., Perry, C., & Mugnier, J. L. Control of detachment geometry on lateral variations in exhumation rates in the Himalaya: Insights from low-temperature thermochronology and numerical modeling, Journal of Geophysical Research: Solid Earth 116 (B5) (2011).

Whipp, D. M., Ehlers, T.A., Blythe, A.E., Huntington, K.W., Hodges, K.V. and Burbank, D.W., 2007, Plio-Quaternary exhumation history of the central Nepalese Himalaya: 2. Thermokinematic and thermochronometer age prediction model, Tectonics, 26 (3).

Wobus, C., Heimsath, A., Whipple, K., and Hodges, K., 2005, Active out-of-sequence thrust faulting in the central Nepalese Himalaya, Nature, 434 (7036), 1008-1011.

Along-strike continuity in quartz recrystallization microstructures adjacent to the MCT: deformation temperatures, strain rates and implications for flow stresses

Richard D. Law[1]

[1] Department of Geosciences, Virginia Tech., Blacksburg, Virginia 24061, USA, rdlaw@vt.edu

Traced for ~ 1500 km along the foreland edge of the Himalaya from NW India to Bhutan published reports indicate a remarkable along-strike continuity of quartz recrystallization microstructures in the footwall and hanging wall to the Main Central Thrust (MCT). Recrystallization in Lesser Himalayan Series (LHS) rocks in the footwall to the MCT is dominated by grain boundary bulging (BLG) microstructures, while recrystallization in Greater Himalayan Series (GHS) rocks in the hanging wall is dominated by grain boundary migration microstructures (GBM I and II using terminology of Stipp et al. 2002a,b) that traced structurally upwards transition in to the anatectic core of the GHS.

In the high-strain rocks adjacent to the MCT recrystallization is dominated by subgrain rotation (SGR) with transitional BLG-SGR and SGR-GBM microstructures being recorded at structural distances of up to a few hundred meters below and above the MCT, respectively. Correlation with available information on temperatures of metamorphism indicated by mineral phase equilibria and RSCM data suggests that recrystallization in the structural zones dominated by BLG, SGR and GBM occurred at temperatures of ~ 350-450, 450-550 and 550- > 650 °C, respectively. It should be kept in mind, however, that these temperatures are likely to be 'close-to-peak' temperatures of metamorphism, whereas penetrative shearing and recrystallization may have continued during cooling.

The dominance of SGR along the more foreland-positioned exposures of the MCT intuitively suggests that shearing occurred under a relatively restricted range of deformation temperatures and strain rates. Plotting the 'close-to-peak' 450-500 °C temperatures of metamorphism indicated for SGR-dominated rocks located at up to a few hundred meters below/above the MCT on the quartz recrystallization map developed by Stipp et al. (2002b) would indicate 'ball-park' strain rates of ~ 10^{-13} to 10^{-10} sec^{-1} (Fig. 1a). If shearing continued during retrograde cooling while remaining in the SGR field, then the recrystallization map suggests that a significant drop in deformation temperature (> ~ 75-100 °C) would result in a decrease in strain rate.

In general, however, the presence of a single recrystallization microstructure traced over a large (regional scale) distance does not necessarily mean that deformation temperature (or strain rate) remains constant but could, for example, indicate that spatial variations in deformation temperature are compensated for by changes in strain rate, with grain-scale deformation remaining within a particular recrystallization regime (Fig. 1a).

Constant stress conditions plot along a straight line in the 1/T versus log strain rate space used in the quartz recrystallization mechanism map (Fig. 1b). This opens up the possibility that the observed along strike consistency of observed SGR-dominated recrystallization microstructures may indicate near to constant stress boundary conditions (albeit with varying temperatures and strain rates) prevailing along what are now the more foreland-positioned exposures of the MCT (Fig. 1a).

If such processes do operate along the MCT then, for a given foreland-hinterland position a constant recrystallized grain size would be predicted traced along strike as, at least under experimental conditions, grain size correlates with flow stress, but is independent of temperature, strain rate and water content (Stipp et al., 2006). Recrystallized quartz grain sizes of 35-65 microns (SGR-dominated microstructures) are recorded at 70-75 m above the MCT in the western part of the Sutlej River Valley in NW India, indicating flow stresses of 28-18 MPa using the Stipp and Tullis (2003) piezometer (Law et al., 2013).

Cite as: Law, R.D., 2014, Along-strike continuity in quartz recrystallization microstructures adjacent to the MCT: deformation temperatures, strain rates and implications for flow stresses, in Montomoli C., et al., eds., proceedings for the 29th Himalaya-Karakoram-Tibet Workshop, Lucca, Italy.

However, flow stresses based on quartz recrystallized grain sizes have not yet been quantified for other MCT transects along the Himalaya.

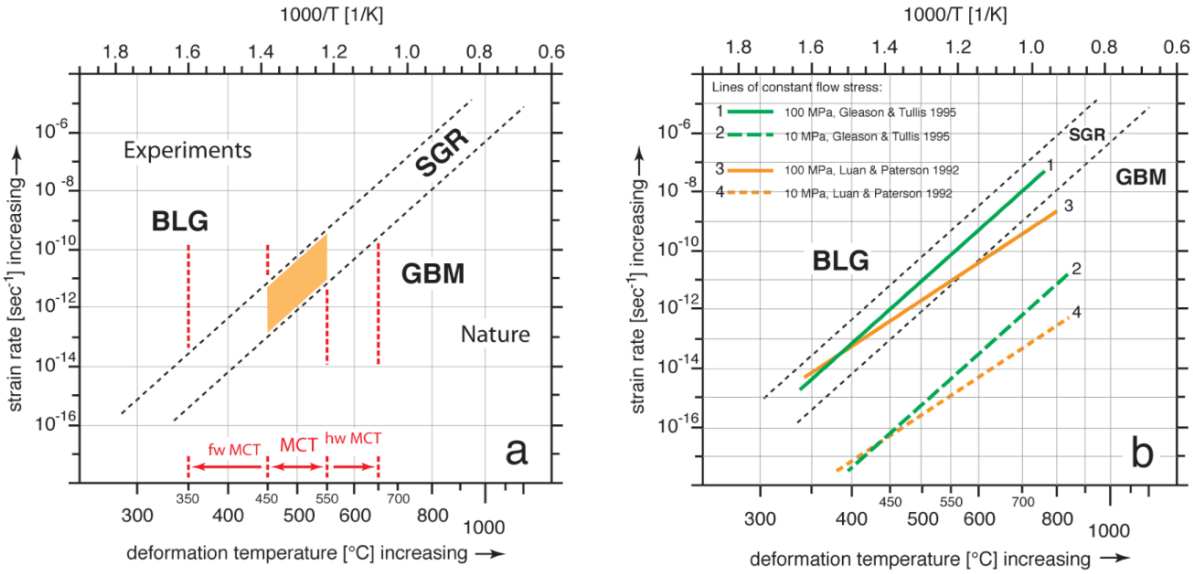

Figure 1. a) Quartz recrystallization mechanism map (Law in press, adapted from Stipp et al., 2002b) for the Main Central Thrust (MCT) with temperature ranges of close-to-peak metamorphism indicted by petrology-based thermometry. Footwall (fw) and hanging wall (hw) to MCT dominated by BLG and GBM recrystallization, respectively; recrystallization adjacent to MCT (< ~ 100-300 m above or below fault) dominated by SGR; orange field indicates predicted range of strain rates for SGR-dominated shearing on the MCT, if shearing occurred at close-to-peak temperatures of metamorphism. b) Recrystallization mechanism map displaying lines of constant flow stress from quartz flow laws of Luan and Paterson (1992) and Gleason and Tullis (1995).

References

Gleason, G.C., and Tullis., 1995, A flow law for dislocation creep of quartz aggregates determined with the molten salt cell, Tectonophysics, 247, 1-23.

Law, R.D., in press, Deformation thermometry based on quartz c-axis fabrics and recrystallization microstructures: a review, Journal of Structural Geology.

Luan, F.,C., and Paterson, M.S., 1992, Preparation and deformation of synthetic aggregates of quartz, Journal of Geophysical Research, 97, 301-320.

Law, R.D., Stahr, D.W., Francsis, M.K., Ashley, K.T., Grasemann, B. and Ahmad, T., 2013, Deformation temperatures and flow vorticities near the base of the Greater Himalayan Series, Sutlej Valley and Shimla Klippe, NW India, Journal of Structural Geology, 54, 21-53.

Stipp, M., Stünitz, H., Heilbronner, R. and Schmid, S., 2002a, The eastern Tonale fault zone: a natural laboratory for crystal plastic deformation of quartz over a temperature range from 250 to 700 °C, India, Journal of Structural Geology, 24, 21-53.

Stipp, M., Stünitz, H., Heilbronner, R. and Schmid, S., 2002b, Dynamic recrystallization of quartz: correlation between natural and experimental conditions. In: De Meer, S., Drury, M. R., De Bresser, J. H. P., Pennock, G. M. (Eds.), Deformation Mechanisms, Rheology and Tectonics: Current Status and Future Perspectives. Geological Society of London, Special Publications, 200, 171–190.

Stipp, M. and Tullis, J., 2003, The recrystallization grain size piezometer for quartz, Geophysical Research Letters, 30, 2088, doi:10.1029/2003GL018444,

Stipp, M., Tullis, J. and Behrens, H., 2006, Effect of water on the dislocation creep microstructure and flow stress of quartz and implications for the recrystallized grain size piezometer, Journal of Geophysical Research, 111, B042201, doi: 10.1029/2005JB003852.

Uplift-driven denudation rates and associated channel response across Bhutan, Himalaya

Romain Le Roux-Mallouf[1], Vincent Godard[2], Matthieu Ferry[1], Rodolphe Cattin[1], Jean-François Ritz[1], Dowchu Drukpa[3], Jampel Gyeltshen[3]

[1] Laboratoire Géosciences Montpellier - Université Montpellier 2 – 34090 Place Eugène Bataillon, lerouxmallouf@gm.univ-montp2.fr
[2] CEREGE - Aix-en-Provence - 13545, Aix en Provence cedex 4
[3] Department of Geology & Mines - Post Box No. 173 - Thimphu, BHUTAN

The Himalaya belt separates the southern edge of the Tibetan Plateau from the Indus-Gangetic Plain and is one of the most active areas in the world in terms of tectonic and climatic processes. Previous studies documented active deformation along the Himalaya in Nepal as well as major earthquakes (M>8) that have struck this area over the last centuries (e.g. Chen & Molnar 1977; Lavé & Avouac, 2000; Kumar & al., 2010). Lateral variations in instrumental seismicity may be observed from western Nepal to Bhutan with a significant decrease in rate from west to east (Drukpa et al., 2006). To better understand this major result and establish its consequences for seismic hazard assessment, observations are needed over a longer time frame.

Recently, Berthet et al. (2014) studied deformed Holocene alluvial terraces along the main front in southern central Bhutan and identified two major surface ruptures (M>8) for the last 1100 years. These first results are similar to what is observed 200 km further west in Nepal (Sapkota et al., 2013). Following this preliminary study, here we quantify the Holocene deformation through a joint approach including both the assessment of the spatial and temporal distribution of denudation rates and a detailed geomorphological analysis of drainage features (stream power, steepness index). We use ^{10}Be concentrations in river sands, along a North-South profile to quantify catchment-scale denudation over 100-1000 yr time-scale and to investigate the relationship between denudation and tectonic processes (Brown et al., 1995).

Analysis of main channel profiles reveal well defined knickpoints at 90 km and 160 km from the Main Frontal Thrust (MFT), which are not associated with a weak-to-resistant lithological transition (Fig 1A). These morphological features are marked by a significant increase in both normalized channel steepness index (Ksn) and stream power (Fig. 1B). This preliminary drainage analysis suggests that cosmogenic ^{10}Be concentrations may yield a higher denudation rate in this area.

Based on this impending result, we suggest that the regional geomorphology results from a flat-and-ramp geometry of the Main Himalayan Thrust at depth, similarly to what is observed in the Nepal Himalaya, but with different characteristics (e.g. distance from the front, depth or ramp dip angle).

Cite as: Le Roux-Mallouf et al., 2014, Uplift-driven denudation rates and associated channel response across Bhutan, Himalaya, proceedings for the 29th Himalaya-Karakoram-Tibet Workshop, Lucca, Italy

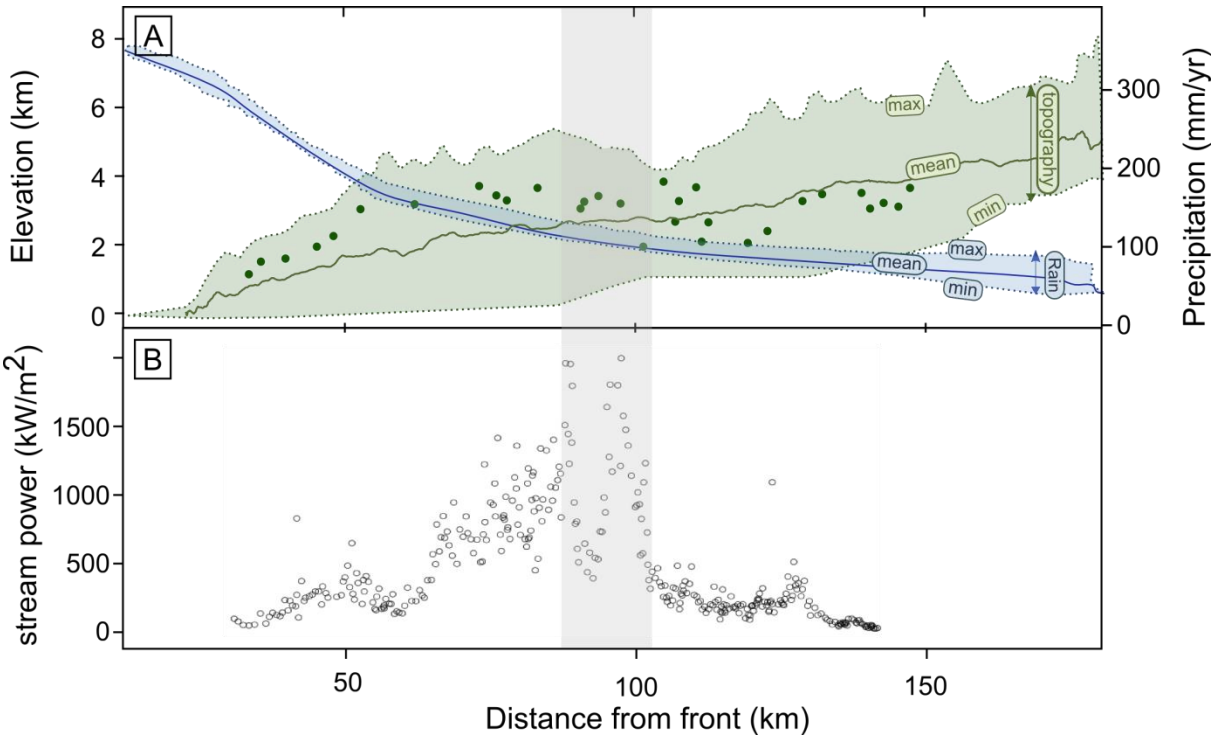

Figure 1. Cross-range section of the Himalaya in west Bhutan. (A) Topography (green) and precipitation (blue) along a 50-km-wide profile. Green dots are average elevation of sampled watershed basins. (B) Stream power. Shaded rectangles show the knickpoint section.

References

Berthet, T., Ritz, J. F., Ferry, M., Pelgay, P., Cattin, R., Drukpa, D., and Hetényi, G., 2014. Active tectonics of the eastern Himalaya: New constraints from the first tectonic geomorphology study in southern Bhutan, Geology, 42(5), 427-430.

Brown, E.T., Stallard, R.F., Larsen, M.C., Raisbeck, G.M., and Yiou, F., 1995, Denudation rates determined from the accumulation of in situ-produced 10Be in the luquillo experimental forest, Puerto Rico, Earth and Planetary Science Letters, 129, 1-4, 193-202, doi:10.1016/0012-821X(94)00249-X.

Chen, W.-P., and P. Molnar, 1977, Seismic moments of major earthquakes and the average rate of slip in central Asia, J. Geophys. Res., 82(20), 2945-2969, doi:10.1029/JB082i020p02945.

Drukpa, D., Velasco, A.A., and Doser, D.I., 2006, Seismicity in the Kingdom of Bhutan (1937–2003): Evidence for crustal transcurrent deformation, Journal of Geophysical Research: Solid Earth (1978–2012), 111(B6).

Godard, V., Bourlès, D.L., Spinabella, F., Burbank, D.W., Bookhagen, B., Fisher, G. B., and Léanni, L., 2014, Dominance of tectonics over climate in Himalayan denudation, Geology, G35342-1.

Kumar, S., Wesnousky, S.G., Jayangondaperumal, R., Nakata, T., Kumahara, Y. and Singh, V., 2010, Paleoseismological evidence of surface faulting along the northeastern Himalayan front india: Timing, size, and spatial extent of great earthquakes, J. Geophys. Res., 115(B12), B12422.

Lavé, J., and J. P. Avouac, 2000, Active folding of fluvial terraces across the Siwaliks Hills, Himalayas of central Nepal, J. Geophys. Res., 105(B3), 5735-5770, doi:10.1029/1999JB900292.

Sapkota, S. N., Bollinger, L., Klinger, Y., Tapponnier, P., Gaudemer, Y., and Tiwari, D., 2013, Primary surface ruptures of the great Himalayan earthquakes in 1934 and 1255, Nature Geoscience, 6(1), 71-76.

Time constraints on partial melting and deformation of the Himalayan Crystalline Sequence, Nyalam Tibet: implications for orogenic models

Philippe Hervé Leloup[1], Xiaobing Liu[1,2,3], Gweltaz Mahéo[1], Jean-Louis Paquette[4], Nicolas Arnaud[5], Alexandre Aubray[1], Xiaohan Liu[2]

[1] Laboratoire de Géologie de Lyon, CNRS UMR 5276, Université Lyon1 – ENS Lyon, Villeurbanne, France, herve.leloup@univ-lyon1.fr
[2] Key Laboratory of Continental Collision and Plateau Uplift, Institute of Tibetan Plateau Research, Chinese Academy of Sciences, Beijing 100085, China.
[3] Research Institute of Petroleum Exploration and development, Petrochina, Beijing 100083, China
[4] Laboratoire Magmas et Volcans, CNRS UMR 6524, Clermont Université, Clermont-Ferrand, France.
[5] Géosciences Montpellier, UMR CNRS 5243, Université de Montpellier, Montpellier, France.

The processes leading to the formation of the Himalayan belt are still vividly debated. For some, the main process is that of a crustal wedge with Indian rocks being underthrusted in the lower plate and deeply buried, before to be accreted to the upper plate and then overthrusted and exhumed (e.g., Mattauer, 1986). Following numerical experiments analysis, a second class of models considers that the main process is that of a lower crustal melted layer expulsed outwards from beneath Tibet (e.g., Jamieson et al, 2006). Both models intend to explain the main geological characteristic of the High Himalaya: a zone of high-grade metamorphic rocks (the Himalayan crystalline series [HCS]) overthrusting less metamorphosed rocks along the Main central thrust (MCT), and overlain by unmetamorphosed rocks above the South Tibet detachment (STD). The internal structure and the Oligo-Miocene inverse metamorphism and high degree of melting observed in the HCS, have been interpreted as characteristic of either an accretionary prism, tectonic wedging, or Lower channel flow.

We present new structural, U-Th/Pb and Ar/Ar data along the Nyalam section across the HCS. From south (bottom) to north (top) we distinguish four tectono-stratigraphic units between the main central thrust (MCT) and the south Tibet detachment system (STDS). Unit 1 corresponds to the MCT zone and contains the upper MCT, unit 2 shows migmatitic othogneiss, units 3 contains in situ migmatites and marbles, and unit 4 consists of paragneiss and marbles intruded by leucogranites. The top of unit 4 is the ~ 300m thick STD shear zone. 15 new U-Th/Pb ages in monazites and zircons of magmatic rocks from units 2, 3 and 4 (Fig. 1) indicate : a) Intrusion of N-S steep dykes between 15 and 17.5 Ma; b) Prograde metamorphism (M1) occurred at ~35 Ma followed by onset of partial fusion (M2) at ~30 Ma in units 2 and 3; c) End of partial melting at ~18 Ma in unit 2 and ~20 Ma in unit 3; d) 7 new Ar/Ar ages of micas in late N-S gashes span between 18 and 5 Ma (Fig. 1) and suggest fast cooling right after the end of partial melting in unit 2.

When combined with published P-T results, Ar/Ar, AFT, ZFT data from Nyalam as well as published results from the Lantang and Dudh Kosi Valleys these data imply that: a) magmatic rocks of unit 4 are produced in units 1, 2 and 3; b) ductile deformation was restricted to the base of unit 1 (MCT 1) and the top of unit 4 (STD shear zone) after ~17.5 Ma, more specifically motion ended at ~13 Ma on the STD and ~9 Ma on the MCT; c) Partial melting ended several Ma before the end of motion on the MCT and the STD. In Nyalam, these structure never where the boundary of a partially molten channel; d) A first phase of rapid cooling occurs right after the end of partial fusion (at ~20 Ma in Dudh Kosi and ~17 Ma in Nyalam) (FC1, Fig. 1) prior to or during the intrusion of the last dykes that seal any ductile deformation in between the MCT and STD; e) A second phase of rapid cooling from ~16 to 13 Ma corresponds to the exhumation of the STDsz footwall up to near surface (FC2, Fig. 1); f) The third, and last, rapid cooling event since ~5 Ma (FC3, Fig. 1) only affects the southern part of the section (units 1 and 2); g) The STDsz has a more complex geometry than the straight low-angle fault often depicted. We propose that it follows flat and ramps, rooting south of the South Tibetan domes and that it initiated at ~24.5 Ma with a total offset of ~40 km.

Cite as: Leloup, P. H. et al., 2014, Time constraints on partial melting and deformation of the Himalayan Crystalline Sequence, Nyalam Tibet: implications for orogenic models, in Montomoli C., et al., eds., proceedings for the 29th Himalaya-Karakoram-Tibet Workshop, Lucca, Italy.

Several of these observations are barely compatible with the lower crustal channel flow model for the exhumation of the HCS. We rather propose a wedge model where HCS partial melting results from decompression above the MCT with an erosion and deformation front located at least ~100 km south of the present day exposure of the MCT in Langtang, Nyalam and Dudh Kosi sections. Shaping of the South slope of the high Himalaya took place since less than 5 Ma and is related to erosion triggered by uplift above a ramp of the MHT not to focussed erosion linked with the main exhumation of the HCS.

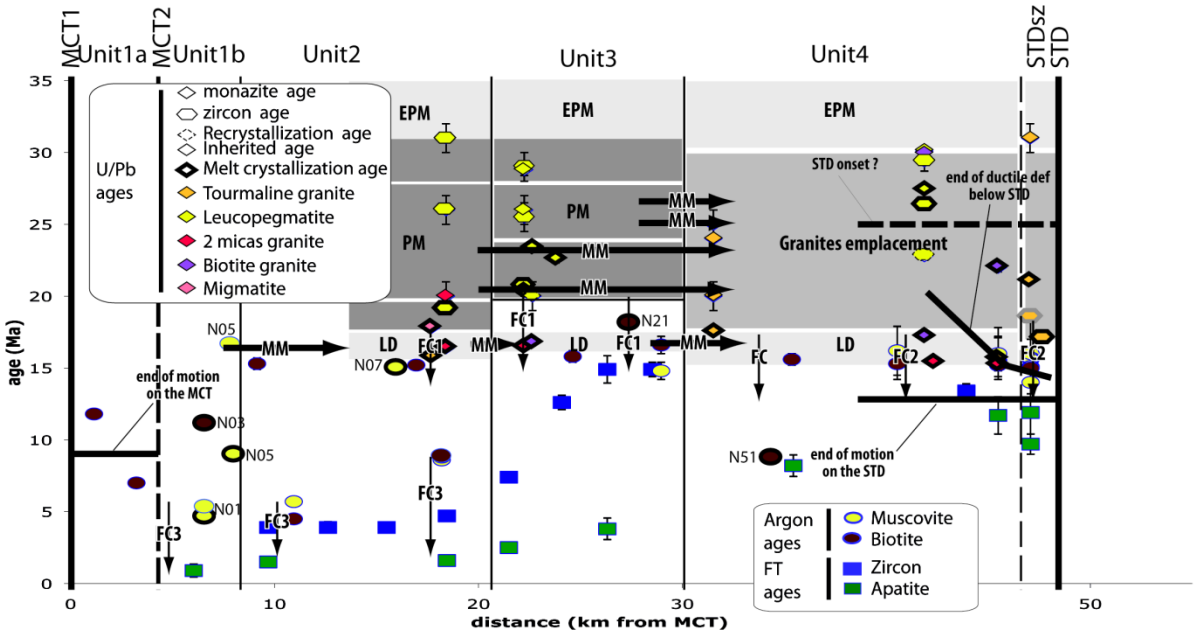

Figure 1. Available ages plotted as a function of the distance from the MCT along the Nyalam cross-section. Symbols colour / shapes refer to the geochronological / mineral systems and the type of rock. U/Pb data from units 2, 3 and 4 are from this study. Ar/Ar data are from Maluski et al. (1988), Wang et al. (2006), and this study (N standing for T11N samples). Zircon fission track data from Wang et al. (2010). Apatite fission track (AFT) data from Wang et al. (2001) and Wang et al. (2010). Grey area are interpretation: EPM: early prograde metamorphism, PM: partial melting, LRM: late retrograde metamorphism, LD: late undeformed dykes. The black arrows show fast cooling periods (FC), and inferred melt migration (MM).

References

Jamieson, R. A. et al., 2006, Provenance of the Greater Himalayan Sequence and associated rocks: predictions of channel flow models, in Channel Flow, Ductile Extrusion and Exhumation in Continental Collision Zones, edited, 165-182.

Maluski, H. et al., 1988, Argon-39-Argon-40 Dating of Metamorphic and Plutonic Events in the North and High Himalaya Belts (Southern Tibet - China), Tectonics, 7, 299-326.

Mattauer, M., 1986, Intracontinental subduction, crust-mantle decollement and crustal-stacking wedge in the Himalayas and other collision belts, Geological Society, London, Special Publications, 19, 37-50.

Wang, Y. et al., 2001, Thermochronological evidence of tectonic uplift in Nyalam, South Tibetan Detachment System, Bulletin of mineralogy, petrology and geochemistry, 20, 292-294 (in Chinese with english abstract).

Wang, Y. et al., 2006, Ar-40/Ar-39 thermochronological constraints on the cooling and exhumation history of the South Tibetan Detachment System, Nyalam area, southern Tibet, in Channel Flow, Ductile Extrusion and Exhumation in Continental Collision Zones, edited by R. D. Law, et al., Geological Society of London Special Publication, London, 327-354.

Wang, A. et al., 2010, Episodic exhumation of the Greater Himalayan Sequence since the Miocene constrained by fission track thermochronology in Nyalam, central Himalaya, Tectonophysics, 495, 315–323.

Field Study of the 12 February 2014 Yutian Ms7.3 Earthquake: A Special Surface Rupture Zone

Haibing Li[1], Zhiming Sun[2], Jiawei Pan[1], Dongliang Liu[1], Jiajia Zhang[3, 1], Chenglong Li[4, 1], Kang Liu[5, 1], Kun Yun[3, 1], Zheng Gong[1]

[1] State Key Laboratory of Continental Tectonics and Dynamics, Institute of Geology, Chinese Academy of Geological Sciences, Beijing 100037, lihaibing06@163.com
[2] Institute of Geomechanics, Chinese Academy of Geological Sciences, Beijing 100081
[3] Chengdu University of Technology, Chengdu, Sichuan 610059
[4] China University of Geosciences(Wuhan), Wuhan, Hubei 430074
[5] National Earthquake Response Support Service, Beijing 100049

On February 12, 2014, a Ms7.3 earthquake struck the eastern region of the West Kunlun Mountains in Yutian County, Xinjiang. Immediate (Feb 20th) field investigation following the earthquake shows that it produced surface ruptures at an altitude of 4600~5100 m. The surface rupture zone consists of a series of en-echelon tensional, shear-tensional to shear cracks, mole-tracks, and sag ponds. Striking NEE–SWW with a total length of about 25 km (Figure 1), the surface rupture zone is characterized by left-lateral strike slip motion with normal component. Maximum sinistral displacement along the surface rupture zone is about 1 m. What is particularly interesting here is that the surface rupture is distributed along two parallel faults, the Ashikule-Xor Kol fault and the south Xor Kol fault, which is rarely seen. The seismogenic fault of the earthquake is one splay at the southwestern end of the Altun fault. This fault combined with the Gozha Co fault and the Longmu Co fault constitutes a "new Altun fault".

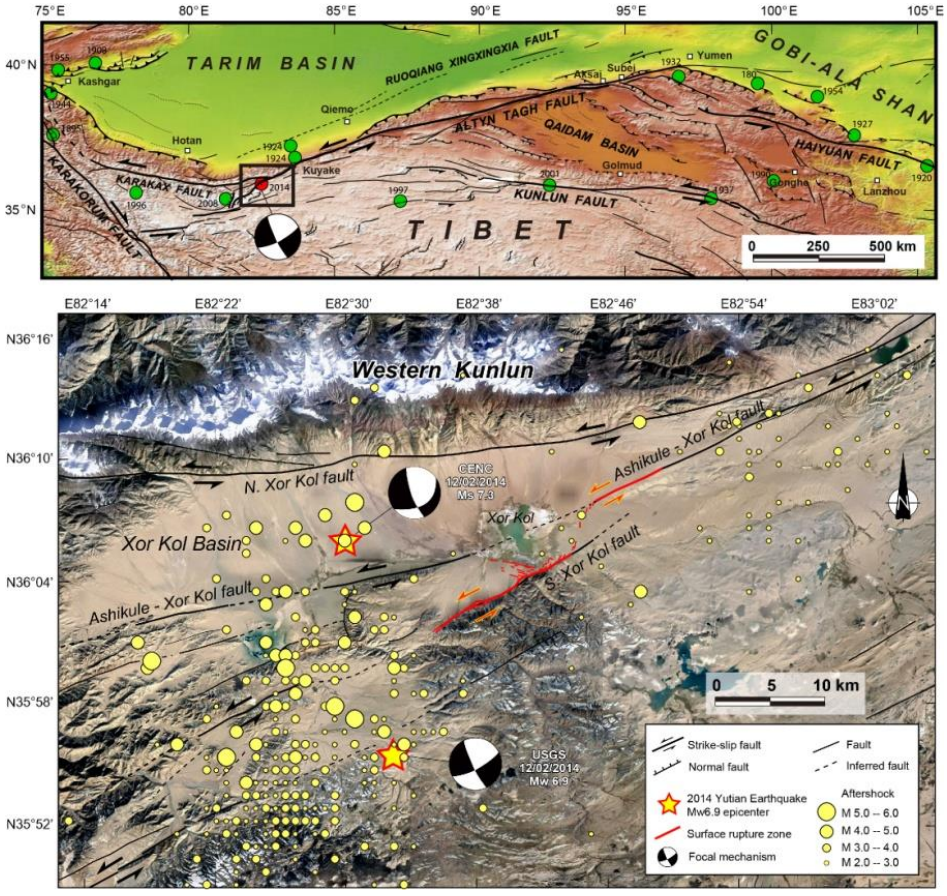

Figure 1. Active faults in northern Tibetan Plateau (upper) and surface rupture zone of the 12 February 2014 Yutian earthquake (lower)

Cite as: Li et al., 2014, Field Study of the 12 February 2014 Yutian Ms7.3 Earthquake: A Special Surface Rupture Zone, in Montomoli C., et al., eds., proceedings for the 29th Himalaya-Karakoram-Tibet Workshop, Lucca, Italy.

Moissanite and chromium-rich olivine in the Luobusa mantle peridotite and chromitite, Tibet: Deep mantle origin implication

Fenghua Liang[1], Jingsui Yang[1], Zhiqin Xu[1], Jianan Zhao[1]

[1] State Key Laboratory of Continental Tectonics and Dynamics, Institute of Geology, Chinese Academy of Geological Sciences, Beijing, 100037, China, liangfenghua1026@gmail.com

The Luobusa ophiolite lies in the eastern part of the Indus-Zangbo suture zone, Tibet and contains the biggest chromitite deposit in China. In recent years, lots of ultrahigh pressure and highly reduced minerals were surprisingly discovered in the Luobusa mantle peridotite and chromitite. They indicate a deep mantle (> 300 km) origin contrary to previously SSZ origin thought (Yang et al., 2014). Here, we report our new discoveries of in-situ natural moissanite and chromium-rich included olivines in Luobusa. They also suggest a lower mantle or transition zone origin.

The moissanite occurs as a twinned grain in Cr-spinel hosted by enveloped dunite of a podiform chromitite in the Luobusa ophiolite (Liang et al., 2014). The moissanite is green in color, and has parallel extinction. Its Raman spectrum has shifts at 967-971 cm^{-1}, 787-788 cm^{-1}, and 766 cm^{-1}. The absorption peaks in the infra-red spectra are at 696 cm^{-1}, 767 cm^{-1}, 1450 cm^{-1}, and 1551 cm^{-1}, which are distinctly different from the peaks for synthetic silicon carbide.Chromium-rich included olivines were found in harzburgite, dunite, disseminated chromitite, nodular chromitite and massive chromitite respectively. These olivines are included by spinels or chromites with crystal shape of subhedral to hedral. No matter in what lithology, included olivines contain obviously higher Cr_2O_3 (0.1-1.49 wt %) and lower FeO than other olivines (Cr_2O_3 < 500 ppm). Especially, they contain the highest Cr_2O_3 content (up to 1.49 wt %) by far in the world and much higher than those in chondrite olivines (~ 0.7 wt %) (Dodd, 1975). Except for a weak negative correlation of Cr_2O_3 vs FeO, no other correlations of Cr_2O_3 vs MnO and of Cr_2O_3 vs MgO were observed. Aluminum is near background levels and minors of manganese (~0.1 wt%) and nickel (0.3~0.5 wt %) were detected in the chromium-rich included olivines.

Moissanite is one of the deepest mantle minerals known to reach the surface. All moissanite grains analysed thus far have very depleted carbon isotope compositions ($\delta^{13}C$ from −18 to −35‰), much lighter than the main carbon reservoir in the upper mantle ($\delta^{13}C$ near −5‰). They were suggested to form in the lower mantle since the ^{13}C-depleted carbon is supported by extraterrestrial carbon, and there have been no other explanations until now (Trumbull et al., 2009).

Although the substitution of chromium in olivine is controversial for a long time, most evidences proved that chromium in olivine is divalent and precipitate in high pressure, high temperature and extremely reducing conditions (e.g. Brenker, 2002). For those chromium-rich included olivines in the Luobusa ophiolite, Cr^{2+} is believed to be the controlled valence in the octahedral site of olivine since the in-situ moissanite in the same sample has been discovered. A possible vacancy substitution mechanism is proposed to explain the uncorrelated characteristic between Cr and other metal elements. Combing with many other findings of ultra-high pressure and extremely reducing minerals reported by previous studies, the chromium-rich olivines in the Luobusa mantle peridotite and chromitite might originate from mantle transition zone or lower mantle and their precursor phase might be wadsleyite or ringwoodite.

References

Brenker, F.E., Stachel, T. and Harris, J.W., 2002, Exhumation of lower mantle inclusions in diamond: ATEM investigation of retrograde phase transitions, reactions and exsolution, Earth and Planetary Science Letters, 198, 1-9.

Butler, P.J., 1972, Compositional characteristics of olivines from Apollo 12 samples, Geochimica et Cosmochimica Acta, 36, 773-786.

Dodd, R.T., Morrison-Smith, D.J. and Heyse, J.V., 1975, Chromium-bearing olivine in the St. Mesmin chondrite, Geochemica et Cosmochimica Acta, 39, 1621-1627.

Liang, F.H., Xu, Z.Q. and Zhao, J.N., 2014, In-situ moissanite in dunite: Deep mantle origin of mantle peridotite in Luobusa ophiolite, Tibet, Acta Geologica Sinica (English Edition), 88, 517-529.

Trumbull, R.B., Yang, J.S. and Robinson, P.T., et al., 2009, The carbon isotope composition of natural SiC (moissanite) from Earth's mantle: New discoveries from ophiolites, Lithos, 113, 612-620.

Yang, J.S., Robinson, P.T. and Dilek, Y., 2014, Diamonds in ophiolites, Elements, 10, 127-130.

Cite as: Liang, F.H., Yang, J.S., Xu, Z.Q. and Zhao, J.N., 2014, Moissanite and chromium-rich olivine in the Luobusa mantle peridotite and chromitite, Tibet: Deep mantle origin implication, in Montomoli C., et al., eds., proceedings for the 29th Himalaya-Karakoram-Tibet Workshop, Lucca, Italy.

Frontier of the underthrusting Indian lithosphere beneath the central Tibet from finite frequency tomography

Xiaofeng Liang[1], Yun Chen[1], Xiaobo Tian[1], Zhongjie Zhang[1]

[1]Institute of Geology and Geophysics, Chinese Academy of Sciences, Chaoyang, Beijing 100029, China, liangxf@mail.iggcas.ac.cn

Combining the new collected teleseismic body waves recorded by Cuoqin-Dangxiong passive seismic array of 59 broadband stations with waveforms from several previous temporary local seismic arrays of 301 broadband stations, we carried out finite-frequency tomographic inversions to image the three-dimensional velocity structure beneath southern-central Tibet to examine the roles of the upper mantle in the formation of the Tibetan plateau. This new dataset significantly improved the station coverage for the teleseismic body-wave tomography research of eastern Tibetan plateau.

There are some new features shown in our preliminary tomographic images. The strong low P- and S-wave velocity anomalies that extends from the lower crust to at least 200 km depth beneath the Coma rift, Yadong-Gulu rift, Tangra Yum Co rift, suggesting that rifting in southern Tibet is probably a process that involves the entire lithosphere. At the same time these low velocities are limited in southern Tibet and do not extend further north to central Tibet. This observation implies that the underthrusted Indian lithosphere may not go further than 31°N, where our Cuoqin-Dangxiong array is located. Another low velocity anomaly is occupied northeast of Gyaring Co fault, showing a possible transfering zone linking north-south trending Cenozoic extensional structures in the Lhasa and Qiangtang Terranes. A high velocity anomaly locates at northeast of Peng Co fault, where the Amdo basement is. The strong velocity contrast reflects the Central Tibet conjugate fault zone might develop under the ancient micro plate structure.

Cite as: Liang, X., Chen, Y., Tian, X. and Zhang, Z., 2014, Frontier of the underthrusting Indian lithosphere beneath the central Tibet from finite frequency tomography, in Montomoli C., et al., eds., proceedings for the 29th Himalaya-Karakoram-Tibet Workshop, Lucca, Italy.

Upper mantle structure beneath central Tibet by teleseismic S wave tomography along INDEPTH-III profile

Zhen Liu[1,2],Xiao-bo Tian[1], Xiao-feng Liang[1], Ji-wen Teng[1]

[1] Institute of Geology and Geophysics, Chinese Academy of Sciences, Beijing, 100029, China, liuzhen@mail.iggcas.ac.cn
[2] University of Chinese Academy of Sciences, Beijing, 100049, China

Tibetan Plateau is produced by the continental- continental collision between the India and Eurasian plates as well as the subsequent convergence. It has become a consensus that the crustal thickness beneath the plateau is twice of the normal continental crust, while the deformation of its mantle lithosphere, as an important part of the developing plateau, is in disputes. This ambiguity about the upper mantle structure is resulted from uneven distributed seismologic observations in Tibet, when upper mantle structure is possibly heterogeneous along the east-west direction, and the seismic wave speed contrast between the continental mantle lithosphere and asthenosphere might not be significant to detect by current seismic methods. Because the geodynamic of mantle lithosphere is closely related to the process of plateau uplift and the presence of volcanic rocks, revealing the geometric configuration of Indian and Eurasian mantle lithosphere is conducive to study the dynamic processes of mantle lithosphere as well as the evolution of the plateau. In this paper, we obtain the travel times of teleseismic S wave from the INDEPTH-III broad-band waveforms, and calculate the perturbation of S wave speed beneath the profile. Our results show that a north-dipping S wave high-velocity anomaly presents in depth range of 100 to 300 km beneath Bangong-Nujiang suture, with a dipping angle about 65°. We suggest that it is the roll-backed Indian lithosphere or/and remnant of Indian mantle lithosphere from convective removal.

Cite as: Liu, Z., Tian, X., Liang, X. and Teng, J., 2014, Upper mantle structure beneath central Tibet by teleseismic S wave tomography along INDEPTH-III profile, in Montomoli C., et al., eds., proceedings for the 29th Himalaya-Karakoram-Tibet Workshop, Lucca, Italy.

Imaging the subduction of continental crust and lithosphere beneath the northern margin of the Tibet-Pamir plateau

James Mechie[1], Rainer Kind[1], Xiaohui Yuan[1], Bernd Schurr[1], Felix Schneider[1], Christian Sippl[1], Wenjin Zhao[2], Mei Feng[3], Zhenhan Wu[2], Danian Shi[2], Heping Su[2], Guangqi Xue[2], Hui Qian[2], Prakash Kumar[4], Vlad Minaev[5], Mustafo Gadoev[5], Ilhomjon Oimahmadov[5], Ulan Abdybachaev[6], Bolot Moldobekov[6], Sagynbek Orunbaev[6], Sobit Negmatullaev[7]

[1] Deutsches GeoForschungsZentrum – GFZ, Telegrafenberg, 14473 Potsdam, Germany, jimmy@gfz-potsdam.de
[2] Chinese Academy of Geological Sciences, 26 Baiwanzhuang Road, Beijing, 100037, China
[3] Institute of Geomechanics, Chinese Academy of Geological Sciences, 11 Minzudaxuenan Road, Beijing, 100081, China
[4] National Geophysical Research Institute (CSIR), Hyderabad 500037, India
[5] Institute of Geology, Earthquake Engineering and Seismology, Academy of Sciences of the Republic of Tajikistan, Dushanbe 734063, Republic of Tajikistan
[6] Central Asian Institute for Applied Geosciences, 720027 Bishkek, Kyrgyz Republic
[7] PMP International, 59 Shevchenko St., Dushanbe 734025, Republic of Tajikistan

The main goal of this contribution will be to present recent results on the imaging of the subduction of continental crust and lithosphere from two seismological projects across the northern margin of the Tibet-Pamir plateau. The first project runs across the eastern end of the Qaidam basin and the Qilian Shan in the northeastern Tibetan plateau. The second project, the TIPAGE (TIen shan—PAmir GEodynamic program) project, is located in the Pamir and southern Tien Shan. The northern margin of the Tibet-Pamir plateau represents an important boundary as it is here that most of the outward growth of the plateau possibly occurs. Important faults occur here, such as the Kunlun fault which hosted the M8.1 Kokoxili earthquake in November 2001. Further, the large Qaidam basin in the northeastern part of the plateau is important for its mineral and hydrocarbon reserves.

For a period of about one year between the summers of 2010 and 2011, 25 broadband seismographs were deployed in a roughly linear array across the eastern end of the Qaidam basin and the Qilian Shan in the northeastern Tibetan plateau (Feng et al. 2014). This region is probably the most suitable place to study the ongoing convergence interaction between the high Tibetan plateau and the main Asian continental plate. Low-frequency *P* receiver function analysis of the data provides an image of the crust and mantle down to 700 km depth. In addition to the Moho at 45-65 km depth beneath the profile, the 410 and 660 km discontinuities bounding the mantle transition zone can be identified at 400-410 km and 650-660 km depths respectively. A possible increase in temperature in the upper mantle thought to exist beneath the northern part of the high Tibetan plateau is thus confined to this part of the plateau and lower upper mantle temperatures similar to those beneath southern Tibet occur beneath the Qaidam basin and Qilian Shan. When higher frequencies are included in the *P* receiver function analysis, a positive *Ps* converter dipping down to the south from 70-75 km depth at 37.9°N to about 110 km depth at 36°N is imaged. As this feature is only seen in high-frequency images and not in the low-frequency image, it is modelled as the positive *Ps* conversion from the base of an approximately 5 km thick anisotropic layer at the top of the Asian mantle lithosphere which is currently subducting. This south-dipping converter continues to the south on the INDEPTH IV profile (Zhao et al. 2011). *S* receiver function analysis completes the image of the structure below the Qilian Shan profile with the identification of the lithosphere-asthenosphere boundary (LAB). The LAB of the Asian plate is identified at 12-14 s (95-110 km depth) between 38 and 41°N below the northern part of the *S* receiver function profile. To the south it increases in depth such that it is at about 19 s (150 km depth) between 34 and 35°N at the southern end of the profile. The LAB of the Asian plate occurs at similar depths on the INDEPTH IV profile at the latitudes where the INDEPTH IV and Qilian Shan profiles overlap (Zhao et al. 2011). As on the INDEPTH IV profile to the south, between 34 and 35°N at the southern end of the Qilian Shan profile there is evidence from the *S* receiver functions for the LAB of a separate Tibetan plate (Zhao et al. 2011).

Cite as: Mechie, J., et al., 2014, Imaging the subduction of continental crust and lithosphere beneath the northern margin of the Tibet-Pamir plateau,, in Montomoli C., et al., eds., proceedings for the 29th Himalaya-Karakoram-Tibet Workshop, Lucca, Italy.

The recent TIPAGE project in the Pamir and southern Tien Shan has produced new insights into this part of the Alpine-Himalayan orogenic belt (Mechie et al. 2012, Schneider et al. 2013, Sippl et al. 2013a, b, Schurr et al. 2014). Along the main seismic profile of the TIPAGE project, guided waves have been observed. These guided waves are associated with a south-dipping low-velocity channel in the upper mantle recognized from receiver function studies (Schneider et al. 2013). The low-velocity channel is coincident with the Pamir seismic zone and has been interpreted to represent Eurasian lower continental crust being subducted southwards beneath the Pamir (Schneider et al. 2013, Sippl et al. 2013a, b). Modelling of the guided waves should place further constraints on the average velocity within and the thickness of the low-velocity zone. Very preliminary results to date suggest that the low-velocity channel may have an average velocity as low as around 6.2 km/s and is on the order of about 10 km thick. This thickness is in agreement with the thickness of 10-15 km derived by Schneider et al. (2013). The low average velocity of 6.2 km/s would indicate either that upper crustal rocks are also being subducted to greater depths or that significant amounts of water are being transported to greater depths or that anisotropy with the slow axis oriented in the down-dip direction of the low-velocity channel exists.

References

Feng, M. et al., 2014, Structure of the crust and mantle down to 700 km depth beneath the East Qaidam basin and Qilian Shan from *P* and *S* receiver functions, submitted to Geophysical Journal International.

Mechie, J. et al., 2012, Crustal and uppermost mantle velocity structure along a profile across the Pamir and southern Tien Shan as derived from project TIPAGE wide-angle seismic data, Geophysical Journal International, 188, 385-407, doi:10.1111/j.1365-246X.2011.05278.x.

Schneider, F. M. et al., 2013, Seismic imaging of subducting continental lower crust beneath the Pamir, Earth and Planetary Science Letters, 375, 101-112, doi:10.1016/j.epsl.2013.05.015.

Schurr, B., et al., 2014, Seismotectonics of the Pamir, submitted to Tectonics.

Sippl, C. et al., 2013a, Geometry of the Pamir-Hindu Kush intermediate-depth earthquake zone from local seismic data, Journal of Geophysical Research, 118, 1438-1457, doi:10.1002/jgrb.50128.

Sippl, C. et al., 2013b, Deep burial of Asian continental crust beneath the Pamir imaged with local earthquake tomography, Earth and Planetary Science Letters, 384, 165-177, doi:10.1016/j.epsl.2013.10.013.

Zhao, W. et al., 2011, Tibetan plate overriding the Asian plate in central and northern Tibet, Nature Geoscience, 4, 870-873, doi:10.1038/ngeo1309.

The Early Neogene decelerated denudation of the Red River-Ailao Shan shear zone, SE Asia: new sedimentary and paleomagnetic constraints on the Middle Miocene deposits

Kai Meng[1], Guoli Wu[1], Erchie Wang[1], Haijian Lu[2]

[1] Institute of Geology and Geophysics, Chinese Academy of Sciences, Beijing, 100029, China, Michael.meng@mail.iggcas.ac.cn
[2] Institute of Geology, Chinese Academy of Geological Sciences, Beijing, 100037, China

The current tectonic framework in Southeast Asia is considerably recognized as a direct resultant of the continental collision between Indian and Eurasian since ~50 Ma (Rowley, 1996; Dupont-Nivet *et al.*, 2010). The collision led to the comprehensive orogeny along the Himalayan, crustal thickening in internal of the Tibetan plateau (TP) and lateral extrusion of lithospheric material along a series of major strike-slip fault belts surrounding the TP (Molnar and Tapponnier, 1975; Tapponnier *et al.*, 1986, 1990; Wang *et al.*, 1997, 1998; Burchfiel and Wang, 2003). In recent couple of decade, as a significant tectonic boundary of the Indochina block, lots of tectonic, thermo-chronological and paleomagnetic studies have been conducted on the Red River-Ailao Shan shear zone (RRAS) for the purpose of constructing the tectonic evolution pattern of the southeast TP during the Cenozoic (Schärer *et al.*, 1990, 1994; Harrison *et al.*, 1992, 1996; Leloup *et al.*, 1995, 2001; Schoenbohm et al., 2006a, 2006b; Sato et al., 2007; Searle et al., 2010).

The RRAS linearly founded by four metamorphic complexes in northwest-southeast direction, including Xuelong Shan, Diancang Shan, Ailao Shan in China and Day Nui Con Voi in Vietnam, extends over 1500 km from the southeast TP to the South China Sea (Fig. 1). The current Red River fault (RRF) is composed of two branches: 1) inactive Range-front fault, bounding the Ailao Shan metamorphic belt on the northeast, is characterized by normal faulting in Late Oligocene to Early Miocene, and 2) active Mid-valley fault, extending along the current Red River valley, is dominated by right-lateral strike slip after the Late Pliocene. Numerous researches pointed out that the RRAS undergone 1) left shearing and sny-kinematic metamorphism, and denudation accommodated by the Range-front fault in the Late Oligocene-Early Miocene, and 2) right-lateral strike slip activity along the Mid-valley fault after the Late Pliocene (Harrison *et al.*, 1992, 1996). But, we still do not clearly know what has happened on the RRAS in interval between these two tectonic events. We here show our newest sedimentary and paleomagnetic evidence from a set of the Late Oligocene-Early Miocene deposits distributed along the Red River valley in the northeast of the Ailao Shan metamorphic belt, and exert reliable constraints on the tectonic evolution of the RRAS during the Early Neogene.

The sampling section is located about 34 km northwest of Yuanjiang County, SE China. This section spans a thickness of more than 700 m and is mainly composed of yellow or brown silty mudstone or mudstone in the upper part, purple mudstone interbedded with angular debris or conglomerates layers in the central part and medium-coarse sandstone interbedded with in the lower part. The whole Cenozoic strata, dipping to SW about 30ºin general, uncomformably rested on the underlying Upper Triassic mudstone and sandstone in northeast and contacted with Ailao Shan metamorphic rocks along the Range-front fault in the southwest. The gradual lithic facies change of the sequence from bottom to top implies the sedimentary environment transited from fluvial to lacustrine or fan-delta facies, which further indicates the deceleration of local sedimentation.

We systematically collected 417 samples and conducted paleomagnetic analysis at the Paleomagnetism and Geochronology Laboratory in the Institute of Geology and Geophysics, Chinese Academy of Sciences. Finally, a linear extrapolation of the average sedimentation rate yielded an age of 8.5 and ~12 Ma for the top and base of the section, respectively. Consistent with the sedimentary analysis, paleomagnetic data also indicate that the normal faulting along the Range-front fault and the rapid denudation of the RRAS decelerated from ~12 Ma to 8.5 Ma at least. Therefore, we proposed that there might exist a tectonic "quiescence epoch" on the RRAS in the Middle Miocene.

Cite as: Meng, K., et al., 2014, The Early Neogene decelerated denudation of the Red River-Ailao Shan shear zone, SE Asia: new sedimentary and paleomagnetic constraints on the Middle Miocene deposits, in Montomoli, C., et al., eds., Proceedings for the 29th Himalaya-Karakoram-Tibet Workshop, Lucca, Italy.

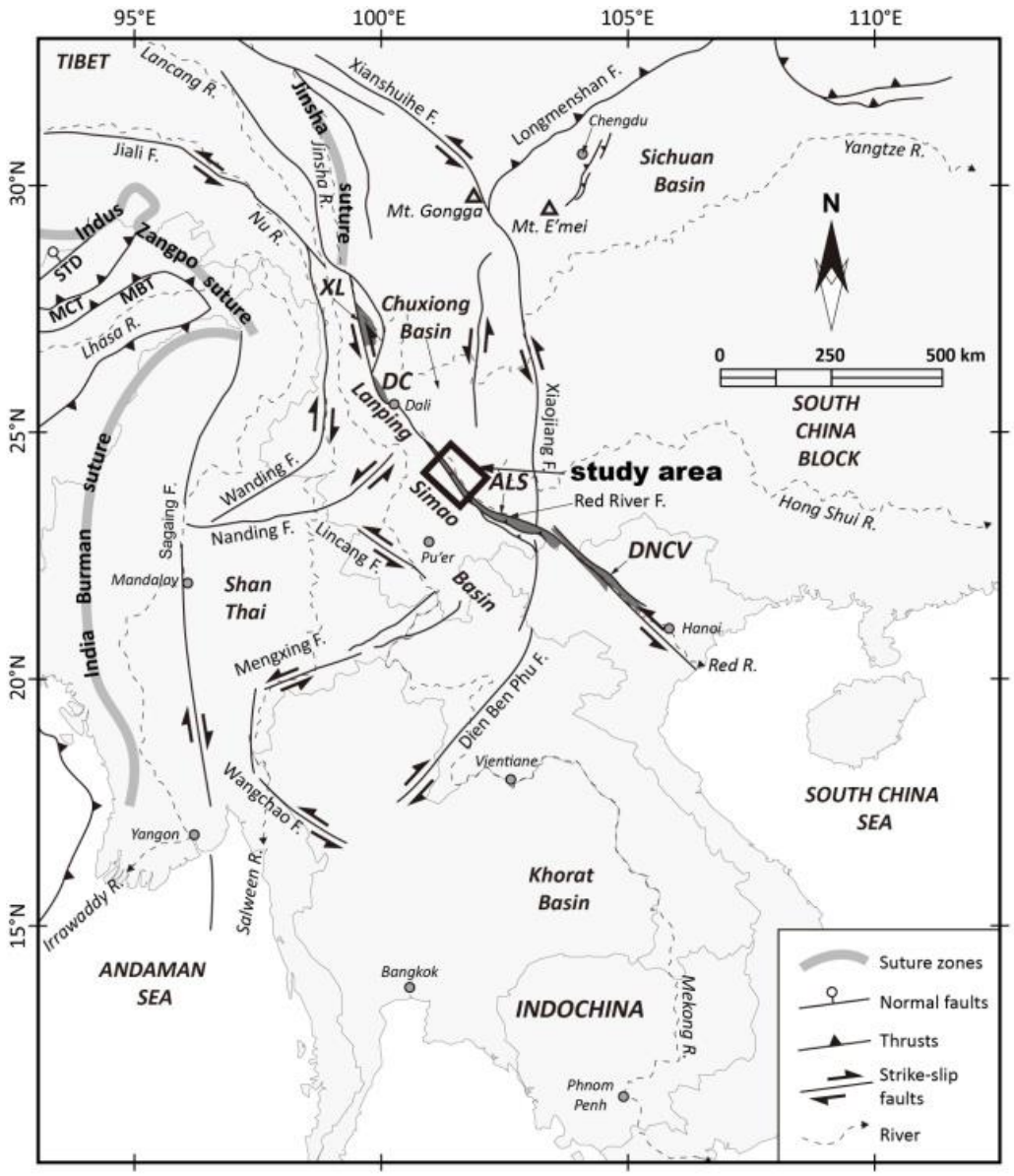

Figure 1. General tectonic sketch map of SE Asia. Major sutures and faults have shown in this figure. The black bold box shows the location of the paleomagnetic section in this study. STD, South Tibetan Detachment; MCT, Main Central Thrust; MBT, Main Boundary Thrust; XL, Xuelong Shan; DC, Diancang Shan; ALS, Ailao Shan; DNCV, Day Nui Con Voi.

References

Burchfiel, B.C. and Wang, E., 2003, Northwest-trending, middle Cenozoic, left-lateral faults in southern Yunnan, China, and their tectonic significance, Journal of Structural Geology, 25, 781-792.

Dupont-Nivet, G., Lippert, P.C., van Hinsbergen, D.J.J., Meijers, M.J.M., and Kapp, P., 2010, Palaeolatitude and age of the Indo-Asia collision: palaeomagnetic constraints, Geophysical Journal International, 182, 1189-1198.

Harrison, T.M., Chen, W.J. and Leloup, P.H., 1992, An early Miocene transition in deformation regime within the Red River fault zone, Yunnan, and its significance for Indo-Asian tectonics, Journal of Geophysical Research, 97, 7159–7182.

Harrison, T.M., Leloup, P .H., Ryerson, F.J., Tapponnier, P., Lacassin, R. and Chen, W.J., 1996, Diachronous initiation of transtension along the Ailao Shan-Red River Shear zone, Yunnan and Vietnam, in Harrison, T.M. and Yin, A., eds., The tectonic evolution of Asia, The Tectonics of Asian Cambridge University Press, 208-226.

Leloup, P.H., Lacassin, R., Tapponnier, P., Schärer, U., Zhong, D.L., Liu, X.H., Zhang, L.S., Ji, S.C. and Phan, T.T., 1995, The Ailao Shan-Red River shear zone (Yunnan, China), Tertiary transform boundary of Indochina, Tectonophysics, 251, 3-84.

Leloup, P .H., Arnaud, N., Lacassin, R., Kienast, J.R., Harrison,T.M., Phan Trong, T.T., Replumaz, A. and Tapponnier, P., 2001, New constraints on the structure, thermochronology, and timing of the Ailao Shan-Red River shear zone, SE Asia, Journal of Geophysical Research, 106, 6683–6732.

Molnar, P. and Tapponnier, P., 1975, Cenozoic tectonics of Asia: Effects of a continental collision, Science, 189, 419-426.

Rowley, D.B., 1996, Age of initiation of collision between India and Asia: A review of stratigraphic data, Earth and Planetary Science Letters, 145, 1–13.

Sato, K., Liu, Y.Y., Wang, Y.B., Yokoyama, M., Yoshioka, S., Yang, Z. and Otofuji, Y.I., 2007, Paleomagnetic study of Cretaceous rocks from Pu'er, western Yunnan, China: Evidence of internal deformation of the Indochina block, Earth and Planetary Science Letters, 258, 1–15.

Schärer, U., Tapponnier, P., Lacassin, R., Leloup, P.H., Dalai, Z. and Ji, S.C., 1990, Intraplate tectonics in Asia: A precise age for large-scale Miocene movement along the Ailao Shan-Red River shear zone, China, Earth and Planetary Science Letters, 97, 65-77.

Schärer, U., Zhang, L.S., and Tapponnier, P., 1994, Duration of strike-slip movements in large shear zones: The Red River belt, China, Earth and Planetary Science Letters, 126, 379-397.

Schoenbohm, L.M., Burchfiel, B.C. and Chen, L.Z. 2006a, Propagation of surface uplift, lower crustal flow, and Cenozoic tectonics of the southeast margin of the Tibetan Plateau, Geology, 34, 813-816.

Schoenbohm, L.M., Burchfiel, B.C., Chen, L.Z. and Yin, J.Y., 2006b, Miocene to present activity along the Red River fault, China, in the context of continental extrusion, upper-crustal rotation, and lower-crustal flow, GAS bulletin, 118, 672-688.

Searle, M.P., Yeh, M.W., Lin, T.H. andChung, S.L., 2010, Structural constraints on the timing of left-lateral shear along the Red River shear zone in the Ailao Shan and Diancang Shan Ranges, Yunnan, SW China, Geosphere, 6, 316-338.

Tapponnier, P., Peltzer, G. and Armijo, R., 1986, On the mechanics of the collision between India and Asia, in Coward, M.P. and Ries, A.C., eds., Collision tectonics, Geological Society of London Special Publication, 19, 115-157.

Tapponnier, P., Lacassin, R., Leloup, P.H., Schärer, U., Zhong, D.L., Liu, X.H., Ji, S.C., Zhang, L.S. and Zhong, J.Y., 1990, The Ailao Shan/Red River metamorphic belt: Tertiary left-lateral shear between Indochina and South China, Nature, 343, 431-437.

Wang, E. and Burchfiel, B.C., 1997, Interpretation of Cenozoic tectonics in the right-lateral accommodation zone between the Ailao Shan Shear Zone and the eastern Himalayan syntaxis, International Geology Review, 39, 191-219.

Wang, E., Burchfiel, B.C., Royden, L.H., Chen, Z.L., Chen, J.S., Li, W.X. and Chen, L.Z., 1998, Late Cenozoic Xianshuihe-Xiaojiang, Red River, and Dali Fault Systems of Southwestern Sichuan and Central Yunnan, China, Geological Society of American Special Paper, 327, 1-108.

The South Tibetan Detachment between Karta and Tingri (South Tibet Himalaya)

Giancarlo Molli[1], David Iacopini[2], Piero C. Pertusati[1]

[1] Dipartimento Scienze della Terra, Università di Pisa, I, gmolli@dst.unipi.it
[2] Geology & Petroleum Geology Department - University of Aberdeen, UK

The South Tibetan Detachment System (STDS) represents a major geological structure within the Himalaya orogen (e.g. Burg et al., 1984; Burchfiel et al., 1992; Carosi et al., 1998; Hodges, 2000; Godin et al., 2001; Searle et al., 2003, Cottle et al., 2011). It can be traced for c.3000 Km along the entire length of the belt between the Zanksar region (NW India) to Arunachal Pradesh (NE India).

At the regional scale it is described as a network of Low Angle Normal Faults (LANF's) and/or Normal Sense Shear Zones (NSSZ's) separating Tethyan zone sediments in the north from medium-high grade metamorphic rocks including migmatites and granites of the Higher Himalayan Crystalline (HHC) series to south.

Different and contrasted architectures, strain features and kinematic characters are locally reported and regionally used as the base of various and debated tectonic models (e.g. Beamount et al., 2001; Webb et al., 2007 and references therein; Kellett and Grujic, 2012 and references therein).

Our study reports structural data collected during an 2005's expedition in Himalaya-Tibet with observation focused on an area between Karta and Tingri bounded by the Ama Drime Range to the est and the Rongbuck valley to the west.

Four structural logs separated by an along-strike distance of c.30 Km and an along-dip direction distance of c.22 Km were analysed with the aim to constrain fault zone pattern, strain distribution and fault-rock types.

In all analysed transects and studied sites, the STDS is formed by a footwall normal sense shear zone (South Tibetan shear zone) and an upper low angle brittle fault (Chomalonga detachment) in marked contrast with that described for the close Dzakaa Chu area (Cottle et al., 2007a).

The shear zone is represented by at least 1000 m thick zone of mylonites with diffuse lower boundary within the HHC series and comprising the entire and variable thickness of the North Col fm. (biotite-chlorite phyllites, metagreywacke, quartzites, impure marbles and calc-silicates). Strongly non-coaxial deformation with top-to-NE kinematics is testified by well developed kinematic indicators, asymmetric folds (up to hectometer-scale) and shear bands systems.

The upper low angle brittle fault consists of meter-thick cataclastic zone where R-types, P-foliation and asymmetric folds point to a top-to-NE sense of transport the same of the lower shear zone. Different kinds of fault rocks (crush breccia, black and green cataclasites and vein derived calc-mylonites) can be observed attesting a prolonged history and multistage reactivations.

Micro- and mesostructural features, leucogranites-fabrics relationships, metamorphic history and a revision of the available radiometric data allowed us to enlighten deformation history for hanging wall and footwall. Moreover, large scale geometry of the structures indicates that the lower shear zone as well as the upper brittle fault are folded by high amplitude (plurikilometer scale) dome and basins and overprinted by a system of N-S trending active normal fault (Molli et al., 2007; Kali et al., 2010 and and references therein).

Cite as: Molli, G., et al., 2014, The South Tibetan Detachment between Karta and Tingri (South Tibet Himalaya)., in Montomoli C., et al., eds., proceedings for the 29th Himalaya-Karakoram-Tibet Workshop, Lucca, Italy.

References

Beaumont, C., Jamieson, R.A., Nguyen, M.H. and Lee B., 2001, Himalayan tectonics explained by extrusion of a low-viscosity crustal channel coupled to focused surface denudation, Nature, 414, 738–742, doi:10.1038/414738a.

Burg, J.-P., Brunel, M., Gapais, D., Chen, G.M., and Liu G.H., 1984, Deformation of leucogranites of the crystalline Main Central Sheet in southern Tibet (China), Journal of Structural Geology, 6(5), 535–542, doi:10.1016/ 0191-8141(84)90063-4.

Burchfiel, B.C., Chen, Z., Hodges, K.V., Liu, Y., Royden, L.H., Deng, C. and Xu J., 1992, The South Tibet Detachment System, Himalayan orogen: Extension contemporaneous with and parallel to shortening in a collisional mountain belt, Geological Society of America Special Paper, 269, 1–41.

Carosi, R., Lombardo B., Molli, G., Musumeci, G. and Pertusati P.C., 1998, The south Tibetan detachment system in the Rongbuk valley, Everest region. Deformation features and geological implications, Journal of Asian Earth Sciences, 16(2–3), 299–311, doi:10.1016/S0743- 9547(98)00014-2.

Cottle, J.M., Jessup, M.J., Newell, D.L., Searle, M.P., Law, R.D. and Horstwood M.S.A., 2007, Structural insights into the early stages of exhumation along an orogen-scale detachment: The South Tibetan Detachment System, Dzakaa Chu section, Eastern Himalaya, Journal of Structural Geology, 29(11), 1781–1797, doi:10.1016/j.jsg.2007.08.007.

Cottle, J.M., Waters, D.J., Riley, D., Beyssac, O. and Jessup M.J., 2011, Metamorphic history of the South Tibetan Detachment System, Mt. Everest region, revealed by RSCM thermometry and phase equilibria modeling, Journal of Metamorphic Geology, 29, 561–582, doi:10.1111/j.1525-1314.2011. 00930.x.

Godin, L., Grujic, D., Law, R. and Searle M.P., 2006, Crustal flow, extrusion, and exhumation in continental collision zones: An introduction, in Channel Flows, Ductile Extrusion and Exhumation in Continental Collision Zones, edited by R. D. Law, M. P. Searle, and L. Godin, Geol. Soc. Spec. Publ., 268, 1–23, doi:10.1144/GSL.SP.2006.268.01.01.

Hodges, K.V., 2000, Tectonics of the Himalaya and southern Tibet from two perspectives, Geological Society of America Bulletin, 112(3), 324–350, doi:10.1130/ 0016-7606(2000)112<324:TOTHAS>2.0.CO;2.

Kali, E., Leloup, P.H., Arnaud, N., Mahéo, G., Liu, D., Boutonnet, E., Van der Woerd, J., Liu, X., Liu-Zeng J. and Li H., 2010, Exhumation history ofthe deepest central Himalayan rocks, Ama Drime range: Key pressure temperature- deformation-time constraints on orogenic models, Tectonics, 29, TC2014, doi:10.1029/2009TC002551.

Kellett, D.A. and Grujic, D.. 2012, New insight into the South Tibetan detachment system: Not a single progressive deformation, Tectonics, 31, TC2007, doi:10.1029/2011TC002957.

Molli G., Iacopini D., Musumeci G. and Pertusati, P., 2007, Architecture, strain features and fault rock types of the south Tibetan detachment system between Karta and Tingri (South Tibet Himalaya). Continental tectonics and mountain building, Peach and Horne Meeting, Ullapool 12-20th May, 2007, Volume Abstract.

Searle, M., Simpson, R.L., Law, R.D., Parrish, R.R. and Waters D.J., 2003, The structural geometry, metamorphic and magmatic evolution of the Everest massif, High Himalaya of Nepal-South Tibet Journal of the Geological Society, 160, 345–366, doi:10.1144/0016-764902-126.

Webb, A.A.G., Yin, A., Harrison, T.M., Célérier, J. and Burgess, W.P., 2007, The leading edge of the Greater Himalayan Crystalline complex revealed in the NW Indian Himalaya: Implications for the evolution of the Himalayan orogen, Geology, 35, 955–958, doi:10.1130/G23931A.1.

Awaran, Pakistan, earthquake of Mw 7.7 in Makran Accretionary Zone, 24 September 2013: focal-mechanism solution and tectonic implications

MonaLisa[1,2], M. Qasim Jan[3]

[1] COMSATS Institute of Information Technology (CIIT) Islamabad, Pakistan, monalisa@comsats.edu.pk
[2] Quaid-i-Azam University (QAU), Islamabad, Pakistan, lisa_qau@yahoo.com
yeatsr@geo.oregonstate.edu
[3] National Centre of Excellence in Geology (NCEG), University of Peshawar, Peshawar, Pakistan

On 24 September, 2013 an earthquake with focal depth of 10 km (by local observatory), identical magnitude (Mw 7.7) and sinistral focal mechanism solution, shook the town of Awaran and surrounding area in Makran Accretionary Zone (MAZ) in the province of Balochistan Pakistan. Named here as Awaran Earthquake (AE), it occurred in a remote and poorly accessible region of Balochistan. AE was followed by a major aftershock of Mw 7.2, occurred about 90 km NNE of Awaran on 28 September 2013. It took a death toll of about 826 (unofficially 1100) human lives and caused a widespread destruction in Awaran and surrounding area. Based on the information obtained from the print and electronic media (and for some areas from the field studies), an intensity of IX on MMI scale has been assigned to the epicenter of the main shock. The damages to construction and loss of lives occurred due to the poor construction of structures within 100 km of the main shock. About 90% of Awaran has been completely destroyed, and this damage was increased further after the occurrence of its largest aftershock. Fault-plane solutions of the main event and its largest aftershock on 28 September 2013 and the aftershock distribution suggest that the NNE-SSW-trending left-lateral strike-slip Awaran Fault (AF) is currently active. However, more fault-plane solutions of aftershocks data are required to confirm this contention. The emergence of an island about 200m long and 100m wide a few hours after the main shock in waters off the port town of Gwadar is the result of the formation of a mud volcano. Liquefaction of sand and mud layers may take place after an earthquake, but it takes a strong one to produce an island such as the island off Gwadar. The other possibility can be a rotational landslide, rather than a conical mud volcano, which moves along a rupture surface that is curved or concave. Further, the emission of methane gas is not an exception as the energy released by the seismic movement of these faults in MSZ activates inflammable gases in the seabed. The seabed near the Makran coast has vast deposits of gas hydrates, or frozen gas having large methane content. On the one hand, this event has released high seismic energy in NE-SW direction along the Chaman fault zone and MSZ, and on the other it has increased the tectonic stresses in the northern and SE directions, which may cause high seismicity in the near future. It is also worth noting that such a big event in the area has triggered many offshoots and splays of the larger faults (data to be presented separately). Thus the possibility of large earthquakes in the future, causing serious damage in the cities situated in the area cannot be excluded.

Cite as: MonaLisa, and Qasim Jan, M., 2014, Awaran, Pakistan, earthquake of Mw 7.7 in Makran Accretionary Zone, 24 September 2013: focal-mechanism solution and tectonic implications, in Montomoli C., et al., eds., proceedings for the 29th Himalaya-Karakoram-Tibet Workshop, Lucca, Italy.

Relations between the South Tibetan Detachment and leucogranite emplacement in Western Nepal: consequences for exhumation of the Greater Himalayan Sequence

Chiara Montomoli[1], Rodolfo Carosi[2], Dario Visonà[3], Salvatore Iaccarino[1], Antonio Langone[4]

[1] Dipartimento di Scienze della Terra, University of Pisa, Pisa, Italy, chiara.montomoli@unipi.it
[2] Dipartimento di Scienzedella Terra, University of Torino, Torino, Italy
[3] Dipartimento di Geoscienze, University of Padova, Padova, Italy
[4] Istituto di Geoscienze e Georisorse, CNR, Pavia, Italy

The South Tibetan Detachment System divides the lower rocks of the Greater Himalyan Sequence (GHS), deformed under medium to high-grade metamorphic conditions from the overlying medium-low-grade to non metamorphic rocks of the Tethyan Himalayan Sequence (THS). It show a complex architecture being characterized by a lower ductile shear zone, affecting the upper part of the GHS (Carosi et al., 1998) and the amphibolites facies rocks at the bottom of the THS (lower THS) and by an upper brittle fault, above which the very-low-grade to non metamorphic rocks of the THS (upper THS) crop out. According to most workers the High Himalayan granites (HHG), located in the upper part of the GHS, intrude and are deformed by the lower ductile shear zone of the STDS.

We report data from a geological transect located in Western Nepal where the STDS shows a peculiar structural setting.

In the study area the upper portion of the Greater Himalayan Sequence is made by gneiss, migmatites and calcsilicates.

The THS is characterized by a lower portion made by garnet and cordierite bearing gneisses. P-T pseudosection modelling, reveal as the observed assemblage is stable in the range of 0.53-0.65 GPa and 610-720°C.

The upper portion the THS is made by biotite-bearing quartzites, impure limestone, metarenites and subordinate metapelites with a metamorphic assemblage of calcite, quartz, muscovite, biotite ± chlorite and scapolite, indicating greenschist facies conditions. Detrital zircon ages indicate a depositional age from upper Jurassic to lower Cretaceous.

The boundary between the GHS and the THS is intruded by a large leucogranitic body showing a crystallization age at 23-24 Ma (Bertoldi et al., 2011; Carosi et al. 2013), constraining the time of youngest shearing event between the two tectonic units.

Dykes from the upper portion of the granite intrude the low-grade metamorphic rocks of the THS causing contact metamorphism within few meters from the granite contact. The low grade foliation in the THS is overgrown by biotite and muscovite. The intrusion closest samples show static crystallization of amphibole, clinopiroxene and annealing of calcite-plagioclase-quartz (± kfeldspar) matrix. On these samples, in order to quantify the depth of pluton emplacement, a set of geothermobarometric methods have been applied. A broad consistency of all the methods points out a T of equilibration around 600-640°C and a P of nearly 0.5 GPa.

Structural relations and time of emplacement of the leucogranite cast doubts on the exhumation models widely adopted till now for the Himalayan belt. According to Montomoli et al. (2013) the MCT in the study area has been active later than 18 Ma and as a consequence STD and MCT were active in different time precluding their contemporaneous activity and the tectonic models based on it.

References

Bertoldi, L., Massironi, M., Visonà, D., Carosi, R., Montomoli, C., Gubert, F., Naletto, G. and Pelizzo, M.G., 2011, Mapping the Buraburi granite in the Himalaya of Western Nepal: remote sensing analysis in a collisional belt with vegetation cover and extreme variation of topography, Remote Sensing of Environment ,115, 1129-1144.

Carosi, R., Lombardo, B., Molli, G., Musumeci, G. and Pertusati, P.C., 1998, The South Tibetan Detachment System in the Rongbuk valley, Everest region. Deformation features and geological implications, Journal of Asian Earth Sciences, 16, 299-31.

Carosi, R., Montomoli, C., Rubatto, D. and Visonà, D., 2013, Leucogranite intruding the South Tibetan Detachment in western Nepal: implications for exhumation models in the Himalayas, Terra Nova, 25, 478-489.

Cite as: Montomoli C. et al., 2014, Relations between the South Tibetan Detachment and leucogranite emplacement in Western Nepal: consequences for exhumation of the Greater Himalayan Sequence, in Montomoli C., et al., eds., proceddings for the 29th Himalaya-Karakoram-Tibet Workshop, Lucca, Italy.

Tectono-metamorphic discontinuities within the Greater Himalayan Sequence, a local or a regional feature?

Chiara Montomoli[1], Rodolfo Carosi[2], Salvatore Iaccarino[1]

[1] Dipartimento di Scienze della Terra, v. S. Maria, 53 56126 Pisa, Italy
[2] Dipartimento di Scienze della Terra, v. Valperga Caluso, 35 10125 Torino, Italy

The Greater Himalayan Sequence (GHS) has been considered as a coherent tectonic unit bounded by the South Tibetan Detachment and the Main Central Thrust. However thrusts within it have been recognized in several places and have been mainly interpreted as out of sequence thrusts (Mukherjee et al., 2012). Recent integrated studies allow to recognise several ductile shear zones in the core of the GHS along the belt, with top-to-the SW sense of shear (Higher Himalayan Discontinuity, HHD: Montomoli et al., 2013). U-Th-Pb in situ monazite ages provide ages older than the Main Central Thrust. HHD was active since 28-26 Ma (Montomoli et al., in press). Different P and T conditions have been often recorded in the hanging-wall and footwall of the HHD. Moreover the activity of the HHD since the Oligocene affected the metamorphic path of the GHS: when the hanging wall was exhumed the footwall continued to be buried reaching its peak conditions later than the hanging wall. Kinematics, P-T-t evolution and geochronology are the key tools to detect the occurrence of the HHD within the GHS along the Himalayan belt and several tectonic discontinuities have been recognized along the Himalayan belt from western Nepal to Bhutan, through Sikkim and Eastern and Central Nepal. Some discontinuities, such as the "Bhanuwa Thrust", the "Tama Kosi P-T-t-d discontinuity" and the "Hidden discontinuity 1" (Fig. 1) correspond in fact to the Main Central Thrust and are localized at the base of the GHS. The other discontinuities, localized within the GHS, divide the GHS into two portions an upper one (Upper Greater Himalayan Sequence- GHS_u) and a lower one (Lower Greater Himalayan Sequence- GHS_l (Fig. 1) (Montomoli et al., 2013).

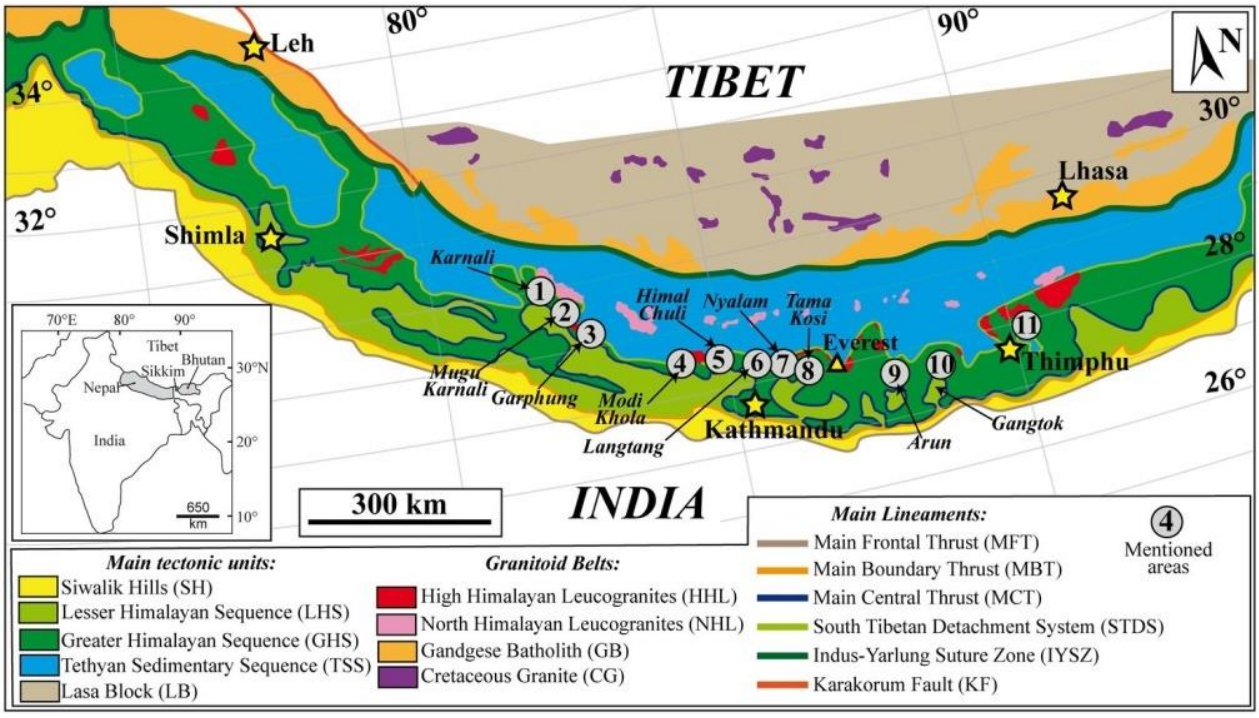

Figure 1. Schematic geological map of the Himalayan Belt. Numbered grey dots represent the location of the main tectonic and metamorphic discontinuities recognized along the belt: 1) Metamorphic discontinuity; Yakymchuk and Godin, 2012; 2) Mangri Shear Zone; Montomoli et al. 2013; 3) Tojiem Shear Zone; Carosi et al. 2010; 4) Bhanuwa and Sinuwa Thrusts; Corrie & Kohn, 2011; Martin et al. 2010; 5) Himal Chuli; Larson et al. 2010; 6) Langtang Thrust; Fraser et al. 2000; Harris and Massey 1994; Kohn 2008 and reference therein; 7) Tama Kosi; Larson et al.

2013; 8) High Himal Thrust; Goscombe et al. 2006 ; Imayama et al., 2012; Hidden Discontinuity 1, Hidden Discontinuity 2; Groppo et al. 2009; 9) Age Discontinuity; Rubatto et al., 2012; 10) Bhutan Discontinuity; Swapp & Hollister 1991. SH: Siwalik Hills- Sub-Himalayan Molasse; LHS: Lesser Himalayan Sequence; GHS: Greater Himalayan Sequence; TSS: Tethyan Sedimentary Sequence; LH: Lhasa Batholith; HHL: High Himalayan Leucogranite; NHG: North Himalayan Leucogranite; GB: Gandgese Batholith; CG: Cretaceous Granite; MFT: Main Frontal Thrust; MBT: Main Boundary Thrust; STDS: South Tibetan Detachment System; MCT: Main Central Thrust; IYSZ: Indus Yarlung Suture Zone; KT: Karakorum Fault).

The correlation of the HHD with other discontinuities recognized in the GHS led to propose that it is a tectonic feature running for several hundreds kilometers, documented at the regional scale with the following characteristics:

- it is a ductile shear zones showing a contractional top-to-the S and SW sense of shear;
- it divides the GHS in two portions; an upper GHS and a lower GHS;
- the upper GHS is made of sillimanite-kyanite bearing migmatites with a high-degree of melting;
- the HHD started its activity before the initiation of the MCT, at 28-26 Ma and continued up to 17 Ma;
- the HW and FW rocks attained peak metamorphic conditions in different times. The FW attained peak metamorphism later than the HW;
- the HW often registered lower P with respect to the FW;
- the HW underwent earlier exhumation, i.e. before MCT and STD activities.

The actual proposed models of exhumation based mainly on the MCT and STD activities are not able to explain the occurrence of the HHD. Any model of the tectonic evolution of the GHS should account for the occurrence of the HHD and its consequences on the tectonic and metamorphic path.

References

Carosi, R., Montomoli, C., Rubatto, D. and Visonà, D., 2010, Late Oligocene high-temperature shear zones in the core of the Higher Himalayan Crystallines (Lower Dolpo,Western Nepal), Tectonics, 29, TC4029. http://dx.doi.org/10.1029/2008TC002400.

Corrie, S.L. and Kohn, M.J., 2011, Metamorphic history of the Central Himalaya, Annapurna region, Nepal, and implication for tectonic models, Geological Society of American Bulletin, 123, 1863-1879.

Fraser, G., Worley, B. and Sandiford, M., 2000, High-precision geothermobarometry across the High Himalayan metamorphic sequences, Langtang valley, Nepal. Journal of Metamorphic Geology, 18, 665-685.

Goscombe, B., Gray, D. and Hand, M., 2006, Crustal architecture of the Himalayan metamorphi front in eastern Nepal, Gondwana Research, 10, 232–255.

Groppo, C., Rolfo, F. and Lombardo, B., 2009, P–T evolution across the Main Central Thrust Zone (Eastern Nepal): hidden discontinuities revealed by petrology, Journal of Petrology, 50, 1149-1180.

Harris, N. and Massey, J., 1994, Decompression and anatexis of Himalayan metapelites, Tectonics, 13, 1537-1546.

Imayama, T., Takeshite, T., Yi, K., Cho, D.-Y., Kitajima, K., et al., 2012, Two-stage partial melting and contrasting cooling history within the Higher Himalayan Crystalline Sequence in the far-eastern Nepal Himalaya, Lithos, 134-135, 1-22.

Kohn, M.J., 2008, P-T-t data from Nepal support critical taper and repudiate large channel flow of the Greater Himalayan Sequence, Geological Society of America Bulletin, 120, 259-273.

Larson, K.P., Godin, L. and Price, R.A., 2010, Relationships between displacement and distortion in orogens: linking the Himalayan foreland and hinterland in central Nepal, Geological Society of American Bulletin, 122, 1116-1134.

Larson, K.P., Gervais, F. and Kellett, D.A., 2013, A P–T–t–D discontinuity in east-central Nepal: Implications for the evolution of the Himalayan mid-crust, Lithos, 179, 275-292.

Montomoli, C., Carosi, R., and Iaccarino, S., 2013, Tectono-metamorphic discontinuities in the Greater Himalayan Sequence and their role in the exhumation of crystalline units. In: "Tectonics of Himalayas" (Editors: S. Mukherjie, R. Carosi, B. Mukherjie, D. Robinson, P. van Der Beck), Geol. Soc. London Special Publication, in press.

Montomoli, C., Iaccarino, S., Carosi, R., Langone, A. and Visonà, D., 2013, Tectonometamorphic discontinuities within the Greater Himalayan Sequence in Western Nepal (Central Himalaya): Insights on the exhumation of crystalline rocks, Tectonophysics, 608, 1349-1370.

Martin, A.J., Ganguly, J. and DeCelles, P.G., 2010, Metamorphism of Greater and Lesser Himalayan rocks exposed in the Modi Khola valley, central Nepal. Contributions to Mineralogy and Petrology, 159, 203-223.

Rubatto, D., Chakraborty, S. and Dasgupta, S., 2012, Timescale of crustal melting in the Higher Himalayan Crystallines (Sikkim, Eastern Himalaya) inferred from trace element-constrained monazite and zircon chronology, Contributions to Mineralogy and Petrology, 165, 349-372.

Swapp, S.M. and Hollister, S., 1991, Inverted metamorphism within the Tibetan slab of Bhutan: evidence for a tectonically transported heat sources, Canadian Mineralogist, 29, 1019-1041.

Yakymchuk, C.J.A. and Godin, L., 2012, Coupled role of deformation and metamorphism in the construction of inverted metamorphic sequences: an example from farnorthwest Nepal, Journal of Metamorphic Geology, 30, 513-535.

P-T-d path of chloritoid schist of the Tethyan Sedimentary Sequence (SE Tibet)

Chiara Montomoli[1], Salvatore Iaccarino[1] , Boria Antolin[2], Erwin Appel[2], Istvàn Dunkl[3], Lin Ding[4], Dario Visonà[5]

[1] Dipartimento di Scienze della Terra, University of Pisa, Pisa, Italy, chiara.montomoli@unipi.it
[2] University of Tübingen, Germany,
[3] University of Göttingen, Germany,
[4] Instititute of Tibetan Plateau Research, CAS, Beijing, China,
[5] Dipartimento di Geoscienze, University of Padova, Padova, Italy

The Tethyan Sedimentary Sequence (TSS) is characterized by a sequence spanning from Lower Paleozoic to Eocene deposited on the Indian passive margin. The TSS is bounded by the South Tibetan Detachment System (STDS) that puts it in contact with the lower Greater Himalayan Sequence, and by the upper Great Counter Thrust getting it in contact with the Lhasa batholit.

In SE Tibet the TSS is mainly represented by a Triassic flysch (Antolin et al., 2010) deformed under very-low to low-grade metamorphic conditions (Crouzet et al., 2007, Dunkl et al. 2011).

Most of the attention has been paid till now to the relations between the TSS and the STDS (Godin 2003; Carosi et al., 2207; Kellet and Godin, 2009) focusing on the relations between the development of several generations of folds and the activity of this important tectonic discontinuity.

In the study area two main deformation phases have been recognized both of them developed in a contractional tectonic setting. The first tectonic phase (D1) is related to the development of south-facing F1 fold with related axial plane foliation, while the D2 phase is associated to north verging F2 folds and backthrusts. The further tectonic evolution is characterized by the development of brittle-ductile shear zones often localized on the inverted limbs of F2 folds. Kinematic indicators are mainly represented by S-C structures and point to a top-to-the-north sense of movement.

During this work we focused on the early P-T-d evolution of Chloritoid bearing schist sampled SE of Lhasa (Gyatsa area), where a quite complex relationships between deformation and mineral growth has been observed.

Microstructural analyses led to recognize a much more complex structural framework for the D1 tectonic phase. The early development of S1 foliation (S1a), classified as a continous foliation, is associated to the recrystallization of white mica and chlorite, followed by the synkinematic growth of chloritoid, white mica and chlorite defining a spaced to continous foliation, S1b, interpretated as composite foliation during D1. Locally, decussate chloritoid, overgrowing S1b is also observed, testyfing a complex (continous) growth of this mineral from late S1a up to post S1b. Moreover, chloritoid grains are optically zoned, with an inclusion rich greenish core and pale-green rim.

The late foliation (S2) is a spaced foliation, where pressure solution is the main deformation mechanism, associated with locally passive rotation of micas grains.

A detailed SEM-EMPA mineral chemistry work has been done in order to quantify any chemical difference between grains in different position and any chloritoid zoning. SEM based chemical maps and EMPA profiles reveal how a core to rim increase of Mg, compensate by decrease of Fe and Mn, systematically present in chloritoid (XMg from 0.12 up to 0.17). Moreover, white mica shows a statistically change in composition as function of microstructural position, where S1a white micas have a lower Si^{4+} (3.02-3.07 a.p.f.u.) content respect to S1b white micas (3.09-3.15 Si^{4+} a.p.f.u.).

Cite as: Montomoli et al., 2014, P-T-d path of chloritoid schist of the Tethyan Sedimentary Sequence (SE Tibet), in Montomoli C., et al., eds., proceedings for the 29th Himalaya-Karakoram-Tibet Workshop, Lucca, Italy.

A P-T pseudosection in the MnO-Na_2O-CaO-K_2O-FeO-MgO-Al_2O_3-SiO_2-H_2O-TiO_2 model chemical system, constructed with the software Perple_X (Connolly, 1990), shows how the P-T condition of S1a equilibration is close to 0.45-0.50 GPa / 400-425 °C, while the P-T condition of S1b developing is around 0.75-0.80 GPa / 500-530 °C. Virtually the same temperature of 510-540 °C have been obtained with the empirical chloritoid-chlorite Fe-Mg exchange thermometer of Vidal et al., (1999) for the chloritoid rim, while the lack of suitable chlorite grains in the core of the chloritoid prevents the application of this thermometer for the chloritoid core.

These observations suggest an increase of P as well as T (buring) during the D1 tectonic event.

References

Antolín, B., Appel, A., Montomoli, C., Dunkl, I., Ding, L., Gloaguen, R., El Bay, R., 2011, Kinematic evolution of the eastern Tethyan Himalaya: Constraints from magnetic fabric and structural properties of the Triassic flysch in SE Tibet. In: J. Poblet and R. Lisle, Editors, Kinematic Evolution and Structural Styles of Fold-and-Thrust Belts, Geological Society of London Special Publications, 349, 99-121 DOI 10.1144/SP349.6

Carosi, R., Montomoli, C. and Visonà, D., 2007, A structural transect in the Lower Dolpo: insights on the tectonic evolution of Western Nepal, Journal of Asian Earth Sciences, 29, 407-423.

Connolly, J.A.D., 1990, Multivariable phase diagrams: an algorithm based on generalized thermodynamics, American Journal of Science, 290, 666-718.

Crouzet, C., Dunkl, I., Paudel, L., Arkai, P., Rainer, T. M., Balogh, K. and Appel, E., 2007, Temperature and age constraints on the metamorphism of the Tethyan Himalaya in Central Nepal: a multidisciplinary approach, Journal of Asian Earth Sciences, 30, 113-130.

Dunkl, I., Antolín, B., Wemmer, K., Rantitsch, G., Kienast, M., Montomoli, C., Ding, L., Carosi, R., Appel, E., El Bay, R., Xu, Q. and von Eynatten, H., 2011, Metamorphic evolution of the Tethyan Himalayan flysch in SE Tibet, In: R. Gloaguen and L. Ratschbacher, Editors, Growth and Collapse of the Tibetan Plateau, Geological Society of London Special Publications, 353, 45-69. DOI: 10.1144/SP353.

Godin, L., 2003, Structural evolution of the Tethyan sedimentary sequence in the Annapurna area, central Nepal Himalaya, Journal of Asian Earth Science, 22, 307-328.

Kellet, D.A. and Godin, L., 2009, Pre-Miocene deformation of the Himalayan superstructure, Hidden valley, central Nepal. Journal of the Geological Society, London, 166, 1-14, doi: 10.1144/0016-76492008.

Vidal, O., Goffé, B., Bousquet, R. and Parra, T., 1999, Calibration and testing of an empirical chloritoid-chlorite Mg-Fe exchange thermometer and thermodynamic data for daphnite, Journal of Metamorphic Geology, 17, 25-39.

Geological map of the Eastern Nepal Himalaya

Pietro Mosca[1], Chiara Groppo[2], Franco Rolfo[1,2]

[1]Institute of Geosciences and Earth Resources – CNR, Torino, Italy, p.mosca@csgt.to.cnr.it
[2] Department of Earth Sciences, University of Torino, Italy

We present a geological map of a sector of the Himalaya in Eastern Nepal, from the Rolwaling Himal to the border with Sikkim. The map has been drawn on the basis of original geological mapping, structural and petrological investigations along several cross sections, variably integrated with published data. According to the major subdivision proposed for the Himalaya, the geological setting of the Eastern Nepal Himalaya is characterized by a few major lithotectonic units striking E-W and separated by tectonic contacts, north-dipping at a regional scale. From lower to upper structural levels (and from south to north) these are the sub-Himalaya, the metamorphic Lesser Himalayan Sequence (LHS) and Greater Himalaya sequence (GHS), and the Tibetan Sedimentary Series.

The LHS typically consists of grey to pale-green fine-grained quartz-sericite schists, slates and phyllites, showing m-scale intercalations of either massive quartzites (±Grt ±Ctd) and chlorite-sericite schists. Graphite-rich schists occur mainly in the lower structural levels. Cm-scale intercalations of garnet-amphibole quartzites are also observed. In the upper structural levels, peculiar two micas augen-gneiss occurs, marking an abrupt change in lithology. The augen-gneiss contains metric to plurimetric layers of Phl- ± Ky-bearing phyllonite and chloritoschist, likely representing the product of a metasomatic transformation of the granitic protolith along shear zones.

The overlying GHS has been subdivided in two different domains considering lithological, structural and metamorphic criteria.

The lower domain (GHS-L) consists of two micas + Grt (± St, ± Ky) coarse-grained micaschist and gneiss. These rocks are associated to metric to decametric thick levels of two-micas quartzitic gneiss, Grt + Zo granofels and small lenses of impure marbles (± Phl, ± Wm). Locally, they host intercalations of phyllitic Ank-bearing micaschist (+ greenish Bt). Moving toward their uppermost levels, the GHS-L consists of Bt (± Grt, ± Sil) gneiss showing local evidence of partial melting and a pervasive growth of late Wm flakes.

The upper domain of the GHS (GHS-U) partially corresponds to the High Himalayan Crytallines of various authors and consists mainly of Grt + Bt + Kfs + Ky/Sil anatectic paragneiss, reported as Barun Gneiss by Lombardo et al. (1993). In its central and upper portions, the Barun Gneiss is associated with a fine-grained Kfs + Bt + Sil ± Grt paragneiss (reported as Black Gneiss by Lombardo et al., 1993), showing Sil + Qtz nodules up to few cm in size. Up section, the GHS-U anatectic paragneisses are characterized by Crd-bearing assemblages and record a progressive decrease of peak-pressure conditions upward. The GHS-U contains also large bodies of Bt ± Sil ± Grt anatectic augen-gneiss, whose occurrence significantly increases toward the upper structural levels. Metric to plurimetric thick layers of calc-silicate granofels and impure marbles (Di + Pl + Qtz ± Kfs ± Scp) are also widespread. Large bodies of leucogranites and a network of pegmatitic dikes are notably intruded in the middle-upper levels of the GHS-U.

The Main Central Thrust zone, notably one of the major features of the Himalaya system, is here indentified as a km-thick highly sheared zone involving rocks of the upper LHS and the lower GHS-L. Across this zone, structural observations integrated with petrography, mineral chemistry, and petrologic modeling revealed the juxtaposition of rock packages characterized by different P-T evolution and T/depth gradients. A similar setting suggests an imbricate nature of the MCTZ, thus emphasizing the complexity of tectonic processes operating during the exhumation of the metamorphic units in the Himalaya.

The graphical editing of the geological map is also supported by suitable databases where all the represented geological features (i.e. geological units, boundaries, foliations, samples, …) are stored and harmonized using standard criteria in order to describe their typology and quality.

References

Lombardo,B., Pertusati, P. and Borghi, A.,1993, Geology and tectono-magmatic evolution of the eastern Himalaya along the Chomolungma-Makalu transect. In: (Eds) Treloar P.J. and Searle M.P., Himalayan Tectonics. Geological Society of London, Special Publication, 74, 341–355.

Cite as: Mosca, P., Groppo, C. and Rolfo, F., 2014, Geological map of the Eastern Nepal Himalaya, in Montomoli C., et al., eds., Proceedings for the 29th Himalayan-Karakoram-Tibet Workshop, Lucca, Italy

Two-stage Petrogenetic Evolution of the Miocene Higher Himalayan Leucogranite from Migmatites

P.K. Mukherjee[1], A.K. Jain[2], Saptarishi Ghosh[3], Preety Singh[4]

[1] Wadia Institute of Himalayan Geology, 33 GMS Road, Dehradun,India, mukherjee_pk@wihg.res.in
[2] CSIR-Central Building Research Institute, Roorkee, India
[3] Department of Earth Sciences,Indian Institute of Technology, Roorkee, India
[4] Department of Geology & Geophysics, Indian Institute of Technology, Kharagpur, India

The metamorphic core of the Higher Himalayan Crystalline (HHC) is characterized by extensive migmatites with varying degree of in situ melting and leucogranite dykes. The Miocene leucogranite magmatism in the HHC is generally linked to these migmatites. In this study, various components of migmatites from two contrasting protoliths, i.e. an orthogneissic migmatite from Bhutan and paragneissic migmatite from Dhauliganga section in Garhwal (western Himalaya) have been investigated to understand the petrogenesis of derivation of leucogranite magmatism from the HHC migmatites. In Bhutan, migmatite is developed on the western flank of the Kuri Chu half-window, a few kilometres up the section of the HHC, while the Dhauliganga section in Garhwal exposes the migmatite in the upper parts of the HHC near the South Tibetan Detachment System (STDS).

The leucosomes are characteristically enriched in Sr but depleted in Rb compared to the mesosome protolith while opposite is true in case of melanosome residue. Compatible behavior of Sr and incompatible of behavior Rb suggest Kf in the residue in preference to plagioclase which diminished into melt. Though the protolith has ubiquitous negative anomaly but a significant positive Eu anomaly is observed in leucosome with melanosome illustrating enhanced Eu negative anomaly compared to the protolith. These features together with the major elemental composition of leucosome suggest preferential plagioclase melting in preference to K-feldspar. These characteristics are observed in both, orthogneissic migmatites as well as in paragneissic migmatites alike.

Consistent with the textural and petrographical observation following fluid saturated melting reaction can be suggested for the para-gneissic migmatite:

Ms + Pl + Qtz = Melt + Kfs + Sil + Bt

However, in case of orthogneisses, melting reaction may be related to ternary eutectic melting or melting starting from eutectic and the residual solid composition moves on K-feldspar-quartz join through consumption plagioclase into melt phase.

Trace elemental modelling using batch melting model suggest very high degree of partial melting (>70%) for both type of protoliths. This is also consistent with (i) relative proportions of melanosome (restite) and leucosome (melt) observed in field as well as macro-scale specimens, and (ii) proximity of major and trace elemental abundances of the leucosome and mesosome or protolith gneiss with melanosome fraction plot far away in the tie-line (Figure 1).

However, temperature estimates of melting are within a range of about 650 - 750^{0}C. At this moderate temperature range, such high degree of melting is possible only in presence of plentiful fluids. It is therefore inferred that the fluid requirement was met externally possibly from the dehydration of metasedimentary rocks.

The leucosome composition is markedly differing from the compositions of leucogranite plutons in the HHC. However, the leucogranite compositions show a linear trend emanating from the field of leucosome compositions (Figure 2). This would mean that the leucogranite magma was derived from the pristine

Cite as: Mukherjee, P.K., et al., 2014, Two-stage Petrogenetic Evolution of the Miocene Higher Himalayan Leucogranite from Migmatites, in Montomoli C., et al., eds., proceedings for the 29th Himalaya-Karakoram-Tibet Workshop, Lucca, Italy.

melt (leucosome) through AFC processes. And this trend being parallel to plagioclase fractionation, it is possible that plagioclase fractionation (~30-40%) would be required to derive most of the leucogranite plutons in the HHC (fig.2). It is also important to note that leucosome compositions with lower degree of melting of paragneiss probably did not yield leucogranite magma through segregation and migration.

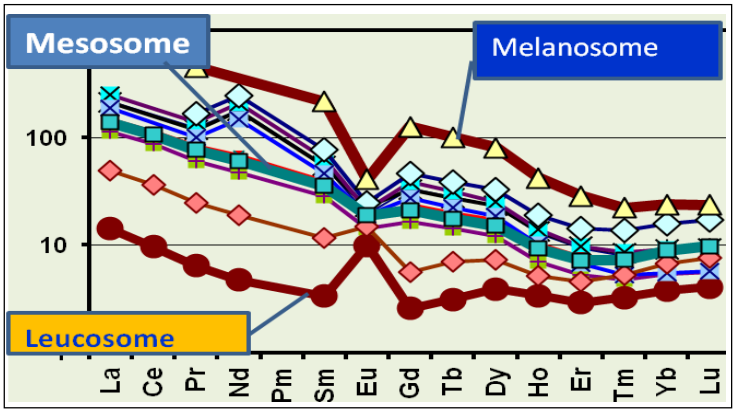

Figure 1. Normalized REE pattern of three components of paragneissic migmatite. Leucosome is strongly depleted in REE with a prominent positive Eu anomaly while melanosome is equally enriched with a negative anomaly; producing a mirror image across the mesosome protolith composition. Other plots are migmatites with variable amounts of mixture of these three components.

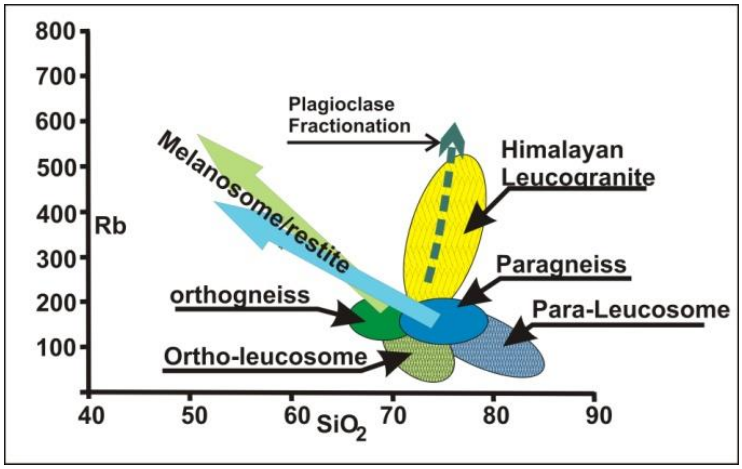

Figure 2. Representative compositional plot of migmatite showing mutual relationships of mesosome protolith, leucosome melt and melanosome residue for both ortho- and paragneissic source migmatites. The average of various HHC leucogranites plot along a trend parallel to a plagioclase fractionation line suggesting derivation of leucogranite through fractionation of calcic-plagioclase during ascent of the accumulated melt. The HHC leucogranite average compositions are taken from various sources.

The above results lead us to conclude that both types of migmatites derived from ortho- and para-gneisses are equally potential source for leucogranite melt generation. High degree of melting involved externally-sourced plentiful fluid flux from dehydration of subducting metasediments of northward moving Indian plate. Partial melting was promoted by external fluid flux and not by dehydration of biotite as it occurs as dominant residual phase. Plagioclase played a dominant role both as melting phase as well as fractionating phase that fashioned a two-stage development of the Miocene Himalayan leucogranite magmatism in the upper parts of the HHC.

What collided with India at 50 Ma in the western (Ladakh) Himalaya?

Yani Najman[1], Dan Jenks[1], Laurent Godin[2], Marcelle Boudagher-Fadel[3], Paul Bown[3], Matt Horstwood[4], Eduardo Garzanti[5], Laura Bracciali[1&4], Ian Millar[4]

[1] LEC, Lancaster University, Lancaster, LA1 4YQ, UK. y.najman@lancs.ac.uk
[2] Dept of Geology, Queens University, Canada
[3]Dept of Geology, UCL, London, UK
[4] NIGL, BGS-Keyworth, Nottingham, UK.
[5] Dept of Geology, University of Milano-Bicocca, Milan, Italy

The timing of India-Asia collision is critical to the understanding of crustal deformation processes, since, for example, it impacts on calculations regarding the amount of convergence that needs to be accommodated by various mechanisms. In the NW Himalaya, a number of workers have proposed a ca 55-50 Ma age for collision along the Indus suture zone which separates India from the Kohistan-Ladakh Intraoceanic Island arc (KLA) to the north. This is based on a number of factors including the age of youngest marine sediments in the Indus suture (e.g. Green et al. 2008), age of eclogites indicative of onset of Indian continental subduction (e.g. de Sigoyer et al. 2000), and first evidence of detritus from north of the suture zone deposited on the Indian plate (e.g. Clift et al. 2002). Such evidence can be interpreted as documenting the age of India-Asia collision if one takes the KLA to have collided with the Asian plate prior to its collision with India (e.g. Petterson 2010 and refs therein). However, an increasing number of workers propose that the KLA collided with Asia subsequent to its earlier collision with India, dated variously at 85 Ma (Chatterjee et al. 2013), 61 Ma (Khan et al. 2009) and 50 Ma (Bouilhol et al. 2013). This, plus the questioning of earlier provenance work (Clift et al. 2002) regarding the validity of that data for constraining the timing of material north of the suture arriving on the Indian plate (Henderson et al. 2011) suggests that the time is right for a reappraisal of this topic. We use a provenance-based approach here, using combined U-Pb and Hf on detrital zircons, along with petrography and biostratigraphy, to identify first arrival of material from north of the Indian plate to arrive on the Indian continent, to constrain the time of collision. With the recent discovery that the Indus Group sediments in the suture zone cannot be used for this purpose as previously proposed (Henderson et al. 2011) we turn to the 50 Ma Kong and Chulung La Formation youngest Tethyan sediments on the Indian margin (Garzanti et al. 1987) to investigate whether we can identify such material, and whether it be Spong arc (Fuchs and Willems 1990), KLA or Trans-Himalayan derived, thus determining what collided with India at 50 Ma.

References

Bouilhol, P., Jagoutz, O., Hanchar, J.M. and Dudas, F.O., 2013, Dating the India-Eurasia collision through arc magmatic records. Earth and Planetary Science Letters, 366, 163-175.

Chatterjee S., Goswami A. and Scotese C.R., 2013, The longest voyage: Tectonic, magmatic, and paleoclimatic evolution of the Indian plate during its northward flight from Gondwana to Asia, Gondwana Research, 23, 238-267.

Clift, P., Carter, A., Krol, M. and Kirby, E., 2002, Constraints on India-Eurasia collision in the Arabian sea region taken from the Indus Group, Ladakh Himalaya, India. The tectonic and climatic evolution of the Arabian Sea region Geological Society of London Special Publication, 195, 97-116.

de Sigoyer, J., Chavagnac, V., Blichert-Toft J., Villa I.M., Luais B., Guillot S., Cosca M. and Mascle G., 2000, Dating the Indian continental subduction and collisional thickening in the northwest Himalaya: Multichronology of the Tso Morari eclogites, Geology, 28, 487-490.

Fuchs, G. and Willems, H., 1990, The final stages of sedimentation in the Tethyan zone of Zanskar and their geodynamic significance (Ladakh - Himalaya), Jahrbuche Geologische Bundenstalt, 133: 259-273.

Garzanti, E., Baud, A. and Mascle, G., 1987, Sedimentary Record of the Northward Flight of India and Its Collision with Eurasia (Ladakh Himalaya, India), Geodinamica Acta 1, 297-312.

Green, O.R., Searle, M.P., Corfield, R.I. and Corfield, R.M., 2008, Cretaceous-tertiary carbonate platform evolution and the age of the India-Asia collision along the Ladakh Himalaya (northwest India), J Geol, 116, 331-353.

Henderson, A,L,, Najman, Y, Parrish, R., Mark, D. and Foster, G.L, 2011, Constraints to the timing of India–Eurasia collision; a re-evaluation of evidence from the Indus Basin sedimentary rocks of the Indus–Tsangpo Suture Zone, Ladakh, India, Earth Science Reviews, 106, 265-292.

Khan, S.D., Walker, D.J., Hall, S.A., Burke, K.C., Shah, M.T. and Stockli, L., 2009, Did the Kohistan-Ladakh island arc collide first with India? Geological Society of America Bulletin, 121, 366-384.

Petterson, M.G., 2010, A review of the geology and tectonics of the Kohistan island arc, north Pakistan. in The Evolving Continents: Understanding Processes of Continetnal Growth (eds. TM Kusky, M-G Zhai, W Xiao), pp. 287-327. Journal of the Geological society of London Special publication.

Cite as: Najman, et al., 2014, What collided with India at 50 Ma in the Western Himalaya, Ladakh? in Montomoli C., et al., eds., proceedings for the 29th Himalaya-Karakoram-Tibet Workshop, Lucca, Italy.

Thermodynamic phase equilibria modelling of retrograde amphibole and clinozoisite in mafic eclogite from the Tso Morari massif, northwest India: Insights into the source and behavior of metamorphic fluid during exhumation

Richard M. Palin[1,2], Marc R. St-Onge[3], David J. Waters[1], Michael P. Searle[1], Brendan Dyck[1]

[1] Department of Earth Sciences, University of Oxford, South Parks Road, Oxford, OX1 3AN, United Kingdom
[2] Now at Institute of Geoscience, University of Mainz, D-55128 Mainz, Germany, richardmpalin@gmail.com
[3] Geological Survey of Canada, 601 Booth Street, Ottawa, Ontario, K1A 0E8, Canada

Retrograde epidote and/or clinozoisite poikiloblasts associated with compositionally zoned amphibole—the latter typically containing a substantial sodic component—are common in exhumed (ultra)high pressure – (U)HP – mafic eclogite (e.g., Massonne, 2012 and references therein). This mineral pairing is present in many subduction-related (U)HP terranes that form during continental collision and can be used to provide valuable constraints on the geodynamic/physico-chemical conditions experienced by (U)HP eclogite during the subduction–exhumation cycle (Palin et al., 2014; Waters et al., 2014).

In this work, we present the results of detailed thermodynamic phase equilibria modelling of such amphibole–clinozoisite-bearing post-peak metamorphic mineral assemblages in (U)HP mafic eclogite from the Tso Morari massif, Ladakh Himalaya, northwest India. These data have provided new insight into the behavior and source of metamorphic fluid during exhumation and constrained the P–T conditions of hydration. Serial P–M(H_2O) pseudosections constructed in the Na_2O–CaO–K_2O–FeO–MgO–Al_2O_3–SiO_2–H_2O–TiO_2–O (NCKFMASHTO) compositional system show that a number of petrographically distinct hydration episodes most likely occurred during exhumation from peak P–T conditions (~640 °C, 27–28 kbar; St-Onge et al., 2013). Initial hydration of a peak assemblage dominated by garnet and omphacite is interpreted to have occurred as a result of the destabilization of talc following isothermal decompression to P ~23 kbar, which led to the formation of barroisite–winchite amphibole core domains. A subsequent externally-sourced episode of hydration at P ~19 kbar, with or without syn-decompressional cooling to ~560 °C, resulted in additional barroisitic–winchitic amphibole growth, followed by the formation of clinozoisite poikiloblasts. Continued buoyancy-driven exhumation to the base of the lower crust is constrained to have taken place with no additional fluid input. A final hydration event, characterized by the formation of magnesiohornblende rims on the barroisite–winchite cores, was associated with later prograde overprinting in the middle crust during the final stages of exhumation. Significantly, the vast majority of externally sourced H_2O, comprising just over half of the current bulk rock fluid content, was added during this final hydration event. In a middle crustal setting, this fluid infiltration is interpreted to have occurred due to devolatilization reactions occurring in migmatitic host orthogneiss and/or metasedimentary units, or following the crystallization of partial melt.

References

Massonne, H.-J., 2012, Formation of amphibole and clinozoisite-epidote in eclogite owing to fluid infiltration during exhumation in a subduction channel, J. Petrol., 53, 1969–1998, doi:10.1093/petrology/egs040.

Palin, R.M., St-Onge, M.R., Waters, D.J., Searle, M.P. and Dyck, B., 2014, Phase equilibria modelling of retrograde amphibole and clinozoisite in mafic eclogite from the Tso Morari massif, northwest India: constraining the *P*–*T*–M(H_2O) conditions of exhumation, J. Metamorph. Geol. (in press), doi:10.1111/jmg.12085.

St-Onge, M.R., Rayner, N., Palin, R.M., Searle, M.P. and Waters, D.J., 2013, Integrated pressure–temperature–time constraints for the Tso Morari dome (NW India): Implications for the burial and exhumation path of UHP units in the western Himalaya, J. Metamorph. Geol., 31, 469–504, doi:10.1111/jmg.12030.

Waters, D.J., Airaghi, L. and Czertowicz, T., 2014, Amphibole equilibria as monitors of P–T path and process in the exhumation of HP/UHP terranes, EGU General Assembly 2014, Geophysical Research Abstracts, 16, EGU2014-5045.

Cite as: Palin, R. M., St-Onge M. R., Waters D. J., Searle M. P. and Dyck B., 2014, Thermodynamic phase equilibria modelling of retrograde amphibole and clinozoisite in mafic eclogite from the Tso Morari massif, northwest India: Insights into the source and behavior of metamorphic fluid during exhumation, in Montomoli C., et al., eds., proceedings for the 29th Himalaya-Karakoram-Tibet Workshop, Lucca, Italy.

Kinematic evolution of the Greater Himalayan Sequence, Annapurna-Dhaulagiri Himalaya, central Nepal

Andrew J. Parsons[1], Richard J. Phillips[1], Geoffrey E. Lloyd[1], Michael P. Searle[2], Richard D. Law[3]

[1] School of Earth & Environment, University of Leeds, Leeds, LS2 9JT, UK. eeap@leeds.ac.uk
[2] Department of Earth Sciences, University of Oxford, Oxford, OX1 3PR, UK.
[3] Department of Geosciences, Virginia Polytechnic Institute and State University Tech, Blacksburg, VA, 24061, USA.

The channel flow model for the Himalayan orogen suggests that the Greater Himalaya Sequence (GHS) represents a partially molten, rheologically weak, mid-crustal channel, bound above and below by rigid continental crust (Beaumont et al., 2001). Extrusion and exhumation of the channel requires coeval ductile shearing on the underlying, reverse-sense, Main Central Thrust Zone (MCTZ) and the overlying, normal-sense, South Tibetan Detachment System (STDS) (see Godin et al., 2006 for a review). The vertical distribution of strain across the GHS is one aspect of the channel flow model that has yet to be investigated. Here, we present the first quantified vertical strain profile for the GHS produced from crystallographic preferred orientation (CPO) measurements of rocks collected through the Annapurna-Dhaulagiri Himalaya, central Nepal. By combining this data with observed macro- and microstructural deformation fabrics identified in the field and in thin sections, we reveal the kinematic evolution of the GHS. Results suggest that the GHS in this area was not rheologically weak enough to sustain mid-crustal channel flow and cooled prematurely to form a rigid 'channel plug'. Consequently, the increased rheological strength of the GHS later resulted in post-peak metamorphic reverse-sense shearing on the STDS. These interpretations highlight the importance of melt distribution and rheology as controls on crustal scale deformation during orogenesis.

With increasing strain, the degree of alignment of minerals, and thus CPO strength, in a rock also increases. As such, CPO strength in deformed rocks provides a proxy for relative strain magnitude (e.g. Bunge & Morris, 1982). CPOs are measured via electron back scattered diffraction (EBSD), from samples collected along a N-S transect through the Kali Gandaki Valley, in the Annapurna-Dhaulagiri Himalaya of central Nepal. Intensity, I (Lisle, 1985) which is used to describe the strength of each CPO fabric is calculated for each sample and stratigraphically arranged into a single plot to produce the first quantified relative strain magnitude profile for the GHS and bounding units. Additionally, deformation temperatures are estimated from microstructures and accompanying metamorphic mineral assemblages in thin sections (e.g. Stipp et al., 2002), and from identification of the active crystal slip-systems in CPO fabrics (e.g. Lister et al., 1978). Combining deformation temperature estimates with the quantified strain profile reveals the thermo-tectonic evolution of the GHS in the Annapurna-Dhaulagiri Himalaya and provides a unique data set to test the validity of the channel flow model for the GHS in this region.

Along the strain profile, variations in I show that relative strain magnitudes are greatest in the bounding shear zones above and below the amphibolite facies mid-crustal rocks of the Upper GHS.
These high strain zones correspond to the MCTZ and STDS. Within these shear zones, I decreases incrementally, away from the Upper GHS towards the over- and underlying tectonic units of the Tethyan Himalayan Sequence (THS) and Lesser Himalayan Sequence (LHS). Deformation microstructures and metamorphic mineral assemblages in these shear zones also indicate a gradual decrease in estimated deformation temperatures from ~500°C to ~300 °C away from the Upper GHS. In both the THS and LHS, relative strain magnitudes and estimated deformation temperatures are low (<300-400 °C). Notably, within the amphibolite facies mid-crustal rocks of the Upper GHS, estimated deformation temperatures are high (~600-700 °C), however, shear fabrics are rarely observed and CPO intensity is low. This suggests that these rocks have undergone little deformation whilst at the conditions suitable for mid-crustal flow. Furthermore, evidence of sillimanite grade retrogression and extensive annatexis and leucogranite production, which is commonly observed in the GHS elsewhere in Nepal (e.g., Everest

Cite as: Parsons, A. J., Phillips R. J., Lloyd, G. E., Searle, M. P. and Law R. D., 2014, Kinematic evolution of the Greater Himalayan Sequence, Annapurna-Dhaulagiri Himalaya, central Nepal, in Montomoli C., et al., eds., proceedings for the 29th Himalaya-Karakoram-Tibet Workshop, Lucca, Italy.

region - Searle et al., 2003; Makalu region - Streule et al., 2010; Manaslu region - Larson et al., 2011), also appears to be absent or severely lacking in the Annapurna-Dhaulagiri Himalaya.

Synthesis of these results suggests that the GHS exposed in the Kali Gandaki Valley may not have been rheologically weak enough to sustain mid-crustal channel flow (c.f. Beaumont et al., 2001). It is proposed that premature cooling of the GHS below sub-solidus temperatures effectively froze the GHS to produce a rigid channel 'plug', preventing significant mid-crustal flow. This was subsequently followed by post-peak metamorphic reverse-sense shearing on the STDS, possibly due to the increase in strength gained by the GHS during its cooling. These observations and interpretations provide an insight into the mid-crustal processes that occur during continental collision and imply that the channel flow model cannot sufficiently explain kinematic evolution of the GHS in the Annapurna-Dhaulagiri Himalaya. Significantly, these results demonstrate that crustal melting and rheology play an important role during the kinematic development of orogenic belts.

References

Beaumont, C., Jamieson, R. A., Nguyen, M. H. and Lee, B., 2001, Himalayan tectonics explained by extrusion of a low-viscosity crustal channel coupled to focused surface denudation. Nature, 414, 738-742.

Bunge, H. J. and Morris, P. R. 1982, Texture analysis in materials science: mathematical methods, Butterworths, London, 593 pp.

Godin, L., Grujic, D., Law, R. D.and Searle, M. P., 2006, Channel flow, ductile extrusion and exhumation in continental collision zones: an introduction. In: Law, R. D., Searle, M. P. Godin, L. (eds.) Channel Flow, Ductile Extrusion and Exhumation in Continental Collision Zones.The Geological Society, London, 268, 1-23.

Larson, K. P., Cottle, J. M. and Godin, L. 2011, Petrochronologic record of metamorphism and melting in the upper Greater Himalayan sequence, Manaslu–Himal Chuli Himalaya, west-central Nepal. Lithosphere, 3, 379-392.

Lisle, R. J., 1985, The Use of the Orientation Tensor for the Description and Statistical Testing of Fabrics. Journal of Structural Geology, 7, 115-117.

Lister, G. S., Paterson, M. S. and Hobbs, B. E., 1978,The simulation of fabric development in plastic deformation and its application to quartzite: The model. Tectonophysics, 45, 107-158.

Searle, M. P., Simpson, R. L., Law, R. D., Parrish, R. R. and Waters, D. J., 2003, The structural geometry, metamorphic and magmatic evolution of the Everest massif, High Himalaya of Nepal-South Tibet. Journal of the Geological Society, 160, 345-366.

Stipp, M., Stunitz, H., Heilbronner, R. and Schmid, S. M., 2002, The eastern Tonale fault zone: a 'natural laboratory' for crystal plastic deformation of quartz over a temperature range from 250 to 700 degrees C. Journal of Structural Geology, 24, 1861-1884.

Streule, M. J., Searle, M. P., Waters, D. J. and Horstwood, M. S. A., 2010, Metamorphism, melting, and channel flow in the Greater Himalayan Sequence and Makalu leucogranite: Constraints from thermobarometry, metamorphic modeling, and U-Pb geochronology. Tectonics, 29, TC5011.

Quantified vertical strain profile through the Greater Himalayan Sequence, Annapurna-Dhaulagiri Himalaya, central Nepal

Andrew J. Parsons[1], Richard J. Phillips[1], Geoffrey E. Lloyd[1], Michael P. Searle[2], Richard D. Law[3]

[1] School of Earth & Environment, University of Leeds, Leeds, LS2 9JT, UK. eeap@leeds.ac.uk
[2] Department of Earth Sciences, University of Oxford, Oxford, OX1 3PR, UK.
[3] Department of Geosciences, Virginia Polytechnic Institute and State University Tech, Blacksburg, VA, 24061, USA.

Determining the kinematic evolution of the Greater Himalayan Sequence (GHS), which forms the metamorphic core of the Himalayan orogen, represents the central focus of all models of Himalayan orogenesis (e.g. Beaumont et al., 2001; Webb et al., 2007; Faccenda et al., 2008). Whilst much is known about the geothermobarometric evolution of the GHS, the spatial and temporal distribution of strain within the GHS is less well understood. This is largely due to the difficulty of finding reliable strain markers within high grade metamorphic rocks, as they are often overprinted during late stage static recrystallisation. Here, we present the first quantified vertical strain profile for the GHS derived from crystallographic preferred orientation (CPO) data from samples collected in the Annapurna-Dhaulagiri Himalaya of central Nepal. We explore interpretations of this profile and their implications for models of Himalayan orogenesis, and also look at the wider implications for our understanding of crustal scale deformation within continental collision zones. We further assess the strengths and weaknesses of this approach and its applicability to other settings.

CPO describes the degree of crystal alignment of a selected mineral in a rock with respect to an external reference frame such as sample or geographic coordinates. With increased crystal plastic strain, the degree of mineral alignment, and thus CPO strength, increases. As such, CPO strength in deformed rocks provides a proxy for relative strain magnitude (e.g. Bunge & Morris, 1982). An advantage to this approach is that deformation-related CPOs can be resilient to late-stage static recrystallisation, a process commonly observed in deformed rocks that can overprint and remove geometric strain markers such as shape preferred orientations. Here, we use electron back scattered diffraction (EBSD) to measure CPOs of bulk mineral assemblages in samples collected along a N-S transect through the Kali Gandaki Valley and neighbouring foothills, in the Annapurna-Dhaulagiri Himalaya. We use the Intensity parameter, *I* (Lisle, 1985), calculated from the eigenvalues of the orientation distribution functions used to define each CPO to quantify CPO fabric strength. Whilst there are numerous parameters available to describe CPO strength (e.g. *strength parameter, c*, Woodcock, 1977; *J-index*, Bunge & Morris, 1982; *PGR index*, Vollmer, 1990; *misorientaion index*, Skemer et al., 2005) we graphically demonstrate that the intensity parameter, I is the most suitable parameter to use as a proxy for relative strain magnitude. By plotting values of I against the relative structural/stratigraphic height of the samples from which they are derived, we have produced the first vertical strain profile for the whole of the GHS and bounding units that shows changes in relative strain magnitudes across the sample transect. Furthermore, as *I* is calculated from the *c*-axis CPOs of all major mineral phases (quartz, calcite, dolomite, mica and feldspar) we may also explore how deformation partitions into specific mineral phases in different polymineralic rocks.

Along the strain profile, variations in I demonstrate that relative strain magnitudes are greatest in the bounding shear zones above and below the GHS. These high strain zones correspond to the reverse-sense Main Central Thrust Zone (MCTZ) at the base of the GHS and the normal-sense South Tibetan Detachment (STDS) at the top of the GHS. Within these shear zones, I decreases incrementally, away from the GHS towards the over- and underlying tectonic units of the Tethyan Himalayan Sequence (THS) and Lesser Himalayan Sequence (LHS), respectively. Pairing CPO data with deformation temperatures derived from deformation microstructures and metamorphic mineral assemblages (e.g. Stipp et al., 2002) shows how deformation migrated outwards away from the GHS as it cooled during extrusion/exhumation. Within the amphibolite facies rocks of the GHS, I is low and shear fabrics are rarely seen, whilst

Cite as: Parsons, A. J., Phillips, R. J., Lloyd, G. E., Searle, M. P. and Law, R. D., 2014, Quantified vertical strain profile through the Greater Himalayan Sequence, Annapurna-Dhaulagiri Himalaya, central Nepal, in Montomoli C., et al., eds., proceedings for the 29th Himalaya-Karakoram-Tibet Workshop, Lucca, Italy.

estimated deformation temperatures are high (~600-700 °C). This suggests that these rocks have undergone little deformation whilst at conditions suitable for mid-crustal flow and instead suggest that the GHS has exhumed as a rigid body with little internal deformation, facilitated by ductile to brittle shearing at its margins.

Such observations suggest that current channel flow models (e.g. Beaumont et al., 2001) that invoke extensive mid-crustal flow of the GHS may not be applicable to the GHS of the Annapurna-Dhaulagiri Himalaya. The channel flow model for the Himalayan orogen suggests that the GHS represents a rheologically weak, mid-crustal channel driven laterally southwards and towards the surface, by the overburden of the Tibetan Plateau and the underthrusting of the Indian lower crust. Whilst there is good evidence to support the occurrence of channel flow elsewhere in the Himalaya (e.g., Everest region - Searle et al., 2003; Makalu region - Streule et al., 2010; Manaslu region - Larson et al., 2011), the weak CPO observed in the GHS of the Annapurna-Dhaulagiri Himalaya, combined with a lower than average volume of partial melting and a marked absense of sillimanite grade metamorphism suggests that channel flow did not play a significant role in the extrusion and exhumation of the GHS in this area.

The technique outlined here, presents a new approach for unravelling the structural evolution of mid-crustal terranes in situations where visual strain markers are hard to find. The observations and interpretations made from this study provide a new insight into the kinematic evolution of the Himalayan orogen and into the crustal proccesses that occurr during continental collision. Further work should be carried out to develop this technique further and to explore its usefulness and applicability to other settings.

References

Beaumont, C., Jamieson, R. A., Nguyen, M. H. and Lee, B. 2001, Himalayan tectonics explained by extrusion of a low-viscosity crustal channel coupled to focused surface denudation. Nature, 414, 738-742.

Bunge, H. J. and Morris, P. R., 1982, Texture analysis in materials science: mathematical methods, 593 pp, Butterworths, London.

Faccenda, M., Gerya, T. V. and Chakraborty, S., 2008, Styles of post-subduction collisional orogeny: Influence of convergence velocity, crustal rheology and radiogenic heat production. Lithos, 103, 257-287.

Larson, K. P., Cottle, J. M. and Godin, L., 2011, Petrochronologic record of metamorphism and melting in the upper Greater Himalayan sequence, Manaslu–Himal Chuli Himalaya, west-central Nepal. Lithosphere, 3, 379-392.

Lisle, R. J., 1985, The use of the orientation tensor for the description and statistical testing of fabrics. Journal of Structural Geology, 7, 115-117.

Searle, M. P., Simpson, R. L., Law, R. D., Parrish, R. R. and Waters, D. J., 2003, The structural geometry, metamorphic and magmatic evolution of the Everest massif, High Himalaya of Nepal-South Tibet. Journal of the Geological Society, 160, 345-366.

Skemer, P., Katayama, I., Jiang, Z. and Karato, S.-I., 2005, The misorientation index: Development of a new method for calculating the strength of lattice-preferred orientation. Tectonophysics, 411, 157-167.

Stipp, M., Stunitz, H., Heilbronner, R. and Schmid, S. M., 2002, The eastern Tonale fault zone: a 'natural laboratory' for crystal plastic deformation of quartz over a temperature range from 250 to 700 degrees C. Journal of Structural Geology, 24, 1861-1884.

Streule, M. J., Searle, M. P., Waters, D. J. and Horstwood, M. S. A., 2010, Metamorphism, melting, and channel flow in the Greater Himalayan Sequence and Makalu leucogranite: Constraints from thermobarometry, metamorphic modeling, and U-Pb geochronology. Tectonics, 29, TC5011.

Vollmer, F. W., 1990, An application of eigenvalue methods to structural domain analysis. Geological Society of America Bulletin, 102, 786-791.

Webb, A. G., Yin, A., Harrison, T. M., Celerier, J. and Burgess, 2006, The leading edge of the Greater Himalayan Crystalline complex revealed in the NW Indian Himalaya: Implications for the evolution of the Himalayan orogen. Geology, 35, 955-958.

Woodcock, N. H., 1977, Specification of fabric shapes using an eigenvalue method. Geological Society of America Bulletin, 88, 1231-1236.

Facies analysis in the southern part of Kathmandu basin and its significance for lake delta deposits during late stage of ancient lake

Mukunda Raj Paudel[1]

[1]Department of Geology, Trichandra Campus, Tribhuvan University, Ghantaghar, Kathmandu, Nepal
mukunda67@gmail.com

Thick sandy and muddy sequence covered the open lacustrine facies of the Kalimati Formation from the southern part of the Kathmandu Basin. Following five facies association (Fig.1) are recognized within the sandy and muddy facies of Sunakothi Formation: (a) facies association (pd): it is composed by muddy rhythmites and silt and laminated to ripple sand bed of the prodeltaic origin (b) Facies association (df): it is composed by the cross-stratification, ripple-drift and parallel lamination of the lacustrine delta front origin (c) facies association (dp): it is characterized by muddy flood-plain and alteration of the fine and coarse sediments, which indicates delta-plain origin (d) facies association (ml): it is characterized by sandy to silty rhythmites of the marginal shallow lacustrine origin above the delta-plain (e) fluvial association (Ff).

Former three associations is interbedded by the thick gravel deposits of the gravelly braidded river origin. It indicates that the transition from lacustrine to alluvial environments in the southern part of the Kathmandu Basin is characterized by fluvial and deltaic system in the south. Sedimentological study of the Sunakothi Formation indicates that these sediments were deposited during the rapid lake level rise and fell indicated by the thick channelized fluvial gravel beds within the sandy and muddy sequence. The cause of this change is due to climatic and activity of the basin margin tectonics of the Kathmandu Basin. On the basis of this study, lake delta of Sunakothi Formation is the southern counterpart of the Thimi-Gokarna Formation distributed in the northern part of the basin

Cite as: Paudel, M.R., 2014, Facies analysis in the southern part of Kathmandu basin and its significance for lake delta deposits during late stage of ancient lake, in Montomoli C., et al., eds., proceedings for the 29th Himalaya-Karakoram-Tibet Workshop, Lucca, Italy.

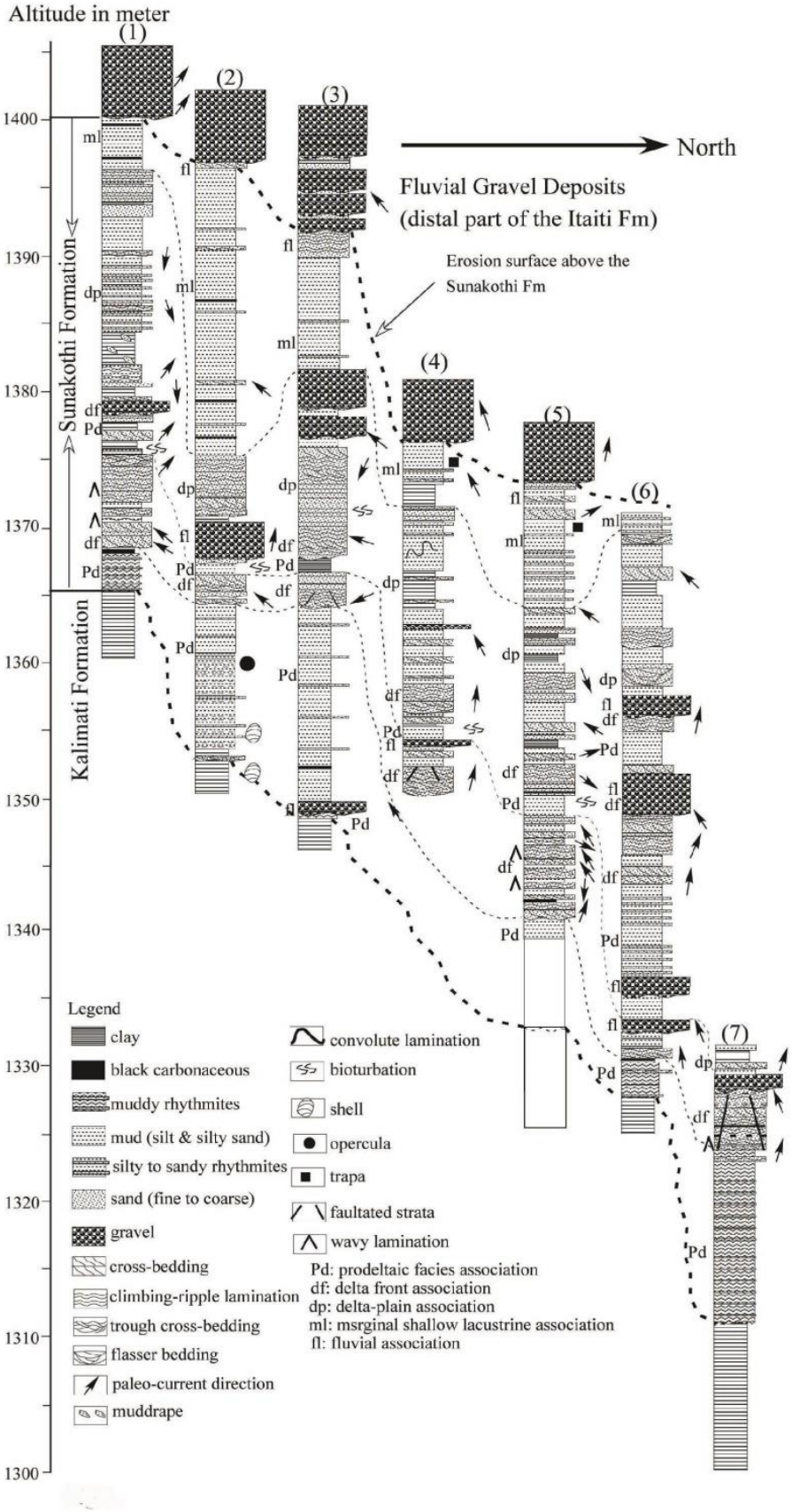

Figure 1. Detail columnar sections of the southern part of the basin showing different lithofacies. Number 1 to 7 indicates location of the columnar section within the study area.

Geological Structures, deformation and metamorphism of Lesser Himalaya between Mugling-Damauli area, central Nepal

K. R. Paudyal[1], L. P. Paudel[1]

[1] Central Department of Geology, Tribhuvan University, Kathmandu, Nepal, paudyalkabiraj@yahoo.com

Geological study was carried out in the Lesser Himalaya between Mugling-Damauli sections of central Nepal. This area consists of both autochthonous and allochthonous successions of Lesser Himalaya. The autochthonous units are called the Nuwakot Group while the allochthonous units are mapped as the Kahun Klippe. There are several nappes and klippes in Nepal Himalaya. The origin of these nappes and klippes (root zone) has been a matter of debate among the researchers. The Kahun Klippe located at central Nepal in Tanahu District is one of the least studied thrust sheets in the region. In the present study, geological mapping (1:25000 scale), structural analysis, petrographic study and illite crystallinity measurements were carried out covering both the Kahun Klippe and underlying autochthon. The study was also concentrated to compare the tectonics and stratigraphy of the Kahun Klippe with the adjacent Kathmandu Nappe and the Main Central Thrust (MCT) zone as it is believed that all the crystalline klippes of the Lesser Himalaya have been thrusted from the Higher Himalaya.

The Mugling-Damauli area forms a part of a large duplex structure. The Dubung Thrust is the roof thrust, the MBT is the floor thrust, the Dewachuli Thrust is the imbricate fault and the Bhangeri Thrust is a back-thrust. The origin of the Lesser Himalayan crystalline nappes can be explained on the basis of single thrust model, i.e., the southward extension of the MCT.

The area shows polyphase deformation (D1-D5) and metamorphism (M0-M3) as in the other parts of the Lesser Himalaya. At least two deformation events (D1 and D2) and one metamorphic event (M0) are pre-Himalayan. The M0 is normal burial metamorphism with grade increasing stratigraphically downwards and peak temperature reaching up to 370°C. The area suffered three deformation events (D3, D4 and D5) and three metamorphic events (M1, M2 and M3) after India-Eurasia collision. The second event (M1) is Eohimalayan event causing garnet-grade prograde metamorphism in the Tanahun Group. This is pre-MCT event. The MCT-related Neohimalayan metamorphism (M2) is inverted also in the low-grade zone of the Lesser Himalaya just below the Kahun Klippe. It is shown by both the illite and graphite crystallinity values.

Cite as: Paudyal, K.R. and Paudel L.P., 2014, Geological Structures, deformation and metamorphism of Lesser Himalaya between Mugling-Damauli area, central Nepal, in Montomoli C., et al., eds., proceedings for the 29th Himalaya-Karakoram-Tibet Workshop, Lucca, Italy.

Geological map of Chomolumgma (Everest), Cho-Oyu and Makalu area (Nepal-Tibet)

Pier Carlo Pertusati[1], Bruno Lombardo[2], Rodolfo Carosi[3], Chiara Frassi[1], Chiara Groppo[3], David Iacopini[4], Giancarlo Molli[1], Chiara Montomoli[1], Giovanni Musumeci[1], Franco Rolfo[3], Dario Visonà[5]

[1] Dipartimento di Scienze della Terra, Univeristy of Pisa, Italy, pertusati.piero@gmail.com
[2] IGG-CNR, Torino, Italy
[3] Dipartimento Scienze della Terra, University of Torino, Italy
[4] University of Aberdeen, UK
[5] Dipartimento di Geoscienze, University of Padova, Italy

A geological map, at the 1:100.000 scale, regarding the Chomolumgma, Cho-Oyu and Makalu area will be presented. The mapped area comprise the region of Chomolumgma extending from the Northern Nepal to the South Tibet. The main tectonic units (Higher Himalayan Crystallines- HHC; Tibetan Sedimentary Sequence – TSS) and the main tectonic discontinuities (Main central Thrus –MCT; South Tibetan Detachement –STD) of the Himalayan chain have been investigated during field expeditions in the years 1990-2010. Legend, tectonic scheme and geological cross sections are joined.

Cite as: Pertusati, et al., 2014, Geological map of Chomolumgma (Everest), Cho-Oyu and Makalu area (Nepal-Tibet), in Montomoli C., et al., eds., proceedings for the 29th Himalaya-Karakoram-Tibet Workshop, Lucca, Italy.

A record of shift in climate and orogenic events in Tethys Himalaya: evidence from geochemistry and petrography of Permo-Carboniferous sandstones from the Spiti region, Himachal Pradesh, India

Shaik A. Rashid[1], Javid Ahmad Ganai[1]

[1] Department of Geology, Aligarh Muslim University, Aligarh 202002, India, rashidamu@hotmail.com (+91-571-2700615)

Through a multidisciplinary approach, including petrology and geochemistry, the sedimentary provenance and paleoweathering of the Permo-Carboniferous Spiti sandstones (Lipak, Po and Ganmachidam formations) of Tethys Himalaya is investigated. The Spiti region consists of texturally immature to mature sandstones composed of unsorted to sorted and subangular to subrounded clastic grains dominated by variable amounts of quartz and feldspar accompanied by lithic fragments (mostly metasedimentary, sedimentary and plutonic grains). Uniform REE patterns (Fig. 1) similar to UCC with LREE enrichment (La_N/Sm_N= 3.91), flat HREE (Gd_N/Yb_N=1.21-2.5) and negative Eu anomalies with variable amounts of ΣREE and Eu anomalies (0.4-0.8) suggest that hydraulic sorting is significant. The striking similarities of the multi-elemental spider diagrams of the Spiti sandstones and the Himalayan granitoids indicate that the sediments are sourced from the Proterozoic and Cambro-Ordovician orogenic belts of the Himalayan region. The nature of the feldspar observed in thin sections from most altered to euhedral pristine minerals corresponding to Carboniferous to lower Permian sandstones strongly indicate a change in climate from most favorable conditions for rapid feldspar alteration (humid) to conditions where negligible alteration is possible (arid and glacial). It is found that the CIA values of these sandstones accorded with inferences based on sedimentologic and paleontological evidence, discriminating well between warm-humid (indicated by high CIA values) and arid- glacial (representing low CIA) conditions in the Spiti basin. Thus these results document a complete record of glacial and interglacial phases in the Permocarboniferous Spiti sandstones and the interpretations are consistent with other such studies on the Phanerozoic glaciation events on Gondwana supercontinent.

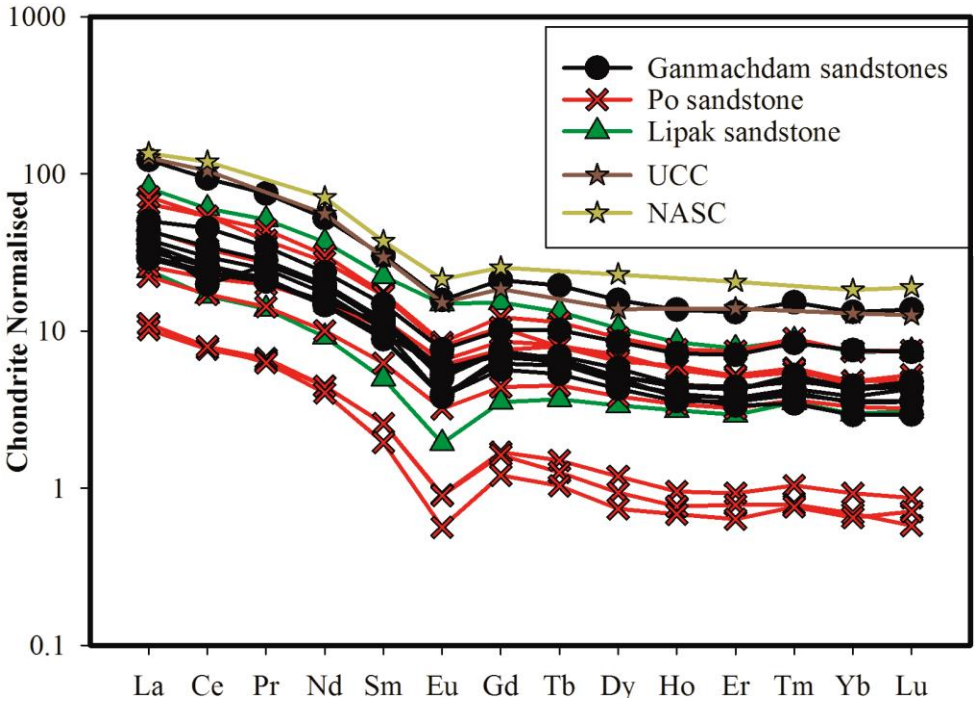

Figure 1. Chondrite-Normalised REE patterns of the Permo-Carboniferous sandstones from the Spiti region, Tethys Himalaya.

Cite as: Rashid, S.A., and Ganai, J.A., 2014, A record of shift in climate and orogenic events in Tethys Himalaya: evidence from geochemistry and petrography of Permo-Carboniferous sandstones from the Spiti region, Himachal Pradesh, India, in Montomoli C., et al., eds., proceedings for the 29th Himalaya-Karakoram-Tibet Workshop, Lucca, Italy.

The development of the Geological Reference Model for some key infrasctutural project in Indian Himalaya

Alessandro Riella[1], Mirko Vendramini[1], Attilio Eusebio[1], Elena Rabbi[1], Pasqualino Notaro[2], Massimo Spanò[2], Daniele Grandis[2], Alessandro Fassone[1]

[1] Geodata Engineering S.p.A., Corso Duca degli Abruzzi 48/e, Torino, Italia, ari@geodata.it
[2] SEA Consulting srl, Corso Bolzano 14, Torino, Italia, notaro@seaconsult.eu

In the last years Geodata Engineering S.p.A. has been involved in design of some infrastructural key - projects located in the Indian Himalaya. In each study the definition of a detailed and reliable Geological Reference Model (GRM) has been essential for a proper development of the projects and for the assessment of the risks connected to the construction. Define the geological context where a project is located means to identify some reference scenarios and conditions, pointing out limits and uncertainties for which the appropriate design countermeasures should be taken.

The development and improvement of a GRM passes through a multidisciplinary study conducted in sequential steps using different methodologies (bibliographic study, remote sensing analysis, geological and structural surveys, geophysical surveys, drillings, sampling and testing, etc...). In this context the geological survey plays a role of paramount importance because it let to define an appropriate reference model starting from the earliest design phase with reduced time and costs. Furthermore, the geological survey can easily cover the entire project area defining both the main potential geological hazards occurring in the site of the project and the most critical area to be studied with additional site investigations (location and characterization of tectonic disturbed zones, water inflow, presence of karst phenomena, potential presence of noxious and dangerous gases, high temperature expected at tunnel level, etc...).

The vastness and complexity of the Himalayan Region reflects also on the job of the geologists working as specialists for the design of large infrastructures. One of the main difficulties that must be faced defining a detailed GRM arise from the scarcity, in several areas, of a reliable geological model, built and accepted by the scientific community, usable as a base for the studies. Consequently, in some contexts followed in Himalaya by Geodata it has been necessary develop the GRM starting from few scientific reference papers, while in other cases the available scientific papers illustrated heterogeneous or contrasting geological conditions (i.e. definition of different geological Formations, discrepant position and characteristics of tectonic structures, etc..).

To face this problem Geodata's geologist had to perform exhaustive and detailed geological mappings to identify the main lithological, stratigraphic and structural characteristics of the different project areas. Specifically, the geological maps have been drawn up according to a rigorous approach based on the following logical steps:

1. on site identification and location of outcrops and geological features (mapping);
2. on site description of the rocks exposed at the surface and the geometric relationships of the different lithologies (mapping) (Figure 1);
3. the on-site checking of the main structures described in the bibliography and better geometry definition according to the scale of mapping (mapping);
4. the on-site checking and integration of geological and geomorphological features defined by the Remote Sensing Analysis (mapping);
5. checking and homogenization of data collected by different components of the mapping team (mapping / desktop);
6. checking and homogenization of all collected data (lithology, structures, etc..) with the available bibliographic reference (mapping / desktop);
7. drawing of representative geological maps and sections.

Cite as: Riella, a., et al., 2014, The development of the Geological Reference Model for some key infrasctutural project in Indian Himalaya, in Montomoli C., et al., eds., proceedings for the 29th Himalaya-Karakoram-Tibet Workshop, Lucca, Italy.

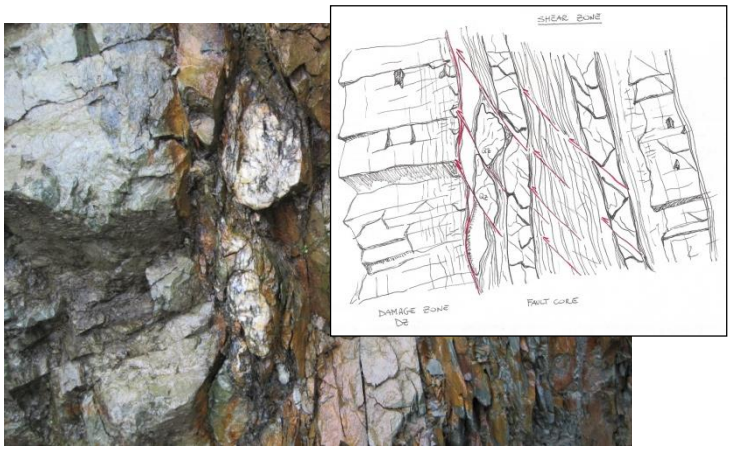

Figure 1. Picture and conceptual sketch of a relevant shear zone referred to the Main Boundary Thrust (MBT) in West Bengal. In evidence the main fault plane cut by recent minor brittle structures. Geodata, 2010.

As result of these activities, detailed geological maps (Figure 2) have been done so far in the following sectors of the Indian Himalaya:

- Sub Himalaya (Siwalik Group) and Lesser Himalaya (Darjeeling Group) in Sikkim and West Bengal *(Broad Gauge Rail Link between Sivok in West Bengal and Rangpo in the State of Sikkim with future connectivity to Gangtok)*
- Sub Himalaya (Murree Formation) in Jammu & Kashmir *(Rehabilitation, Strengthening and four Laning of Chenani to Nashri Section of NH-1A, from km 89.00 to km 130.00 - new alignment - including 9 km long tunnel - 2 lanes - with parallel escape tunnel, on BOT - Annuity - basis, on DBFO Pattern in the State of Jammu & Kashmir)*
- Higher Himalaya (Ramsu Formation and Machal Formation) in Jammu & Kashmir. *(Detailed Design Consultancy, 3D Monitoring & Supervision of Tunnel T-74R - between km 134 & 145 - in connection with construction of Dharam-Qazigund Section of Udhampur-Srinagar-Baramulla New BG Railway Line Project).*
- Kashmir Basin (Panjal Volcanic Group, Nagmarg Group, Madmatti Group) in Jammu & Kashmir *(Consultancy service for Detailed Feasibility Study and Framing Up of Phase Wise Proposal –DPR- for construction of 18 Km long Highway Tunnel across Razdhan Pass on Bandipur-Gurez road in Jammu&Kashmir State in India).*
- Lesser Himalaya (Subathu Formation, Tal Group, Krol Group, Baliana Group, Jaunsar Group, Garhwal Group) in Uttarakhand. *(Development of New Alignment including Refinements, Geological & Geophysical mapping, Final Location Survey and detailed Abstract Cost Estimating of 125 km long Broad Gauge New Rail Link Between Rishikesh and Karanprayag via Devprayag in the State of Uttarakhand, India).*

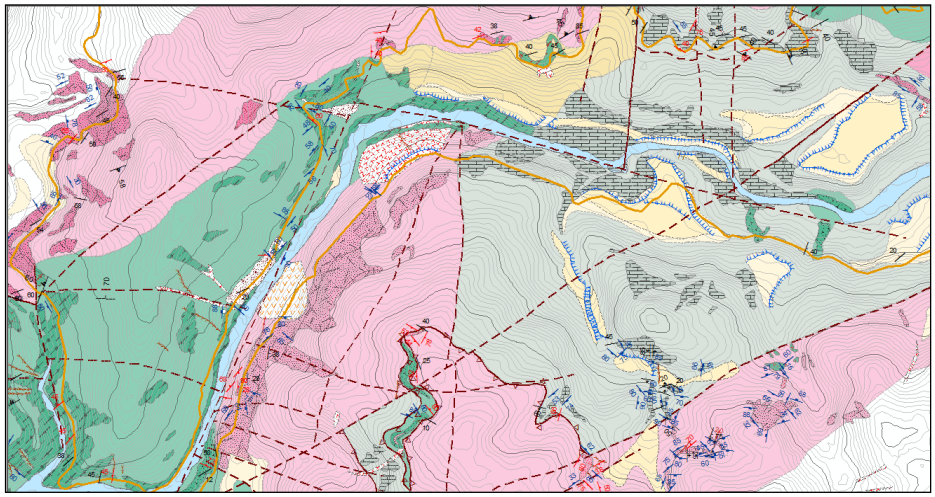

Figure 2. Extract of detailed geological map in a sector of Garhwal Group in Uttarakhand. Geodata, 2013

Evidence for a far traveled thrust sheet in the Greater Himalayan thrust system, and an alternative model to building the Himalaya

Dolores M. Robinson[1], Subodha Khanal[1], Matthew J. Kohn[2] , Subho Mandal[1]

[1] Department of Geological Sciences, University of Alabama, Tuscaloosa, Alabama, USA, dmr@ua.edu
[2] Department of Geosciences, Boise State University, Boise, Idaho, USA

New U-Pb zircon data from a Galchhi shear zone orthogneiss in central Nepal yield a 467.25 +2.5/-9.7 Ma crystallization age and metamorphic overgrowths of 26.2±1.7 Ma. To the northeast, the shear zone is crosscut by two undeformed pegmatite veins with U-Pb zircon crystallization ages of 24.7±0.6 Ma and 22.5±1.3 Ma, caused by motion on a thrust that initiated at ~26-22 Ma. This time is older than the 22-16 Ma Main Central thrust. Two micaceous quartzite samples from the hanging wall and footwall of the Galchhi shear zone yield youngest detrital zircon peak ages of ~584 and ~570 Ma, respectively. Toward the northern Himalaya, two quartzite samples from the hanging wall and footwall of the Langtang thrust, which has similar timing to the Galchhi shear zone, yield youngest detrital zircon peak ages of ~765 Ma and ~660 Ma, respectively. An augen orthogneiss from the hanging wall of the Langtang thrust yields a 474 +7/-3 Ma crystallization age. Rocks at Galchhi are younger than at Langtang suggesting that either the Langtang thrust cuts up section to the south or that the shear zone at Galchhi is another fault in the Greater Himalayan thrust system. Thus, the southward dipping Galchhi shear zone brought Greater Himalayan rocks from north of the Langtang thrust southward, and were subsequently passively folded into their present position by younger faults in the Lesser Himalayan duplex. We suggest a model with top-to-the-south shearing on the Langtang thrust or another intra-Greater Himalayan thrust to form the Galchhi shear zone.

Cite as: Robinson, D. M, Khanal, S., Kohn, M. J. and Mandal, S., 2014, Evidence for a far traveled thrust sheet in the Greater Himalayan thrust system, and an alternative model to building the Himalaya, in Montomoli C., et al., eds., proceedings for the 29th Himalaya-Karakoram-Tibet Workshop, Lucca, Italy.

Petrologic assesment of deep CO_2 production in the active Himalayan orogen

Franco Rolfo[1,2], Chiara Groppo[1], Pietro Mosca[2]

[1] Department of Earth Sciences, University of Torino, Italy, franco.rolfo@unito.it
[2] IGG – CNR, Torino, Italy

Active collisional orogens may have strong impact on the global carbon cycle through metamorphic degassing, which would supply a significant fraction of the global solid-Earth derived CO_2 to the atmosphere, thus playing a fundamental role even in today's Earth carbon cycle.

The Himalayan belt, a major active "hot" collisional orogen, is a likely candidate for the production of significant amounts of metamorphic CO_2 that may have caused changes in long-term climate of the past, present and near future. Large metamorphic CO_2 fluxes are likely to be triggered by rapid prograde metamorphism of big volumes of impure carbonate rocks coupled with facile escape of CO_2 to the Earth's surface. So far, the incomplete knowledge of the nature, magnitude and distribution of the CO_2-producing processes hampered a reliable quantitative modeling of metamorphic CO_2 fluxes from the Himalayan belt, as well as from any other collisional orogens.

We focus on the metamorphic decarbonation processes occurring during the Himalayan collision in the framework of the Ev-K2-CNR SHARE (Stations at High Altitude for Research on the Environment) Project. Consequently, the distribution of different types of metacarbonate rocks in the Eastern Himalaya, their petrography and petrological data about the nature of the CO_2-producing reactions in garnet-bearing calc-silicate rocks are discussed.

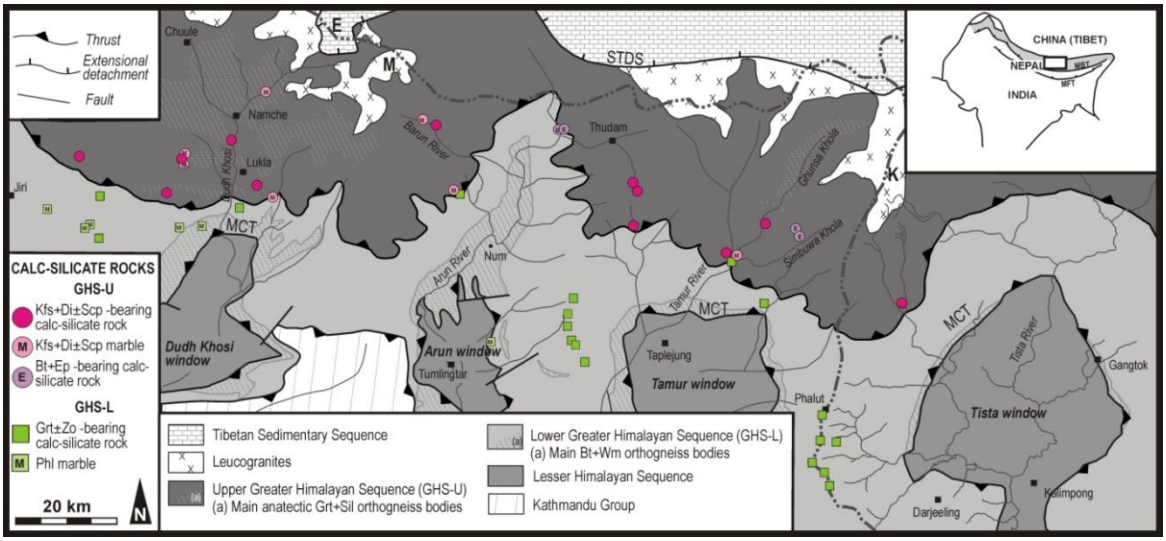

Figure 1. Simplified geological map of the central-eastern sector of the Himalayan belt (modified from Goscombe et al. 2006, Dasgupta et al. 2004, Mosca et al. 2012, Mosca et al. 2013) showing sample locations (squares: Grt+Zo calc-silicate assemblages and Phl marbles of the GHS-L; circles: Kfs+Di+Scp calc-silicate rocks and marbles of the GHS-U). The double-dashed grey line is the approximate political boundary between Nepal to the south, west, China (Tibet) to the north, India (Sikkim) to the east. MCT: Main Central Thrust; STDS: South Tibetan Detachment System; E: Everest, K: Kangchenjunga, M: Makalu. Inset shows the location of the study area (white rectangle) in the framework of the Himalayan chain. The grey shaded belt approximates the location of the Greater Himalayan Sequence. MFT: Main Frontal Thrust; MBT: Main Boundary Thrust.

In the eastern Himalaya, calc-silicate rocks are widespread in the lower (GHS-L) and upper (GHS-U) structural levels of the Greater Himalayan Sequence (Fig. 1). Different modes of occurrence have been distinguished for these lithologies:

(i) in the GHS-L, calc-silicate rocks generally occur as dm to metre-thick levels or boudins within medium- to high-grade, locally anatectic, staurolite- and/or kyanite-bearing metapelites (Fig. 2a,b);

Cite as: Rolfo, F., Groppo, C. and Mosca, P., 2014, Petrologic assesment of deep CO_2 production in the active Himalayan orogen, in Montomoli C., et al., eds., proceedings for the 29th Himalaya-Karakoram-Tibet Workshop, Lucca, Italy.

(ii) in the GHS-U, calc-silicate rocks are hosted in anatectic kyanite-sillimanite- bearing gneisses (i.e. Barun Gneiss) and often occur as tens to hundreds of meter thick, folded or boudinated, levels occasionally associated to layers of impure marbles. The transition between the paragneiss and the calc-silicate granofels is generally gradual and is characterized by the progressive disappearance of biotite, the appearance of clinopyroxene and the modal increase of plagioclase (Fig. 2c,d).

A banded structure is locally observed in the calc-silicate rocks, defined by the different modal proportion of the rock-forming minerals in adjacent layers. This suggest that calc-silicate rocks derive from former marly intercalations within a thick sedimentary sequence.

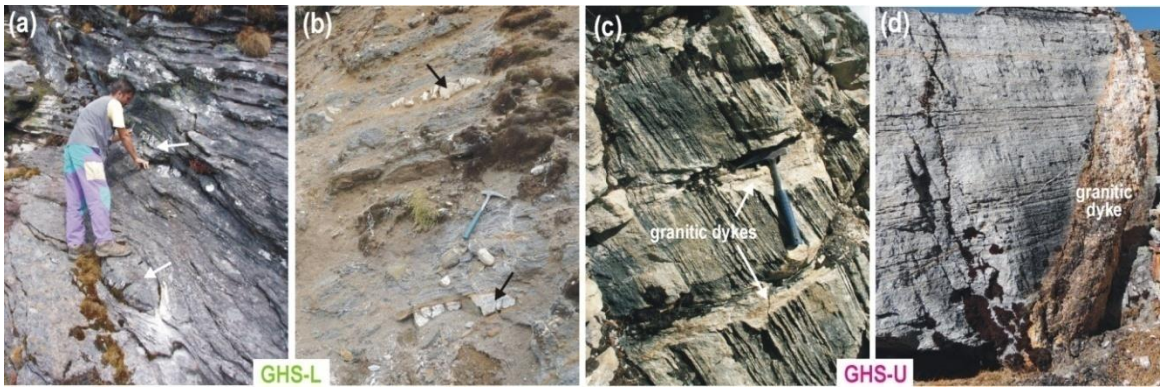

Figure 2. Field occurrence of calc-silicate rocks from the GHS-L (a,b) and GHS-U (c,d). The arrows in (a) and (b) indicate the calc-silicate boudins.

Mineral assemblages are systematically different in the GHS-L and GHS-U (Fig. 1):

(i) in the GHS-L, the equilibrium assemblage consists of plagioclase + clinopyroxene + quartz + garnet. Garnet is locally very abundant and it is often intergrown with quartz. Microstructural evidence suggest that garnet grew at the expense of zoisite, clinopyroxene and calcite, the latter being only locally observed as inclusion in garnet. Coarse-grained graphite is abundant.

(ii) in the GHS-U, calc-silicate rocks consist of K-feldspar + clinopyroxene + calcite + scapolite + plagioclase + quartz ± zoisite, relict biotite and muscovite. The ubiquitous mineral scapolite occurs both in the matrix and as oriented inclusions in clinopyroxene and zoisite; it is locally partially replaced by fine-grained dusty aggregates of plagioclase + calcite and/or it is overgrown by coarse-grained epidote.

The nature of the CO_2-producing reactions in the calc-silicate rocks may be petrologically investigated using activity-corrected P-T phase diagrams at fixed fluid composition, isobaric T-X(CO_2) phase diagram sections, and phase diagram projections in which fluid composition is not explicitly constrained (Groppo et al. 2013). Petrologic data demonstrate that both garnet- and scapolite- bearing calc-silicate rocks may act as CO_2-source during prograde heating, releasing internal-derived CO_2-rich fluids through garnet forming reactions and scapolite consuming reactions.

However, if the system remains closed, fluid-rock interactions may induce hydration of the calc-silicate assemblages and the in-situ graphite precipitation, thereby removing carbon from the fluid. The interplay between these two contrasting processes – i.e. production of metamorphic CO_2-rich fluids vs. carbon sequestration through graphite precipitation – must be taken in account when dealing with a global estimate of the role exerted by decarbonation processes on the orogenic CO_2-cycle.

References

Dasgupta, S., Ganguly, J. and Neogi, S., 2004, Inverted metamorphic sequence in the Sikkim Himalayas: crystallization history, P–T gradient and implications, J. metamorphic Geol., 22, 395–412.

Gaillardet, J. and Galy, A., 2008, Himalaya-carbon sink or source?, Science, 320, 1727–1728.

Goscombe, B., Gray, D. and Hand, M., 2006, Crustal architecture of the Himalayan metamorphic front in eastern Nepal, Gondwana Res., 10, 232–255.

Groppo, C., Rolfo, F., Castelli, D. and Connolly, J.A.D., 2013, Metamorphic CO_2 pro-duction from calc-silicate rocks via garnet-forming reactions in the CFAS-H_2O-CO_2 system, Contrib. Mineral. Petrol., 166, 1655–1675.

Mosca, P., Groppo, C. and Rolfo, F., 2012, Structural and metamorphic features of the Main Central Thrust Zone and its contiguous domains in the eastern Nepalese Himalaya, J. Virtual Expl. Electronic Edition, 41, paper 2.

Mosca, P., Groppo, C. and Rolfo, F., 2013, Main geological features of the Rolwaling-Khumbu Himal between the Khimti Khola and Dudh Khosi valleys (eastern-central Nepal Himalaya), Rend. Online Soc. Geol. It., 29, 112-115.

Preliminary chemical and isotopic characterization of cold and hot-spring waters from Nepal

Franco Rolfo [1,2], Emanuele Costa[1], Enrico Destefanis[1], Chiara Groppo[1], Pietro Mosca[2], Krishna P.Kaphle[3], Bhoj R. Pant[4]

[1] Department of Earth Sciences, University of Torino, Torino, I-10125, Italy, franco.rolfo@unito.it
[2] IGG – CNR, Torino, I-10125, Italy
3 Central Department of Geology, Tribhuvan University, Kathmandu, Nepal
4 Environment Research Division, Nepal Academy of Science and Technology, Kathmandu, Nepal

Metamorphic degassing from active collisional orogens supplies a significant fraction of CO_2 to the atmosphere, thus playing a fundamental role even in today's Earth carbon cycle. Appealing clues for a contemporary metamorphic CO_2 production are represented by the widespread occurrence, along the whole Himalayan belt, of CO_2 rich hot-springs mainly localized along the major tectonic discontinuities such as the Main Central Thrust (Becker et al., 2008; Evans et al., 2008; Perrier et al., 2009), and by the recent discovery of gaseous CO_2 ground discharges which may be variably associated with the hot-springs (Perrier et al., 2009; Girault et al., 2014). Recent geochemical and isotopic studies suggest that CO_2 is released at mid-crustal depth by metamorphic reactions within the Indian basement, transported along pre-existing faults by meteoric hot water circulation, and degassed before reaching surface. Thus, further studies should be undertaken to better constrain the carbon budget of the Himalaya, and, more generally, the contribution of collisional orogens to the global carbon balance.

In order to test the occurrence of CO_2 gas discharges not associated to hot-springs, a systematic chemical and isotopic characterization of cold-springs located along major tectonic discontinuities is needed; the isotopic signature of stable isotopes of carbon, hydrogen and oxygen is, in fact, useful to identify the water source and to individuate possible mixing phenomena.

Few chemical and almost no isotopic data are actually available for cold-springs of the Nepal Himalaya, especially regarding those located at high-altitude and in remote areas. In the framework of the Ev-K_2-CNR SHARE (Stations at High Altitude for Research on the Environment) Project, we have therefore started a preliminary chemical and isotopic study on high-altitude cold-springs located at different structural levels in the eastern Nepal Himalaya. The preliminary chemical and isotopic data obtained from these high-altitude cold-springs are compared with those obtained from well-known hot-springs located along or close to the Main Central Thrust.

Twelve cold-springs have been sampled from the Khimti Khola, Likhu Khola, Dudhkhund Khola and Irkhuwa Khola catchments. The Khimti, Likhu, Dudhkhund and Irkhuwa rivers cross the main tectonostratigraphic units of eastern Nepal Himalaya, flowing across the Greater Himalayan Sequence (GHS) and the Lesser Himalayan Sequence (LHS) and crossing the Main Central Thrust Zone (MCTZ). Four of the investigated cold-springs are located in the MCTZ, and eight are located in the upper GHS domain (GHS-U) (Fig. 1a). As concerning the hot-springs, seven samples have been collected from the well-known localities of Tatopani-Kodari, Tatopani and Ratopani in the Kaligandaki valley (Fig. 1b), Tatopani in the Myagdi valley, Syabru Bensi and Trisuli in the Langtang Himal. All these hot-springs are located within the MCTZ except for Tatopani and Ratopani in the Kaligandaki valley and Tatopani in the Myagdi valley, which are located in the LHS, immediately below the MCTZ.

The analyzed cold-springs are characterized by low discharge temperature varying between 3°C and 23°C. They are characterized by a very low salinity (TDS<150 mg/L, except for one sample, in which TDS <500 mg/L) and a correspondent very low conductivity (<200 μS/cm). The pH varies between 6.5 and 7.3 and the samples are Ca–Mg–HCO_3^- in composition (Fig. 1c) (see also: Evans et al. 2001, Becker et al. 2008).

The analysed hot-springs show different compositions, ranging from Na–Cl to Na–Ca–Cl types, are typically characterized by high amounts of total dissolved solids (TDS up to 4700 mg/L), vary in

Cite as: Rolfo, F., et al., 2014, Preliminary chemical and isotopic characterization of cold- and hot-spring waters from Nepal, in Montomoli C., et al., eds., proceedings for the 29th Himalaya-Karakoram-Tibet Workshop, Lucca, Italy.

temperature between 40 to 60 °C and have a pH in the range 6.8–7.7 (see also Evans et al., 2004; Becker et al. 2008, Perrier et al., 2009). Interestingly, the chemical composition of the hot-springs associated with gaseous CO_2 discharges from the ground (Syabru Bensi and Trisuli, sample 4A and 4B) is partially overlapped with that of some cold-springs (Fig. 1c).

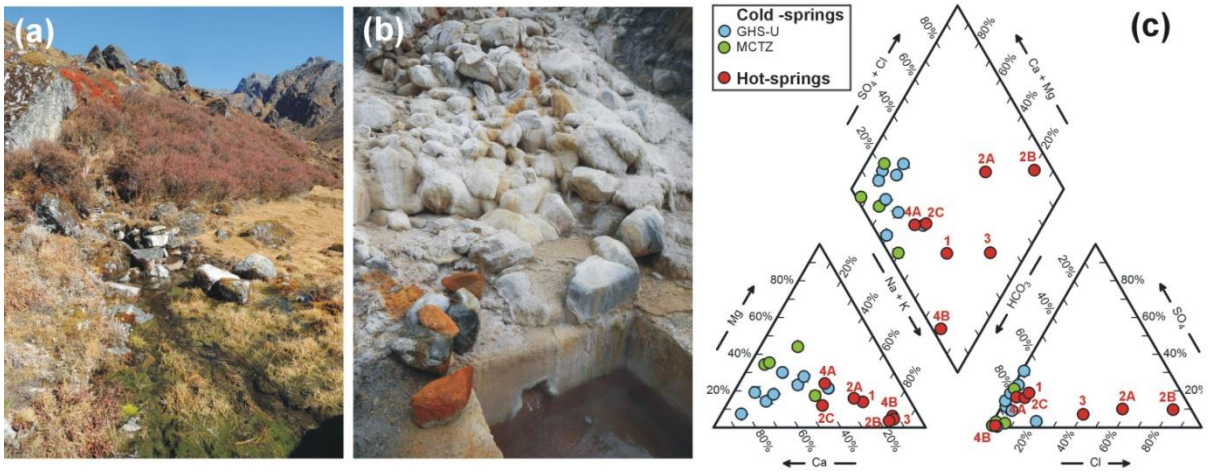

Figure 1. (a) Example of a high-altitude cold-spring in the Likhu Khola valley of eastern Nepal. (b) Example of a hot-spring with associated travertine deposits in the Kaligandaki valley (sample 2B). (c) Piper Diagram of the investigated water samples, showing the Ca-Mg–HCO_3^- composition of the cold-springs and the variable compositions of the hot-springs, from Na–Cl to Na–Ca–Cl types.

The very low total dissolved solids (TDS) of most of the analysed cold-springs hampered the possibility of analyzing their carbon isotopic composition; only for one sample the TDS was high enough to precipitate significant carbon for the isotopic measurement of the Dissolved Inorganic Carbon (DIC). The measured $\delta^{13}C_{(DIC)}$ value of this cold-spring water is strongly negative (-22 ‰) and contrasts with the moderate negative to significantly enriched $\delta^{13}C_{(DIC)}$ values measured for the hot-spring waters (-18‰ to +5‰). The more enriched $\delta^{13}C_{(DIC)}$ values have been measured for the hot-springs associated with gaseous CO_2 discharges from the ground (Syabru Bensi and Trisuli, sample 4A and 4B).

The hydrogen and oxygen isotopic values of both cold- and hot-springs are typical of meteoric waters and show a very good correlation with the Global Meteoric Water Line (GMWL) of precipitation (IAEA 1970, 2005), lying directly upon or very near the GMWL. The close correlation suggests that the contribution of metamorphic H_2O is negligible (e.g. Becker et al., 2008).

References

Becker, J.A., Bickle, M.J., Galy, A. and Holland T.J.B., 2008, Himalayan metamorphic CO_2 fluxes: Quantitative constraints from hydrothermal springs, Earth Planet. Sci. Lett., 265, 616-629.

Evans, M.J., Derry, L.A., Anderson, S.P.and France-Lanord, C., 2001, Hydrothermal source of radiogenic Sr to Himalayan rivers, Geology, 29, 803-806.

Evans, M.J., Derry, L.A. and France-Lanord, C., 2008, Degassing of metamorphic car-bon dioxide from the Nepal Himalaya, Geochem. Geophys Geosyst., 9, Q04021.

Evans, M.J., Derry, L.A. and France-Lanord, C., 2004, Geothermal fluxes of alkalinity in the Narayani river system of central Nepal, Geochem. Geophys Geosyst, 5, Q08011.

Girault, F., Perrier, F., Crockett, R., Bhattarai, M., Koirala, B.P., et al., 2014, The Syabru-Bensi hydrothermal system in Central Nepal. Part I – Characterization of carbon dioxide and radon fluxes, J. Geophys. Res. Solid Earth, 119, doi:10.1002/2013JB010301.

IAEA, 1970, Technical report IAEA-116, Interpretation of environmental isotope data in hydrology, International Atomic Energy Agency, Vienna.

IAEA, 2005, Isotopes in the Water Cycle: Past, Present and Future of a developing science, International Atomic Energy Agency, Vienna.

Perrier, F., Richon, P., et al., 2009, A direct evidence for high carbon dioxide and radon-222 discharge in Central Nepal, Earth Planet. Sci. Lett., 278, 198–207.

A geophysical perspective on the lithosphere-asthenosphere system of the Qinghai-Tibet plateau and its adjacent areas

Fabio Romanelli[1,2], Giuliano F. Panza[1,2,3,4]

[1] Department of Mathematics and Geosciences, University of Trieste, Via Weiss 4, 34127, Trieste, Italy, enrico.brandmayr@gmail.com
[2] The Abdus Salam International Centre for Theoretical Physics, Strada Costiera 11, 34014 Trieste, Italy
[3] Institute of Geophysics, China Earthquake Administration, Minzudaxuenanlu 5, Haidian District, 100081 Beijing, China
[4] International Seismic Safety Organization (ISSO) - www.issoquake.org

The Tibetan Plateau and the North China Craton (NCC), two key areas in mainland China, offer excellent laboratories to understand continental tectonics over a broad span of Earth history. Particularly, the deep structure of the lithosphere as imaged from geophysical data on the Tibetan Plateau and the NCC provide important clues in understanding orogeny and cratonization. The Tibetan Plateau is the largest and highest plateau on Earth in terms of mean altitude, and it is an important region for understanding the mechanisms of continent–continent collision and Cenozoic plateau uplift. The NCC is an Archean craton that underwent lithospheric disruption during the Mesozoic. Here we reconstruct the main features of the structure of the crust and upper mantle from surface wave tomography and gravity modeling in Tibet and its neighboring regions, as a clue to understand the modality of the convergence and collision process between the Indian and Eurasian plates, and the influence of this process on the uplift of the plateau. In the NCC, geological, geochemical, geophysical and tectonic investigations demonstrate that lithospheric destruction mainly occurred in the Eastern Block.

Data and method

The 3D model is obtained through the ensemble of cellular models expressed in terms of shear waves velocity (V_S), thickness and density of the layers, to a depth of 350 km. These physical properties are obtained by means of advanced non-linear inversion techniques, such as the "hedgehog" inversion method of group and phase velocity dispersion curves for the determination of V_S (e.g. Panza et al., 2007 and references therein) and the non-linear inversion of gravity data by means of the method GRAV3D (Li and Oldenburg, 2008). The "hedgehog" method allows for the definition of a set of structural models without resorting to any a priori model, considering the V_S and the thickness of the layers as independent variables. Given the well-known non-uniqueness of the inverse problem, the representative solution of each cell is determined through the application of optimization algorithms (Boyadzhiev et al., 2008) and is also validated with the use of independent geological, geophysical and petrological data.

Results

From the 3D density structure beneath the Tibetan Plateau, a 3D gravitational potential energy (GPE) map can be constructed (e.g Zhang et al. 2014, Deng et al., 2014). The GPE difference with respect to the average GPE to the depth of 350 km under the Tibetan Plateau along seven sections, A-A, B-B, C-C, D-D, E-E, F-F, and G-G, is shown in Figure 1a. Along most of these NE-SW sections not only the distribution in space of Vs and ρ but also that of the GPE difference evidence that, in some instances, the subducted lithosphere is less dense than the ambient rocks, and thus, the lithosphere cannot be driven by its negative buoyancy (i.e., slab pull). Therefore, the subduction process requires the presence of another dynamical force that is able to drag the upper plate lithosphere over the Indian plate. These observations highlight that the top asthenosphere (LVZ) acts as the lithosphere base decoupling, and the underlying mantle should flow NE-ward to SE-ward along the tectonic mainstream (e.g. see Panza et al. 2010).

The Vs absolute tomography (Foulger et al., 2013) and the density (ρ) models of the crust and upper mantle (to about 350 km depth) demonstrate the lateral variation of the thickness of the metasomatic lid (see Figure 1b) between the south and north of the Bangong–Nujiang suture (BNS) and the west and east of Tibet, which suggest that the leading edge of the subducting Indian slab reaches the BNS. The subduction angle of Indian Plate indicates a transition from steep to shallow from the west to east Tibet.

Cite as: Romanelli, F. and Panza, G.F., 2014, A geophysical perspective on the lithosphere-asthenosphere system of the Qinghai-Tibet plateau and its adjacent areas, in Montomoli C., et al., eds., proceedings for the 29th Himalaya-Karakoram-Tibet Workshop, Lucca, Italy.

Both Vs and ρ models suggest the following: (1) north–southward lower-crust flow beneath the eastern NCC and interaction between the westward mantle flow and eastward escape flow beneath the central NCC (in addition to the earlier proposed mechanisms of delamination and thermal erosion) played important roles in the lithospheric disruption of the Archean craton; (2) mantle flow plays an important role in the continental tectonic transition between neighboring tectonic blocks and within the cycle between orogeny and cratonization.

The direction of the Himalaya subduction is along the trend of the tectonic equator that deviates from NE to SE moving from India to China as indicated both by plate motions in the last 50 Ma and the GPS data in the no-net rotation and net rotation reference frameworks (e.g. Panza et al., 2010). Therefore, the W-E extension in the Tibetan Plateau is compatible with the global flow of plates, and it may be related to the back-arc extension operating along the western margin of the Pacific realm and not necessarily to tectonic escape.

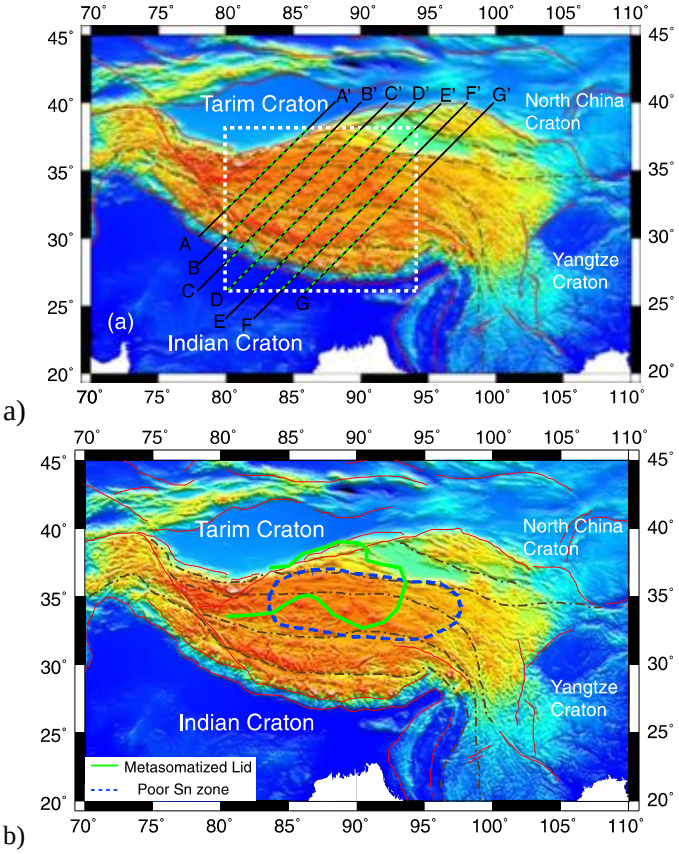

Figure 1. a) Spatial distribution of seven sections labeled A-A′, B-B′, C-C′, D-D′, E-E′, F-F′, and G-G′ in black lines. All of these sections were constructed from Vs cellular models (e.g. Zhang et al., 2014). The dashed white rectangle denotes the region wherein density inversion has been made. The tectonic units are: ID, Indian Craton; QDM, Qaidam Basin. AST, Asthenosphere.
b) Spatial distribution of the metasomatic lid in the Tibetan Plateau.

Acknowledgments

We thank all co-authors (see references) for their contribution and we acknowledge partial financial support from PRIN 2011- 2010PMKZX7 (MIUR) and from PNRA projects 2004/2.7-2.8, 2009/A2.17.

References

Boyadzhiev, G., Brandmayr, E., Pinat, T. and Panza, G.F., 2008, Optimization for non linear inverse problem. Rendiconti Lincei: Sci. Fis. e Nat., 19, 17-43.

Deng, Y., Panza, G.F. Zhongje, Z., Romanelli, F., Ma, T., Doglioni, C., Wang, P., Zhang, X. and Teng, J., 2014. Transition from continental collision to tectonic escape? A geophysical perspective on lateral expansion of the northern Tibetan Plateau, Earth, Planets and Space, doi:10.1186/1880-5981-66-10.

Foulger, G.R., Panza, G.F., Artemieva, I.M., Bastow, I.D., Cammarano, F., Evans, J.R., Hamilton, W.R., Julina, B.R., Lustrino, M., Thybo, H. and Yanovskaya, T.B., 2013, Caveats on tomographic images. Terra Nova, 25, 259-281.

Li, Y. and Oldenburg, D.W., 1998, 3D inversion of gravity data, Geophysics, 63, 109-119.

Panza, G.F., Doglioni, C. and Levshin, A., 2010, Asymmetric ocean basins. Geology, 38, 59-62. 10.1130/G30570.1

Zhang, Z., Teng, J., Romanelli, F., Braitenberg, C., Ding, Z., Zhang, X., Fang, L., Zhang, S., Wu, J., Deng, Y., Ma, T., Sun, R. and Panza, G.F., 2014, Geophysical constraints on the link between cratonization and orogeny: Evidence from the Tibetan Plateau and the North China Craton, Earth-Science Reviews, 130, 1-48, ISSN 0012-8252.

Dental hypoplasia in Siwalik Rhinos: additional information on Neogene climate of South Asia

Ghazala Roohi[1], S. Mahmood Raza[2], Muhammad Akhtar[3]

[1] Pakistan Museum of Natural History, Islamabad, Pakistan, roohi@pmnh.gov.pk
[2] Peabody Museum, Harvard University, Cambridge, MA, USA
[3] Zoology Department, University of the Punjab, Lahore, Pakistan

The developmental or usage patterns experienced by certain mammals during their growing age or later in their life often are preserved in their fossilized remains which have extensively been used in reconstructing their life-history or the habitat in which the animals lived. One such, though lesser emphasized, feature is the *enamel hypoplasia* (*hypo*-low and *plasis*-forming), which is a failure for the enamel to form properly leaving distinct linear or curved marking(s) on the teeth. *Enamel hypoplasia* (EH) is caused by environmental or physiological stresses in an animal life at that particular time when the growth was taking place. Hence, the EH analysis in a faunal accumulation have been used for providing a unique perspective into environmental conditions present during the growing years of an extinct animal's life, which indirectly reflects the climatic conditions prevailing during that period of time (for example: Franz-Odendaal, 2004; Franz-Odendaal et al., 2004). Another line of evidence used for interpreting local environment is the stable Oxygen and Carbon isotope analysis in fossilized mammalian bones (Balasse et al., 2002). For interpreting the Neogene environmental and climatic changes in South Asia, scholars have coupled the studies of microwear patterns on mammalian teeth with stable isotopes of carbon and oxygen in paleosols carbonates from the Miocene Siwalik of Pakistan (Martin et al., 2011; Morgan et al., 2009; Nelson 2007). The present study on enamel hypoplasia of Siwalik Rhinocerotids has provided another tool for not only understanding their past life-history but also reconstructing local paleoenvironment and regional paleoclimate of the region.

The Rhinocerotid dental remains collected from the entire Neogene continental sediments (colloquially termed as the Siwaliks in South Asia) exposed in the Himalayan Foreland belt in Pakistan and India were examined for this study on enamel hypoplasia. A total of 1754 Rhinocerotid teeth housed in major museums and institutes of Pakistan (Islamabad and Lahore), France (Paris and Toulouse), UK (BMNH, London) and the USA (New York, Yale and Harvard) were examined for the presence or absence of hypoplasia, if present its location on the crown, shape and measurements, eruption state and wear stage of the tooth, etc. The Siwaliks Rhino teeth studied included 34 species in which 11 species have enamel hypoplasia and represented a time period ranging from 25 Myr to about 2 Myr from a vast area extending from the Bugti Hills in central Pakistan, through Potwar Plateau and Kashmir in northern Pakistan to the Siwalik Hills in western India (Fig. 1).

The 11 species showing hypoplasia occur almost at all the intervals of the Neogene. It is difficult to directly correlate the hypoplasia occurrences with global or regional climate changes but there exists a broad relationship, which is discussed here. The Rhino species with EH are apparently more prevalent at four time periods; around 22-20 Myr, ~16 Myr, 12-8 Myr and ~2 Myr in the Pliocene. It has been argued that climate, especially seasonality with prolonged draught periods, might have been the cause of stress for these animals having hypoplasia. It would, however, bring credence to the hypothesis proposed here that climate change has caused the EH in Rhinos if other mammalian groups are also examined for the same time span. This is my next project which will examine another common Siwalik herbivore, the giraffids.

References

Balasse, M., Ambrose, S.H., Smith, A.B. and Price, T.D., 2002, The seasonal mobility model for prehistoric herders in the South-western Cape of South Africa assessed by isotopic analysis of sheep tooth enamel, Journal of Archaeological sciences, 29, 917-932.

Franz-Odendaal, T.A., 2004, Enamel hypoplasia provides insights into early systematic stress in wild and captive giraffes (Giraffa camelopardalis), Journal of Zoology, 263, 197-206.

Franz-Odendaal, T.A., Chinsamy, A. and Lee-Thorp, J., 2004, High prevalence of enamel hypoplasia in an early Pliocene giraffid (Sivatherium hendeyi) from South Africa, Journal of Vertebrate Paleontology, 24 (1), 235-244.

Cite as: Roohi, G. et al., 2014, Dental hypoplasia in Siwalik Rhinos: additional information on Neogene climate of South Asia, in Montomoli C., et al., eds., proceedings for the 29th Himalaya-Karakoram-Tibet Workshop, Lucca, Italy.

Martin, C., Bentaleb, I. and Antoine, P.–O., 2011, Pakistan mammal tooth stable isotopes show paleoclimatic and paleoenvironmental changes since the early Oligocene, Palaeogeography, Palaeoclimatology, Palaeoecology, 31, 19-29.

Morgan, M.E., Behrensmeyer, A.K., Badgley, J., Barry, J.C., Nelson, S. et al., 2009, Lateral trends in carbon isotope ratios reveal a Miocene vegetation gradient in the Siwaliks of Pakistan, Geology, 37 (2), 103-106.

Nelson, S.V., 2007, Isotopic reconstructions of habitat change surrounding the extinction of Sivapithecus, a Miocene hominoid, in the Siwalik Group of Pakistan, Palaeogeography, Palaeoclimatology, Palaeoecology, 243 (1–2), 204–222.

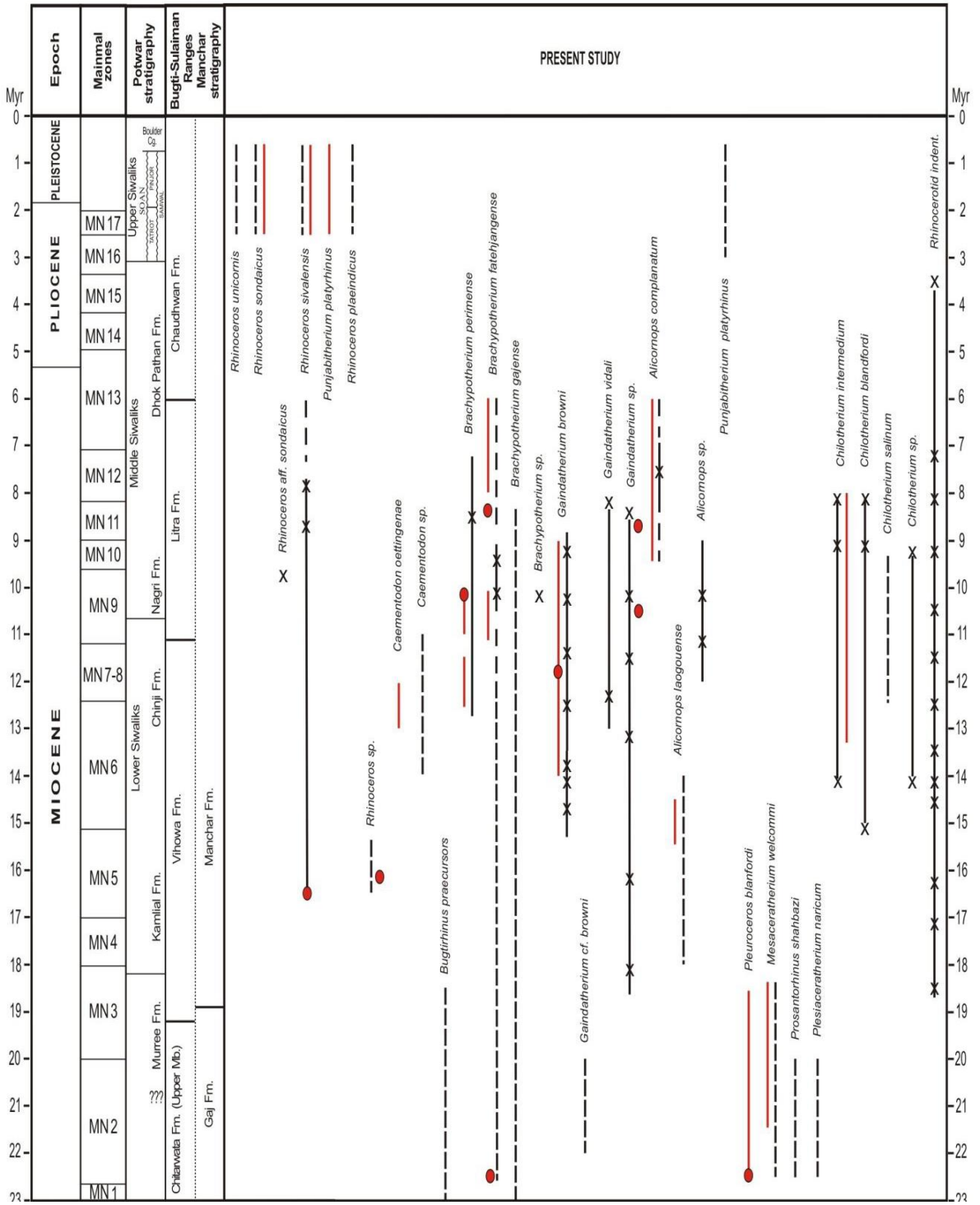

Figure 1. Ranges of 34 species in which 11 species have hypoplasia at one or more time period in their total range.

Exhumation history of the Tethyan Himalaya based on apatite (U-Th-Sm)/He dates from the Takkhola graben and the Mustang granite (Nepal)

Ruben V. Rosenkranz[1], Mohammad S. Sohi[1], Cornelia Spiegel[1]

[1] Geodynamics of the Polar Regions, University of Bremen, Klagenfurter Str., D-28359 Bremen, Germany, ruben.rosenkranz@uni-bremen.de

The exhumation of the Himalayan arc has been studied intensively throughout the last decades. For the Tethyan Himalaya, however, the youngest exhumation history is still unclear, mostly because of the lack of a significant apatite content in most Tethyan sediments (Crouzet et al. 2007). For this study we are using apatite (U-Th-Sm)/He thermochronology for investigating exhumation and denudation of the Tethyan Himalaya back through time. Apatite (U-Th-Sm)/He thermochronology is sensitive to temperatures of ~40 to 85°C and thus to movements within the upper ~1.5 to 3 km of the earth´s crust.

During a recent field campaign, we sampled the Mustang granite and the Takkhola-Graben. The former intrudes the Tethyan marine sediments, but far northwards than other Himalayan leucogranites; the latter is a magnificent graben, which can be seen as an inusual southern part of the normal faulting system affecting the whole Tibetan Plateau, where the faults have the same submeridional orientation (Colchen, 1999), while the timing of the activation of the faulting is still highly debated. The syntectonics filling of the Takkhola-Mustag graben consists of Mio-Pliocene fluvio-lacustrine deposits (Garzione et al. 2003). These were described as containing significant amounts of apatite, derived from the past erosion of the Mustang granitic body (Adhikari and Wagreich, 2011). Being only up to 1km thick, a post depositional thermal resetting of the apatite (U-Th-Sm)/He system is unlikely, so that the (U-Th-Sm)/He dates of the sediments are expected to have retained their information regarding source area exhumation. We took several sand samples from the Kali Gandaki River draining the present-day exposure of the Mustang granite. Furthermore, we sampled different stratigraphic levels of the Mio-Pliocene sedimentary rocks, i.e., from the Tetang and Takkahola formation deposited between 11 and 7 Ma. One sample was taken at high altitude from a dyke of the Mustang granite, whereas, due to the remoteness of the area, it was not possible to access the main granitic body. This sampling approach will not only provide information about the youngest denudation history of the Mustang granite /Tethyan Himalaya, but will also reveal insights into its past denudation and changes of denudation rates through time for the region past the South Tibetan Detachment.

It is our expectation to link the results to the tectonic behavior of the South Tibetan Detachment or to the newly recognized Western Nepal Fault System. Corroborating our results with other ages and diverse methods will provide a robust constraint on the exhumation history of the Tethyan Himalaya, as well as insights on the U-Th/He dating technique.

References

Adhikari, B.R. and Wagreich, M., 2011, Provenance evolution of collapse graben fill in the Himalaya-The Miocene to Quaternary Thakkhola-Mustang graben (Nepal), Sedimentary Geology, 233, 1-14.

Blythe, A.E., Burbank, D.W., Carter, A., Schmidt, K. and Putkonen, J., 2007, Plio-Quaternary exhumation history of the central Nepalese Himalaya: 1. Apatite and zircon fission track and apatite [U-Th]/He analyses, Tectonics, 26(3).

Crouzet, C. et al., 2007, Temperature and age constraints on the metamorphism of the Tethyan Himalaya in Central Nepal: A multidisciplinary approach, Journal of Asian Earth Sciences, 30, 113-130.

Garzione, C.N, DeCelles, P.G., Hokinson, D.G., Ojha, T.P. and Upreti, B.N., 2003, East-west extension and Miocene environmental change in the southern Tibetan plateau: Thakkhola graben, central Nepal, Geological Society of America Bulletin, 115, 3-20.

Colchen, M., 1999, The Takkhola-Mustang graben in Nepal and the latee Cenozoic extension in the Higher Himalayas, Journal of Asian Earth Sciences, 17, 683-702.

Cite as: Rosenkranz, R.V., Sohi, M.S. and Spiegel, C., 2014, Exhumation history of the Tethyan Himalaya based on apatite (U-Th-Sm)/He dates from the Takkhola graben and the Mustang granite (Nepal), in Montomoli C., et al., eds., proceedings for the 29th Himalaya-Karakoram-Tibet Workshop, Lucca, Italy.

Seismicity and convergence partitioning in the eastern Himalaya

Adi Saric[1], Djordje Grujic[1]

[1] Dalhousie University, Department of Earth Sciences, Halifax, Canada (dgrujic@dal.ca,)

Seismotectonics of the eastern Himalaya appears fundamentally different to the one in central and western Nepal. Potentially, this may indicate a current tectonic reorganisation of the Himalaya.

Present-day seismicity of the Himalaya has been interpreted in terms of (1) fault interaction by transfer of stress, both on timescales of earthquake sequences and aftershocks, and on longer timescales where the seismicity is associated with the inter-event time of the largest shocks that occur in a given region (Stein, 1999); and (2) the combination of crustal processes governing the Pliocene-Quaternary deformation of the Himalayan orogen. For example, kinematic models of seismic data in the central Himalaya (Cattin and Avouac, 2000) suggest that since the M 8.4 Bihar earthquake (1934), the Main Himalayan Thrust (MHT) in central and eastern Nepal has remained locked from the trace of the Main Frontal thrust (MFT) to ~100 km downdip. This process has resulted in stress build-up, triggering seismic activity observed in Nepal in a belt about 100 km from the foothills. The Himalayan seismic belt extends actually along the entire Himalayan arc, but the frequency of the earthquakes is not uniform, with the largest seismic gap in the Bhutan Himalaya (Gahalaut et al., 2011).

Causes of the Bhutan seismic gap may be multiple: (a) The entire MHT beneath the Bhutan Himalaya has been locked and a large (> M 8) earthquake is overdue; (b) The M ~8.1 "Great Assam earthquake" of 12 June 1897 that hit the northern Shillong Plateau (North-eastern India), has caused a stress shadow in the Bhutan Himalaya; (c) The partitioning of Himalayan contraction into the MHT and strike slip faults that dominate the seismotectonics of the eastern Himalaya.

We investigate the two latter possibilities by calculating the Coulomb stress changes along two seismically active faults and the resulting Coulomb stress changes along dozen potential receiver faults. Our calculations demonstrate that the Great Assam Earthquake caused only minor stress drop along the MFT of Bhutan, and it did not affect the MHT. However, the event has caused major stress loading in the eastern part of the Dauki fault, which is the principal fault bounding the Shillong plateau to its south. Dextral, NW striking Kopili fault has also received modest stress loading in its central segment. The M 6.9 Sikkim earthquake of 18 September 2011 and its aftershocks occurred along a zone parallel to the known Tista strike-slip fault, and is here named Gangtok fault. This event has caused moderate stress drip along a narrow segment of the MHT in Sikkim, and moderate stress increase along the seismically active strike slip faults along India-Bhutan border.

References

Cattin, R. and Avouac, J., 2000, Modeling mountain building and the seismic cycle in the Himalaya of Nepal, Journal of Geophysical Research, 105, B6, 13,389-313,407.

Gahalaut, V., Rajput, S. and Kundu, B., 2011, Low seismicity in the Bhutan Himalaya and the stress shadow of the 1897 Shillong Plateau earthquake, Physics of the Earth and Planetary Interiors, 186, 97-102.

Stein, R.S., 1999, The role of stress transfer in earthquake occurrence, Nature, 402, 605-609.

Cite as: Saric, A. and Grujic, D., 2014, Seismicity and convergence partitioning in the eastern Himalaya, in Montomoli C., et al., eds., proceedings for the 29th Himalaya-Karakoram-Tibet Workshop, Lucca, Italy.

Imaging continental collision and subduction in the Pamir mountain range by seismic attenuation tomography

Bernd Schurr[1], Christian Haberland[1], Christian Sippl[2], Xiahui Yuan[1], Jim Mechie[1], Felix Schneider[1]

[1] Deutsches GeoForschungsZentrum – GFZ, Telegrafenberg, 14473 Potsdam, Germany, schurr@gfz-potsdam.de
[2] Research School of Earth Sciences, Australian National University, Canberra, Australia

Subduction of continental crust is the mode of shortening in continental collision that is the least well understood. It is known to occur, as testified e.g., by now exhumed ultra-high-pressure rocks, despite the fact that continental crust is generally too buoyant to submerge into the mantle. Continental crust may, however, subduct in tow of a leading dense oceanic plate at the last stage of the plate tectonic Wilson cycle. Alternatively, if upper and lower crust detach, the latter, together with the underlying cold mantle lithosphere, may become negatively buoyant, enabling their descend. The Pamir mountains in Central Asia have been one of the few places on Earth, where on-going continental subduction has been postulated based on an active Wadati-Benioff zone. The Pamir is situated on an orographic node northwest of Tibet, between the Tarim and Tajik basins, where the Hindu Kush, Karakorum, western Kunlun Shan and Tien Shan ranges coalesce. It formed in the late Paleogene to Neogene, i.e. approximately during the second half of the India-Asia collision, north of the Western Himalayan Syntaxis, on the Asian (retro)continent.

We use tomography of seismic attenuation to image the lithospheric-scale structure of the Pamir orogen. Attenuation tomography has been shown to be a powerful tool to study deep process-related structures particularly in oceanic subduction zones. Attenuation at this scale may be seen as a proxy for rheology and hence is very sensitive to e.g., homologous temperature and deformation. We use data from a two-year seismic deployment of the Tian Shan-Pamir Geodynamic Program (TIPAGE, Mechie et al. 2012). The whole path attenuation parameter t* is determined by inversion of P-wave velocity spectra from 1790 earthquakes and then inverted for a 3D attenuation model employing a recently published 3D velocity model (Sippl et al. 2013). We find a prominent continuous crescent-shaped high attenuation anomaly (HAA) that penetrates from upper crustal levels to depths of more than 100 km. At mantle depths the HAA follows the seismicity and coincides with low seismic velocities and most probably presents subducted crustal rocks. The HAA appears to be squeezed between regions of low attenuation. To the north and west this probably presents cold Asian lithospheric mantle. To the south the low attenuation maybe an indication of the (Indian?) indenter. The structures we image here are distinctively different from oceanic subduction zones, where HAAs usually occur in the mantle wedge above low attenuation oceanic slabs.

References

Sippl, C. et al., 2013, Deep burial of Asian continental crust beneath the Pamir imaged with local earthquake tomography, Earth and Planetary Science Letters, 384, 165-177, doi:10.1016/j.epsl.2013.10.013.

Mechie, J. et al., 2012, Crustal and uppermost mantle velocity structure along a profile across the Pamir and southern Tien Shan as derived from project TIPAGE wide-angle seismic data, Geophysical Journal International, 188, 385-407, doi:10.1111/j.1365-246X.2011.05278.x.

Cite as: Schurr, B. et al., 2014, Imaging continental collision and subduction in the Pamir mountain range by seismic attenuation tomography, in Montomoli C., et al., eds., proceedings for the 29th Himalaya-Karakoram-Tibet Workshop, Lucca, Italy.

Tectonics of the Mogok Metamorphic Belt, Myanmar (Burma) and its correlations from the East Himalayan Syntaxis to the Malay Peninsula

Mike P. Searle[1], N.J. Gardiner[1], C.K. Morley[2,3] U. Kyi Htun[4]

[1] Dept. Earth Sciences, Oxford University, South Parks Rd., Oxford OX1 3AN, mikes@earth.ox.ac.uk
[2] PTT Exploration & Production, 555 Vibhavadi Rangsit Road, Chatuchak, Bangkok, 10900, Thailand
[3] also at: Dept. of Geology, Chiang Mai University, Thailand
[4] Consultant Geologist, B201, B14 Ward, Thanthumar Street, Okkalapa Township, Yangon, Myanmar

The Mogok Metamorphic belt (MMB) in Myanmar (Burma) is thought to be a southward continuation of the Lhasa block of south Tibet around the East Himalayan syntaxis. South of Burma the MMB may extends into the tin granite province of the Mergui coast and south to Phuket. The MMB in Burma is a sequence of high-grade metamorphic rocks including phlogopite + diopside + spinel ± olivine ± ruby corundum marbles, scapolite + garnet + biotite calc-silicates, clinopyroxene-bearing quartzites and gneisses intruded by rare nepheline syenites (occasionally sapphire-bearing) and associated ultramafic rocks and a variety of granitic rocks. Pre-collisional hornblende and biotite bearing diorites and granodiorites are related to supra-subduction zone magmatism prior to Indian plate collision. Mogok gneisses show high-temperature paragenesis with sillimanite + muscovite replacing earlier andalusite (Kyaushe gneiss) in pelites and peak metamorphic anatexis resulting in tourmaline + garnet + muscovite leucogranites (Kyanikan). An earlier metamorphic event and fabric formation is preserved at Belin quarry where a post-kinematic biotite granite dyke has been dated at ~59 Ma. Evidence of older metamorphism along the Mogok belt has largely been overprinted by a Cenozoic high-temperature metamorphism constrained by U-Th-Pb ID-TIMS and in situ LA-ICPMS dating of metamorphic monazite and zircon. Growth of metamorphic monazite at sillimanite grade (680ºC; 4.4 - 4.9 kbar) and growth of zircon rims occurred between 47-43 Ma. Syn-peak metamorphic tourmaline granites have ages ranging between 45.5 – 24.5 Ma. The tourmaline granites are *in situ* partial melts from a biotite + muscovite + K-feldspar augen gneiss protolith and their ages record Cenozoic periods of peak sillimanite grade metamorphism. Kyanite gneisses in the Katha Gangaw range record higher pressures. The MMB has little in common with the Western granite belt of peninsula Malaysia, dominated by Triassic tin-bearing biotite granites, which is regarded as a separate terrane.

Cite as: Searle, M.P., Gardiner, N.J., Morley, C.K. and Kyi Htun, U., 2014, Tectonics of the Mogok Metamorphic Belt, Myanmar (Burma) and its correlations from the East Himalayan Syntaxis to the Malay Peninsula, in Montomoli C., et al., eds., proceedings for the 29th Himalaya-Karakoram-Tibet Workshop, Lucca, Italy.

Records of Proterozoic magmatism and Himalayan exhumation in sulphide minerals and fluid inclusions from the klippen rocks of Lesser Himalayan tectonic domain

Rajesh Sharma, D.R. Rao, Dinesh S. Chauhan[1]

Wadia Institute of Himalayan Geology, Dehra Dun, India, *sharmarajesh@wihg.res.in*
[1]Present address: Geological Survey of India, Dehra Dun, India

The genetic environment of sulphide ores from the klippen rocks of the Lesser Himalaya in Garhwal and Kumaun has been investigated to understand the processes operated in the Proterozoic rock suit. The characteristic minerals, together with chemical data point to the primary deposition of ores, and in turn the Proterozoic environment of the host crystalline rocks. Features of complex mineral assemblage suggest activity of hydrothermal fluids. The composition of cubanite lamellae reveals its transformation from high temperature form, myrmekitic intergrowth of stannoidite in chalcopyrite and Zn content in it, togther with $\delta^{34}S$ values in range of 0.9 to 6.8 ‰ attribute to the shallow magmatic process during syngenetic ore formation in the crystalline rocks. Arsenopyrite compositions further imply 450±20°C formation temperatures. Fluid inclusions in the ore mineral assemblage suggest high volatile contents in the ore forming fluid, and the micro Raman spectroscopy confirms CO_2 with significant CH_4 in the fluid, which is unusual to general metamorphic sequence in Lesser Himalaya. Liquid-vapour coexistence and fluid separation was prominent in the shallow magmatic system. These features are in alignment with the chemical signatures of granitoids from the mineralized Askot and Chiplakot klippen, which are interpreted to have hybrid source, and represent active arc around 1800 Ma.

The fluid inclusions in the selected minerals from the assemblage help to understand the imprints of the exhumation of the host rock sequence. Early fluid inclusions in gneisses show their re-equilibration to the stretched cavities as a result of dissolution-crystallization process. Such inclusions occurring in the fluid inclusion arrays are oriented perpendicular to the stress, and were deformed subsequent to a regional stress generated by Himalayan thrusting. The Himalayan exhumation is apparent from the excess internal pressure developed within inclusions in the exhumed rocks. The features observed near the thrust plane further points to the isothermal decompression and rapid uplift.

Cite as: Sharma, et al., 2014, Records of Proterozoic magmatism and Himalayan exhumation in sulphide minerals and fluid inclusions from the klippen rocks of Lesser Himalayan tectonic domain, in Montomoli C., et al., eds., proceedings for the 29th Himalaya-Karakoram-Tibet Workshop, Lucca, Italy.

Morpho-dynamic characteristics and their controls, Bagmati River of Central Nepal Himalaya

Pramila Shrestha[1,2], Naresh Kazi Tamrakar[2]

[1] Department of Irrigation, Jawalakhel, Lalitpur, Nepal, pramisht05@gmail.com
[2] Central Department of Geology, Tribhuvan University, Kirtipur, Nepal

The Bagmati River has unique geological characteristics of terrains, diverse climatic regime, and topographic variations from the head to the mouth, which give rise to various patterns of the river along its course. The main stem Bagmati River that originates at the eastern hills of the Kathmandu Valley is the eighth order perennial river that stretches for about 206 km with an elongated catchment of area 3761 km^2 within different geological terrains as the Kathmandu Valley sediments, the Lesser Himalaya, the Siwalik Group and the Indogangatic Plains.

Seven representative segments from upstream to downstream are classified based on geomorphological characteristics in to C2, F2, F2, B2a, F3, D4 and F3 stream types. Morphological characteristics and river dynamics of the segments at different geological terrains are variable and are controlled by topography and local geology. The C2 stream-type developed at the Kathmandu Valley sediment is stable, the F2 and B2a stream-types developed at the Lesser Himalaya are potentially degradational and those of F3, D4 and C3 stream-types at the Siwaliks are potentially aggradational. The dimensionless shear stresses in F2, B2a and F3 stream-types exceed the corresponding critical dimensionless shear stresses, and the existing bankfull depths and water surface slopes exeed the corresponding required mean depths and bankfull water surface slopes. The stream powers at these segments are conspicuously higher compared to the rest of the study segments. Hence, the F2, B2a streams in the Lesser Himalayan terrain and the F3 streams in the Siwalik terrain are competent enough to transport their available bed materials load probably due to change in topography, slopes, and morphology.

Cite as: Shrestha, P. and Tamrakar, N.K., 2014, Morpho-dynamic characteristics and their controls, Bagmati River of Central Nepal Himalaya, in Montomoli C., et al., eds., proceedings for the 29th Himalaya-Karakoram-Tibet Workshop, Lucca, Italy.

Towards a high-resolution seismic image of the lithospheric structure of the Himalayan orogenic wedge beneath Bhutan

Julia Singer[1], György Hetényi[1,2], Edi Kissling[1], Tobias Diehl[2]

[1] Department of Geophysics, ETH Zürich, Zürich, Switzerland, julia.singer@erdw.ethz.ch
[2] Swiss Seismological Service, ETH Zürich, Zürich, Switzerland

In the Eastern Himalaya the main lithospheric structure of the orogenic wedge across and perpendicular to the Himalayan range is only poorly constrained compared to the Western and Central Himalaya. Neither the detailed geometry of the dipping crust-mantle boundary (Moho) of the Indian lithosphere, nor the major crustal detachment of the Main Himalayan Thrust (MHT) have been yet well resolved for this region. For a better understanding of the orogenic wedge kinematics in this part of the Himalaya, like crustal exhumation rates or thrust faulting the geometry of these structures is essential.

We use data from a temporary seismological network in Bhutan (GANSSER project) to determine the first order lithospheric and seismic structure in the Eastern Himalaya with receiver functions and a minimum 1-D velocity model. First results of the receiver function study show a significant variation in their characteristics across the network, between Western and Eastern Bhutan, and across the Himalaya. This indicates a non-uniform dipping geometry of the Indian Moho beneath the Eastern Himalaya and an intra-crustal interface with a major velocity contrast, likely corresponding to the MHT. In combination with the minimum 1-D velocity model we provide first insights into the crustal velocity structure of the Bhutan Himalaya and physical properties of the crustal wedge material.

Cite as: Singer, J., Hetényi, G., Kissling, E. and Diehl, T., 2014, Towards a high-resolution seismic image of the lithospheric structure of the Himalayan orogenic wedge beneath Bhutan, in Montomoli C., et al., eds., proceedings for the 29th Himalaya-Karakoram-Tibet Workshop, Lucca, Italy.

Climate Variability during the past 50 ka in the Trans Himalaya- a case study from Tangtse Valley, Ladakh

Randheer Singh[1], Binita Phartiyal[1], S.K. Patil[2]

[1] Birbal Sahni Institute of Palaeobotany, Lucknow, 226007, India, randheer.singh@gmail.com
[2] Dr. K. S. Krishnan Geomagnetic Laboratory, Allahbad, Jhunsi

The Tangtse valley encompasses the eastern most tip of the Indian territory of Ladakh. In this area, the strike–slip Karakoram Fault (KKF) bifurcates in two strands viz. the SW Tangtse Strand and NE Pangong Strand (Rutter, 2007). The River Tangtse, a tributary of River Shyok has served as a spillway during the high strands (Norin, 1946) of the Pangong Tso (lake), occupies a 94.18 km long course in the KKF zone and covers almost 2170 sq km basin area. Active nature of KKF in the area is evident by presence of various features like strath terraces (28 m), offset of streams (200-400 m), wide valley filled with debris flow, abandoned channels, gorges, straight river course with the swirls and fluvio-lacustrine sediments at the height of ~50-60 m above from the present day river level. Lacustrine, fluvial and flood facies are exposed below the Shachukul village (the type section (ST)). Two phases of fluvial regime at 48 ± 4 and between 30 ± 6 to 21 ± 2 ka draining Pangong Tso into the River Shyok and a lacustrine phase between ~9.6 to ~5.1 ka inundating the whole valley are recorded. A flood event dated to ~3.4 ka is also recorded.

The lacustrine phase between ~9.6 to ~5.1 ka (ST-A of 7.40 m and ST-B of 17.5 m sections) was analysed to decipher the climatic variability using environmental magnetism (χ_{lf}, ARM, χ_{ARM}, χ_{ARM}/χ_{lf}, SIRM, SIRM/ARM, S-ratio and SIRM/χ_{lf}) and loss on ignition. The variations in the fundamental mineral magnetic parameters are correspondent to the changes in catchment weathering, detrital influx and authigenic productivity and are used to indicate the climatic variability between warm and cold conditions. Enhanced susceptibility (χ_{lf}), high χ_{ARM} and enhanced SIRM, indicate increased catchment weathering, increasing concentration of detritus input and show a drier and colder phase. During warm periods, on the other hand, fine sediments were deposited and the magnetic signals of concentration are therefore reduced in this high altitude cold desert region. Therefore it is assumed that the low values of χ_{lf}, SIRM and soft IRM values correspond to comparatively warmer climatic conditions. The variations in the studied parameters divide the lacustrine span (~9.6 to ~5.1 ka) this span in 5 Magneto-zones (MZ-I to MZ-V).

The sections are composed of thick, massive buff coloured clays with intermittently placed sand and silt beds. The MZ1 (~9.6 to ~8.4 ka), MZ-3 (~7.8 to ~7.2 ka) and MZ 5 (~6.8 to ~6 ka) shows a stable lake condition with a warm climate record. While in MZ-2 (~8.4 to ~7.9 ka and MZ-4 (~7.2 to ~6.8 ka) a shift towards cold climate conditions is seen. Perhaps the ~11 ka flooding (Dortch et al., 2011) and the early Holocene warming may have led to the lake formation in this valley with very stable conditions during MZ1.

For ST-A section majority of the pronounced peaks in χ_{lf} positively correlate with the susceptibility of ARM (χ_{ARM}), suggesting predominance of Single Domain (SD) magnetite that is characterizes authigenic forms favouring restricted and calm bottom water conditions and/or (ii) those generated during poorly drained soil forming processes in lake catchments. At ~5 ka an 8 m thick deposit constituting fine to medium sand having clay lens and clay ball at different levels,is recorded with a high sedimentation rate. Later at ~3 ka, a 9.7 m flood facies section of intermittent clay and sand having cross bedded sand, slity sand layers is seen. The authigenic SD magnetite indicate less oxygenated water condition for a short while due to the turbid water of flood event in Flood facies section. High magnetic susceptibility indicates high ferromagnetic content.

A detailed work on chronology, textural and geochemical analysis is in progress and will strengthen this dataset of Quaternary researches from the Ladakh area.

References

Dortch, J.M., Owen, L.A., Caffee, M.A., Kamp, U., 2011, Catastrophic partial drainage of Pangong Tso, northern India and Tibet, Geomorphology, 125, 109-121.

Norin, E., 1946, Geological Explorations in Western Tibet Reports from the Scientific Expedition to the North-Western Provinces of China under the Leadership of Dr. Sven Hedin /3, Thule, 214p.

Rutter, E.H., Faulkner, D.R., Brodie, K.H., Phillips, R.J., Serale, M.P., 2007, Rock Deformation processes in the Karakoram fault zone, Eastern Karakoram, Ladakh, NW India, J. Struct. Geol., 29, 1315-1326.

Cite as: Singh, R., Phartiyal, B. and Patil, S.K., 2014, Climate Variability during the past 50 ka in the Trans Himalaya- a case study from Tangtse Valley, Ladakh, in Montomoli C., et al., eds., proceedings for the 29th Himalaya-Karakoram-Tibet Workshop, Lucca, Italy.

Pan-African Magmatism and Himalayan Collisional Tectonism

Sandeep Singh[1]

[1] Department of Earth Sciences, IITRoorkee, Roorkee – 247 667, India, sandpfes@iitr.ernet.in

The Himalayan orogenic belt provides unique opportunity to investigate the Cenozoic collision and crustal shortening of a remobilised Proterozoic basement and cover sediments within a major northeast-dipping 15 -20 km thick intracontinental ductile shear zone. The remobilized Proterozoic basement has been exposed as the Himalayan Metamorphic Belt (HMB) and has been thrust south-westward over the Lesser Himalayan sedimentary sequence along the Main Central Thrust (MCT) and its various splays, e. g. the Jutogh/Vaikrita Thrusts etc. Just north of this major tectonic boundary a granite belt is exposed from Pakistan to eastern Nepal as independent isolated plutons occurring as tabular concordant sheet within the Himalayan Metamorphic Belt (HMB). These bodies have almost similar tectonic, petrographic and geochemical characters in distinct tectonic zone as elongated medium to large size intrusive bodies within low to medium grade metamorphic rocks, absolute ages around 500 Ma, high Sr ratios around 0.72, marginally well foliated, coarse grained gneissose bodies having undeformed massive to porphyritic core, development of thermal contact areoles, presence of abundant metasedimentary xenoliths, and is superposed by Himalayan deformation and metamorphism.

The Pan-African magmatism has been a known phenomenon in Himalaya. The southern limit of this magmatism is Main Central Thrust (MCT). This magmatism represent a part of large thermo-magmatic episode and is associated with a mega-zone of crustal extension, thinning and melting of the lower crust. The magmatism has been recognized from three different regions within the Himalaya; (i) The Lesser Himalayan Granite Belt (LHGB), (ii) Granites at the northern limit of Higher Himalayan Crystallines (HHC) and (iii) North-Himalayan Granite Belt comprises of a series of domes.

These granitic belts are S-type peraluminous, porphyritic in character with discontinous gneissoe and non-gneissic bodies and accompanied by post-magmatic deformation leading to development of mylonitic fabric along their margins. An attempt has been made to date the LHGB (Mandi and Dalhousie body) as well as North-Himalayan Granite Belt (Jispa body). The Mandi and Dalhousie bodies are intruding within the Jutogh Group of rocks. Mandi body has the development of foliation paralleling the main foliation of the schist and psammite sequences. Within the country rock the presence of tight fold having flame-type hinge developed during the D1-pre-Himalayan deformation on lithological/metamorphic banding S0. This deformational phase is missing within the Mandi Granite body. This indicate that the granite body is having only main Himalayan fabric development and the country rock has two fabrics causing the main fabric as a composite fabric. Out of these two fabrics one is pre-Mandi Granite fabric. The date of Mandi Granite indirectly tells about the timing of the formation of the fabric which was already there at the time of crystallization of Mandi Granite (i.e. 469 ± 8 Ma U-Pb SHRIMP age). It has aalso been observed that Mandi body do not inherit any older zircon whereas Dalhousie Body show single population for the body to be 463 ± 8 Ma (U-Pb SHRIMP age) with older inherited near-concordant cores scattered with ages ranging from about 1200 Ma to 700 Ma without clear peaks indicating involvement of mid to late Proterozoic crust. However, Jispa body having TIMS U-Pb lower intercept age to be 457 ± 41 Ma having upper intercept at ~2500 Ma.

These ages substantiate that there has been a wide magmatic activity around Cambro-Ordovician time which can be attributed to Pan African orogeny. These magmatic ages have coeval Pan-African garnet ages along the Himalaya ranging from 548 ± 24 Ma (Alakhnanda Valley) to 436 ± 8 Ma (Barun Gneiss) as well as several unconconformities in the Lesser and the Tethyan Himalaya, including a distinct angular relationship between the Cambrian and Ordovician sequences in the Tethyan part and folded Cambrian sediments sealed by Ordovician strata.

Cite as: Singh, S., 2014, Pan-African Magmatism and Himalayan Collisional Tectonism, in Montomoli C., et al., eds., proceedings for the 29th Himalaya-Karakoram-Tibet Workshop, Lucca, Italy.

Role of Internal Thrusts in NW Sub-Himalaya, India, for SHA

Tejpal Singh[1], A. K. Awasthi[2], Daisy Paul[3], R. Caputo[4]

[1] CSIR-Centre for Mathematical Modelling and Computer Simulation, Bangalore 560037, India, geotejpal@yahoo.co.in; tejpal@cmmacs..ernet.in
[2] Department of Petroleum Engineering, Graphic Era University, Dehradun, India
[3] Vellore Institute of Technology (VIT) University, Vellore (India)
[4] Department of Physics of Earth Sciences, University of Ferrara, Ferrara (Italy)
formerly at: Department of Earth Sciences, Indian Institute of technology Roorkee, Roorkee 247667, India

Continuous convergence of the Indian and Eurasian plates along the Himalayan arc is manifested as uplifted topography, short and long term shortening rates and inter-seismic strain. The proportion in which each of the above said elements contributes is, however, different along different sectors of the Himalaya. For example, the bulk shortening along the central part of the Himalaya is mainly accommodated along the Himalayan Frontal Thrust (HFT) (Wesnousky et al., 1999; Lave and Avouac, 2000). Accordingly, it has been hypothesized that the tectonic wedge of the Sub-Himalaya represents an expanding mountain front, in the central part. The present study is aimed at testing this hypothesis in the NW Himalaya of India by integrating field observations and results of geomorphic investigations.

The Himalayan arc is marked by significant along-strike lateral variations in the geology, structure and seismicity (Singh et al., 2012; Gahalaut and Arora, 2012). In the NW Sub-Himalaya of India the deformation front is conspicuously characterized by actively deforming frontal anticlines running parallel to the mountain front (Singh and Jain, 2012). Here the sedimentation pattern indicates fold growth initiation as young as 0.78 Ma (Rao et al., 1998). Field mapping and observations about the presence of typical geomorphic surfaces along mapped internal thrust faults, here, amply demonstrate that the deformation is not restricted to the HFT alone; rather it is distributed across different thrusts running parallel to the Sub-Himalayan belt. Previous work on the stream profiles by the authors had clearly indicated that major internal thrust fault, eg. Nahan Thrust, is active (or in fact reactivated) to absorb the impact of continuous convergence (Singh and Awasthi, 2010). However, the present work in detail has highlighted active shortening along the internal thrust system in the Kangra area. Many of these thrusts cut and/or override the Quaternary deposits to the north of the HFT. Studies on surficial deposits, geometrical patterns and morphological analyses of streams patterns indicate that such deformation have been going on even during the last few thousand years along these internal thrusts.

The new results draw us to infer that the tectonic wedge of the Sub-Himalayan Fold Thrust Belt is mechanically constrained internally by thrust faults other than the range-bounding HFT. Similar inferences have also been drawn, alternatively, by statistical analysis of the taper parameters of the tectonic wedge (Singh et al., 2012). However, owing to the curvilinear surface trace of the thrust faults, the internal thrusts tend to merge with the main range-bounding thrusts (HFT and MBT in the present case); thereby placing much importance (or prominence) to the range-bounding thrusts rather than the internal thrusts. In such a case, the role of internal thrusts that are relatively limited in spatial dimensions seem to be undermined. Moreover, in areas with widely spaced range-bounding thrusts, the impact of internal thrusts, though smaller in dimension but larger in number becomes significant. This observed scenario becomes important in evaluating the seismic hazard of any region characterized by a large number of internal thrusts. This becomes even more important where the width of the Sub-Himalayan belt varies significantly from as much as ~ 80 km in the Kangra sector to ~20 km in the Nahan sector of India. This present study emphasizes that the internal thrusts play a very significant role in the seismicity of the NW Sub-Himalaya of India. Also, it clearly indicates that the cumulative role/impact of the internal thrusts in the NW Himalaya is much more in accommodating the overall India-Asia convergence than the range bounding thrusts. Further, this style of deformation is in clear contrast to that observed in the Central Himalaya. It is therefore surmised that the internal thrusts should be seriously considered for any seismic hazard evaluation program to be more realistic and successful.

References

Gahalaut, V.K. and Arora, B.R., 2012, Episodes, 35, 493-500.
Lave, J. and Avouac, J.P., 2000, J. Geophys. Res., 105 (B3), 5735-5770.
Rao, A.R., Agarwal, R.P., Sharma, U.N., Bhalla, M.S. and Nanda, A.C., 1998, J. Geol. Soc. India, 31, 361-385.
Singh, T. and Awasthi, A.K., 2010, Curr. Sc., 98, 95-98.
Singh, T., Awasthi, A.K. and Caputo, R., 2012, Tectonics TC6002, 1-18.
Singh, T. and Jain, V., 2009, Geomorphology, 106, 231-241.
Wesnousky, S.G., Kumar, S., Mohindra, R. and Thakur, V.C., 1999, Tectonics, 18, 967-976.

Cite as: Singh, T., Awasthi, A. K., Paul, D. and Caputo, R. 2014, Role of Internal Thrusts in NW Sub-Himalaya, India, for SHA, in Montomoli C., et al., eds., proceedings for the 29th Himalaya-Karakoram-Tibet Workshop, Lucca, Italy.

Paleo-denudation history of the Ladakh Batholith - new constraints from bedrock and detrital apatite (U-Th-Sm)/He thermochronology

Mohammad S. Sohi[1], Ruben Rosenkranz[1], Cornelia Spiegel[1]

[1] Departement of Geoscience, Universität Bremen, Klagenfurter straße, 28359 Bremen, Germany, sohi@uni-bremen.de

The Ladakh Batholith is part of the Transhimalayan Plutonic Belt and records the early exhumation history of the Himalayan orogen. The evolution of the Ladakh Batholith is complex and was controversially discussed in the literature (see Kirstein, 2011 for details). Recent data by Kirstein et al. (2006 & 2009) suggest a trend of exhumation rates across the batholith, with earlier exhumation along its southern margin and later exhumation in the north.

Apart from methodological purpose aimed at refining the apatite (U-Th-Sm)/He technique, the goal of our study is to investigate the earliest denudation history of the Ladakh Pluton and thereby that of the Himalayan orogen, using apatite (U-Th-Sm)/He thermochronology (i) applied to bedrocks from the southern margin of the batholith, and (ii) to sediments from the adjacent Upper Indian Group sediments such as Chogdo and Sumda Formations with Oligo−Miocene in age (coincident with initiation of the paleo−Indus River system) and Choksti and Hemis conglomerates. These sediments are thought to be sourced from the Ladakh Batholith (Henderson et al., 2011).

Apatite (U-Th-Sm)/He dating is sensitive to temperatures between ~85 and 40°C and thus to geodynamic movements of the upper ~1.5 to 3 km of the earth´s crust. While thermochronology data from present-day bedrock exposures provides denudation rates integrated over the time between cooling age and the present, the earlier denudation history is eroded away from the present exposures and stored in the syn-tectonic sediments. Thus, dating sediments of the Indian Group will yield the paleo-denudation history of the (southern) Ladakh area, including changes of denudation rates back through time. This will reveal new insights into the relation between tectonics, climate, and erosion.

References

Henderson, A.L., Najman, Y., Parrish, R., Mark, D.F. and Foster, G.L., 2011, Constraints to the timing of India–Eurasia collision; a re-evaluation of evidence from the Indus Basin sedimentary rocks of the Indus–Tsangpo Suture Zone, Ladakh, India, Earth-Science Reviews, 106(3), 265-292.

Kirstein, L.A., Sinclair, H., Stuart, F.M. and Dobson, K., 2006, Rapid Early Miocene exhumation of the Ladakh batholith, western Himalaya, Geology 34, 1049-1052.

Kirstein, L.A., Foeken, J.P.T., Van Der Beek, P., Stuart, F.M., and Phillips, R.J., 2009, Cenozoic unroofing history of the Ladakh Batholith, western Himalaya, constrained by thermochronology and numerical modelling, Journal of the Geological Society, 166(4), 667-678.

Kirstein, L.A., 2011, Thermal evolution and exhumation of the Ladakh Batholith, northwest Himalaya, India, Tectonophysics, 503(3), 222-233.

Cite as: Sohi, M.S., Rosenkranz, R.V. and Spiegel, C., 2014, Reassessment of the exhumation history of the Ladakh Batholith (AHe technique), in Montomoli C., et al., eds., proceedings for the 29th Himalaya-Karakoram-Tibet Workshop, Lucca, Italy.

Recognition of the South Tibetan Detachment in the Karnali klippe, western Nepal: implications for emplacement of Himalayan external crystalline nappes

Renaud Soucy La Roche[1], Laurent Godin[1], Zoe Braden[1]

[1] Department of Geological Sciences & Geological Engineering, Queen´s University, Kingston, ON K7L 3N6, Canada, 13rslr@queensu.ca

The Himalayan external crystalline nappes are traditionally viewed as a series of Greater Himalayan Sequence (GHS) klippen carried southward on the Main Central Thrust (MCT) (Ganser, 1964), and therefore represent the southernmost exposure of the metamorphic core. Larson et al. (2010) have recently proposed that a transition exists from older mid-crustal ductile flow in the hinterland to younger thrust-fold wedge deformation propagating into the foreland. The style and timing of deformation and metamorphism in the external klippen could therefore highlight this postulated transition. In contrast, an alternative tectonic model states that the South Tibetan Detachment (STD) and the MCT merge in southern Nepal, which implies a tectonic wedge geometry for the GHS (Yin, 2006; Webb et al. 2007, 2011). If the GHS is a tectonic wedge, external klippen are consequently crucial locations to study the geometrical relationships between the MCT and STD.

Our study is located at the eastern termination of the Almora-Dadeldhura klippe in western Nepal, which was originally investigated by Frank and Fuchs (1970), Arita et al. (1984) and Hayashi et al. (1984). More recently, from observations on the northern flank of the Karnali klippe, He (2013) proposed that the MCT and the STD merge at depth, thus suggesting a tectonic wedge geometry. This interpretation, however, warrants complementary data from the southern flank of the klippe. Consequently, one of the main objectives of our study is to investigate both the northern and southern flanks of the klippe and assess the relationships between the MCT and the STD. Our mapping was carried out along a ~125 km long transect from Jumla to Dailekh in a section of the klippe commonly referred to as the Karnali klippe (e.g. Upreti and LeFort, 1999; Johnson, 2005). This area occupies an intermediate geographic position between the typical homoclinal exposure of the GHS to the north and the southernmost crystalline klippen.

The Karnali klippe is an east-west trending synform defined at the base by a ~2 km thick folded top-to-the-southwest reverse-sense shear zone. Greenschist to amphibolite metamorphic-facies rocks consist of abundant granitic orthogneiss with common metapelite and local calcsilicate gneiss, quartzite and meta-arenite. The metamorphic field gradient increases from biotite grade near the basal shear zone to kyanite grade in the upper structural levels. On the southwestern flank, however, a decrease to staurolite grade is observed towards the top-bounding shear zone. The metamorphic rocks record both coaxial and top-to-the-southwest non-coaxial strain. Quartz deformation textures suggest temperatures of deformation in excess of 500 °C. In contrast, the structurally highest levels of the klippe exposes a ~1 km thick top-to-the-northeast shear zone that separates footwall metamorphic units from lower greenschist facies to subgreenschist sedimentary rocks in the hanging wall. This shear zone corresponds to a drastic change in lithology and break in metamorphic grade; above it, rocks vary structurally upwards from calcareous meta-arenite to micaceous crystalline limestone and silty laminated limestone. Quartz deformation textures suggest that temperatures of deformation decrease rapidly from >500 °C in the lower part of the top-to-the-northeast shear zone to 400 °C in its upper part. Calcite twining types in the upper part of the shear zone suggest temperatures of deformation >250 °C, whereas the weakly metamorphosed limestone above the shear zone was likely deformed at lower temperatures around 150-200 °C.

We correlate the amphibolite metamorphic-facies units of the Karnali klippe with the GHS, which is exposed less than 20 km northeast of Jumla, on the basis of lithologic and metamorphic similarities. The sedimentary rocks at the structurally highest levels are tentatively correlated with the Cambro-Ordovician Tethyan sedimentary sequence (TSS) 'Yellow marble' (Robinson et al. 2006) and phyllite, quartzite and

Cite as: Soucy La Roche, R., Godin, L., and Braden, Z., 2014, Recognition of the South Tibetan detachment in the Karnali klippe, western Nepal: Implications for emplacement of Himalayan external crystalline nappes, in Montomoli C., et al., eds., proceedings for the 29th Himalaya-Karakoram-Tibet Workshop, Lucca, Italy.

marble (Murphy and Copeland, 2005) in western Nepal, and to the Annapurna-Yellow-Larjung Formation (Colchen et al. 1981, 1986) in central Nepal. This interpretation implies that the basal top-to-the-southeast shear zone represents the MCT and the top-to-the-northeast shear zone is the STD. The presence of the STD on the north and west flanks of the folded TSS and the presence of GHS rocks southwest of the TSS contradicts conclusions that the STD and the MCT merge at depth in the core of the klippe (He, 2013), and therefore weakens the argument for tectonic wedging in western Nepal. The geology of the Karnali klippe is similar to that of the Dadeldhura klippe in far western Nepal (Antolín et al. 2013). Although both klippen expose medium to high metamorphic grade rocks bounded by a lower top-to-the-southwest shear zone and an upper top-to-the-northeast shear zone with low metamorphic grade rocks at the highest structural levels, lithological correlation between the two klippen is uncertain. Metapelitic rocks are near absent in the metamorphic part of the Dadeldhura klippe, where slate and phyllite comprise the structurally highest units. In contrast, metapelitic rocks are common in the metamorphic part of the Karnali klippe and carbonate rocks comprise the structurally highest units. The lithologic differences between the Dadeldhura and Karnali klippen could be a reflection of lateral protolith variation, contrasting structural levels of the TSS cut by the STD (e.g. Searle and Godin, 2003), or the fundamental and independent nature of the Dadeldhura and Karnali klippen (e.g. Upreti and LeFort, 1999).

References

Antolín, B., Godin, L., Wemmer, K., Nagy, C., 2013, Kinematics of the Dadeldhura klippe shear zones (W Nepal): implications for the foreland evolution of the Himalayan metamorphic core, Terra Nova, 25(4), 282-291.

Arita, K., Shiraishi, K., Hayashi, D., 1984, Geology of western Nepal and a comparison with Kumaun, India. J. Faculty of Sci, Hokkaido University. Series 4, Geology and mineralogy, 21(1), 1-20.

Colchen, M., LeFort, P., Pêcher, A., 1981, Geological map of Annapurnas-Manaslu-Ganesh Himalaya of Nepal, in Gupta, H.K., and Delany, F.M., eds., Zagros–Hindu Kush–Himalaya geodynamic evolution, Washington, D.C., American Geophysical Union, scale 1:200,000.

Colchen, M., LeFort, P., Pêcher, A., 1986, Geological research in the Nepal Himalayas, Annapurna– Manaslu–Ganesh Himal: Paris, Centre National de la Recherche Scientifique, scale 1:20,000, 137 p.

Frank, W., Fuchs, G.R., 1970, Geological investigations in west Nepal and their significance for the geology of the Himalayas. Geologische Rundschau, 59(2), 552-580.

Gansser, A., 1964, Geology of the Himalayas: London,Wiley Interscience, 289 p.

Hayashi, D., Fujii, Y., Yoneshiro, T., Kizaki, K., 1984, Observations on the geology of the Karnali Region, West Nepal: J. Nepal Geol. Soc., 4, 29-40.

He, D., 2013, Contractional tectonics: the Himalayan orogen and Perdido fold-thrust belt, Ph.D. thesis, Louisiana State University, Baton Rouge, United States of America, 163 p.

Johnson, M.R.W., 2005, Structural settings for the contrary metamorphic zonal sequences in the internal and external zones of the Himalaya. J. Asian Earth Sci., 25(5), 695-706.

Larson, K., Godin, L., Price, R.A., 2010. Relationships between displacement and distortion in orogens: linking the Himalayan foreland and hinterland in central Nepal, Geol. Soc. Am. Bull., 122(7-8), 1116–1134.

Murphy, M.A., Copeland, P., 2005, Transtensional deformation in the central Himalaya and its role in accommodating growth of the Himalayan orogen, Tectonics, 24, TC4012.

Robinson, D.M., DeCelles, P.G., Copeland, P., 2006, Tectonic evolution of the Himalayan thrust belt in western Nepal: Implications for channel flow models, Geol. Soc. Am. Bull., 118(7-8), 865-885.

Searle, M.P., Godin, L., 2003, The South Tibetan detachment and the Manaslu leucogranite: A structural reinterpretation and restoration of the Annapurna-Manaslu Himalaya, Nepal, J. Geol., 111, 505– 523.

Upreti, B.N., Le Fort, P., 1999, Lesser Himalayan crystalline nappes of Nepal: problem of their origin, Geol. Soc. Am. Spec. Pap., 328, 225-238.

Webb, A.A.G., Yin, A., Harrison, T.M., Célérier, J., Burgess, W.P., 2007, The leading edge of the Greater Himalayan Crystallines revealed in the NW Indian Himalaya: Implications for the evolution of the Himalayan Orogen: Geology, 35, 955-958.

Webb, A.A.G., Schmitt, A.K., He, D., Weigand, E.L., 2011, Structural and geochronological evidence for the leading edge of the Greater Himalayan Crystalline complex in the central Nepal Himalaya, Earth Planet. Sci. Lett., 304, 483-495.

Yin, A., 2006, Cenozoic tectonic evolution of the Himalayan orogen as constrained by along-strike variation of structural geometry, exhumation history, and foreland sedimentation, Earth Sci. Rev., 76, 1-131.

The NE-directed Shikar Beh nappe in the Himalayan orogenic prism of Lahul and Ladakh

Albrecht Steck[1], Jean-Luc Epard[1], Martin Robyr[2], Micha Schlup, Jean-Claude Vannay

[1] University of Lausanne, Geopolis, CH-1015 Lausanne, Switzerland, Albrecht@unil.ch
[2] University of Bern, Baltzerstrasse 1-3, 3012 Bern

Two belts of SW-verging folds and thrusts dominate the structure of the Himalaya. The North Himalayan nappes are composed of the north Indian Tethys shelf sediments and their Paleozoic and Precambrian base. They are situated between the Indus-Tsangpo suture to the north and the Zanskar shear zone to the south. The High Himalayan nappe with its frontal Main Central and Main Boundary thrusts occupies the southern part of the orogenic prism. These, SW-directed nappes have been formed by underthrusting of the Indian margin below Asia since 55 Ma. Structural and metamorphic investigations in the Chenab, Miyar, Kullu and the Spiti valley regions of the Higher Himalaya show the existence of older NE-verging folds and thrusts, associated with an older up to amphibolite facies metamorphism. This is the Shikar Beh nappe that extends from the Suru valley to the NW to the Spiti valley to the SE over a distance of 400 and a width of 60 km. The overprint of the Shikar Beh nappe structures by the North Himalayan frontal thrusts is observed in the Chandra valley at Batal and in the Spiti valley to the East of Kiato. SW-verging folds of the High Himalayan nappe deform the NE-verging Tandi syncline composed of Permian to Triassic limestones. Similar fold interference structures are responsible for the fan-shape folds in the upper Chenab and lower Miyar valley. Radiometric dating indicate an age of 53 Ma for the Tso Morari ultra-high pressure metamorphism, 48-30 Ma for the North Himalayan nappes and >22 – 18 Ma for the Zanskar Shear Zone and the High Himalayan nappe extrusion. Younger cooling ages indicate continuous movements on the Main Central and Main Boundary Thrusts up to the present. Radiometric ages of the polymetamorphic Higher Himalaya give >42 – 30 Ma for the Shikar Beh nappe Barrovian metamorphism. New Th-Pb monazite ages of 42 ± 2 and 38 ± 0.7 Ma were obtained for the Miyar thrust zone associated to the same event. The formation of the intra-continental NE-directed Shikar Beh nappe testifies of compressional forces acting on the Indian crust during its underthrusting. This fact suggests that slab-pull was probably not the exclusive force acting on the Indian crust during its underthrusting below Asia.

References

De Sigoyer, J., Chavagnac, V., Blichert-Toft, J., Villa, I.M., Luais, P., Guillot, S., Cosca, M. and Mascle, G., 2000, Dating the Indian continental subduction and collisional thickening in the northwest Himalaya: Multichronology of the Tso Morari eclogites, Geology, 28, 487-490.

Epard, J.-L. and Steck, A., 2008, Structural development of the Tso Morari ultra-high pressure nappe of the Ladakh Himalaya, Tectonphysics, 451, 242-264.

Frank, W., Thöni, M. and Purtscheller, F., 1977, Geology and petrography of the Kulu-South Lahul area, Colloques internationaux du CNRS, 268, 147-160.

Honegger, K.H., 1983, Struktur und Metamorphose im Zanskar Kristallin, Ph.D. thesis, ETH-Zürich.

Leech, M.L., Sing, S., Jain. A.K., Klemperer, M.R. and Manickavasagam, R.M., 2005, The onset of India-Asia continental collision: early steep subduction required by the timing of UHP metamorphism in the western Himalaya, Earth Planet. Sci. Lett., 234, 83-97.

Robyr, M., Vannay, J.-Cl., Epard, J.-L. and Steck, A., 2002, Thrusting, extension and doming during the polyphase tectonometamorphic evolution of the High Himalayan Crystalline Zone in NW India, J. Asian Earth Sci., 25, 221-239.

Schlup, M., Steck, A., Carter, A., Cosca, M., Epard, J.-L. and Hunziker, J., 2011, Exhumation history of the NW Indian Himalaya revealed by fission track and $^{40}Ar/^{39}Ar$ ages, J. Asian Earth Sci., 40, 334-350.

Steck, A., 2003, Geology of the NW Indian Himalaya, Eclogae Geologicae Helvetiae (Swiss Journal of Earth Sciences), 96, 147-196.

Weinberg, R.F. and Dulap, W.J., 2000, Growth and deformation of the Ladakh Batholith, Northwest Himalayas: implications for timing of continental collision and origin of Calc-Alcaline Batholiths, The Journal of Geology, 108, 303-320.

Cite as: Steck, A., Epard, J.-L., Robyr, M., Schlup, M. and Vannay, J.C., 2014, The NE-directed Shikar Beh nappe in the Himalayan orogenic prism of Lahul and Ladakh, in Montomoli C., et al., eds., proceedings for the 29th Himalaya-Karakoram-Tibet Workshop, Lucca, Italy.

Great Earthquakes Recurrence Times in the Eastern Himalayas

Paul Tapponnier[1], Laurent Bollinger[2], Elise Kali[3], Aurelie Coudurier-Curveur[1], Çağıl Karakaş[1], Magali Rizza[4], Soma N. Sapkota[5], Saurabh Baruah[6], Swapnamita Choudhury[7], Jerome Van der Woerd[3], Yann Klinger[8], Emile Okal[9]

[1] Earth Observatory of Singapore, Nanyang Technological University, Singapore 639798, Singapore, tappon@ntu.edu.sg
[2] Département Analyse et Surveillance Environnement, CEA, DAM, DIF, F-91297 Arpajon, France
[3] Institut de physique du Globe de Strasbourg, UMR CNRS/UdS 7516, 67084 Strasbourg, France
[4] CEREGE, Aix-Marseille Université, Marseille, France
[5] National Seismic Center, Department of Mines and Geology, Lainchaur, Kathmandu, Nepal
[6] North-East Institute of Science and Technology, Jorhat, India
[7] Wadia Institute of Himalayan geology, Dehradun, India
[8] Institut de Physique du Globe de Paris, UMR 7154, 75238 Paris, France
[9] Department of Earth and Planetary Sciences Northwestern University, Evanston, IL, United States

Contrary to consensus, the two great Himalayan earthquakes of the mid-20th century were not blind. In eastern Nepal, the surface rupture of the Mw ≈ 8.4, 1934 "Bihar-Nepal" earthquake, unambiguously exposed in the region of Bardibas, probably extended at least 150 km along the Main Frontal Thrust (MFT). In Arunachal Pradesh, we recently discovered unmistakable field evidence for the surface rupture of the great, Mw ≈ 8.7, 1950 Assam earthquake. Both ruptures bound hanging walls with spectacularly uplifted fluvial terraces.

In the easternmost part of Nepal, the penultimate great event was the AD 1255 earthquake. Given preliminary observations of characteristic slip, the hanging-wall of the Patu thrust – one of two overlapping strands of the MFT near Bardibas - likely recorded 3 more great events in the last 3650 ± 450 years. Each would have accommodated 15 ± 2.5 m of slip on the 25° ± 5° dipping thrust, in keeping with an uplift rate of 8.5 ± 1.5 mm/yr and with the shortening deficit accumulation rate (≈ 18 mm/yr) derived from cGPS measurements. In the past 4500 ± 50 years, up to 7 events appear to have been recorded on the other local MFT strand, the Bardibas Thrust. Hence, since the mid-Holocene, the average return time of great MFT earthquakes in eastern Nepal has probably been between 750 ± 150 and 875 ± 250 years.

In Arunachal Pradesh, along a remarkably fresh thrust rupture found near Wakro, the bedrock and strath terrace co-seismic uplifts are ≈ 7 m, with nearly identical surface throw in the penultimate event. The rupture, most likely that of the 1950 earthquake, continues northwards along the Mishmi thrust, then eastwards along the MFT past Pasighat after a high-angle bend at the Dibang valley outlet. The ≈ 90 km-wide, ≈ 350 km-long source of the great Assam earthquake was thus composed of two nearly orthogonal patches, with perhaps similarly oriented slip-vectors along an intersection near 95°30' E. Dating of uplifted terraces is still in progress, but the average return time of mega-thrust earthquakes around the Arunachal syntaxis may turn out to be longer than in eastern Nepal.

Cite as: Tapponnier, P., et al, 2014, Great Earthquakes Recurrence Times in the Eastern Himalayas, in Montomoli C., et al., eds., proceedings for the 29th Himalaya-Karakoram-Tibet Workshop, Lucca, Italy.

Climate change impacts on Chitral-Kabul trans-boundary rivers, Northern Pakistan

Shahina Tariq[1], Maqbool Ahmad[2], Irfan Mahmood[1]

[1] Department of Meteorology, COMSATS Institute of Information Technology, Islamabad, Pakistan, shahinatariq@comsats.edu.pk
[2] Albadar Model School and College, District, KPK, Pakistan.

Climate change presents the most significant environmental challenges and its impacts on water resources is quite uncertain, and can strongly affect the river flows system in many countries. Many rivers and lakes are shared by two or more nations and crosses political borders. Because of economic instability and technological deficiency, a number of developing countries are incapable to take firm policy-decisions for rapid actions to address the environment and climate-related problems. The case study is based on monitoring the impacts of climatic changes on trans-boundary river basin of Chitral in the northern areas of Pakistan. The basin occupies an area of 15,322.4 sq. km out of which the glacier area is about 1,903.7 sq. km (Figure.1). Kabul River flows between two countries specifically Pakistan and Afghanistan. It is considered as a central river of Asia, originates from the Kohi-Baba Mountain in Afghanistan and flows past the valley of Chitral of Hindu Kush Mountains, and Peshawar valley of Himalayas Pakistan. The study area covers a trans-boundary watershed, left part of the watershed lie in northern areas of Pakistan and right part of it wraps the Afghanistan region. The Kabul river water resources are shared between Afghanistan and Pakistan and the river is mostly composed of glacier and snow fed water and naturally flows throughout the year with additional runoff during the monsoon period and playing a vital role in assisting the irrigation and other domestic activities. The trans-boundary watershed and Kabul River are facing climate change impacts via changing pattern of precipitation, temperature and water discharge. Kabul River is a strong water contributing source for Indus River in Pakistan and backbone of the most water based economical activities. The construction of new reservoirs on Kabul River in Afghanistan and variability of water will affect the flow and can cause drought or flood in Pakistan that mainly affect the agriculture sector, especially a fast growing urbanization and industrialization in and around the major cities of Peshawar and Chitral can become a threatening state to the climate as well as groundwater resource system of both valleys.

In this way the water resource system proved to possess more sensitivity towards climate change particularly on conditions like rainfall, flood and water supply to the rivers. The assessment of these impacts is carries importance for an efficient, effective and sustainable planning for water resource. Meteorological data and Landsat Satellite Remote Sensing data were used to observe the effect of climate change indicators on trans-boundary river sites. The variability is measured at gauging station of Chitral and Warsak. Statistics are shown that the temperature and rainfall has increasing pattern for the Chitral and Peshawar valleys, indicating the negative impacts on the future environmental sustainability. The supervised and un-supervised classification and change detection techniques were adopted to assess the land use and land cover features to salvage its class boundaries. The results obtained have shown an increase in both barren land as well as urbanization from 58.168 km^2 to 264.35 km^2 and decreases in the dense areas and as well as light vegetation land from 608.85 km^2 to 411.69 km^2 and 173.25 km^2 to 105.77 km^2 respectively. The accuracy evaluation test was applied for the determination of image of 1985, which reflected the overall accuracy equal to 91.67% while Kappa statistics was calculated as 0.8657. However the user accuracy indicated 92.31%, for rocks while for rocks mix vegetation it was 93.88%, for soil 98.66%. From the result for image of 2011, the assessment reported was 93.65% for rocks, 92.50% for rocks mix vegetation and 83.33% for soil. The overall user accuracy was 91.67% and overall Kappa statistics was given as 0.8682. Our findings are in relation to the facts proved already from the current research that valleys are highly prone to climatic and environmental change.

Cite as: Tariq, S., Ahmad, M. and Mahmood, I., 2014, Climate change impacts on Chitral-Kabul trans-boundary rivers, Northern Pakistan, in Montomoli C., et al., eds., proceedings for the 29th Himalaya-Karakoram-Tibet Workshop, Lucca, Italy.

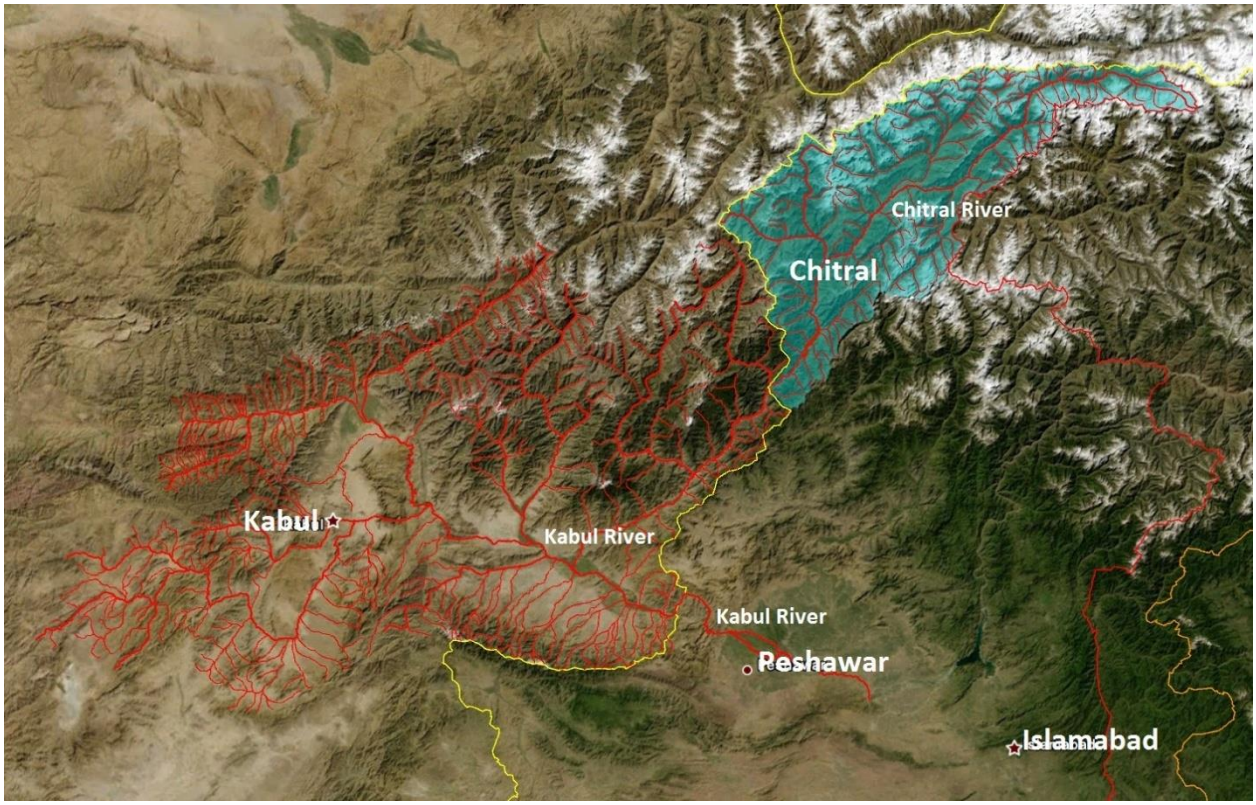

Figure 1. Satellite Image of Chitral-Kabul trans-boundary river.

Precipitation and snow resources in the Hindu-Kush Karakoram Himalaya mountains: current picture and expected changes

Silvia Terzago[1], Elisa Palazzi[1], Jost von Hardenberg[1], Antonello Provenzale[1]

[1]Institute of Atmospheric Sciences and Climate ISAC-CNR, Torino, Italy, s.terzago@isac.cnr.it

The Hindu-Kush Karakoram Himalaya and the Tibetan Plateau extend for about 5 million Km^2 and they are the largest mountain range in the world, including the 14 world's highest peaks above 8,000 m. This mountain range shapes the atmospheric circulation and the climate of South-Eastern Asia. In fact the HKKH mountains act as an orographic barrier that forces the impinging humid air masses to rise and cool, producing precipitation in the form of rain or snow.

Two main dynamical mechanisms bring humidity to the HKKH region: the summer Indian monsoon, which transports warm and moist air from the Indian Ocean northward, producing heavy precipitation during summer months, and the Western Weather Patterns (WWPs), which are weather disturbances coming from the Mediterranean and Caspian Sea and propagating eastward, mainly during winter months (Singh 1995). While the summer Indian monsoon mainly affects the southeastern slope of the Himalaya, the WWPs discharge precipitation mainly over the Hindu-Kush Karakoram mountains, feeding the glaciers and the snow reservoirs. Both summer monsoon and WWPs deeply influence human activities ,,with the former supplying water for agriculture in the dry season in the form of intense and widespread precipitation, and the latter accumulating snow resources that assure continuous river flow also in the driest months.

Changes in the spatial patterns and timing of precipitation, both liquid and solid, in HKKH would impact heavily on water resources availability in lowlands. This study evaluates the properties of precipitation in the Hindu-Kush Karakoram Himalaya region, in term of spatial pattern and temporal variability, using currently available data sets, i.e. satellite rainfall estimates (Tropical Rainfall Measuring Mission), reanalyses (ERA-Interim), gridded in situ rain gauge data (Asian Precipitation Highly Resolved Observational Data Integration Towards Evaluation of Water Resources, Climate Research Unit, and Global Precipitation Climatology Centre), and a merged satellite and rain gauge climatology (Global Precipitation Climatology Project). The results are discussed in relation to those obtained from the Global Climate Models (GCM) simulations participating in the Climate Model Intercomparison Project Phase 5 (CMIP5; Taylor et al., 2012). We highlight the strengths and weaknesses of all datasets, the skill of the GCMs and the related uncertainties.

A similar analysis has been carried out on the snowpack dynamics, still poorly known due to the difficulties in performing regular meteorological observations in high elevation areas (Qian et al., 2003). We studied the representation of snowpack, in terms of snow depth and snow water equivalent, in the HKKH region, given by a set of Global Climate Models, comparing with the main observational datasets (the National Snow and Ice Data Center Global Monthly EASE-Grid Snow Water Equivalent Climatology, the AMSR-E/Aqua Monthly L3 Global Snow Water Equivalent, the Canadian Meteorological Centre Daily Snow Depth Analysis Data) and reanalyses (ERA-Interim/Land, NCEP-CFSR, 20th Century Reanalysis V2).

We analysed precipitation trends in winter (December-April) and summer (June-September) over the "historical" period (1850-2005) covered by GCM simulations and, particularly for the winter seasons, we related the precipitation changes to the snow depth trends. For both variables we investigated the future projections up to the end of the XXI century under two climate change scenarios, RCP4.5 and RCP8.5, in order to highlight the changes that will likely affect the water cycle and water availability in the HKKH region.

References

Qian, Y.F., Zheng, Y.Q., Zhang, Y. and Miao, M.Q., 2003, Responses of China's summer monsoon climate to snow anomaly over the Tibetan Plateau, International Journal of Climatology, 23, 593-613.

Singh, P., Ramasastri, K. and Kumar, N., 1995, Topographical influence on precipitation distribution in different ranges of Western Himalayas, Nord. Hydrol., 26 (4-5), 259-284.

Taylor, K.E., Stouer, R.J. and Meehl, G.A., 2012, An Overview of CMIP5 and the Experiment Design, Bulletin American Meteorological Society, 93, 485-498.

Neotectonic modeling of Central Asia

Lavinia Tunini[1], Ivone Jiménez-Munt[1], Manel Fernàndez[1] , Jaume Vergès [1]

[1] Institute of Earth Sciences Jaume Almera (ICTJA-CSIC), Barcelona, Spain, ltunini@ictja.csic.es

Two of the most prominent deformed areas on Earth, the Zagros and Himalaya-Tibet orogens, are located along the southern margin of Eurasian plate. They are the result of Arabia/Eurasia and India/Eurasia collisions occurred in Cenozoic times. In both cases, the collision occurred between the strong and resistant lithospheres of Arabia and India (with Archean-Proterozoic shields) and weaker material along the southern edge of the Eurasian plate. Major pre-existing sutures and/or large-scale fault zones between the different accreted Gondwana-derived continental blocks are responsible for the weakness of the Eurasia margin. The convergence resulted not only in the building of mountain ranges over the north-eastern edges of the Arabian and Indian plates, but also in widespread deformation several hundreds of km inwards with respect to the suture zones. Thus, the understanding of the deformation patterns in Zagros and Himalaya-Tibet orogens requires the study of the lithospheric structure and the analysis of the deformation of the whole Central Asia region.

This work aims to study the neotectonics of Central Asia (Fig. 1), and in particular the Himalaya-Tibetan orogen. To this end, we use the thin-shell finite element code SHELLS (Bird 1999), in which the horizontal components of the momentum equation are solved using a 2-D finite element grid, and the horizontal velocities do not change in depth. Some characteristics of three-dimensional methods are incorporated, since volume integrals of density and strength are performed numerically in a lithosphere of laterally varying crustal and lithospheric mantle thicknesses.

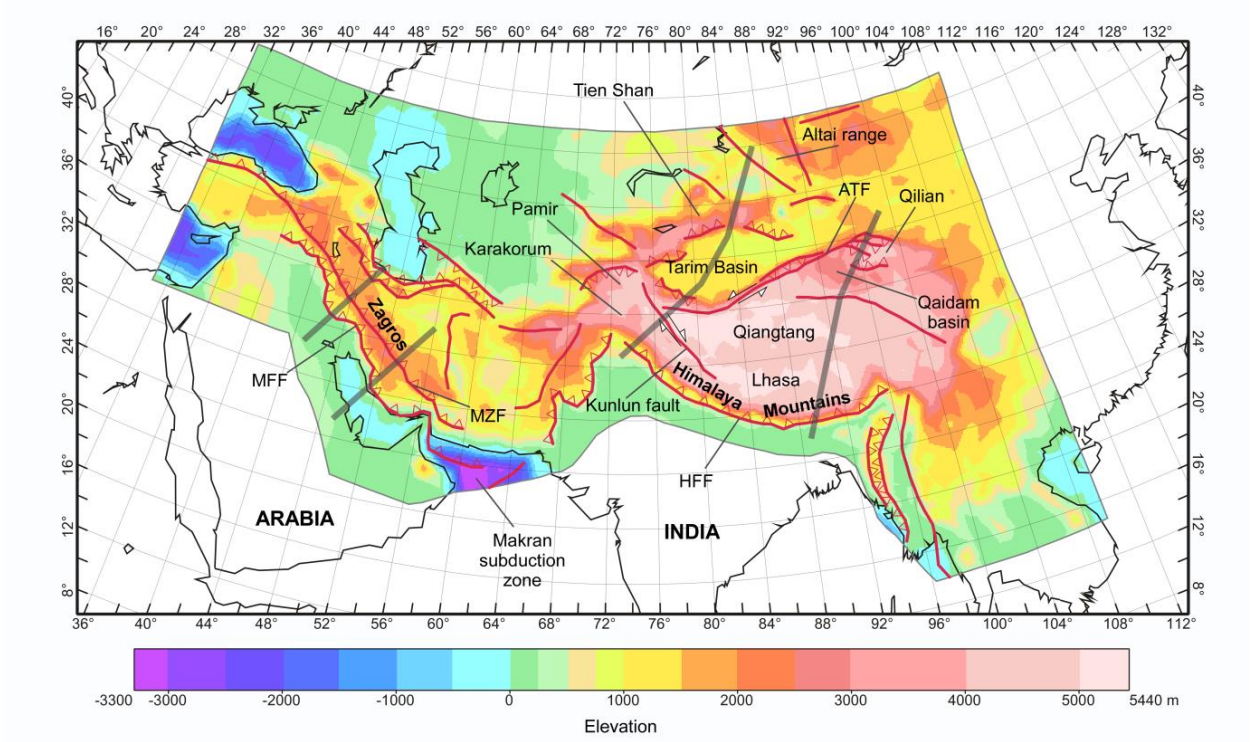

Figure 1. Topography map and main tectonic features in Central Asia. Thick light grey segments crossing Zagros and Himalaya-Tibetan orogens indicate the location of 2-D modelled cross-sections coming from the geophysical-petrological previous study. Their results on crustal and lithospheric structure are incorporated to the model.

Cite as: Tunini, L., Jiménez-Munt, I., Fernàndez, M., Vergès, J., 2014, Neotectonic modelling of Central Asia, in Montomoli C., et al., eds., proceedings for the 29th Himalaya-Karakoram-Tibet Workshop, Lucca, Italy.

In order to determine the lateral variations of the lithospheric strength, elevation, heat-flow, crustal and lithospheric thickness are calculated assuming steady-state thermal regime and local isostasy. In the updated version of the code (Bird et al., 2008) two additional adjustable parameters are incorporated at each node in order to reduce locally large departures from isostasy: i) density anomaly of compositional origin in the lithosphere; ii) extra quadratic curvature of geotherm due to transient cooling/heating.

The input crust and lithospheric mantle structures are derived from elevation and geoid anomaly, assuming local isostasy and thermal analysis (Robert et al., in prep.). Previous results using a geophysical-petrological approach along four 2D lithospheric profiles down to 400 km depth (Fig. 1) are also incorporated to the model (Tunini et al., in rev; Tunini et al., in prep.). These profiles reveal a strong strain partitioning between the crust and the lithospheric mantle affecting the Zagros and Tibet orogens. A crustal thickening along the suture zone in the Zagros range corresponds to a thinning of the subyacent lithospheric mantle (LAB depth difference ~100 km). The lithospheric mantle below the north-eastern Tibetan Plateau (eastern Lhasa and Qiangtang regions), is thin (LAB depth ~120 km), weak and warm and characterized by a typical composition of supra-subduction mantle wedge as inferred by xenolith samples. A thick, fertile and strong lithosphere characterizes the Indian plate at the southern margin of Tibetan Plateau, plunging northwards with a progressive shallower angle from east to west.

The (potentially) active faults, defined with low friction coefficient, are taken from Taylor and Yin (2009) database, Berberian and Yeats (2001) and Holt et al. (2000). Boundary conditions are selected in a fixed-Eurasia reference frame, testing different Euler rotation poles from DeMets et al. (2010) and Liu and Bird (2008) for Arabia and India plates. Model predictions include velocities, fault slip rates, strain rates and stress tensors. Preliminary results will be compared with measured GPS, slip faults and stress data.

References

Berberian, M. and Yeats, R.S., 2001, Contribution of archaeological data to studies of earthquake history in the Iranian Plateau, Journal of Structural Geology, 23, 563-584.

Bird, P., 2003, An updated digital model of plate boundaries, Geochemistry Geophysics Geosystems, 4(3), doi:10.1029/2001GC000252.

Bird, P., Liu Z., and Rucker W.K., 2008, Stresses that drive the plates from below: Definitions, computational path, model optimization, and error analysis, Journal of Geophysical Research, 113, B11406, doi:10.1029/2007JB005460.

DeMets, C., Gordon, R.G., Argus, D.F., 2010, Geologically current plate motions, Geophysical Journal International, 181, 1-80.

Holt, W.E., 2000. Correlated crust and mantle strain fields in Tibet, Geology, 28(1), 67-70.

Liu, Z. and Bird, P., 2008, Kinematic modelling of neotectonics in the Persia-Tibet-Burma orogen, Geophysical Journal International, 172, 79-797.

Robert, A., Fernandez, M., Jiménez-Munt, I., Verges, J., Lithospheric structures in Central Eurasia derived from elevation, geoid anomaly and thermal analysis, in prep.

Taylor, M. and Yin A., 2009, Active structures of the Himalaya-Tibetan orogen and their relationships to earthquake distribution, contemporary strain field and Cenozoic volcanism, Geosphere, 5 (3), 199-214.

Tunini, L., Jiménez-Munt, I., Fernandez, M., Verges, J., Villaseñor, A., Lithospheric mantle heterogeneities below the Zagros Mountains and the Iranian Plateau: a petrological-geophysical study, in rev.

Tunini, L., Jiménez-Munt, I., Fernandez, M., Verges, J., Villaseñor, A., Looking at the roots of the highest mountains: the lithospheric structure of the Himalaya-Tibetan orogen form a geophysical-petrological study, in prep.

Inherited basement controls on the development of Neogene thrust faults in the Northeast Tibetan Plateau

Rowan Vernon[1], Dickson Cunningham[1,2], Zhang Jin[3], Richard England[1]

[1] Department of Geology, University of Leicester, rv52@le.ac.uk
[2] Department of Environmental Earth Science, Eastern Connecticut State University
[3] Institute of Geology, Chinese Academy of Geological Sciences, Beijing

The Qilian Mountains of the northeast Tibetan Plateau represent one of the most actively deforming regions of the Plateau, and may provide an analogue for the formation and evolution of its older regions. The crust of the Qilian Mountains is an orogenic collage of island arc derived meta- volcanic and sedimentary rocks, accreted to the North China Craton during the Palaeozoic. Northeast-directed compression related to the Indo-Asia collision began here in the early Miocene. The resulting northwards-propagating deformation is characterised by uplift of fold-thrust mountain ranges which splay south-eastwards from the sinistral northeast-trending Altyn Tagh Fault (ATF).

In this project, we investigate the extent of inherited structural and lithological controls on the post-Oligocene tectonics around the Changma Basin at the very northeast corner of the Plateau, where the ATF forms a triple junction with the Qilian Nan Shan. Our research involves synthesis of previous geological and geophysical data, remote sensing analysis and structural mapping along key transects.

The Changma Basin (Fig. 1) is being uplifted through thrusting at the front of the Qilian Nan Shan and inverted due to back-thrusting of the Yumen Shan, related to transpression against the ATF. It is not possible to trace major structures from the basin into the surrounding ranges to demonstrate unequivocal evidence of basement reactivation. Field data and previous geological mapping show that some of the main range-building thrusts are approximately strike-parallel to basement structures within the ranges, while some are strongly discordant to these structures. Pre-existing foliations are exploited by some range-bounding faults, but intra-range reactivation of older fabrics has not been observed. In ranges containing thick limestone units intra-range uplift is accommodated by thrust faults both within and below the limestones, however in ranges lacking these units uplift is focused on the range-front. These observations suggest that inherited basement structures and specific lithologies exert varying degrees of control on the development of thrust faults and the post-Oligocene uplift of mountain ranges in the northeast Tibetan Plateau.

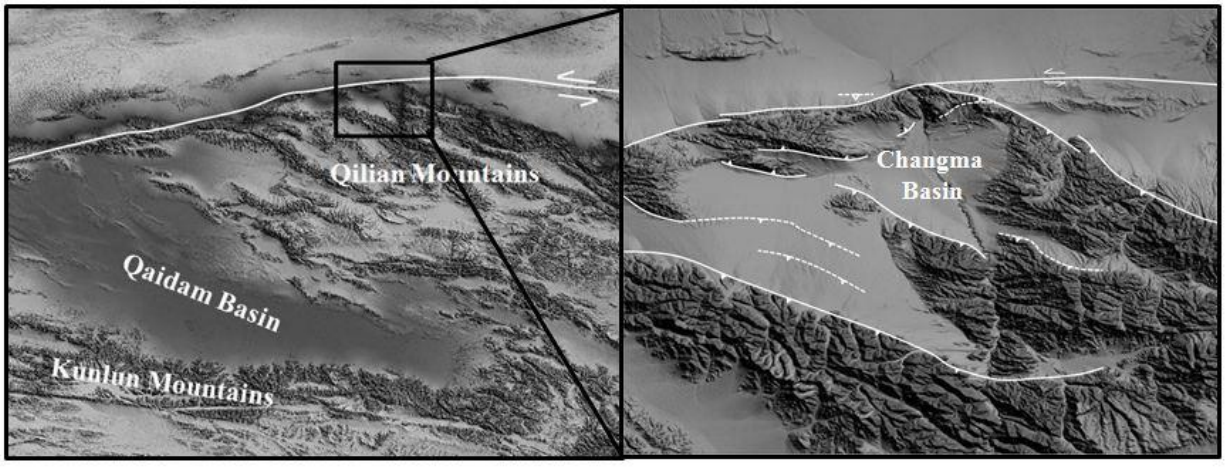

Figure 1- DTM showing the location of the field area and the major Neogene faults surrounding the Changma Basin, NE Tibet.

Cite as: Vernon, R., Cunningham, W.D., Zhang, J. and England, R., 2014, Inherited basement controls on the development of Neogene thrust faults in the Northeast Tibetan Plateau, in Montomoli C., et al., eds., proceedings for the 29th Himalaya-Karakoram-Tibet Workshop, Lucca, Italy.

Plateau growth around the Changma Basin in NE Tibet

Rowan Vernon[1], Dickson Cunningham[2,1], Zhang Jin[3], Richard England[1]

[1] Department of Geology, University of Leicester. rv52@le.ac.uk
[2] Department of Environmental Earth Science, Eastern Connecticut State University
[3] Institute of Geology, Chinese Academy of Geological Sciences, Beijing

The Qilian Mountains form one of the most actively uplifting regions of the northeastern Tibetan Plateau and provide an opportunity to study the ongoing, intermediate stages of plateau growth. The crust of the Qilian Mountains consists of an orogenic collage of mid-Proterozoic to mid-Palaeozoic island arc terranes accreted to the North China Craton during the Palaeozoic. NE-directed compression related to the Indo-Asian collision began in the Early Neogene, uplifting fold-thrust mountain ranges which splay south-eastwards from the sinistral northeast-trending Altyn Tagh Fault (ATF). In this study, we investigate the post-Oligocene tectonic evolution of the northern margin of the Tibetan Plateau around the Changma Basin, at the very northeast corner of the Plateau, where the ATF forms a triple junction with the frontal Qilian Shan thrust. Our research involves synthesis of previous geological and geophysical data, remote sensing analysis and field mapping of structures along key transects.

The Changma Basin (Fig. 1) is a relatively low intra-montane basin in the northeast Tibetan Plateau that is receiving alluvial infill from surrounding ranges, but is also being drained by the Su Le River, one of the largest river systems in the northeast Tibetan Plateau. The basin is also internally deforming and inverting along fault and fold zones, as well as being overthrust along some of its margins. Where older basement trends are parallel to neotectonic faults, some reactivation is inferred and locally documented through field observations. Otherwise, the post-Oligocene thrust and oblique-slip faults which are responsible for uplifting various basement blocks and inverting the Changma Basin appear discordant to nearby basement trends. Range-bounding thrust faults with the greatest along-strike continuity and relief generation are assumed to have the largest displacements, whereas other intra-range thrusts that bound uplifted limestone blocks are assumed to have lower amounts of displacement. Structural transects reveal a lack of intra-range reactivation of inherited structures or fabrics, concentrating uplift on the lithologically-controlled intra-range thrust faults and the major range-bounding thrust and oblique-slip faults. Northeast of the Changma Basin, in the Qilian Shan foreland, an east-trending belt of low folds and faulted ridges along the ATF marks the structural continuation of the Yumen Shan range. We find that uplift and growth of northeastern Tibet is complex with local variations in structural vergence, degree of strain partitioning, fault reactivation and basin inversion. This complexity reflects both the buttressing effect of the rigid Archaean basement directly to the north and the variation in the structural trends and lithologies of the Qilian basement, as well as the competition between uplift and erosion in the region.

Cite as: Vernon, R., Cunningham, W.D., Zhang, J. and England, R., 2014, Plateau growth around the Changma Basin in NE Tibet, in Montomoli C., et al., eds., proceedings for the 29th Himalaya-Karakoram-Tibet Workshop, Lucca, Italy.

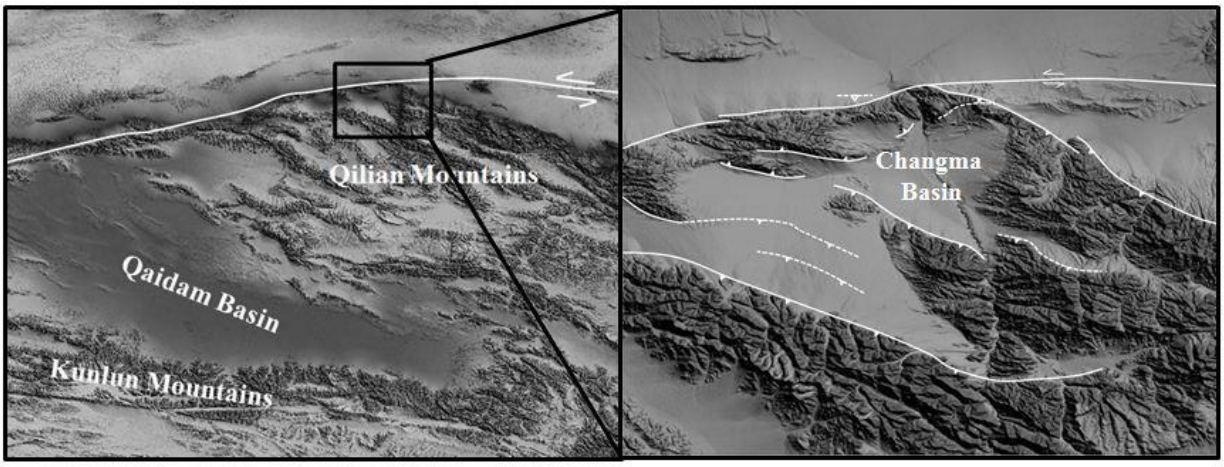

Figure 1. DTM showing the field area location and the major faults surrounding the Changma Basin.

Geochronology from the producer to the consumer

Igor M. Villa[1]

[1] CUDAM, Università di Milano Bicocca, 20126 Milano, Italy; Institut für Geologie, Universität Bern, 3012 Bern, Switzerland

Tectonic modelling requires large amounts of age data. Automated hardware appears capable to deliver numbers at an unprecedented rate. From the consumer's point of view, this may look like paradise.

The problem is, automation has not been the only advance. Improvements in sensitivity and precision have initiated a wave of innovative experiments on age patterns within and between mineral grains. Today we know more than was thought possible two decades ago. More knowledge means that the interpretive paradigm is no longer the simple "closure temperature" scheme fashionable in the early 1960s, yet consumers sometimes struggle to keep up-to-date in an exponentially rising amount of literature. As a consequence, a comment very frequently made by consumers is "I am not interested in your discussions, I want data quickly".

The producers of age data have reached a consensus on the paired geochronology+petrology advances. Pseudosections in P-T-A-X space, developed by petrologists, have taken the place of the "thermal isograds" of yore. Most minerals record internally discordant ages, diffusion being usually overrun by recrystallization. Petrographic relics coincide with isotopic inheritance. Zircon is the most obvious example, but similar observations are being increasingly documented for every single mineral chronometer (Villa & Williams 2013). This requires to no longer view minerals as "thermochronometers", but as *hygrochronometers* instead, and demands that each analysis be provided its complete context at the intercrystalline (retrogression, petrologic disequilibria, etc) and intracrystalline (microchemical gradients, age patches, etc) level. The modelling of exhumation rates by dating context-free detrital minerals, which forgoes the necessary petrologic equilibrium information, is not founded on solid bases. As context-finding is a typically human task, no automated protocol is predicted to reliably provide correct interpretations. One must never forget that accuracy must be laboriously sought and is not a guaranteed by-product of better precision. Today we know more: there are many more factors to be taken into account nowadays than our forefathers thought of half a century ago, and the complexity of the petrology-geochronology dependence is not going to make data production faster. The good news is that taking into account this complexity makes accurate geological reconstructions possible.

References

Villa, I.M. and Williams, M.L., 2013, Geochronology of metasomatic events, In: Harlov, D.E. and Austrheim, H. (eds.), Metasomatism and the Chemical Transformation of Rock, 171-202, Springer, Heidelberg, ISBN 978-3-642-28393-2.

Cite as: Villa, I.M., 2014, Geochronology from the producer to the consumer, in Montomoli C., et al., eds., proceedings for the 29th Himalaya-Karakoram-Tibet Workshop, Lucca, Italy.

A record of weathering, hydrological and monsoon evolution in the Eastern Himalaya since 13 Ma from detrital and organic geochemistry, Kameng River Section, Arunachal Pradesh

Natalie Vögeli[1], Peter van der Beek[1], Pascale Huyghe[1], Yani Najman[2], Dirk Sachse[3]

[1] Institut des Sciences de la Terre, Université Joseph Fourier, 38401 Grenoble, France, natalie.voegeli@ujf-grenoble.fr
[2] Department of Environmental Science, Lancaster University, Lancaster LA1 4YQ, United Kingdom
[3] Institut für Erd- und Umweltwissenschaften, Universität Potsdam, 14476 Potsdam, Germany

The link between tectonics, erosion and climate has become an important subject to ongoing research in the last years (Clift et al. (2008), amongst others). The young Himalayan orogeny is the perfect laboratory for its study. The Neogene sedimentary foreland basin of the Himalaya contains a record of tectonics and paleoclimate since Miocene times, within the so called Siwalik Group. Therefore several sedimentary sections within the Himalayan foreland basin along strike in the Himalayan range have been dated and studied regarding exhumation rates, provenance and paleoclimatology (e.g. Quade and Cerling, 1995; Ghosh et al., 2004; Sanyal et al., 2004; van der Beek et al., 2006). Lateral variations have been observed and changes in exhumation rate as well as climate change in the past especially the onset of the Asian summer monsoon is still debated. Several paleoclimatological studies in the western Himalaya were conducted (Quade and Cerling, 1995; Najman et al., 2003; Huyghe et al., 2005), but the eastern part of the mountain range remains poorly studied.

The Himalaya has a major influence on the regional and global climate. The major force driving the evolution of this mountain belt is the India-Asia convergence, nevertheless it has been suggested that the monsoonal climate plays a major role for the erosion and relief pattern (Bookhagen and Burbank, 2006; Clift et al., 2008; Iaffaldano et al., 2011). Exhumation rates in central Himalaya are more or less constant over last 13 Ma in the order of 1.8 km/myr, whereas exhumation rates in the eastern syntaxis increased post 3 Ma (Chirouze et al., 2013) to reach up to 10km/myr in the recent past.

In this study we use a multidisciplinary approach in order to better understand the interplay of monsoon and weathering regime during the Mid Miocene to Pleistocene in the eastern Himalaya. Therefore a sedimentary section in the eastern Himalaya was sampled. Pairs of fine and coarse grained sediment samples were taken in the Kameng section, Arunachal Pradesh (Fig. 1), which was previously dated by magnetostratigraphy by Chirouze et al. (2012) and ranges from 13 Ma to 1 Ma. A change in provenance of the sediments has been documented between 3-7 Ma and is interpreted as sediments brought from the Paleo-Brahmaputra, which had migrated northwards during this time (Chirouze et al., 2013).

Major elements were analyzed in order to calculate the Chemical Index of alteration (CIA) and to further see a first trend in the weathering intensity over the time span. Ratios of mobile to immobile elements show different trends of weathering, whereas the CIA remains relatively constant over time and values between 65 and 85 indicate a strong and stable weathering regime. In addition, in an ongoing analysis we use organic geochemical methods, such as lipid biomarker analysis, to decipher organic matter sources, alteration as well as possibly climatic and hydrological changes through time. Clay mineralogy should provide information on silicate weathering and possible diagenetic influence (Derry and France-Lanord, 1997).

Cite as: Vögeli, N., van der Beek, P., Huyghe, P., Najman, Y. and Sachse, D., 2014, A record of weathering, hydrological and monsoon evolution in the Eastern Himalaya since 13 Ma from detrital and organic geochemistry, Kameng River Section, Arunachal Pradesh, in Montomoli C., et al., eds., proceedings for the 29th Himalaya-Karakoram-Tibet Workshop, Lucca, Italy.

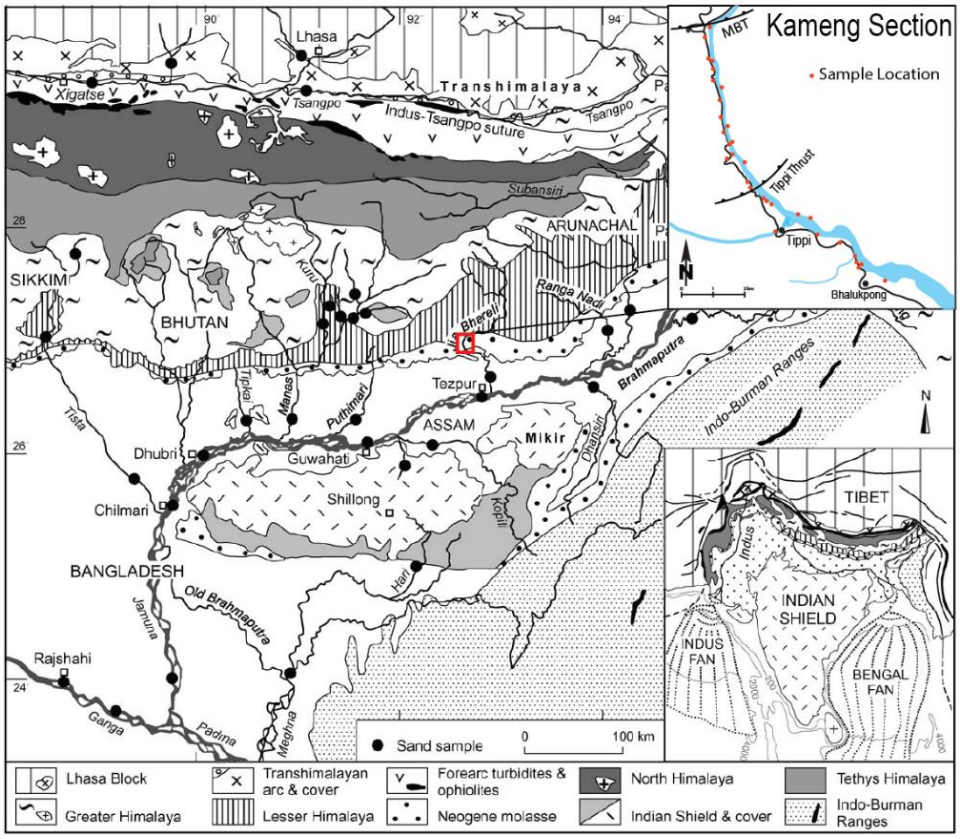

Figure 1. Geological map modified from Garzanti et al. (2004), Kameng river sampling region and locations are indicated.

References

Bookhagen, B. and Burbank, D. W., 2006, Topography, relief, and TRMM-derived rainfall variations along the Himalaya, Geophysical Research Letters, 33, L08405.

Chirouze, F., Dupont-Nivet, G., Huyghe, P., van der Beek, P., Chakraborti, T., Bernet, M. and Erens, V., 2012, Magnetostratigraphy of the Neogene Siwalik Group in the far eastern Himalaya: Kameng section, Arunachal Pradesh, India, Journal of Asian Earth Sciences, 44, 117-135.

Chirouze, F., Huyghe, P., van der Beek, P., Chauvel, C., Chakraborty, T., Dupont-Nivet, G. and Bernet, M., 2013, Tectonics, exhumation, and drainage evolution of the eastern Himalaya since 13 Ma from detrital geochemistry and thermochronology, Kameng River Section, Arunachal Pradesh, Geological Society of America Bulletin, 125, 523-538.

Clift, P.D., Hodges, K.V., Heslop, D., Hannigan, R., Van Long, H. and Calves, G., 2008, Correlation of Himalayan exhumation rates and Asian monsoon intensity, Nature Geoscience, 1, 875-880.

Garzanti, E., Vezzoli, G., Andò, S., France-Lanord, C., Singh, S.K. and Foster, G., 2004, Sand petrology and focused erosion in collision orogens: the Brahmaputra case, . Earth and Planetary Science Letters, 220, 157-174.

Ghosh, P., Padia, J. T. and Mohindra, R., 2004, Stable isotopic studies of palaeosol sediment from Upper Siwalik of Himachal Himalaya: evidence for high monsoonal intensity during late Miocene?, Palaeogeography, Palaeoclimatology, Palaeoecology, 206, 103-114.

Huyghe, P., Mugnier, J.-L., Gajurel, A. P. and Delcaillau, B., 2005, Tectonic and climatic control of the changes in sedimentary record of the Karnali River section (Siwaliks of western Nepal), Island Arc, 14, 311-327.

Iaffaldano, G., Husson, L. and Bunge, H.-P., 2011, Monsoon speeds up Indian plate motion, Earth and Planetary Science Letters, 304, 503-510.

Najman, Y., Garzanti, E., Pringle, M., Bickle, M., Stix, J. and Khan, I., 2003, Early-Middle Miocene paleodrainage and tectonics in the Pakistan Himalaya, Geological Society of America Bulletin, 115, 1265-1277.

Quade, J. and Cerling, T.E., 1995, Expansion of C4 grasses in the Late Miocene of Northern Pakistan: evidence from stable isotopes in paleosols, Palaeogeography, Palaeoclimatology, Palaeoecology, 115, 91-116.

Sanyal, P., Bhattacharya, S. K., Kumar, R., Ghosh, S. K. and Sangode, S. J., 2004, Mio–Pliocene monsoonal record from Himalayan foreland basin (Indian Siwalik) and its relation to vegetational change, Palaeogeography, Palaeoclimatology, Palaeoecology, 205, 23-41.

van der Beek, P., Robert, X., Mugnier, J.-L., Bernet, M., Huyghe, P. and Labrin, E., 2006, Late Miocene – Recent exhumation of the central Himalaya and recycling in the foreland basin assessed by apatite fission-track thermochronology of Siwalik sediments, Nepal, Basin Research, 18, 413-434.

The subduction and exhumation path of one UHP-eclogite from the Tso Morari complex

Franziska D.H. Wilke[1,2], Patrick J. O'Brien[1], Alexander Schmidt[1]

[1] Institut Earth and Environmental Sciences, University of Potsdam, D-14476 Potsdam, Germany, fwilke@geo.uni-potsdam.de
[2] German Research Centre for Geosciences GFZ, Telegrafenberg, D-14473 Potsdam, Germany

Eclogites and their host rocks were sampled from the Higher Himalayan Crystalline, south of the Indus-Tsangpo-Suture Zone, from the Tso Morari Complex, NW India. Peak pressures of around ≥39 kbar, for temperatures of 750°C, were obtained by Mukherjee and Sachan, 2009 for coesite-bearing eclogites from this area. This study of one newly collected eclogite reveals >100 µm large coesite grains, confirmed by raman spectroscopy, included in garnet. Garnets are zoned reflecting the prograde and a small part of the retrograde path. Inclusions can be directly correlated with the compositional zoning and are seen as either relicts of the protolith mineral paragenesis and as "snap shots" of the mineral paragenesis during subduction and under peak conditions. The matrix minerals reflect the multi-stage exhumation history.

Petrography

Ca- and Ca-Na-amphiboles, quartz, dolomite, rutile and ilmenite are present in the Ca- and Mn- rich garnet core (X_{Mg}=0.12) reflecting, most probably, protolith remnants. Ca-Na-amphiboles, paragonite, clinozoisite and quartz are present in the Fe-rich garnet mantle, indicating their appearance during subduction, whereas rutile appears from the garnet mantle into the Mg-rich rim. At the border from garnet mantle to rim, calcite is present accompanied by Fe-oxide. In the Mg-rich garnet rim (X_{Mg}=0.45), omphacite and coesite are preserved, reflecting their growth under peak metamorphic conditions.
In the matrix, primary omphacite with a X_{Jd} of 0.42-0.50 is present. Secondary omphacite overgrowing the primary one has a slightly lower X_{Jd} of 0.38-0.49. Na- and Na-Ca-amphiboles replace omphacite, which are themselves surrounded by Ca- amphiboles, either as granoblastic minerals or as symplectites together with albite. Phengite relicts are associated with paragonite. Clinozoisite and zoisite in places contain omphacite and rutile whereas the interaction with carbonates - large grains are intergrown with, smaller grains overgrow carbonates - points to subduction as well as exhumation-related epidote mineral formation. Matrix carbonate is either dolomite with small magnesite cores or ca. 300 µm long magnesite grains with initial cracks filled with dolomite. Secondary cracks passing through dolomite are filled with calcite and are associated with ca. 2 µm wide, parallel veins filled with iron oxide. Dolomite surrounds the magnesite and the youngest cracks contain Ca-rich dolomite and calcite as a part of a larger network of cracks that continue into adjacent minerals and are clearly associated with fluid influx. Magnesite shows an inhomogeneous chemistry enriched in Fe ($Mgs_{0.76–0.80}\ Sd_{0.20–0.21}$).

REE-geochemistry

Rare earth element (REE) concentrations were obtained by LA-ICP-MS for garnet, mineral inclusions in garnet and matrix minerals. The REE patterns in garnet reflect either mineral decomposition and release of REE or mineral formation and REE uptake during subduction, peak metamorphism and, to a minor extent, during exhumation. REE analyses of mineral inclusions in garnet and minerals from the matrix reveal that white mica and epidote minerals, which normally preferentially incorporate LREEs, reveal higher HREE contents or even equal values of heavy and light REEs.

P-T path reconstruction and conclusions

Standard geothermobarometry reveals peak conditions of 48-51 kbar at 560-750°C, using the most Mg-rich garnet, the most silicic phengite and the most jadeite-rich omphacite. The P-T condition of the subsequent glaucophane formation have been modelled to be at around 500°C at ca. 19 kbar whereas later Ca-amphiboles provide evidence for reheating towards 730°C at pressures as low as 10 kbar.

We applied a Gibbs free energy minimizing modelling to summarize our analytical findings (see Figure 1). The effective bulk rock composition, iteratively corrected for fractionation effects was used for the calculation

Cite as: Wilke, F.D.H. et al., 2014, The subduction and exhumation path of one UHP-eclogite from the Tso Morari complex, in Montomoli C., et al., eds., proceedings for the 29th Himalaya-Karakoram-Tibet Workshop, Lucca, Italy.

of pseudosections. The inclusions in garnet, supported by the REE distribution pattern in garnet to have been grown during subduction, suggest an isothermal subduction path, at least down to 55 km.

Peak P-T conditions as calculated by standard geothermobarometry were supported by modelling inasmuch as omphacite is stable up to 60 kbar within a temperature range of 620-780°C and the reaction curve dolomite ⇔ magnesite + aragonite was touched. The previously described carbonate textures would indicate an early dolomite that was stable throughout most of the prograde and retrograde stages. Dolomite overgrew magnesite during exhumation, while calcite probably replaced aragonite, which however, could not be identified in this sample. Despite these indicators that the eclogite crossed the graphite–diamond transition boundary, no diamond could be confirmed. A possible reason for the lack of diamond is the presence of carbon bound in the carbonates due to a high oxygen fugacity.

The complex exhumation path shows a stage of initial cooling during decompression, which lead to the formation of glaucophane. The subsequent growth of the second stage Ca-amphiboles and albite requires a significant reheating, before final exhumation. All together the results point to the, already reported, S-shape exhumation path characteristic for both the Tso Morari complex (Guillot et al., 2008) and the Kaghan Valley eclogites (Wilke et al., 2010).

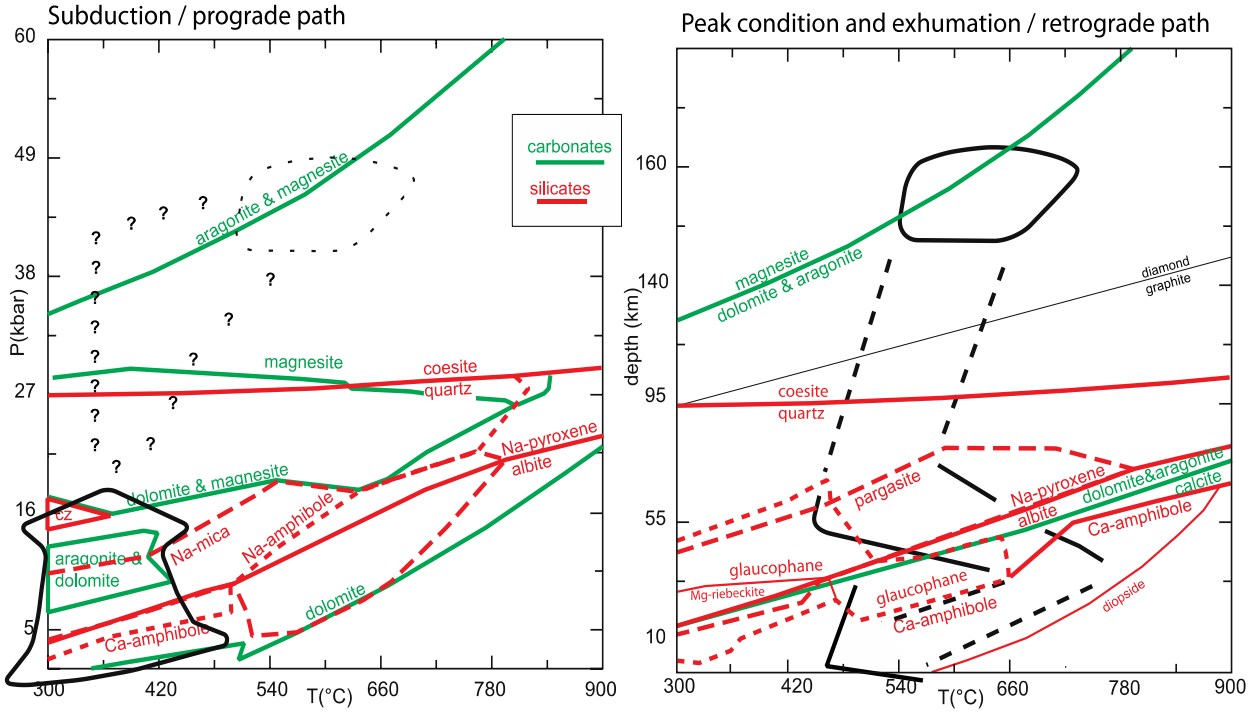

Figure 1. Phase diagrams for garnet-fractionated UHP eclogite bulk rock chemistry calculated with Perple_X. The coesite-quartz and albite = jadeite + quartz equilibria were calculated together with other reaction curves. Mineral phases that were not identified in the eclogite are not given in the diagrams, with the exception of aragonite, diopside and Mg-riebeckite, latter for orientation. Large arrows show our preferred PT-path that was reconstructed with Perple_X phase equilibria modelling for the subduction path and, in addition to that, with conventional geothermobarometry for the exhumation path.

References

Guillot, S., Mahéo, G., de Sigoyer, J., Hattori, K.H., Pêcher, A., 2008, Tethyan and Indian subduction viewed from the Himalayan high- to ultrahigh-pressure metamorphic rocks, Tectonophysics, 451, 225-241.

Mukherjee, B.K., Sachan, H.K., 2009, Fluids in coesite-bearing rocks of the Tso Morari Complex, NW Himalaya: evidence for entrapment during peak metamorphism and subsequent uplift, Geological Magazine, 164, 876-889.

Wilke, F.D.H., O'Brien, P.J., Altenberger, U., Konrad-Schmolke M., and Khan, M.A., 2010, Multi-stage history in different eclogite types from the Pakistan Himalaya and implications for exhumation processes, Lithos, 114, 70-85.

Seismic anisotropy from shear wave splitting across east Kunlun fault

Chenglong Wu[1,2], Tao Xu[1], Zhongjie Zhang[1], Jiwen Teng[1]

[1] State Key laboratory of Lithosphere Evolution, Institute of Geology and Geophysics, Chinese Academy of Sciences, Beijing, 100029, China, wuchenglong@mail.iggcas.ac.cn
[2] University of Chinese Academy of Sciences, Beijing, 100049, China

The northeastern Tibetan plateau is dominated by the Kunlun strike-slip fault system and adjacent Kunlun concealed thrust. In order to investigate the link between surface and internal deformation in the context of crust and mantle structure, we present shear wave splitting results obtained from the analysis of teleseismic SKS and direct S waves from regional earthquakes. We find a contrast in the splitting pattern complexity beneath different parts across the Kunlun fault. The fast directions in the southwest of Kunlun fault trending NW-SE are generally consistent with the strike of Kunlun fault, suggesting that the anisotropy in the lithosphere contributes significantly to the observed shear-wave splitting. While in northeast of Kunlun fault, the anisotropy shows azimuthal dependence of splitting parameters that can be modeled by two anisotropic layers. The fast direction in the upper layer is consistent with the surface movement determined from GPS, and could be associated with middle or lower crustal flow. The fast direction in the lower layer could be related to the flow in the asthenosphere related to the absolute motion of Eurasia. The complexity of seismic anisotropy pattern suggests that no unique geodynamic model can fit all the splitting results suitably.

Cite as: Wu, C.,, Xu, T., Zhang, Z. and Teng, J., 2014, Seismic anisotropy from shear wave splitting across east Kunlun fault, in Montomoli C., et al., eds., proceedings for the 29th Himalaya-Karakoram-Tibet Workshop, Lucca, Italy.

Three Dimensional Exhumation Process of the Greater Himalayan Complex above the Main Himalaya Thrust

Zhiqin Xu[1], Hui Cao[1], Zhihui Cai[1], Lingsen Zeng[1], Santa Man Rai[2], Huaqi Li[1], Zhonghai Li[1], Xijie Chen[1], Wang Qi[3]

[1] State Key Laboratory for Continental Tectonics and Dynamics, Institute of Geology, Chinese Academy of Geological Sciences, Beijing, China, xuzhiqin@gmail.com
[2] Department of Geology, Tri-Chandra Campus, Tribhuvan University, Kathmandu, Nepal
[3] State Key Laboratory for Mineral Deposits Research, Department of Earth Sciences, Nanjing University, Nanjing, China

The Greater Himalayan Complex (GHC) is characterized by high-grade (up to granulite facies) metamorphic rocks exhumed from the middle to lower crust, widespread migmatites from extensive anatectic process and high-temperature ductile deformation, suggesting that the Himalayan orogen is a "hot" collisional orogen. For a long time, the southward exhumation of the GHC was assumed to occur between the Main Central Thrust (MCT) and the South Tibet Detachment (STD) at ~24–10 Ma. However, our previous studies in the GHC revealed the widespread presence of sub-horizontal ductile detachment with orogen-parallel stretching lineation in the upper part of the GHC, which can be traced from the Purang area in the western Himalaya to the eastern Namche Barwa Syntaxis. The U–Pb ages of metamorphic zircon rims and $^{40}Ar/^{39}Ar$ cooling ages of mica and hornblende indicate that the orogen-parallel extension in the GHC is asymmetric: initiated first in the central GHC and moved faster eastward (28–26 Ma in the Nyalam and Jilong areas), but migrated slower westward (22 Ma in the Purang area). The lateral flow along the orogen-parallel detachments continued to 13–11 Ma, coeval with the activation of the MCT and STD.

In this study we revealed a large-scale ductile thrust shear zone in the GHC in the Beni-Jamson cross-section, Central Nepal, which is characterized by high-temperature quartz fabric (>650 °C), syn-tectonic felsic veins and a top-to-the-south shear sense. This thrust shear zone began the high-temperature ductile deformation at 34 Ma in the top of the GHC, and progressively migrated to the south at 26 Ma in the lower part of the GHC, i.e., earlier than the activation of the STD and MCT. Combined with seismic profiles across the Himalaya, we interpret this thrust shear zone as the exposed Main Himalaya Thrust (MHT). Activation of the MHT probably triggered the emplacement of late Eocene leucogranites in the Lagugoi Ganri metamorphic domes of the Tethys Himalaya.

Therefore, we propose a 3-D exhumation process of the GHC as follows: (1) Initial activation of the MHT triggered the partial melting of a thickened crust at 45–36 Ma and resulted in a weak and hot GHC; (2) Top-to-the-south thrusting along the MHT formed a thick shear zone in the GHC in the Oligocene (34–26 Ma); (3) Initial orogen-parallel gravitational collapse occurred in the late Oligocene in central and eastern GHC (28–26 Ma); (4) Widespread orogen-parallel extension and southward extrusion of the GHC in the Early-Middle Miocene, accompanied with the activation of the STD and MCT (24–10 Ma) under upper-amphibolite to greenschist facies metamorphism conditions. Subsequently, the MHT was migrated southward and produced the Main Boundary Thrust and Main Front Thrust between 10 and 5 Ma.

The Luobusa ophiolite lies in the eastern part of the Indus-Zangbo suture zone, Tibet and contains the biggest chromitite deposit in China. In recent years, lots of ultrahigh pressure and highly reduced minerals were surprisingly discovered in the Luobusa mantle peridotite and chromitite. They indicate a deep mantle (> 300 km) origin contrary to previously SSZ origin thought (Yang et al., 2014). Here, we report our new discoveries of in-situ natural moissanite and chromium-rich included olivines in Luobusa. They also suggest a lower mantle or transition zone origin.

References

Searle, M.P. and Szulc, A.G., 2005, Channel flow and ductile extrusion of the high Himalayan slab-the Kangchenjunga–Darjeeling profile, Sikkim Himalaya, J. Asian Earth Sci., 25,173-185.

Singh, S. and Chowdhary, P.K., 1990, An outline of the geological framework of the Arunachal Himalaya, Journal of Himalayan Geology, 1, 189-197.

Xu, Z.Q., Wang, Q., Pêcher, A. et al., 2013, Orogen-parallel ductile extension and extrusion of the Greater Himalaya in the late Oligocene and Miocene, Tectonics, 32, 191-215, doi: 10.1002/tect.20021.

Webb, A.G., Yin, A., Harrison, T.M. et al., 2007, The leading edge of the Greater Himalayan Crystalline complex revealed in the NW Indian Himalaya: Implications for the evolution of the Himalayan orogen, Geology, 35, 955-958.

Hodges, K.V., Whipple, K.X. and Hurtado, J.M., 2001, Himalayan neotectonics may imply active southward extrusion of Tibetan middle crust. Eos Trans., Am. Geophys. Union, 81, 1094.

Cite as: Xu, Z.Q., Cao, H., Cai, Z.H., Zeng, L.S., Rai, S.M., et al., 2014, Three Dimensional Exhumation Process of the Greater Himalayan Complex above the Main Himalaya Thrust, in Montomoli C., et al., eds., proceedings for the 29th Himalaya-Karakoram-Tibet Workshop, Lucca, Italy.

Spatial-temporal evolution of the Indus River and implications for western Himalayan tectonics: constraints from Sr-Nd isotopes and detrital zircon geochronology of Paleogene-Neogene rocks in the Katawaz basin, NW Pakistan

Guangsheng Zhuang[1], Yani Najman[1], Ian Millar[2], Catherine Chauvel[3], Stéphane Guillot[3], Andrew Carter[4]

[1] Lancaster Environment Centre, Lancaster University, Lancaster LA1 4YQ UK, g.zhuang@lancaster.co.uk
[2] NERC Isotope Geosciences Laboratory, Nottingham NG12 5GG, UK
[3] ISTerre, CNRS, Université Grenoble I, BP 53, 38041 Grenoble cedex, France
[4] Department of Earth and Planetary Sciences, Birkbeck, London WC1E 7HX, UK

The Indus River and its antecedence is controversially considered to have been draining various western Himalayan tectonic units since Indo-Asian initial contact and to have deposited sediments in intermontane basin within the suture zone, in the proximal foreland, and down to the Indian Ocean (Chirouze et al., 2014; Clift et al., 2001, 2002; Clift and Blusztajn, 2005; Henderson et al., 2010; Qayyum et al., 1996, 1997a, 1997b, 2001; Sinclair and Jaffey, 2001). Despite active research, fundamental questions regarding the river's origin and spatial-temporal evolution still remain open. The Cenozoic sedimentary sequence in the Katawaz Basin, NW Pakistan was thought to be a product of a fan-deltaic system, analogous to the modern Indus River system (Qayyum et al., 1996, 1997a, 1997b, 2001) and is critical for studying the Palaeo-Indus detritus transport history from source to sink. A preliminary study by Carter et al (2010) demonstrated that source sediment signatures were consistent with material derived from the nascent western Himalaya and associated magmatic arc but this study was based on too few samples to fully understand local changes in drainage and source contributions through time. To better understand the paleodrainage of the Indus River and its tectonic control, we conducted a detailed study of Sr-Nd isotopes and detrital zircons on Paleogene- to Neogene sedimentary rocks from the Katawaz Basin

In this study, we analyzed 22 bulk mudstone samples for Sr-Nd isotopes and 10 medium-grained sandstones for detrital zircon (U-Pb) geochronology. We refined the Cenozoic chronology in the Katawaz Basin based on our newly collected and compiled detrital zircon U-Pb ages and fission track ages. The prominent feature of this series is a positive excursion in Nd isotope value (ε_{Nd}) from ca. -10 to -5 starting in the Early Miocene (>19 Ma). Samples in this positive excursion also have relatively low $^{87}Sr/^{86}Sr$ values (0.7100 ~ 0.7200). We interpret this positive excursion in Nd isotope as reflecting a change in palaeodrainage from predominant input from the Karakoram or its possible western extension, the Helmand Block in Afghanistan (Boulin, 1988; Debon et al., 1987), possibly with a limited drainage area, to increasing contribution from Kohistan-Ladakh arcs that are characterized by high ε_{Nd} and low $^{87}Sr/^{86}Sr$ values. This shift towards increasing inputs from arcs is supported by our densely sampled detrital zircon U-Pb study of the same sedimentary rocks that shows a coincident change in U-Pb spectrum to dominant young zircon (<120 Ma) grains. This finding is consistent with a study on detrital sandstone framework mode in the upper stream, proximal foreland location, which reveals a change in sediment source to dominant arc detritus in the Early-Middle Miocene (Najman et al., 2003); and a new Hf-Sr study from the same location reveals that substantial input from arcs may last until the Middle-Late Miocene (Chirouze et al., 2014). The end of this positive excursion is accompanied by a shift in detrital zircon U-Pb mode towards more Himalayan-derived detritus dominated by old zircon (750-1,200 Ma) grains, possibly due to the stripping of the Kohistan-Ladak arc carapace that had been covering the Nanga Parbat syntaxis of Higher Himalaya affinity. Up-section, the recurrence of dominant young zircons with Neogene grains typical of the present Indus (Alizai et al., 2011), suggests the construction of the modern drainage of the Indus by then, with later eastward shifting of the lower Indus due to eastward propagation of the adjacent Baluchistan thrust belt.

Cite as: Zhuang, G., Najman, Y., Millar, I., Chauvel, C., Guillot, S., et al., 2014, Spatial-temporal evolution of the Indus River and implications for western Himalayan tectonics: constraints from Sr-Nd isotopes and detrital zircon geochronology of Paleogene-Neogene rocks in the Katawaz basin, NW Pakistan, in Montomoli C., et al., eds., proceedings for the 29th Himalaya-Karakoram-Tibet Workshop, Lucca, Italy.

References

Alizai, A., Carter, A., Clift, P.D., VanLaningham, S., Williams, J.C. and Kumar, R., 2011, Sediment provenance, reworking and transport processes in the Indus River by U–Pb dating of detrital zircon grains, Global and Planetary Change, 76, 33-55.

Boulin, J., 1988, Hercynian and Eocimmerian events in Afghanistan and adjoining regions, Tectonophysics, 148, 253-278.

Carter, A., Najman, Y., Bahroudi, A., Bown, P., Garzanti, E. and Lawrence, R.D., 2010, Locating earliest records of orogenesis in western Himalaya: Evidence from Paleogene sediments in the Iranian Makran region and Pakistan Katawaz basin, Geology, 38, 807-810.

Chirouze, F., Huyghe-Mugnier, P., Chauvel, C., van der Beek, P., Bernet, M. and Mugnier, J.-L., 2014, Stable drainage pattern and variable exhumation in the western Himalaya since the Middle Miocene, J. Geol., under revision.

Clift, P., Shimizu, N., Layne, G., Blusztajn, J., Gaedicke, C., Schlüter, H.-U., Clark, M. and Amjad, S., 2001, Development of the Indus Fan and its significance for the erosional history of the Western Himalaya and Karakoram, Geol. Soc. Am. Bull., 113, 1039-1051.

Clift, P.D. and Blusztajn, J., 2005, Reorganization of the western Himalayan river system after five million years ago, Nature, 438, 1001-1003.

Clift, P.D., Carter, A., Krol, M. and Kirby, E., 2002, Constraints on India-Eurasia collision in the Arabian Sea region taken from the Indus Group, Ladakh Himalaya, India, In: Clift, P.D., Carter, A., Krol, M., and Kirby, E. (eds.), The tectonic and climatic evolution of the Arabian Sea region, Geological Society Special Publication, 195, 97-116.

Debon, F., Afzali, H., Le Fort, P. and Sonet, J., 1987, Major intrusive stages in Afghanistan: Typology, age and geodynamic setting, Geologische Rundschau, 76, 245-264.

Henderson, A.L., Najman, Y., Parrish, R., BouDagher-Fadel, M., Barford, D., Garzanti, E. and Andò, S., 2010, Geology of the Cenozoic Indus Basin sedimentary rocks: Paleoenvironmental interpretation of sedimentation from the western Himalaya during the early phases of India-Eurasia collision, Tectonics 29.

Najman, Y., Garzanti, E., Pringle, M., Bickle, M., Stix, J. and Khan, I., 2003, Early-Middle Miocene paleodrainage and tectonics in the Pakistan Himalaya, Geol. Soc. Am. Bull., 115, 1265-1277.

Qayyum, M., Lawrence, R.D. and Niem, A.R., 1997a, Discovery of the palaeo-Indus delta-fan complex, J. Geol. Soc., 154, 753-756.

Qayyum, M., Lawrence, R.D. and Niem, A.R., 1997b, Molasse-Delta-flysch continuum of the Himalayan orogeny and closure of the Paleogene Katawaz Remnant Ocean, Pakistan, Intern. Geol. Rev., 39, 861-875.

Qayyum, M., Niem, A.R. and Lawrence, R.D., 1996, Newly discovered Paleogene deltaic sequence in Katawaz basin, Pakistan, and its tectonic implications, Geology, 24, 835-838.

Qayyum, M., Niem, A.R. and Lawrence, R.D., 2001, Detrital modes and provenance of the Paleogene Khojak Formation in Pakistan: Implications for early Himalayan orogeny and unroofing, Geol. Soc. Am. Bull., 113, 320-332.

Sinclair, H. and Jaffey, N., 2001, Sedimentology of the Indus Group, Ladakh, northern India: implications for the timing of initiation of the palaeo-Indus River, J. Geol. Soc. 158, 151-162.

Journal of Himalayan Earth Sciences
ISSN Print 1994-3237
ISSN Online 2305-6959

Published by: National Centre of Excellence in Geology, University of Peshawar, Peshawar 25120, Pakistan
Phone: ++92-91-9216427, ++92-91-9216767; Fax: ++92-91-9218183
Email: jhes@upesh.edu.pk; Web: http://nceg.upesh.edu.pk/